BioMed Research International

Biomarkers of Brain Function and Injury: Biological and Clinical Significance

Guest Editors: Diego Gazzolo, Giovanni Li Volti, Antonio W. D. Gavilanes, and Giovanni Scapagnini

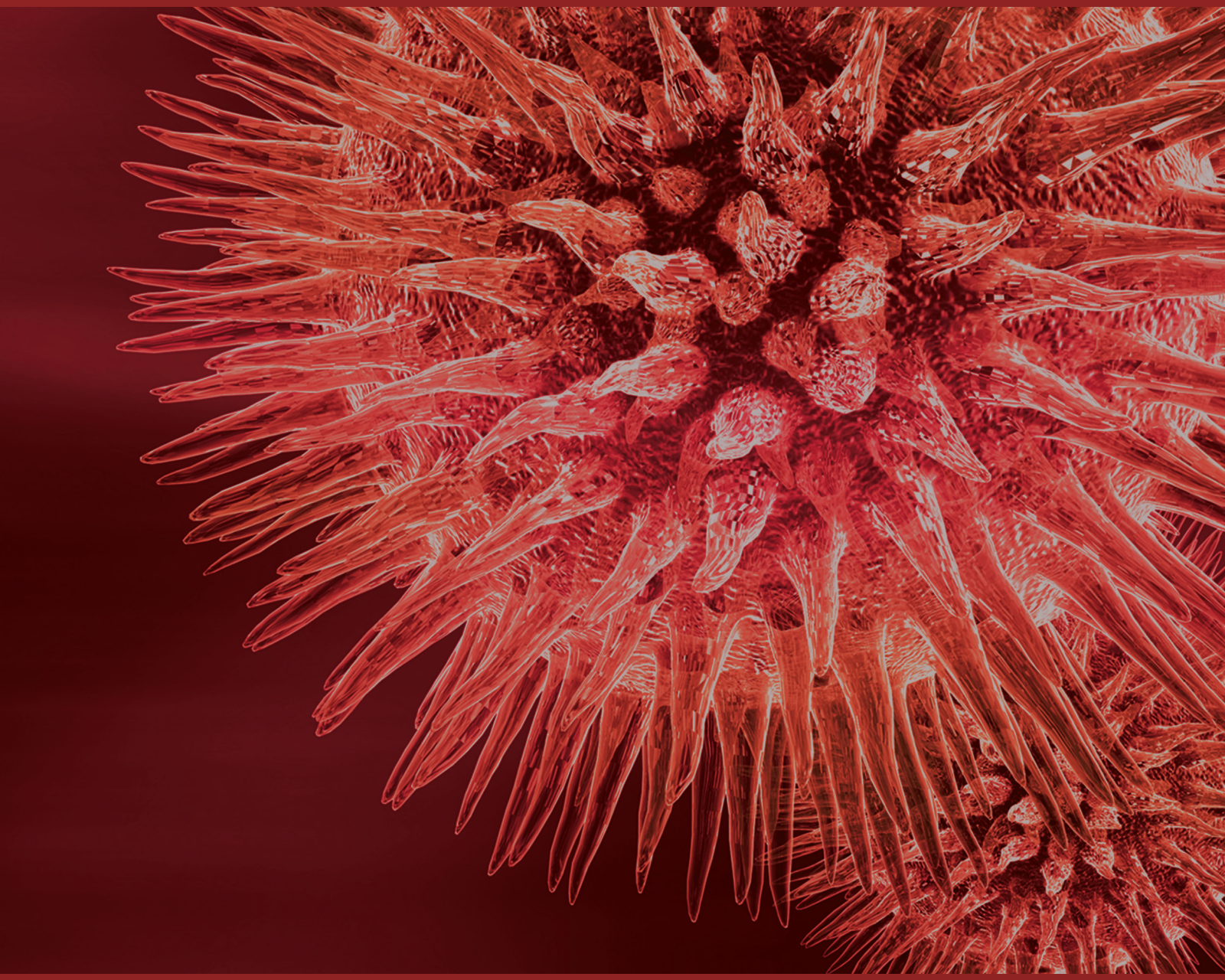

Biomarkers of Brain Function and Injury: Biological and Clinical Significance

BioMed Research International

Biomarkers of Brain Function and Injury: Biological and Clinical Significance

Guest Editors: Diego Gazzolo, Giovanni Li Volti, Antonio W. D. Gavilanes, and Giovanni Scapagnini

Contents

Hindawi Publishing Corporation
BioMed Research International
Volume 2015, Article ID 389023, 2 pages
http://dx.doi.org/10.1155/2015/389023

Editorial

Biomarkers of Brain Function and Injury: Biological and Clinical Significance

Diego Gazzolo,[1] Giovanni Li Volti,[2] Antonio W. D. Gavilanes,[3] and Giovanni Scapagnini[4]

[1]*Department of Maternal Fetal and Neonatal Medicine, C. Arrigo Children's Hospital, 15100 Alessandria, Italy*
[2]*Department of Biomedical and Biotechnological Sciences, University of Catania, 95100 Catania, Italy*
[3]*Department of Pediatrics, Neonatology and Child Neurology, University of Maastricht, 6229 HX Maastricht, Netherlands*
[4]*Department of Medicine and Health Sciences, University of Molise, 86100 Campobasso, Italy*

Correspondence should be addressed to Diego Gazzolo; dgazzolo@hotmail.com

Received 28 June 2015; Accepted 28 June 2015

Over the past decade an increasing interest in the use of biomarkers that are disease-specific to improve the diagnostic, prognostic, and therapeutic approach of different human pathologies has been observed.

Biomarkers have to be measurable in body fluids and able to address unmet clinical needs for the detection of a tissue injury. In particular, biochemical markers of brain damage, both in adult and in paediatric population, have been object of growing interest.

From the 90s onwards, deep evidence about brain plasticity throughout a person's lifespan has been accumulated, in contrast to the previous belief of a nonmutable system. Brain, in effect, is a complex network of different cell subsets that can not only be rewired, but it can also be structurally remodeled. The main consequence of neuroplasticity is the ability of several stimuli, from normal daily experience to damage, or recovery, to modulate the brain activity. The brain compensates for damage by reorganizing and forming new connections between intact neurons. Following a brain injury, in fact, a destructive cascade of biological events continues over hours and days that may worsen the patient's condition. Research studies on markers of brain damage both in humans and in specific animal model might help to understand the underlying mechanisms disrupting this plasticity and giving new insight into several human disease states.

In the current special issue, this topic has been addressed in both experimental and clinical studies, in which biomarkers assessment under different brain damage conditions, affecting central or peripheral nervous system, has been investigated. In detail, neuromarkers currently available have been evaluated (i) in cerebrospinal fluid of healthy adults (L. Hajduková et al.), (ii) in neurodegenerative diseases of adult population such as Alzheimer's disease (L. C. Oliveira-Júnior et al. and K. Weaver et al.), and (iii) in paediatric and adult populations complicated by idiopathic scoliosis, epilepsy, and/or requiring medical/surgical procedures (X. Liu et al., H. W. Lee et al., and D. Tomaszewski), in traumatic brain injury or stroke (A. Mangiola et al. and O. J. Kwon et al.), and in congenital heart diseases surgically treated (A. Varrica et al.). In addition, a space has been given to a novel "omics" science thanks to A. Dessì et al. who reported metabolomics pattern in healthy and intrauterine restricted newborns.

Moving to experimental model the key word "*. . .perinatal origin of adulthood diseases*" has been investigated in (i) a sheep-based model of perinatal asphyxia (E. Strackx et al.), (ii) a rat model of epilepsy (K. Rijkers et al. and C. Ventura-Mejía and L. Medina-Ceja), (iii) a zebrafish model of regeneration to explore the pattern of genes related to brain plasticity and remodelling (C. Kizil et al.), and finally (iv) mouse brain pattern of neural stem cells biomarkers involved in embryonic and adult neurogenesis (S. Zhang and J. Jiao).

Last but not least, this special issue also focuses on the need of trustable biomarkers for early diagnosis of brain damage when insult has already occurred and clinical

symptoms are at a subclinical stage. Future perspectives will regard the role of novel biomarkers in evaluating positive side-effects of neuroprotective strategies.

Diego Gazzolo
Giovanni Li Volti
Antonio W. D. Gavilanes
Giovanni Scapagnini

Hindawi Publishing Corporation
BioMed Research International
Volume 2015, Article ID 379071, 7 pages
http://dx.doi.org/10.1155/2015/379071

Research Article

Biomarkers of Brain Damage: S100B and NSE Concentrations in Cerebrospinal Fluid—A Normative Study

Lenka Hajduková,[1,2] Ondřej Sobek,[1] Darina Prchalová,[1,3] Zuzana Bílková,[1] Martina Koudelková,[1] Jiřina Lukášková,[1] and Inka Matuchová[1,4]

[1] *Laboratory for CSF and Neuroimmunology, Topelex Ltd., 190 00 Prague, Czech Republic*
[2] *Department of Neurology, The Military University Hospital Prague, 169 02 Prague, Czech Republic*
[3] *Department of Biology and Medical Genetics, Charles University 2nd Faculty of Medicine and University Hospital Motol, 150 06 Prague, Czech Republic*
[4] *Department of Biochemistry and Microbiology, The Institute of Chemical Technology, 166 28 Prague, Czech Republic*

Correspondence should be addressed to Ondřej Sobek; ondrej.sobek@likvor.cz

Received 27 June 2014; Revised 31 August 2014; Accepted 20 October 2014

Academic Editor: Diego Gazzolo

NSE and S100B belong among the so-called structural proteins of the central nervous system (CNS). Lately, this group of structural proteins has been profusely used as specific biomarkers of CNS tissue damage. So far, the majority of the research papers have focused predominantly on the concentrations of these proteins in blood in relation to CNS damage of various origins. Considering the close anatomic and functional relationship between the brain or spinal cord and cerebrospinal fluid (CSF), in case of a CNS injury, a rapid and pronounced increase of the concentrations of structural proteins specifically in CSF takes place. This study inquires into the physiological concentrations of NSE and S100B proteins in CSF, carried out on a sufficiently large group of 601 patients. The detected values can be used for determination of a normal reference range in CSF in a clinical laboratory diagnostics.

1. Introduction

Approximately from the 80s, there has been a notable increase of interest in structural proteins of the central nervous system (CNS), including S100B and NSE as biomarkers of CNS tissue damage [1].

1.1. Protein S100B. The exact term is S100 calcium binding protein B or S100B. This protein is the first identified member of the S100 protein multigenic family and participates in an extracellular and intracellular regulation of a cellular calcium metabolism [2]. Protein S100B, which is a major subordinate unit in mammals, is located mostly in glial cells of the central (predominantly astrocytes) and peripheral nervous system, but also in chondrocytes, melanocytes, and adipocytes [3].

S100B might have either a trophic or toxic effect depending on the local concentration. In a low nanomolar physiological concentration it seems to have a neurotrophic effect, it stimulates the growth of neurons, and it increases their survival during development and also during an injury [4–6]. On the other hand, higher concentrations of this protein might be toxic and evoke cell death. Generally, S100B acts like a damage-associated molecular pattern (DAMP), which is released from damaged or activated cells under conditions of cell stress [7]. Furthermore, a more complex role of S100B in the inflammatory processes has been described [8–11].

1.2. Neuron-Specific Enolase (NSE). It is a dimer formed in neurons with subordinate units α-γ or γ-γ, which belongs to the group of hydrolytic enzymes. NSE is an isoenzyme of enolase (2-phospho-D-glycerate hydrolase), which catalyzes the transition of 2-phosphoglycerate into phosphoenolpyruvate [12]. It is present in tissues of neuroectodermal origin. In a small amount, NSE is present in erythrocytes, blood platelets, plasmatic cells, lymphocytes, capillary walls, and myoepithelial cells, which explains its physiologically low concentrations in blood [13, 14].

In case of a CNS injury, accompanied by a nervous tissue and cellular damage, these structural proteins are released from cells, and their concentrations increase extracellularly—including CSF and blood. In these consequences these proteins could be called "biomarkers of brain damage" [1, 15–18].

Considerable number of research papers, engaged in monitoring the concentrations of NSE and S100B protein after a traumatic brain injury (TBI), was published [15, 17, 19–23].

The concrete value and dynamics of the concentrations of S100B protein and NSE also play an important role in the prediction of the outcome of patients who had brain ischemia [15, 23–28] or bleeding [15, 29–31] or after they underwent a cardiac surgery [32, 33] or a neurosurgery [34, 35].

Proteins S100B and NSE are also produced by some tumorous cells of neuroectodermal origin [36, 37].

Furthermore, structural proteins of CNS, including NSE and S100B protein, were researched in relation to prion diseases of CNS [38].

Major part of the research studies focuses on monitoring the concentrations of these biomarkers in blood. Sporadic studies that address the determination of their physiological concentrations in CSF are carried out on relatively small groups of patients [39].

Considering not only the close anatomic relationship between the brain or spinal cord and CSF, but also the small volume of a CSF reservoir, when CNS tissue is damaged, a rapid and pronounced increase of the concentrations of structural proteins specifically in CSF takes place.

In our opinion, a substantial study of the physiological concentrations of NSE and S100B protein in CSF, carried out on a sufficiently large group of patients, is missing.

In the Laboratory for CSF and Neuroimmunology, Prague, there are approximately 5000 CSF samples analyzed per year. Biochemical analysis (CSF total protein, glucose, lactate, and albumin), CSF cytological analysis (cell count and qualitative cytology), immunological analysis (CSF immunoglobulins IgG, IgM, IgA, isoelectric focusing of immunoglobulins and free light chains kappa and lambda, inflammatory markers including IL 1, IL 6, IL 8, and IL 10, autoantibodies including anti-AQP4, Yo, Hu, Ri, NMDA, AMPA, GABA, VGKC, and Gangliosides), microbiological CSF analysis (PCR and antibodies against neurotropic microbial agents, including Borrelia Burgdorferi s.l., Treponema Pallidum, Herpes viruses, TBE virus), and determination of structural proteins of CNS, namely, S100B, NSE are performed in this laboratory workplace.

2. Materials and Methods

We were able to compile a large enough investigated group of approximately 600 patients, on which we determined sufficiently reliable range of normal values of NSE and S100B in CSF.

2.1. Investigated Group. From the group of altogether 28.394 patients whose CSF was obtained and analyzed for diagnostic purposes within the years 2008–2014 (suspected inflammatory, vascular, degenerative, or traumatic impairment of CNS), a file of 601 patients was selected. There were no pathological findings in these patients as well as no clinical or CT/MRI signs of CNS tissue damage. Biochemical, cytological, and immunological values in CSF were normal.

2.2. Inclusion Criteria

Total cell count in CSF <= 4/μL.

Normal cytological finding: 60–80% of lymphocytes, no plasma cells, monocytes without signs of activation, no phagocytosis, no granulocytes, no atypical or tumorous cells.

Total CSF protein <= 0.4 g/L.

Lactate in CSF <= 2 mmol/L.

Glucose in CSF >= 2.2 mmol/L AND <= 4.2 mmol/L.

Coefficient of energy balance (CEB) in normal range (>27) [40, 41].

Negative finding of oligoclonal bands (OCB) in CSF on isoelectric focusing (IEF) of IgG (pattern I-normal finding).

IL 6 in CSF < 18 pg/mL.

Patients signed an informed consent with a further scientific use of their CSF samples.

2.3. Analytical Method. For determination of the concentrations of S100B and NSE in CSF, the sensitive electrochemiluminescence immunoassay (ECLIA, Roche Diagnostics) on Elecsys 2010 analyzer was used.

The method is based on the use of a ruthenium-complex and tripropylamine (TPA). The chemiluminescence reaction for the detection of the reaction complex is initiated by applying a voltage to the sample solution resulting in a precisely controlled reaction.

The standard kits for in vitro diagnostics, NSE catalogue number: 12133113 and S100B catalogue number: 03175243 by Roche Diagnostics GmbH, Sandhofer Strasse 116, D-68305 Mannheim, were used [42].

Interlaboratory comparisons of measurements of the concentrations of S100B and NSE were done in the frame of EQA (External Quality Assessment) organized by SEKK, Pardubice, Czech Republic.

The investigated group was divided into two groups of men and women to determine sex dependency and then into two age groups (20–59 and over 60 years) to establish age consequences.

The obtained data were statistically analyzed and scatter diagrams were created using program MS Excel. We estimated the reference limit as the 2.5th and the 97.5th percentiles for sex and age dependency.

3. Results and Discussion

See Table 1 and Figures 1, 2, 3, 4, 5, 6, 7, 8, 9, 10, 11, and 12.

Table 1: (a) S100B concentrations in CSF (μg/L). (b) NSE concentrations in CSF (μg/L).

(a)

Percentile 2.5	Percentile 97.5
Whole group, n = 601	
0.304	1.600
Men, n = 171	
0.309	1.420
Women, n = 430	
0.303	1.600
Age 20–59 years, n = 477	
0.303	1.437
Age > 60 years, n = 124	
0.326	1.609

(b)

Percentile 2.5	Percentile 97.5
Whole group, n = 601	
3.50	22.98
Men, n = 171	
4.67	23.29
Women, n = 430	
3.47	22.28
Age 20–59 years, n = 477	
3.47	19.98
Age > 60 years, n = 124	
6.46	27.63

The reference intervals were calculated as 2.5th and 97.5th percentiles.

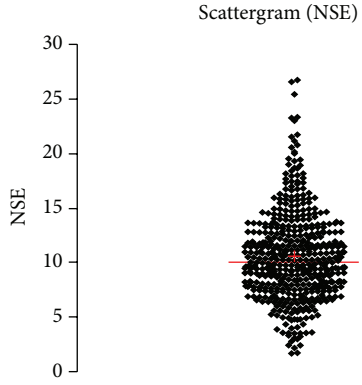

Figure 1: Concentration of NSE (μg/L) in an age group of patients 20–59 years, indiscriminately of sex.

3.1. Sex and Age Dependence. In the investigated group it was possible to observe similar tendencies in relation to age, as it had already been observed in previously published studies [39, 43, 44], that is, increasing concentrations of structural proteins of the CNS with age. In relation to sex, a higher concentration of S100B protein in CSF was observed in women, and, on the contrary, a higher concentration of NSE in CSF was observed in men.

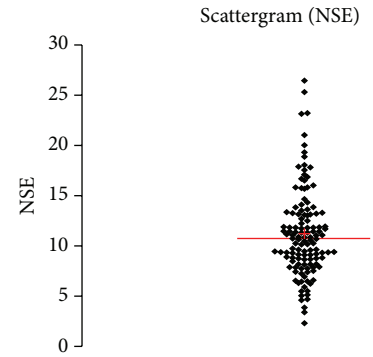

Figure 2: Concentration of NSE (μg/L) in an age group of patients 20–59 years, men.

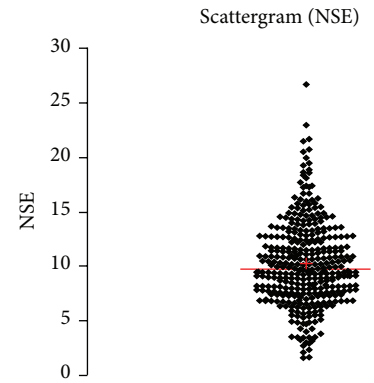

Figure 3: Concentration of NSE (μg/L) in an age group of patients 20–59 years, women.

Explanation of different allocation of both proteins, based on sex, could be most likely found in the dissimilar physiological tasks of each structural protein, eventually in their different distribution within the frame of the CNS—the source of S100B protein is astroglial cells above all, whereas NSE comes from the cellular body of neurons for the most part.

4. Conclusion

NSE and S100B are considered as quite established and specific markers of the CNS tissue damage. So far, clinical-laboratory interpretations mostly relied on studies based on monitoring of these structural proteins in blood.

Nonetheless, besides taking into account the close anatomic relationship between the brain or spinal cord and CSF, and also the small volume of a physiological CSF reservoir, in case of a CNS injury, the most sensitive and specific compartment accessible for a routine laboratory analysis is CSF.

With regard to the intercompartmental dynamics of a protein transportation from CNS to CSF [45], after a brain injury, a rapid and pronounced increase of the concentrations of the structural proteins particularly in CSF takes place.

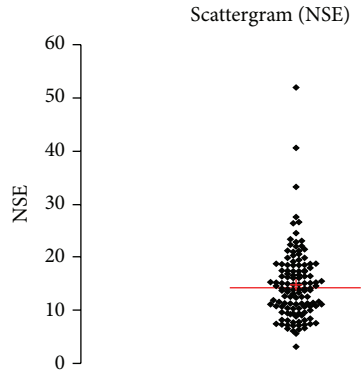

Figure 4: Concentration of NSE (μg/L) in an age group of patients above 60 years, indiscriminately of sex.

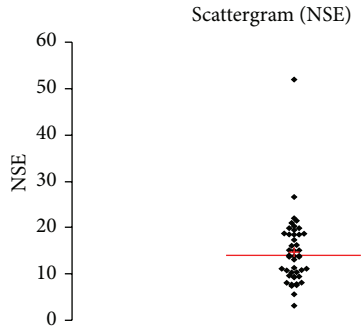

Figure 5: Concentration of NSE (μg/L) in an age group of patients above 60 years, men.

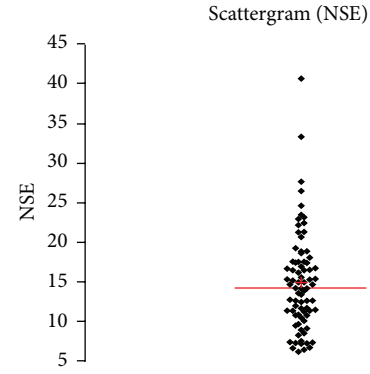

Figure 6: Concentration of NSE (μg/L) in an age group of patients above 60 years, women.

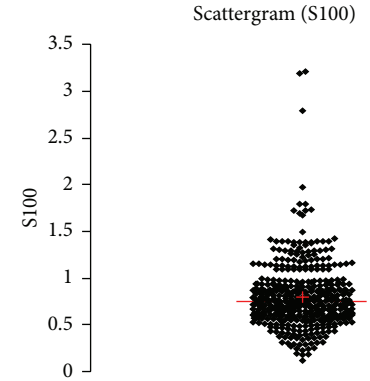

Figure 7: Concentration of S100B (μg/L) in an age group of patients 20–59 years, indiscriminately of sex.

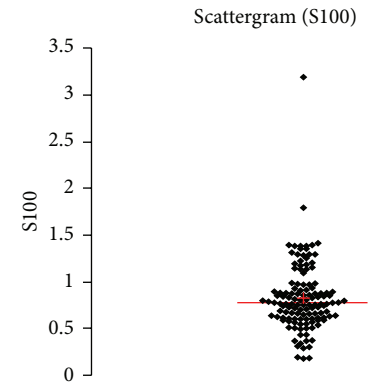

Figure 8: Concentration of S100B (μg/L) in an age group of patients 20–59 years, men.

This study evaluated the physiological concentrations of NSE and S100B protein in CSF, carried out on a sufficiently large group of 601 patients. Correlations of the concentrations of S100B and NSE depending upon age and sex were established as well.

The values detected in this study can be used for stating the normal reference range in CSF in a clinical laboratory diagnostics.

Reliable reference ranges of S100B and NSE are necessary for a clinical interpretation of laboratory findings in CSF in patients with suspected damage of CNS tissue. Preference of determination of concentrations of these proteins in CSF, to their determination in blood, is meaningful especially in a more discrete impairment of CNS (in terms of degenerative or vascular etiology, in traumatic or compressive impairment of brain and spinal cord, etc.). Into a large group of diseases, with a possible tissue damage of CNS, where CSF diagnostics is preferred, belong neuroinflammations, both neuroinfections and autoimmune processes (MS, NMO, ADEM, etc.).

Laboratory analysis used in this study is based on an established and widely accessible ECLIA methodology used in a routine laboratory practice. Presently, there are lots of regular external quality control assessments (EQA) for S100B and NSE available, so that interlaboratory comparability of results is guaranteed. Introduction of these new parameters into the CSF diagnostics brings, in the authors' opinion, a new and potent diagnostic tool for a detection of a CNS tissue damage, which is both independent of and complementary to neuroimaging methods like CT or MRI.

The precise determination of the presence and degree of a structural damage of CNS has a clinical significance for both prognosis of a patient's outcome and a choice of therapeutic approaches.

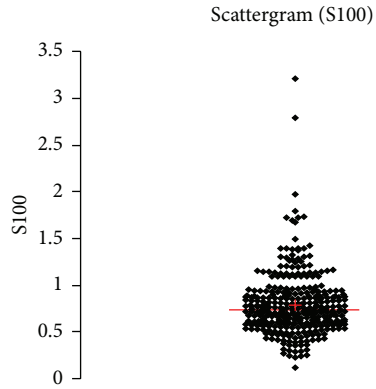

Figure 9: Concentration of S100B (μg/L) in an age group of patients 20–59 years, women.

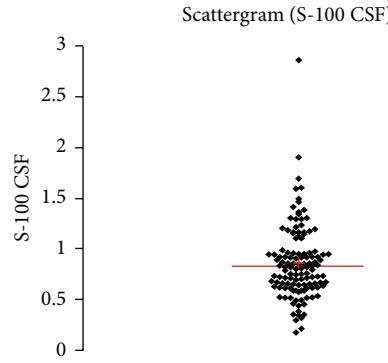

Figure 10: Concentration of S100B (μg/L) in an age group of patients above 60 years, indiscriminately of sex.

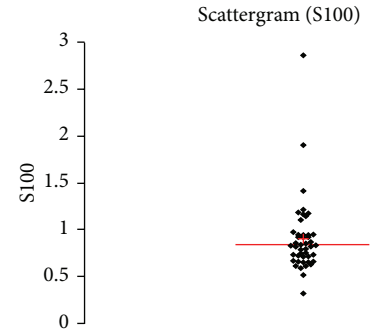

Figure 11: Concentration of S100B (μg/L) in an age group of patients above 60 years, men.

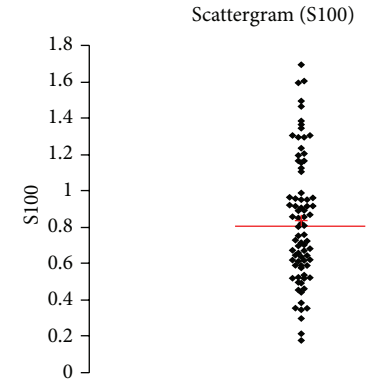

Figure 12: Concentration of S100B (μg/L) in an age group of patients above 60 years, women.

Abbreviations

CNS:	Central nervous system
CSF:	Cerebrospinal fluid
NSE:	Neuron-specific enolase
S100B:	S100B protein. Synonyms: S100 calcium binding protein B
DAMP:	Damage-associated molecular pattern
TBI:	Traumatic brain injury
AQP4:	Aquaporin 4
Anti-Yo:	Anti-Yo antibodies. Synonyms: type 1 Purkinje cell cytoplasmic autoantibodies (PCA-1).
Anti-Hu:	Anti-Hu antibodies. Synonyms: anti-neuronal nuclear antibody type 1 (ANNA-1)
Anti-Ri:	Anti-Ri nuclear antibody type 2 (ANNA-2)
NMDA:	(N-Methyl-D-aspartate) receptor
AMPA:	(α-Amino-3-hydroxy-5-methyl-4-isoxazolepropionic acid) receptor
GABA:	(Gamma aminobutyric acid) receptor
VGKC:	Voltage-gated potassium channel
IEF:	Isoelectric focusing
CEB:	Coefficient of energy balance
ECLIA:	Electrochemiluminescence immunoassay
EQA:	External quality assessment
MS:	Multiple sclerosis
NMO:	Neuromyelitis optica
ADEM:	Acute disseminated encephalomyelitis
CT:	Computed tomography
MRI:	Magnetic resonance imaging.

Conflict of Interests

The authors declare that there is no conflict of interests regarding the publication of this paper.

Acknowledgments

The authors would like to express special thanks to Jitka Doležalová for editorial support and to Ondřej Duchoň for patient database operations.

References

[1] F. Michetti, A. Massaro, G. Russo, and G. Rigon, "The S-100 antigen in cerebrospinal fluid as a possible index of cell injury in the nervous system," *Journal of the Neurological Sciences*, vol. 44, no. 2-3, pp. 259–263, 1980.

[2] B. W. Schäfer and C. W. Heizmann, "The S100 family of EF-hand calcium-binding proteins: functions and pathology," *Trends in Biochemical Sciences*, vol. 21, no. 4, pp. 134–140, 1996.

[3] L. Zhu, S. Okano, M. Takahara et al., "Expression of S100 protein family members in normal skin and sweat gland tumors," *Journal of Dermatological Science*, vol. 70, no. 3, pp. 211–219, 2013.

[4] F. Michetti and D. Gazzolo, "Perinatal S100B protein assessment in human unconventional biological fluids: a minireview and new perspectives," *Cardiovascular Psychiatry and Neurology*, vol. 2010, Article ID 703563, 5 pages, 2010.

[5] R. Donato, G. Sorci, F. Riuzzi et al., "S100B's double life: intracellular regulator and extracellular signal," *Biochimica et Biophysica Acta—Molecular Cell Research*, vol. 1793, no. 6, pp. 1008–1022, 2009.

[6] T. Rainey, M. Lesko, R. Sacho, F. Lecky, and C. Childs, "Predicting outcome after severe traumatic brain injury using the serum S100B biomarker: results using a single (24 h) time-point," *Resuscitation*, vol. 80, no. 3, pp. 341–345, 2009.

[7] D. Foell, H. Wittkowski, T. Vogl, and J. Roth, "S100 proteins expressed in phagocytes: a novel group of damage-associated molecular pattern molecules," *Journal of Leukocyte Biology*, vol. 81, no. 1, pp. 28–37, 2007.

[8] M. C. Guerra, L. S. Tortorelli, F. Galland et al., "Lipopolysaccharide modulates astrocytic S100B secretion: a study in cerebrospinal fluid and astrocyte cultures from rats," *Journal of Neuroinflammation*, vol. 8, article 128, 2011.

[9] G. Sorci, R. Bianchi, F. Riuzzi et al., "S100B protein, a damage-associated molecular pattern protein in the brain and heart, and beyond," *Cardiovascular Psychiatry and Neurology*, vol. 2010, Article ID 65648, 13 pages, 2010.

[10] F. Michetti, V. Corvino, M. C. Geloso et al., "The S100B protein in biological fluids: more than a lifelong biomarker of brain distress," *Journal of Neurochemistry*, vol. 120, no. 5, pp. 644–659, 2012.

[11] J. Sen and A. Belli, "S100B in neuropathologic states: the CRP of the brain?" *Journal of Neuroscience Research*, vol. 85, no. 7, pp. 1373–1380, 2007.

[12] C. C. Rider and C. B. Taylor, "Enolase isoenzymes. II. Hybridization studies, developmental and phylogenetic aspects," *Biochimica et Biophysica Acta*, vol. 405, no. 1, pp. 175–187, 1975.

[13] M. Ondrkalová, T. Kalnovičová, J. Štofko, P. Traubner, and P. Turčáni, "Levels of neuron-specific anolase in focal brain ischaemia," *Klinicka Biochemie a Metabolismus*, vol. 14, no. 4, pp. 202–206, 2006.

[14] V. Planche, C. Brochet, A. Bakkouch, and M. Bernard, "Importance of hemolysis on neuron-specific enolase measurement," *Annales de Biologie Clinique*, vol. 68, no. 2, pp. 239–242, 2010.

[15] L. Persson, H.-G. Hardemark, J. Gustafsson et al., "S-100 protein and neuron-specific enolase in cerebrospinal fluid and serum: Markers of cell damage in human central nervous system," *Stroke*, vol. 18, no. 5, pp. 911–918, 1987.

[16] T. O. Kleine, L. Benes, and P. Zöfel, "Studies of the brain specificity of S100B and neuron-specific enolase (NSE) in blood serum of acute care patients," *Brain Research Bulletin*, vol. 61, no. 3, pp. 265–279, 2003.

[17] H. Zetterberg, D. H. Smith, and K. Blennow, "Biomarkers of mild traumatic brain injury in cerebrospinal fluid and blood," *Nature Reviews Neurology*, vol. 9, no. 4, pp. 201–210, 2013.

[18] L. M. Calderon, F. X. Guyette, A. A. Doshi, C. W. Callaway, and J. C. Rittenberger, "Combining NSE and S100B with clinical examination findings to predict survival after resuscitation from cardiac arrest," *Resuscitation*, vol. 85, pp. 1025–1029, 2014.

[19] T. Ingebrigtsen, B. Romner, S. Marup-Jensen et al., "The clinical value of serum S-100 protein measurements in minor head injury: a Scandinavian multicentre study," *Brain Injury*, vol. 14, no. 12, pp. 1047–1055, 2000.

[20] P. Biberthaler, T. Mussack, E. Wiedemann et al., "Rapid identification of high-risk patients after minor head trauma (MHT) by assessment of S-100B: ascertainment of a cut-off level," *European Journal of Medical Research*, vol. 7, no. 4, pp. 164–170, 2002.

[21] R. P. Berger, M. C. Pierce, S. R. Wisniewski et al., "Neuron-specific enolase and S100B in cerebrospinal fluid after severe traumatic brain injury in infants and children.," *Pediatrics*, vol. 109, no. 2, p. E31, 2002.

[22] T. Hayakata, T. Shiozaki, O. Tasaki et al., "Changes in CSF S100B and cytokine concentrations in early-phase severe traumatic brain injury," *Shock*, vol. 22, no. 2, pp. 102–107, 2004.

[23] P. M. Kochanek, R. P. Berger, H. Bayir, A. K. Wagner, L. W. Jenkins, and R. S. B. Clark, "Biomarkers of primary and evolving damage in traumatic and ischemic brain injury: diagnosis, prognosis, probing mechanisms, and therapeutic decision making," *Current Opinion in Critical Care*, vol. 14, no. 2, pp. 135–141, 2008.

[24] T. Büttner, S. Weyers, T. Postert, R. Sprengelmeyer, and W. Kuhn, "S-100 protein: serum marker of focal brain damage after ischemic territorial MCA infarction," *Stroke*, vol. 28, no. 10, pp. 1961–1965, 1997.

[25] A. Petzold, P. Michel, M. Stock, and M. Schluep, "Glial and axonal body fluid biomarkers are related to infarct volume, severity, and outcome," *Journal of Stroke and Cerebrovascular Diseases*, vol. 17, no. 4, pp. 196–203, 2008.

[26] M. Herrmann, P. Vos, M. T. Wunderlich, C. H. M. M. de Bruijn, and K. J. B. Lamers, "Release of glial tissue-specific proteins after acute stroke," *Stroke*, vol. 31, no. 11, pp. 2670–2677, 2000.

[27] C. Foerch, O. C. Singer, T. Neumann-Haefelin, R. Du Mesnil de Rochemont, H. Steinmetz, and M. Sitzer, "Evaluation of serum S100B as a surrogate marker for long-term outcome and infarct volume in acute middle cerebral artery infarction," *Archives of Neurology*, vol. 62, no. 7, pp. 1130–1134, 2005.

[28] R. Brouns, B. de Vil, P. Cras, D. de Surgeloose, P. Mariën, and P. P. de Deyn, "Neurobiochemical markers of brain damage in cerebrospinal fluid of acute ischemic stroke patients," *Clinical Chemistry*, vol. 56, no. 3, pp. 451–458, 2010.

[29] M. Huang, X.-Q. Dong, Y.-Y. Hu, W.-H. Yu, and Z.-Y. Zhang, "High S100B levels in cerebrospinal fluid and peripheral blood of patients with acute basal ganglial hemorrhage are associated with poor outcome," *World Journal of Emergency Surgery*, vol. 1, no. 1, 2010.

[30] C. S. Jung, B. Lange, M. Zimmermann, and V. Seifert, "CSF and serum biomarkers focusing on cerebral vasospasm and ischemia after subarachnoid hemorrhage," *Stroke Research and Treatment*, vol. 2013, Article ID 560305, 7 pages, 2013.

[31] S. Moritz, J. Warnat, S. Bele, B. M. Graf, and C. Woertgen, "The prognostic value of NSE and S100B from serum and cerebrospinal fluid in patients with spontaneous subarachnoid hemorrhage," *Journal of Neurosurgical Anesthesiology*, vol. 22, no. 1, pp. 21–31, 2010.

[32] P. Johnsson, M. Bäckström, C. Bergh, H. Jönsson, C. Lührs, and C. Alling, "Increased S100B in blood after cardiac surgery is

a powerful predictor of late mortality," *The Annals of Thoracic Surgery*, vol. 75, no. 1, pp. 162–168, 2003.

[33] D. Georgiadis, A. Berger, E. Kowatschev et al., "Predictive value of S-100β and neuron-specific enolase serum levels for adverse neurologic outcome after cardiac surgery," *The Journal of Thoracic and Cardiovascular Surgery*, vol. 119, no. 1, pp. 138–147, 2000.

[34] J. de Vries, W. A. M. H. Thijssen, S. E. A. Snels, T. Menovsky, N. G. M. Peer, and K. J. B. Lamers, "Intraoperative values of S-100 protein, myelin basic protein, lactate, and albumin in the CSF and serum of neurosurgical patients," *Journal of Neurology, Neurosurgery & Psychiatry*, vol. 71, no. 5, pp. 671–674, 2001.

[35] C. Mattusch, K.-W. Diederich, A. Schmidt et al., "Effect of carotid artery stenting on the release of S-100B and neurone-specific enolase," *Angiology*, vol. 62, no. 5, pp. 376–380, 2011.

[36] E. Seregni, S. Massaron, A. Martinetti et al., "S100 protein serum levels in cutaneous malignant melanoma," *Oncology Reports*, vol. 5, no. 3, pp. 601–604, 1998.

[37] M. Harding, J. McAllister, G. Hulks et al., "Neurone specific enolase (NSE) in small cell lung cancer: a tumour marker of prognostic significance?" *British Journal of Cancer*, vol. 61, no. 4, pp. 605–607, 1990.

[38] A. J. E. Green, E. J. Thompson, G. E. Stewart et al., "Use of 14–3–3 and other brain-specific proteins in CSF in the diagnosis of variant Creutzfeldt-Jakob disease," *Journal of Neurology, Neurosurgery & Psychiatry*, vol. 70, no. 6, pp. 744–748, 2001.

[39] Ø. Nygaard, B. Langbakk, and B. Romner, "Age- and sex-related changes of S-100 protein concentrations in cerebrospinal fluid and serum in patients with no previous history of neurological disorder," *Clinical Chemistry*, vol. 43, no. 3, pp. 541–543, 1997.

[40] P. Kelbich, A. Hejčl, I. S. Krulichová et al., "Coefficient of energy balance, a new parameter for basic investigation of the cerebrospinal fluid," *Clinical Chemistry and Laboratory Medicine*, vol. 52, no. 7, pp. 1009–1017, 2014.

[41] K. Bořecká, P. Adam, O. Sobek, L. Hajduková, V. Lánská, and P. Nekola, "Coefficient of energy balance: effective tool for early differential diagnosis of CNS diseases," *BioMed Research International*, vol. 2013, Article ID 745943, 8 pages, 2013.

[42] J. M. G. Bonfrer, C. M. Korse, O. E. Nieweg, and E. M. Rankin, "The luminescence immunoassay S-100: a sensitive test to measure circulating S-100B: its prognostic value in malignant melanoma," *British Journal of Cancer*, vol. 77, no. 12, pp. 2210–2214, 1998.

[43] D. Gazzolo, F. Michetti, M. Bruschettini et al., "Pediatric concentrations of S100B protein in blood: age- and sex-related changes," *Clinical Chemistry*, vol. 49, no. 6, pp. 967–970, 2003.

[44] B. G. M. van Engelen, K. J. B. Lamers, F. J. M. Gabreels, R. A. Wevers, W. J. A. van Geel, and G. F. Borm, "Age-related changes of neuron-specific enolase, S-100 protein, and myelin basic protein concentrations in cerebrospinal fluid," *Clinical Chemistry*, vol. 38, no. 6, pp. 813–816, 1992.

[45] H. Reiber, "Dynamics of brain-derived proteins in cerebrospinal fluid," *Clinica Chimica Acta*, vol. 310, no. 2, pp. 173–186, 2001.

Hindawi Publishing Corporation
BioMed Research International
Volume 2015, Article ID 276049, 9 pages
http://dx.doi.org/10.1155/2015/276049

Research Article

Expression Signatures of Long Noncoding RNAs in Adolescent Idiopathic Scoliosis

Xiao-Yang Liu,[1,2] Liang Wang,[1] Bin Yu,[1] Qian-yu Zhuang,[1] and Yi-Peng Wang[1]

[1]*Department of Orthopedic Surgery, Peking Union Medical College Hospital, Chinese Academy of Medical Sciences & Peking Union Medical College, No. 1 Shuaifuyuan, Wangfujing, Dongcheng District, Beijing 100730, China*
[2]*Department of Spine Surgery, Shandong Provincial Hospital Affiliated to Shandong University, Jinan, Shandong 250000, China*

Correspondence should be addressed to Yi-Peng Wang; ypwang133@163.com

Received 4 June 2014; Accepted 31 October 2014

Academic Editor: Diego Gazzolo

Purpose. Adolescent idiopathic scoliosis (AIS), the most common pediatric spinal deformity, is considered a complex genetic disease. Causing genes and pathogenesis of AIS are still unclear. This study was designed to identify differentially expressed long noncoding RNAs (lncRNAs) involving the pathogenesis of AIS. *Methods*. We first performed comprehensive screening of lncRNA and mRNA in AIS patients and healthy children using Agilent human lncRNA + mRNA Array V3.0 microarray. LncRNAs expression in different AIS patients was further evaluated using quantitative PCR. *Results*. A total of 139 lncRNAs and 546 mRNAs were differentially expressed between AIS patients and healthy control. GO and Pathway analysis showed that these mRNAs might be involved in bone mineralization, neuromuscular junction, skeletal system morphogenesis, nucleotide and nucleic acid metabolism, and regulation of signal pathway. Four lncRNAs (ENST00000440778.1, ENST00000602322.1, ENST00000414894.1, and TCONS_00028768) were differentially expressed between different patients when grouped according to age, height, classification, severity of scoliosis, and Risser grade. *Conclusions*. This study demonstrates the abnormal expression of lncRNAs and mRNAs in AIS, and the expression of some lncRNAs was related to clinical features. This study is helpful for further understanding of lncRNAs in pathogenesis, treatment, and prognosis of AIS.

1. Introduction

Adolescent idiopathic scoliosis (AIS), accounting for 90% of all idiopathic scoliosis (IS) cases, affects more than 2% of the pediatric population and results in more than 600,000 physician visits annually [1]. Approximately, 1.5% patients ultimately need surgical correction for their curvature [2]. However, the causes involved in AIS remain obscure.

Genetic twin studies and observation of familial aggregation have revealed significant genetic contribution to IS [3, 4]. A genetic survey study reported that an overall risk of IS in first-degree relatives was up to 11%, as compared to 2.4 and 1.4% in second- and third-degree relatives, respectively. These studies indicate that IS is an inheritable complex disease. Molecular studies found that some critical regions on chromosomes were potentially important for the occurrence of scoliosis [5, 6]. Genome-wide association studies of AIS in case-control cohorts also located candidate susceptibility genes, and these findings indicate that single nucleotide polymorphisms are valuable for the AIS prognosis [7]. However, inconsistent outcomes were observed among studies concerning the candidate genes in AIS [8–11]. Totally, the inheritance mode and pathogenic gene of AIS is uncertain until today.

Recent technological advances reveal that a major portion of the genome is being transcribed and that protein-coding sequences only account for a minority of cellular transcriptional output. MicroRNAs are endogenously expressed noncoding transcripts, shorter than 20 nucleotides. MicroRNA silences gene expression by targeting specific mRNAs on the basis of sequence recognition [12]. Long noncoding RNAs (lncRNAs) are transcripts longer than 100 nucleotides. lncRNAs in most cases mirror the features of protein-coding

Table 1: Detailed information of the four pairs of participants.

Number	Group	Sex	Height	Age (years)	Illness history (years)	Menarche	Classification	Cobb angle (°)	Risser sign
A1	AIS	F	155	13.7	1	N	PUMCIIc2	50	0
A2	AIS	F	167	15.9	2	Y	PUMCIIc2	40	4
A3	AIS	F	158	15.0	1	Y	PUMCIb	44	5
A4	AIS	F	159	14.2	3	Y	PUMCIIc1	44	3
N1	NC	F	163	17.9	0	Y	—	0	5
N2	NC	F	163	13.2	0	Y	—	0	3
N3	NC	F	158	12.3	0	N	—	0	0
N4	NC	F	170	15.5	0	Y	—	0	4

genes except that the former does not contain a functional open reading frame. A handful of studies have implicated that lncRNAs are involved in a variety of disease states [13] and altered lncRNA levels can result in aberrant expression of gene products that may contribute to many biological processes and human diseases [14–16]. Circulating levels of lncRNAs were reported to reflect local pathophysiological conditions [17, 18]. Expression level of RNA in peripheral blood has been used to evaluate local circumstance of spine [19, 20]. However, the expression of lncRNAs and their functions in AIS are still unknown.

In the present study, we measured lncRNAs expression in AIS patients using microarray and quantitative PCR (qPCR) analysis. Our results disclosed lncRNAs expression profiles and provide new information for further exploration of pathogenesis and prognosis of AIS.

2. Materials and Methods

2.1. Patients. Written informed consent was obtained from all participants. The study was approved by the Institutional Review Board of Chinese Academy of Medical Sciences and Peking Union Medical College Hospital. One hundred and twenty AIS patients (AIS) and twenty normal children (NC) were included in the study. Of these participants, four AIS patients and four children were used for microarray analysis. No significant difference was found between two groups in age, menarche, and Risser sign. Detailed information of the four pairs of participants is summarized in Table 1. The diagnosis of AIS was made only when other causes of scoliosis, including vertebral malformation, neuromuscular disorder, and syndromic disorders, were ruled out. Participants were screened with Adams' forward bend test. Cobb angle measured with a scoliometer was at least 10° [21]. Peripheral blood from each subject was added 3 times volume of Trizol LS reagent (Amboin) and immediately stored at −80°C until use.

2.2. RNA Extraction. Total RNA was extracted using Trizol LS reagent according to the instructions recommended by the manufacturer. The RNA purity and concentration were evaluated with NanoDrop ND-1000 spectrophotometer. RNA integrity was determined with 1% formaldehyde denaturing gel electrophoresis, which revealed a good quality (data not shown).

2.3. RNA Labeling and Hybridization. Double-stranded cDNAs (containing T7 RNA polymerase promoter sequence) were synthesized from 1 mg total RNA according to the manufacturer's instructions (Capitalbio) and labeled with a fluorescent dye (Cy3-dCTP). Labeled cDNA was denatured at 95°C for 3 min in hybridization solution. Agilent human lncRNA + mRNA Array V3.0 was hybridized in an Agilent Hybridization Oven overnight at 42°C and washed with two consecutive solutions (0.2% SDS, 2x SSC for 5 min at 42°C, and 0.2x SSC for 5 min at room temperature).

2.4. Microarray Analysis. The data from lncRNA + mRNA Array were used to analyze data summarization, normalization, and quality control using the GeneSpring software V11.5 (Agilent). The differentially expressed genes were selected if the change of threshold values was ≥ 2 or ≤ -2 folds and if Benjamini-Hochberg corrected P values were <0.05. The data was normalized and hierarchically clustered with CLUSTER 3.0 software. The data were performed to be Tree Visualization with Java Treeview software (Stanford University School of Medicine, Stanford, CA, USA).

2.5. Construction of the Coding-Non-Coding Gene Coexpression (CNC) Network. The CNC network was constructed based on the correlation analysis between the differentially expressed lncRNAs and mRNAs. LncRNAs and mRNAs with Pearson correlation coefficients not less than 0.99 were selected to draw the network using open source bioinformatics software Cytoscape (Institute of Systems Biology in Seattle). In network analysis, red nodes represent the upregulated lncRNAs, dark blue nodes represent the downregulated lncRNAs, pink nodes represent the upregulated mRNAs and light blue nodes represent the downregulated mRNAs, circular nodes represent mRNAs, triangular nodes represent lncRNAs, dashed lines represent a positive correlation, and solid lines represent an inverse correlation.

2.6. qPCR. qPCR was performed using SYBR Premix Ex Taq on Thermal Cycler Dice TP800 instrument. Four lncRNAs (ENST00000440778.1, ENST00000602322.1, ENST00000414894.1, and TCONS_00028768), which revealed differentially expression, were evaluated in all participants. Total RNA (2 μg) was reversely transcribed into cDNA using a PrimeScript RT reagent kit containing a gDNA Eraser (TaKaRa) according to the manufacturer's instructions. PCR

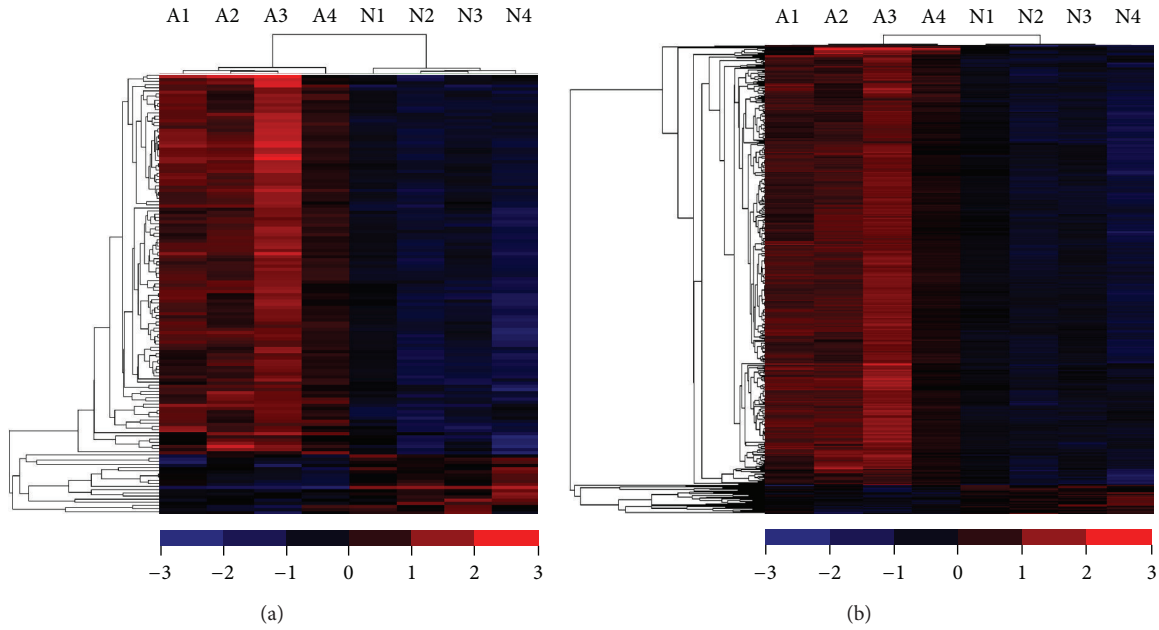

Figure 1: Heat maps of expression ratios (log2 scale) of lncRNAs (a) and mRNAs (b) between AIS patients and normal control. "Red" denotes high relative expression and "blue" denotes low relative expression.

Table 2: Primers used for qPCR.

lncRNAs	Sense primer (5′-3′)	Antisense primer (5′-3′)	Product (bp)
ENST00000602322.1	accttcccacctaccagtct	ctggggaaaccaccatagctt	150
ENST00000440778.1	acttggttgcttttccccaca	gctttgggcttggaaagatgg	107
ENST00000414894.1	agccgccctattcagttcac	tccaagttccgagttgtggg	148
TCONS_00028768	gcaaacctggaaatctcggc	ggccgcagacatcatcttct	142
GAPDH	ctataaattgagcccgcagcc	gcgcccaatacgaccaaatc	154

was performed in 20 μL of reaction system, including 10 μL SYBR Premix Ex Taq (2x), 0.4 μL of PCR forward primer (10 μM), 0.4 μL of PCR reverse primer (10 μM), 1 μL of cDNA, and 8.2 μL of double-distilled water. Primers for lncRNAs and mRNA are listed in Table 2. All experiments were performed in triplicates. All samples were normalized to GAPDH. The median in each triplicate was used to calculate relative lncRNAs concentrations (ΔCt = Ct median lncRNAs-Ct median GAPDH). Folds change was calculated using $2^{-\Delta\Delta Ct}$ methods. The differences of lncRNAs expression between patients and control were analyzed using Student's t-test within SPSS (version 16.0 SPSS Inc.). A value of $P < 0.05$ was considered as statistically significant.

3. Results

3.1. LncRNAs Profiles. Tens of thousands lncRNAs were examined in microarray. A total of 139 lncRNAs revealed significantly different expression in AIS group, compared to NC group (≥2-fold) (Table S1, see Supplementary Material available online at http://dx.doi.org/10.1155/2015/276049). Compared to NC group, a total of 118 lncRNAs were consistently upregulated or downregulated in all tested AIS samples. ENST00000440778.1 was the most significantly downregulated lncRNA (fold change = 9.780566), while NR_024075 (Log2 fold change = 3.8194413) was the most significantly upregulated one. The heat maps of the expression ratios of lncRNAs are shown in Figure 1(a).

3.2. mRNAs Profiles. The expression of coding transcripts (i.e., mRNAs) was examined with microarray containing 33,982 coding transcripts probes. Up to 546 mRNAs showed significant difference between AIS and NC groups (Table S2). A total of 512 mRNAs were upregulated in AIS, while 34 mRNAs were downregulated. The heat map of the expression ratios of mRNAs is shown in Figure 1(b). GO analysis showed that these mRNAs might be involved in bone mineralization, neuromuscular junction, skeletal system morphogenesis, and nucleotide and nucleic acid metabolism. Pathway analysis indicates that the dysregulated mRNAs are involved in cell adhesion molecules, Wnt signaling pathway, Toll-like receptor signaling pathway, MAPK signaling pathway, and so on. Coding RNAs related to major biological processes are listed in Table 3. These results support the viewpoint that AIS may be a genetic disease involving musculoskeletal system.

Table 3: Genes biological processes.

Biological processes	Gene symbol	Gene name	Entrez gene ID	Fold changes
Nervous system development	LTA	"Phosphoinositide-3-kinase, catalytic, delta polypeptide"	5293	2.1513674
	TP53	Tumor protein p53	7157	2.0308032
	MSH2	"mutS homolog 2, colon cancer, nonpolyposis type 1 (E. coli)"	4436	2.0266845
	BCL2	BCL2-associated athanogene 3	9531	2.130905
	TP53	Tumor protein p53	7157	2.0308032
	NCL	Nuclear RNA export factor 1	10482	2.00108
	PAFAH1B1	"Platelet-activating factor acetylhydrolase 1b, regulatory subunit 1 (45 kDa)"	5048	2.1079702
	OLIG1	Oligodendrocyte transcription factor 1	116448	2.129439
	PKD1	Polycystic kidney disease 1 (autosomal dominant)		2.18849
	BTG2	"BTG family, member 2"	7832	2.7636645
Skeletal morphogenesis and development	BCL2	B-Cell CLL/lymphoma 2	596	2.252202
	IL6ST	"Interleukin 6 signal transducer (gp130, oncostatin M receptor)"	3572	2.2222419
	MYC	v-myc myelocytomatosis viral oncogene homolog (avian)	4609	2.768515
	TPP1	Tripeptidyl peptidase I	1200	2.0187664
	AES	Aminoterminal enhancer of split	166	2.2728803
	ALOX15	Arachidonate 15-lipoxygenase	246	2.1062436
Muscle development and function	BCL2	B-Cell CLL/lymphoma 2	596	2.252202
	FLI1	Friend leukemia virus integration 1	2313	2.2254617
	UTRN	Utrophin	7402	2.1682687
	UTS2	Urotensin 2	10911	2.469184
	HIF1A	"Hypoxia inducible factor 1, alpha subunit (basic helix-loop-helix transcription factor)"	3091	2.028285
	TGFBR2	"Transforming growth factor, beta receptor II (70/80 kDa)"	7048	2.1115046
	TTN	Titin	7273	2.7300012
	LEF1	Lymphoid enhancer-binding factor 1	51176	3.1550286
	HIF1A	"Hypoxia inducible factor 1, alpha subunit (basic helix-loop-helix transcription factor)"	3091	2.028285
	FAM65B	"Family with sequence similarity 65, member B"	9750	2.247876
	UTRN	Utrophin	7402	2.1682687
Notch signaling pathway	ADAM17	ADAM metallopeptidase domain 17	6868	2.0420005
	NOTCH2	Notch 2	4853	2.1405845
	CTBP1	C-Terminal binding protein 1	1487	2.050679
MAPK signaling pathway	TAB2	TGF-beta activated kinase 1/MAP3K7 binding protein 2	23118	2.1040483
	SOS1	Son of sevenless homolog 1 (Drosophila)	6654	2.0901704
	DUSP16	Dual specificity phosphatase 16	80824	2.1876025
	MAP3K1	Mitogen-activated protein kinase kinase kinase 1	4214	2.343032
	RPS6KA3	"Ribosomal protein S6 kinase, 90 kDa, polypeptide 3"	6197	2.0745454
	CD14	CD14 molecule	929	2.3363564
	DUSP6	Dual specificity phosphatase 6	1848	2.2230558
	ARRB1	"Arrestin, beta 1"	408	2.004528
	TGFBR2	"Transforming growth factor, beta receptor II (70/80 kDa)"	7048	2.1115046
	AKT3	"v-akt murine thymoma viral oncogene homolog 3 (protein kinase B, gamma)"	10000	2.0013347
	MYC	v-myc myelocytomatosis viral oncogene homolog (avian)	4609	2.768515
	TP53	Tumor protein p53	7157	2.0308032
	NFKB1	Nuclear factor of kappa light polypeptide gene enhancer in B-cells 1	4790	2.0809784

Table 3: Continued.

Biological processes	Gene symbol	Gene name	Entrez gene ID	Fold changes
Wnt signaling pathway	CAMK2G	Calcium/calmodulin-dependent protein kinase II gamma	818	2.1046312
	TCF7	"Transcription factor 7 (T-cell specific, HMG-box)"	6932	2.6018746
	PPARD	Peroxisome proliferator-activated receptor delta	5467	2.1376982
	TCF3	"Transcription factor 7 (T-cell specific, HMG-box)"	6932	2.8202255
	CAMK2D	Calcium/calmodulin-dependent protein kinase II delta	817	2.5258021
	PLCB2	"Phospholipase C, beta 2"	5330	2.2920265
	NFATC1	"Nuclear factor of activated T-cells, cytoplasmic, calcineurin-dependent 1"	4772	2.0340881
	MYC	v-myc myelocytomatosis viral oncogene homolog (avian)	4609	2.768515
	TP53	Tumor protein p53	7157	2.0308032
	LEF1	Lymphoid enhancer-binding factor 1	51176	3.1550286
	CTBP1	C-Terminal binding protein 1	1487	2.050679
	PIAS4	"Protein inhibitor of activated STAT, 4"	51588	2.0654333
	AES	Aminoterminal enhancer of split	166	2.2728803
	INVS	Inversin	27130	2.2433844
	LRRFIP2	Leucine rich repeat (in FLII) interacting protein 2	9209	2.1049194

Gene Ontology and Pathway analysis was performed for differentially expressed mRNAs. mRNAs involving musculoskeletal development are listed in their gene groups with associated Entrez Gene ID and fold changes per gene.

Table 4: Correlation between lncRNAs and mRNAs.

Source[a]	lncRNA	mRNA	Gene symbol	Correlation	*P* value	*cis*-Regulation[b]
p33784	uc002ddj.1	A_21_P0011418	PKD1	0.9967847	$8.29E-08$	Sense
p33788	uc021tnw.1	A_24_P282108	ZZEF1	0.9976724	$3.15E-08$	Sense
p26337	uc021zdc.1	A_23_P122615	PNISR	0.9907335	$1.98E-06$	Sense
p26595	HIT000067310	A_23_P391275	RCAN3	0.9967367	$8.67E-08$	Intergenic
p112	ENST00000577528.1	A_23_P391275	RCAN3	0.9965706	$1.01E-07$	Intergenic
p2444	ENST00000602322.1	A_33_P3210139	PCF11	0.9932224	$7.74E-07$	Antisense
p26595	HIT000067310	A_23_P35205	RCAN3	0.9900216	$2.47E-06$	Sense
p29552	TCONS_00001429	A_23_P35205	RCAN3	0.9956033	$2.12E-07$	Antisense

[a]Probe name of lncRNA. [b]sense: the lncRNAs is a coding transcript exon on the same genomic strand; antisense: the lncRNA is transcribed from the antisense strand; intergenic: there are no overlapping or bidirectional coding transcripts nearby the lncRNA within 10 kbp.

3.3. CNC Network. In the CNC network, there were 76 lncRNAs and 370 mRNAs. A total of 446 network nodes were gained and this was associated with 1121 pairs of coexpression of lncRNAs and mRNAs. The CNC network indicates that one mRNA is correlated with one to tens of lncRNAs and *vice versa*. The whole CNC network might implicate an interregulation between lncRNAs and coding RNAs in AIS. In particular, lncRNA ENST00000602322.1 was correlated with lncRNA ENST00000422231.2 and nine coding RNAs (Figure 2).

More and more evidences indicate that lncRNAs play important roles in gene expression. Thus, we explored the correlation between lncRNAs and mRNA. More than 1000 pairs of lncRNAs and mRNAs reached an absolute correlation coefficient greater than 0.99 and a False Discovery Rate less than 0.01. Target prediction indicated that seven lncRNAs (uc002ddj.1, uc021tnw, uc021zdc.1, HIT000067310, ENST00000577528.1, ENST00000602322.1, and TCONS_00001429) may influence the expression of related mRNAs. ENST00000602322.1 and HIT000067310 may regulate the mRNA expression of PCF11 and RCAN3, respectively. The two mRNAs are expressed in muscle system and encode proteins which regulate mRNA splicing and metabolism. These lncRNAs and mRNAs may play a role in the pathogenesis of AIS. Detailed information of lncRNAs and predicted mRNAs is listed in Table 4.

3.4. LncRNA Classification and Subgroup Analysis. Recently, some special classes or 14 clusters of lncRNAs have been identified with specific function in human cells. Numerous lncRNAs were found to be transcribed from the human homeobox transcription factors (HOX) clusters [22]. These lncRNAs are expressed in temporal and site-specific fashions and may be associated with distinct and diverse biological processes [23, 24], such as cell proliferation, RNA binding complexes, and muscle development. In the present study, our microarray probes targeted 407 discrete transcribed regions of four human HOX loci. None of them was differentially expressed between AIS and NC.

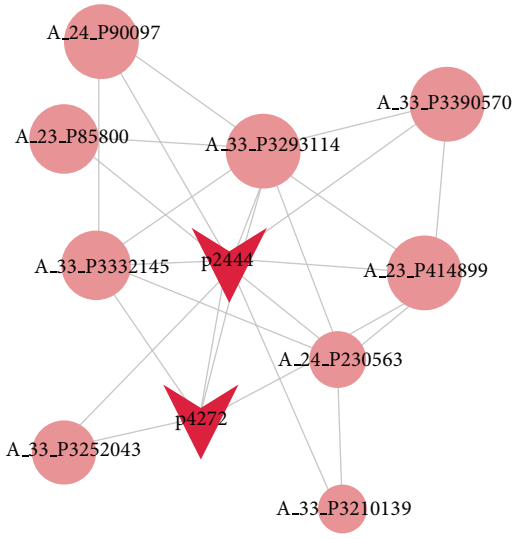

Figure 2: CNC network of lncRNA ENST00000602322.1 (labeled as p2444). Circular nodes represent mRNA; triangular nodes represent lncRNA. Detailed information of lncRNAs and mRNAs is listed in supplementary tables.

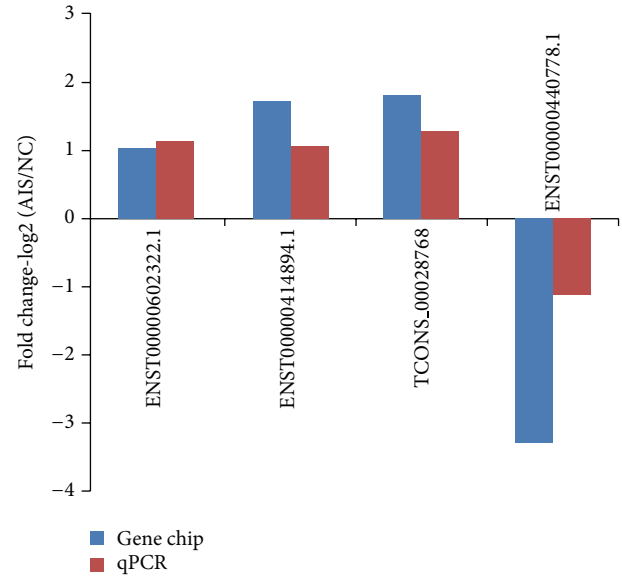

Figure 3: Comparison between microarray and qPCR results. The columns heights represent the log-transformed median fold changes (AIS/NC) in the AIS patients compared to normal control. The validation results of the four lncRNAs indicate that the microarray results match well the qPCR results.

Harrow and his colleagues defined a set of lncRNAs with enhancer-like function in human cell lines [25]. Depletion of these lncRNAs led to decreased expression of their neighboring protein-coding genes. In the present study, 1896 lncRNAs with enhancer-like function were detected while 4 of them were differentially expressed in AIS. The differentially expressed enhancer-like lncRNAs and their nearby coding genes (distance, 300 kb) are shown in Table S3.

3.5. qPCR Validation. Data from microarray were validated by qPCR in twenty pairs of samples. qPCR results revealed that ENST00000602322.1, ENST00000414894.1, and TCONS_00028768 were upregulated and ENST00000440778.1 was downregulated in AIS samples ($P < 0.01$), as compared to the control, which was consistent with those from microarray analysis (Figure 3).

3.6. Clinical Features of Validated lncRNAs. The correlation of lncRNA expression with clinical features was further analyzed. All 120 AIS patients were grouped according to age, height, menarche, classification, severity of scoliosis (measured by Cobb angle), and Risser grade (Table 5). No significant difference of lncRNAs expression was observed when patients were grouped according to menarche. The expression of ENST00000440778.1 and TCONS_00028768 was significantly different when grouped according to height ($P < 0.05$). The expression of ENST00000602322.1 was higher in younger patients ($P < 0.01$). Significant difference was also observed in ENST00000602322.1 expression between patients with single curve and double curves ($P < 0.05$). Lower expression of ENST00000414894.1 was observed in patients with Cobb angle greater than 40° ($P < 0.05$). The expression of ENST00000440778.1 was higher in patients with Risser grade ≤3 ($P < 0.05$).

4. Discussion

Although many clinical, epidemiological, and basic science researches were performed, the etiopathogenesis of AIS is still unclear [26]. Over the past decades, significant achievements have been made in profiling the molecular signatures in diseases using gene expression microarray [27]. Microarray has been recognized as a feasible and useful approach to explore pathogenesis and genetics of diseases and seek specific biomarkers [28]. Recently, hundreds of lncRNAs have been discovered, and altered lncRNAs expression has been considered to be correlated with cancer pathogenesis and muscles differentiation [29, 30]. However, the potential role of lncRNA expression in etiology and pathogenesis of AIS has not been systematically investigated.

To uncover the expression pattern of lncRNAs in AIS, we investigated the lncRNA expression signatures using microarray and found hundreds of differentially expressed lncRNAs in AIS patients. These lncRNAs may be involved in the development and progression of AIS. Based on the previous work and computer analysis, four lncRNAs (ENST00000440778.1, ENST00000602322.1, ENST00000414894.1, and TCONS_00028768) were selected to validate the consistency using qPCR. The expression of ENST00000440778.1 was downregulated in microarray and qPCR. But the expression gap between AIS and normal control was narrower in qPCR than in microarray. The difference may result from selection bias. Samples used in microarray analysis may lack representativeness, and ENST00000440778.1 expression in microarray analysis was not completely coincident between participants. Besides, it is necessary to investigate the specific lncRNAs in bigger size of samples.

Table 5: Expressions of lncRNAs in different clinical features.

Features		ENST00000602322.1	ENST00000440778.1	ENST00000414894.1	TCONS_00028768
Menarche age (y)	≤11	7.29 ± 0.82	4.74 ± 0.88	3.04 ± 0.52	5.51 ± 1.08
	>11	7.75 ± 1.20	5.09 ± 1.25	2.95 ± 0.75	5.62 ± 1.44
Height (cm)	≤160	7.49 ± 1.03	4.40 ± 0.71*	2.98 ± 0.59	5.05 ± 0.99*
	>160	7.73 ± 1.17	5.34 ± 1.45*	2.99 ± 0.78	5.95 ± 1.63*
Onset of AIS (y)	≤12	6.73 ± 0.60**	4.92 ± 1.09	3.09 ± 1.52	5.54 ± 1.19
	>12	7.86 ± 1.29**	5.01 ± 1.17	2.87 ± 1.17	5.63 ± 1.43
Numbers of curves[a]	1	7.09 ± 0.74*	4.95 ± 1.40	2.79 ± 0.66	5.81 ± 1.24
	2	7.98 ± 1.19*	4.98 ± 0.95	3.10 ± 0.66	5.46 ± 1.34
Cobb angle (°)	≤40	7.60 ± 1.36	5.11 ± 1.70	2.47 ± 0.63*	5.59 ± 1.60
	>40	7.58 ± 1.95	4.90 ± 0.72	3.38 ± 0.65*	5.59 ± 1.15
Risser sign[b]	≤3	7.51 ± 1.12	4.33 ± 0.81*	2.93 ± 0.60	5.37 ± 0.97
	>3	7.65 ± 1.07	5.21 ± 1.25*	3.02 ± 0.72	5.76 ± 1.51

Relative lncRNAs levels were normalized to GAPDH (ΔCt = CtlncRNA − CtGAPDH). Results are presented as mean ± standard deviation. $^{*}P < 0.05$, $^{**}P < 0.01$. [a]Curves were counted and classified into single, double, and triple curves according to the apex number. [b]Risser sign refers to the amount of calcification of the human pelvis as a measure of maturity. On a scale of 5, it gives a measurement of ossification progression; the grade of 5 means that skeletal maturity is reached.

In the present study, the differentially expressed mRNAs in AIS patients involve musculoskeletal development processes, including bone mineralization, neuromuscular junction, skeletal system morphogenesis, and nucleotide and nucleic acid metabolism. Pathway analysis indicates that the dysregulated mRNAs are related to cell adhesion molecules, Wnt signaling pathway, Toll-like receptor signaling pathway, MAPK signaling pathway, and so on. Precious studies have revealed the relationship between synapse formation, bone mineralization, and Wnt signaling pathway [31–33]. MAPK signaling pathway was also reported to be related to osteoblast differentiation and intervertebral disc cells degeneration [34, 35]. These biological processes and signaling pathway may play a significant role in the musculoskeletal system and pathogenesis of AIS.

More and more evidences reveal that lncRNAs act in both *cis* and *trans* [36, 37]. LncRNA ENST00000602322.1 locates on chromosome 11q and is adjacent to Pcf11 (Protein 1/Cleavage Factor 1). Pcf11 participates in transcription by coupling pre-mRNA [38]. Pcf11 is also found to play a role in transcription initiation, elongation, and mRNA export from nucleus to cytoplasm [39–41]. Given the key role of Pcf11 in transcription, it may not be surprising that ENST00000602322.1 may relate to the pathogenesis of AIS. The more detailed mechanisms of ENST00000602322.1 in transcription and translation need further investigation.

ENST00000440778.1 was upregulated 9.78-fold in AIS. Its expression was even higher in each AIS patient than that in healthy participants. Little is known about the function of ENST00000440778.1. However, its potential role in AIS pathogenesis was implied not only by its expression change but also by the clinical data from different height and Risser sign.

Our findings demonstrate differential lncRNA expression patterns in AIS when grouped according to different clinical features. This suggests potential significance in treatment and prognosis evaluation. Clinically, classification and curvature angle are important in evaluating surgical treatment and making operation plan in AIS [42, 43]. Onset time and Risser grade also play important roles in evaluating the progression of scoliosis [44]. It has been reported that lncRNAs are more specific than protein-coding mRNAs [45] and are easier to be detected in the blood samples of neoplastic and nonneoplastic patients using conventional PCR method [17, 18]. The differential expression of lncRNAs is potentially valuable in development of specific PCR markers and in providing more support on treatment and prognosis.

Several limitations exist in this study. First, although the different expression patterns of identified lncRNA genes suggest potential function in AIS pathogenesis, direct supporting evidence is lacking. Second, only four pairs of samples were used in microarray analysis. This may lose some important information and decrease the accuracy of biomarker selection. Third, RNA expression in peripheral blood was tested in our study. Regarding the idiopathic scoliosis being a musculoskeletal disease, tissue sample from musculoskeletal system may be more ideal targets. To accurately and comprehensively elucidate the role of lncRNAs in AIS, more comprehensive studies and laboratory and clinical researches are needed.

In summary, to the best of our knowledge, this is the first study that describes the expression profiles of human lncRNAs in AIS using microarray. Altered lncRNAs may play a potential role in the pathogenesis and/or development of this musculoskeletal disease. More work will be needed to confirm whether these lncRNAs play an essential role in the pathogenesis, treatment, and prognosis of AIS.

Conflict of Interests

The authors declare that there is no conflict of interests regarding the publication of this paper.

Authors' Contribution

Xiao-Yang Liu and Liang Wang contributed equally to this work.

Acknowledgment

The work was supported by the National Natural Science Foundation of China under Grant nos. 81171770, 81372007, and 81272054.

References

[1] J. Ogilvie, "Adolescent idiopathic scoliosis and genetic testing," *Current Opinion in Pediatrics*, vol. 22, no. 1, pp. 67–70, 2010.

[2] E. J. Rogala, D. S. Drummond, and J. Gurr, "Scoliosis: incidence and natural history. A prospective epidemiological study," *Journal of Bone and Joint Surgery—Series A*, vol. 60, no. 2, pp. 173–176, 1978.

[3] M. O. Andersen, K. Thomsen, and K. O. Kyvik, "Adolescent idiopathic scoliosis in twins: a population-based survey," *Spine*, vol. 32, no. 8, pp. 927–930, 2007.

[4] C. A. Wise, X. Gao, S. Shoemaker, D. Gordon, and J. A. Herring, "Understanding genetic factors in idiopathic scoliosis, a complex disease of childhood," *Current Genomics*, vol. 9, no. 1, pp. 51–59, 2008.

[5] N. H. Miller, "Genetics of familial idiopathic scoliosis," *Clinical Orthopaedics and Related Research*, vol. 462, pp. 6–10, 2007.

[6] N. H. Miller, C. M. Justice, B. Marosy et al., "Identification of candidate regions for familial idiopathic scoliosis," *Spine*, vol. 30, no. 10, pp. 1181–1187, 2005.

[7] S. Sharma, X. Gao, D. Londono et al., "Genome-wide association studies of adolescent idiopathic scoliosis suggest candidate susceptibility genes," *Human Molecular Genetics*, vol. 20, no. 7, pp. 1456–1466, 2011.

[8] T. Esposito, R. Uccello, R. Caliendo et al., "Estrogen receptor polymorphism, estrogen content and idiopathic scoliosis in human: a possible genetic linkage," *Journal of Steroid Biochemistry and Molecular Biology*, vol. 116, no. 1-2, pp. 56–60, 2009.

[9] J. Wu, Y. Qiu, L. Zhang, Q. Sun, X. Qiu, and Y. He, "Association of estrogen receptor gene polymorphisms with susceptibility to adolescent idiopathic scoliosis," *Spine*, vol. 31, no. 10, pp. 1131–1136, 2006.

[10] Y. Takahashi, M. Matsumoto, T. Karasugi et al., "Lack of association between adolescent idiopathic scoliosis and previously reported single nucleotide polymorphisms in MATN1, MTNR1B, TPH1, and IGF1 in a Japanese population," *Journal of Orthopaedic Research*, vol. 29, no. 7, pp. 1055–1058, 2011.

[11] N. L. S. Tang, H. Y. Yeung, K. M. Lee et al., "A relook into the association of the estrogen receptor α gene (PvuII, XbaI) and adolescent idiopathic scoliosis: a study of 540 Chinese cases," *Spine*, vol. 31, no. 21, pp. 2463–2468, 2006.

[12] R. W. Carthew and E. J. Sontheimer, "Origins and mechanisms of miRNAs and siRNAs," *Cell*, vol. 136, no. 4, pp. 642–655, 2009.

[13] I. I. G. M. van de Vondervoort, P. M. Gordebeke, N. Khoshab et al., "Long non-coding RNAs in neurodevelopmental disorders," *Frontiers in Molecular Neuroscience*, vol. 6, article 53, 2013.

[14] C. A. Klattenhoff, J. C. Scheuermann, L. E. Surface et al., "Braveheart, a long noncoding RNA required for cardiovascular lineage commitment," *Cell*, vol. 152, no. 3, pp. 570–583, 2013.

[15] R. J. Taft, K. C. Pang, T. R. Mercer, M. Dinger, and J. S. Mattick, "Non-coding RNAs: regulators of disease," *Journal of Pathology*, vol. 220, no. 2, pp. 126–139, 2010.

[16] T. Gutschner, M. Hämmerle, M. Eißmann et al., "The noncoding RNA MALAT1 is a critical regulator of the metastasis phenotype of lung cancer cells," *Cancer Research*, vol. 73, no. 3, pp. 1180–1189, 2013.

[17] D. G. Weber, G. Johnen, S. Casjens et al., "Evaluation of long noncoding RNA MALAT1 as a candidate blood-based biomarker for the diagnosis of non-small cell lung cancer," *BMC Research Notes*, vol. 6, no. 1, article 518, 2013.

[18] D. Li, G. Chen, J. Yang et al., "Transcriptome analysis reveals distinct patterns of long noncoding RNAs in heart and plasma of mice with heart failure," *PLoS ONE*, vol. 8, Article ID e77938, 2013.

[19] M. Stuss, P. Rieske, A. Cegłowska et al., "Assessment of OPG/RANK/RANKL gene expression levels in peripheral blood mononuclear cells (PBMC) after treatment with strontium ranelate and ibandronate in patients with postmenopausal osteoporosis," *Journal of Clinical Endocrinology and Metabolism*, vol. 98, no. 5, pp. E1007–E1011, 2013.

[20] R. Nowak, J. Szota, and U. Mazurek, "Vitamin D Receptor gene (VDR) transcripts in bone, cartilage, muscles and blood and microarray analysis of vitamin D responsive genes expression in paravertebral muscles of Juvenile and Adolescent Idiopathic Scoliosis patients," *BMC Musculoskeletal Disorders*, vol. 13, article 259, 2012.

[21] S. L. Weinstein, L. A. Dolan, J. C. Cheng, A. Danielsson, and J. A. Morcuende, "Adolescent idiopathic scoliosis," *The Lancet*, vol. 371, no. 9623, pp. 1527–1537, 2008.

[22] J. L. Rinn, M. Kertesz, J. K. Wang et al., "Functional demarcation of active and silent chromatin domains in human HOX loci by noncoding RNAs," *Cell*, vol. 129, no. 7, pp. 1311–1323, 2007.

[23] M. Guttman, I. Amit, M. Garber et al., "Chromatin signature reveals over a thousand highly conserved large non-coding RNAs in mammals," *Nature*, vol. 458, no. 7235, pp. 223–227, 2009.

[24] A. M. Khalil, M. Guttman, M. Huarte et al., "Many human large intergenic noncoding RNAs associate with chromatin-modifying complexes and affect gene expression," *Proceedings of the National Academy of Sciences of the United States of America*, vol. 106, no. 28, pp. 11667–11672, 2009.

[25] U. A. Ørom, T. Derrien, M. Beringer et al., "Long noncoding RNAs with enhancer-like function in human cells," *Cell*, vol. 143, no. 1, pp. 46–58, 2010.

[26] R. G. Burwell, "Aetiology of idiopathic scoliosis: current concepts," *Pediatric Rehabilitation*, vol. 6, no. 3-4, pp. 137–170, 2003.

[27] Z. Yin, D. Guan, Q. Fan et al., "LncRNA expression signatures in response to enterovirus 71 infection," *Biochemical and Biophysical Research Communications*, vol. 430, no. 2, pp. 629–633, 2013.

[28] F. Yang, L. Zhang, X.-S. Huo et al., "Long noncoding RNA high expression in hepatocellular carcinoma facilitates tumor growth through enhancer of zeste homolog 2 in humans," *Hepatology*, vol. 54, no. 5, pp. 1679–1689, 2011.

[29] F. Yang, L. Zhang, X.-S. Huo et al., "Long noncoding RNA high expression in hepatocellular carcinoma facilitates tumor growth through enhancer of zeste homolog 2 in humans," *Hepatology*, vol. 54, no. 5, pp. 1679–1689, 2011.

[30] M. Cesana, D. Cacchiarelli, I. Legnini et al., "A long noncoding RNA controls muscle differentiation by functioning as a competing endogenous RNA," *Cell*, vol. 147, pp. 358–369, 2011.

[31] R. Velázquez-Cruz, H. García-Ortiz, M. Castillejos-López et al., "WNT3A gene polymorphisms are associated with bone mineral density variation in postmenopausal mestizo women of an urban Mexican population: findings of a pathway-based high-density single nucleotide screening," *Age*, vol. 36, article 9635, 2014.

[32] T. Nagaoka, R. Ohashi, A. Inutsuka et al., "The Wnt/planar cell polarity pathway component Vangl2 induces synapse formation through direct control of N-cadherin," *Cell Reports*, vol. 6, pp. 916–927, 2014.

[33] J. N. Collins, B. J. Kirby, J. P. Woodrow et al., "Lactating Ctcgrp nulls lose twice the normal bone mineral content due to fewer osteoblasts and more osteoclasts, whereas bone mass is fully restored after weaning in association with up-regulation of Wnt signaling and other novel genes," *Endocrinology*, vol. 154, no. 4, pp. 1400–1413, 2013.

[34] Y. Liu, W.-K. Zheng, W.-S. Gao, Y. Shen, and W.-Y. Ding, "Function of TGF-beta and p38 MAKP signaling pathway in osteoblast differentiation from rat adipose-derived stem cells," *European Review for Medical and Pharmacological Sciences*, vol. 17, no. 12, pp. 1611–1619, 2013.

[35] C.-C. Niu, S.-S. Lin, L.-J. Yuan et al., "Hyperbaric oxygen treatment suppresses MAPK signaling and mitochondrial apoptotic pathway in degenerated human intervertebral disc cells," *Journal of Orthopaedic Research*, vol. 31, no. 2, pp. 204–209, 2013.

[36] K. Plath, S. Mlynarczyk-Evans, D. A. Nusinow, and B. Panning, "Xist RNA and the mechanism of X chromosome inactivation," *Annual Review of Genetics*, vol. 36, pp. 233–278, 2002.

[37] M. V. Koerner, F. M. Pauler, R. Huang, and D. P. Barlow, "The function of non-coding RNAs in genomic imprinting," *Development*, vol. 136, no. 11, pp. 1771–1783, 2009.

[38] Z. Zhang and D. S. Gilmour, "Pcf11 is a termination factor in Drosophila that dismantles the elongation complex by bridging the CTD of RNA polymerase II to the nascent transcript," *Molecular Cell*, vol. 21, no. 1, pp. 65–74, 2006.

[39] T. J. Loya, T. W. O'Rourke, and D. Reines, "A genetic screen for terminator function in yeast identifies a role for a new functional domain in termination factor Nab3," *Nucleic Acids Research*, vol. 40, no. 15, pp. 7476–7491, 2012.

[40] M. Rougemaille, G. Dieppois, E. Kisseleva-Romanova et al., "THO/Sub2p Functions to Coordinate 3′-End Processing with Gene-Nuclear Pore Association," *Cell*, vol. 135, no. 2, pp. 308–321, 2008.

[41] Z. Zhang, A. Klatt, A. J. Henderson, and D. S. Gilmour, "Transcription termination factor Pcf11 limits the processivity of Pol II on an HIV provirus to repress gene expression," *Genes & Development*, vol. 21, no. 13, pp. 1609–1614, 2007.

[42] J. S. Hoashi, P. J. Cahill, J. T. Bennett, and A. F. Samdani, "Adolescent scoliosis classification and treatment," *Neurosurgery Clinics of North America*, vol. 24, no. 2, pp. 173–183, 2013.

[43] G. Qiu, J. Zhang, Y. Wang et al., "A new operative classification of idiopathic scoliosis: a Peking Union Medical College method," *Spine*, vol. 30, no. 12, pp. 1419–1426, 2005.

[44] Y. Smorgick, Y. Mirovsky, K. C. Baker, Y. Gelfer, E. Avisar, and Y. Anekstein, "Predictors of back pain in adolescent idiopathic scoliosis surgical candidates," *Journal of Pediatric Orthopaedics*, vol. 33, no. 3, pp. 289–292, 2013.

[45] J. R. Prensner, M. K. Iyer, O. A. Balbin et al., "Transcriptome sequencing across a prostate cancer cohort identifies PCAT-1, an unannotated lincRNA implicated in disease progression," *Nature Biotechnology*, vol. 29, no. 8, pp. 742–749, 2011.

Hindawi Publishing Corporation
BioMed Research International
Volume 2015, Article ID 727542, 14 pages
http://dx.doi.org/10.1155/2015/727542

Review Article

Molecular Biomarkers for Embryonic and Adult Neural Stem Cell and Neurogenesis

Juan Zhang[1,2] and Jianwei Jiao[1,3]

[1]*State Key Laboratory of Reproductive Biology, Institute of Zoology, Chinese Academy of Sciences, 1 Beichen West Road, Chaoyang District, Beijing 100101, China*
[2]*University of Chinese Academy of Sciences, No. 80 Zhongguancun East Road, Chaoyang District, Beijing 100190, China*
[3]*Group of Neural Stem Cell and Neurogenesis, Institute of Zoology, Chinese Academy of Sciences, 1 Beichen West Road, Chaoyang District, Beijing 100101, China*

Correspondence should be addressed to Jianwei Jiao; jwjiao@ioz.ac.cn

Received 27 June 2014; Accepted 19 November 2014

Academic Editor: Giovanni Scapagnini

The procedure of neurogenesis has made numerous achievements in the past decades, during which various molecular biomarkers have been emerging and have been broadly utilized for the investigation of embryonic and adult neural stem cell (NSC). Nevertheless, there is not a consistent and systematic illustration to depict the functional characteristics of the specific markers expressed in distinct cell types during the different stages of neurogenesis. Here we gathered and generalized a series of NSC biomarkers emerging during the procedures of embryonic and adult neural stem cell, which may be used to identify the subpopulation cells with distinguishing characters in different timeframes of neurogenesis. The identifications of cell patterns will provide applications to the detailed investigations of diverse developmental cell stages and the extents of cell differentiation, which will facilitate the tracing of cell time-course and fate determination of specific cell types and promote the further and literal discoveries of embryonic and adult neurogenesis. Meanwhile, via the utilization of comprehensive applications under the aiding of the systematic knowledge framework, researchers may broaden their insights into the derivation and establishment of novel technologies to analyze the more detailed process of embryogenesis and adult neurogenesis.

1. Introduction

Neural stem cells (NSCs) acting as a source of various cell types are a subpopulation of cells that can self-renewal and proliferate identical cells. They are multipotent to generate diversity neural lineages, encompassing neurons, astrocytes, and oligodendrocytes [1]. NSCs serving as an origin of neurons and glia throughout life were one of the milestone events of the past twenty-five years in the neuroscience research field [2], which is quite meaningful to the investigator majoring in the study of NSCs. NSCs with the plasticity to give rise to new neurons and glia play a crucial role in the embryogenesis and adult neurogenesis [3, 4].

The elemental discrimination between embryonic and adult neural stem cells is that the process of adult NSC is not orchestrated and massively paralleled progression as that in the embryonic developmental stages because such stages can occur at any time point [5].

NSCs, a headspring of progenitor cells in the central nervous system (CNS), are born with proliferation capacity of self-renewal and generation of both neurons and glia through a multistep process [6]. During the process of adult neurogenesis, NSCs in the germinal regions undergo numerous stages, including NSCs self-renewal, transient amplifying progenitors, neuroblasts, and terminally mature neurons, astrocytes, and oligodendrocytes [2, 5, 7].

With the various technologies development, a quiet number of molecular biomarkers have been emerging like mushrooms after rain, which will favor the further research in the neuroscience field. However, there is not a systematic framework to illustrate the specific markers' detailed characters and functions. And our summary is tempting to provide

such a commentary on these particular cell types for the best use of these powerful cells.

2. Molecular Biomarkers during Embryogenesis

During the embryogenesis, there are two crucial proliferative zones: ventricular zone (VZ) and subventricular zone (SVZ), which are the springheads of cortical neurons and glia cells [8]. NSCs locate at the VZ of the neural tube and produce all sorts of cell types necessary for the construction of the CNS [9]. The process of embryogenesis can be overviewed in Figure 1.

NSCs in the VZ divide symmetrically and asymmetrically to preserve the stem cell pool and generate progenitor cells, which subsequently migrate to SVZ and then perform the capability of proliferation or differentiation [10]. The SVZ may function as a peculiar zone that instructs the late-born neurons to establish the upper layers and terminally construct the neocortex [11].

The embryogenesis originates from the neural plate which is composed of neuroepithelial cells (NECs). Initially, the NECs divide symmetrically to amplify their own cohorts which are identified as the earliest form of embryonic NSCs [12, 13]. And, after the formation of neural tube, NECs convert to radial glial cells, which locate the soma at the VZ and stretch the long radial fiber out of the neural tube internal surface to the outer (pial) surface [9]. On the one hand, the especial radial glial cells function as a scaffold to guide the migration of neuron. On the other hand, the characterized glial cells present the properties of embryonic NSCs. During this stage, radial glial cells accomplish a process of self-renewal (a newborn radial glial cell) and generate one neuron (or a neuronal progenitor) from each asymmetrical division. Later, radial-glia cells differentiate into ependymal cells forming the neural tube of internal lining, and neurons migrate to the further layers along the radial filaments [14]. At the late stage of embryogenesis, radial glial cells will proliferate to produce oligodendrocytes and eventually astrocytes after the accomplishing of neuron formation. Closing to the date of birth, the radial glial cells change the characteristics to generate NSCs serving as a pool of adult neurogenesis and embryogenesis processes throughout life that can be found at Molecular Biomarkers during Adult Neurogenesis [12, 13].

Given the general frame of embryogenesis, we provide a subsection of this process to get a detailed understanding. The mouse cerebral neocortex can be factitiously partitioned into 6 layers horizontally, each of which contains a specific subpopulation of cells distinguished by singular or multiple markers identifying the characteristics functionally and molecularly [15]. Each layer is composed of pyramidal (glutamatergic excitatory projection) neurons and interneurons (GABAergic inhibitory interneurons). The newborn cortical neurons initially emerge at the mouse gestation of about embryonic day 10.5 (E10.5) and then form the preplate (PP), a cohort of cells located at the surface part (SP) of the cortical mantle.

And at E11.5, the cortical projection neurons present firstly in PP layer and migrate to establish the seminal cortical plate (CP), which whereafter progress to form L2–L6 layers. Before the program of embryonic neurogenesis being launched, the neural progenitor cells (NPCs) in VZ divide symmetrically to amplify the neural progenitor pool. At around E11.5, NPCs get down to divide asymmetrically for self-renewal and to produce neurons which will subsequently migrate to mantle layers (MZ) along the scaffold acted by radial-glia cells (RGCs).

The projection neurons formed at the initial stage locate at the PP and build the nascent CP, which will thenceforth convert into the neocortex L2–6. The increasing CP neurons subsequently crack the PP into SP and MZ. With the neurogenesis progressing, many projection neurons are created in sequence through the continuous asymmetric divisions of NPCs. Gathered together, neurons residing in SP are formed firstly, then those locating at deep layers, and at last those locating at the upper layers (L4, 3, and 2).

The formation of neocortex composed by neurons starts with deep layers; then the newborn neurons will migrate across the older ones to build upper layers. A part of daughter cells of NPCs transform into the IPCs, which will migrate away from VZ and go through symmetric divisions in SVZ, contributing to upper-layer neurons. At around E17.5, closing to the end of neurogenesis, the NPCs convert into gliogenesis, which produce cortical and subependymal zone (SEZ) astrocytes and form the layer of ependymal cells (EL) layer.

During the procedure of embryogenesis, different cell lineages generate different cell types in the different time-courses. And the specific cell types show exclusive cell surface proteins which can be applied to discriminate the particular cell type in specific stage from the NSCs pool. According to the characters above, various cell surface proteins can function as cell markers. And abundant biomarkers have been reported to identify the different cell lineages and different time-courses. Here, we listed the major ones for an illustration.

2.1. Emx2. Emx2, empty spiracles homolog 2, belongs to a homeobox-containing gene [18]. It is a transcription factor participating in the development of mouse cerebral cortex including proliferating neuroblasts originating from the neuroepithelium, VZ, and postmitotic Cajal-Retzius cells. Given the enrichment expression at the outset of corticogenesis, Emx2 is used broadly as a dorsal marker during the corticogenesis [19]. The results of Emx2 null embryos indicated that Emx2 as a transcription factor bears a critical part in regulating the neuroblast proliferation, migration, and differentiation. Moreover, Emx2 is also involved in the molding of the forebrain, the definition of cortical territories, and arealization during neocortical development [20].

2.2. Sox5. Sox5, sex determining region Y-box 5 (Sox5), is a transcription factor belonging to Sox family. It can be detected exclusively in postmitotic neurons of SP and in projection neurons of L6 at high level and in a cohort of L5 projection neurons. And the detectable phenotype persists from E14.5 to P7 (postnatal 7 days). Meanwhile, Sox5 can also

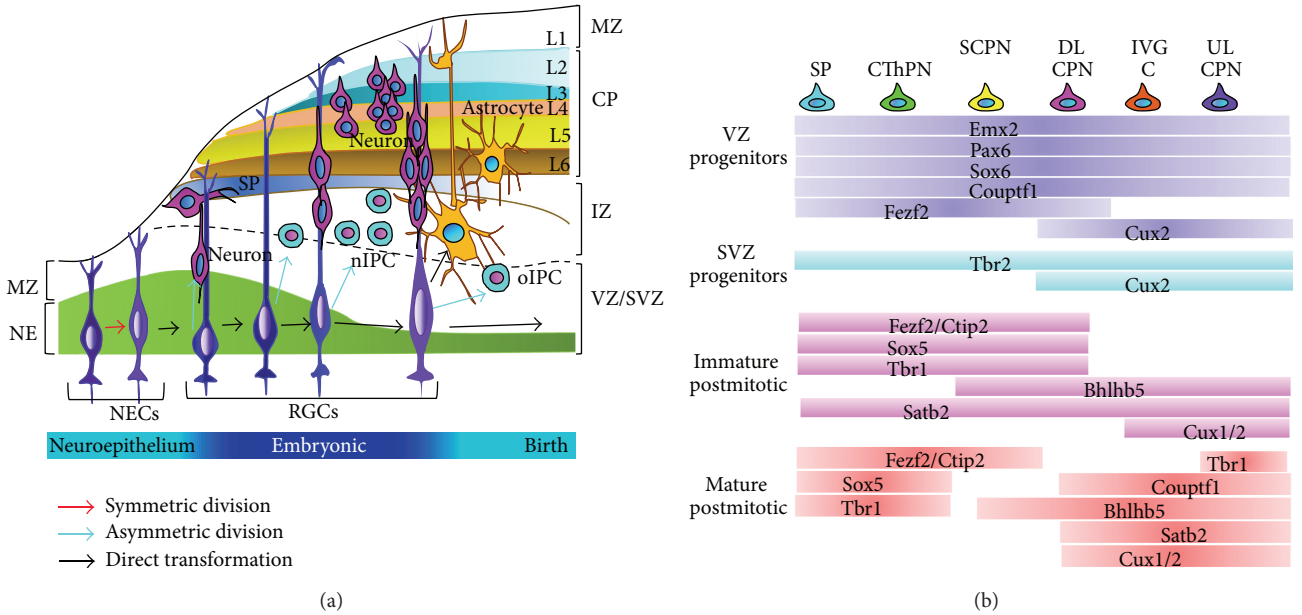

FIGURE 1: The schematic of embryogenesis and the specific markers expressed in specific time-line. (a) The process of embryogenesis. With the beginning of neuroepithelial cells, a series of cell types are produced, including radial glial cells, neurogenic intermediate progenitor cells, oligogenic intermediate progenitor cells, neurons, and astrocytes. (b) The specific markers indicate the specific cell types generated during the process of neurogenesis [16]. CP, cortical plate; DL, deep layer; GC, glial cells; IZ, intermediate zone; L1–6, layers 1–6; MZ, marginal zone; nIPC, neurogenic intermediate progenitor cell; NECs, neuroepithelium cells; oIPC, oligogenic intermediate progenitor cell; UL, upper layer; CPN, callosal projection neurons. RGCs, radial glial cells; SVZ, subventricular zone; SP, subplate; VZ, ventricular zone. CThPN, corticothalamic projection neurons; SCPN, subcerebral projection neurons.

be detected in a few of upper-layer neurons at low levels [21–23].

Otherwise, investigation reported that Sox5 is absent in the progenitor cells residing in VZ and SVZ [23]. In addition, Sox5 is imperative for deep-layer neurons migration across the earlier-born neurons to fix on the more superficial layers. It might manipulate the migration of deep-layer neurons [24].

2.3. Bcl11b. Bcl11b (also called Ctip2), B cell leukemia/lymphoma 11B, is a zinc finger transcription factor, which takes part in the development of L5 subcortical axon and is exclusively expressed in L5 [24, 25].

2.4. Tbr1. Tbr1, T-box brain factor 1, is a transcription factor, which cooperates with Sox5 to regulate early born neurons in multiple lines during the embryonic development. The deletion of Tbr1 inmice indicated that it is necessary for numerous processes in cortical development, such as laminar location, molecular differentiation, and axonal expeditions [26–28]. The research has reported that Tbr1 could be detected at E12.5 in the corticothalamic projection neurons which located in L6 and SP and in MZ Cajal-Retzius neurons, starting from E12.5 [26]. And, in progenitor cells that reside in VZ and SVZ, Tbr1 is not detectable, which may imply the resemblance of Tbr1 to Sox5 in function. And when time-course progresses to the postnatal course, the layer specificity expression of Tbr1 is gradually downregulated but begins to present in several upper-layer neurons [26, 28, 29]. Additionally, Tbr1 is also involved into the regulation of neuronal migration [27].

2.5. Fezf2. Fezf2 (also known as FEZL, ZFP312) belongs to FEZ family zinc finger 2, which also functions as a transcription factor. Fezf2 can be found in L5 cortical spinal (CS) neurons at a high level and plays a pivotal role in the CS tract development. Fezf2 is also found enriching in early progenitors of VZ and in their neuronal progenies which launch into the deep-layer of subcortex. Yet it disappeared in late progenitor cells and upper-layer neurons. Fezf2 is downregulated in L6 neurons during the late embryonic development [27, 28].

2.6. Satb2. Satb2, special AT-rich sequence-binding protein 2 (DNA-binding protein), is a matrix-attachment region interacting transcription factor, which can exclusively conjunct the nuclear matrix-attachment regions and plays a role in regulating the transcription and remodelling chromatin. It regulates the position of laminin and helps to identify the late-born neurons. It enriched the postmitotic neurons of corticocortical L2–L5, which begins to emerge in the E13.5 neurons when these neurons migrate into the IZ (intermediate zone) and will persist postnatally. Yet, in the subcortical projection neurons, it is not expressed [30, 31]. Furthermore, SATB2, as an active transcriptional modulator, regulates a diversity of layer-specific markers for cortical projection neurons. The relative markers are listed as follows: Cdh10, cadherin 10; Cux2, cut-like homeobox 2; Rorb, RAR-related orphan receptor beta [31]. Scientists also reported that Satb2 also regulated the neuron dendritic arborization

in upper layer (Zhang et al., 2011), referring to a wider role during neocortical development [15, 32].

2.7. Cux1/Cux2. Cux1/Cux2, cut-like homeobox 1/2, are upper layer-specific markers for neurons, which participate in the fundamental regulation of the late neuronal differentiation, spine formation, dendritic branching, and synaptogenesis in upper-layer (L2-3) neurons of the cortex [33, 34].

2.8. Pou3f2 and Pou3f3. Pou3f2 (POU class 3 homeobox 2, also called Brn-2) and Pou3f3 (POU class 3 homeobox 3, also called Brn-1) both are the members of the class III POU family transcription factors involved in neural differentiation [35]. POU3F2/POU3F3 is considered to be involved in upper-layer neuronal migration and identification, playing overlapping roles in the regulation of neocortical layers development [36, 37]. Pou3f2 and Pou3f3 emerge in the L2–L5 projection neurons at E14.5 and continue presenting in the progenitor cells which amplify themselves and persist running through the migration and differentiation of postmigratory. Studies reported that the absence of Pou3f2/3 led to reduction of upper layer-specific markers expression but did not affect the expression of markers for neurons in L6 and SP [36–38].

2.9. Pax6. Pax6, paired box 6, plays a pivotal role in the neuronal fate determination and NSCs proliferation. It participates in the neocortex positioning and upper-layer neurons generation via identifying the SVZ progenitor cells [39, 40]. During the late mouse embryonic developmental stage of the cortical SVZ, Pax6 controls the neural progenitor cells proliferation by changing the Sox2 expression [41].

2.10. Nr2f1. Nr2f1 (also known as Coup-tf1), nuclear receptor subfamily 2, group F, member 1, plays a crucial role in the neocortical regionalization. And the late-born neurons migration and the callosal projection neurons (CPNs) differentiation are modulated by Nr2f1 [42, 43].

2.11. Sox1. Sox1 is expressed exclusively in the CNS and probably functions as the earliest marker for neural fate decision of embryonic stem cells. Furthermore, it marks the proliferating progenitors residing in the neural tube [44].

3. Molecular Biomarkers during Adult Neurogenesis

Adult neural stem cells are peculiar cell subpopulations with the character of structural plasticity [17]. In mammals, neurogenesis presents in two germinative regions: SVZ and SGZ throughout life [45]. Currently, various markers expressed at multistep strategies during the progressions of adult hippocampal neurogenesis have been discovered and developed [46, 47], which will be enumerated in the two major procedures of adult neurogenesis. The process of adult neurogenesis can be overviewed in Figure 2.

3.1. Developmental Process of Adult Neurogenesis in the Hippocampus. Radial-glia-like neural stem/precursor cells existing in the SGZ are usually regarded as relatively quiescent but can be activated by internal and external stimulus. They compose a pool of neuroblasts including transit-amplifying and proliferative cells produced by symmetrically and asymmetrically dividing. Only a small bunch of cells in this pool can survive and differentiate into immature neurons. After the postdivision of 7–10 days, cells start to enter a neuronal fate [17, 48].

Radial-glia cells act dual-status during CNS development. On the one hand, they play as neural progenitor cells for neuronal generation and a scaffolding facilitating neuronal migration. And on the other hand, they act as a source of most neurons life-long in the CNS [49, 50].

Adult neurogenesis in the hippocampus germinates from progenitor cells and leads to the birth of granule cell neurons, which goes through approximately six distinct stages experiencing type-1 cells, type-2a cells, type-2b cells, type-3 cells and immature and mature neurons [5].

NSCs can be defined as a cohort that possesses both self-renewal and neurons/glia cells production from a unicell according to their potential capacities [1, 51]. NSCs (defined as type-1 cells) amplify intermediate progenitors (IPs, called as Type-2a cells) which keep expressing the stem/progenitor markers involving Sox2, a transcription factor [52]. And, at latish stage, neuronal determination starts to become obvious, overlapping with the transcription factors expression including Prox1, NeuroD1, and doublecortin (DCX) (type-2b) [53]. These cells produce migratory neuroblasts (classified as Type-3 cells) which amplify but subsequently exit the cell cycle ahead of maturation into granule neurons. Presently, the procedure of adult neurogenesis can be separated into six developmental strategies factitiously according to the currently emerging investigations [5, 54].

Stage 1. Type-1 cells are a group of radial-glia-like neural stem cells with distinct morphology [55], which express astrocytic marker glial fibrillary acidic protein (GFAP) and nestin [56].

Stages 2–4. Type-1 cells assumedly divide asymmetrically generating daughter cells called type-2 cells, which will form subsequently three consistent kinds of putative temporary augmenting progenitor cells, which can be characterized by the proliferation capacities, specific morphology, and their gradually increasing neuronal differentiation [57, 58]. Type-2 cells are GFAP negative and are increasingly capable of proliferation [55, 59]. They enter two subtypes: type-2a, nestin-positive and positive for doublecortin (DCX, an immature neuronal marker); type-2b, nestin and DCX-positive [60]. And type-3 cells, which display the polysialated form of neural cell adhesion molecule (PSA-NCAM), present DCX-positive and nestin-negative features [55, 61]. Meanwhile, the three cell types (type-2a, type-2b, and type-3 cells) share some identical features during the three stages, which are classified into the neuronal lineage and labeled by 5-bromodeoxyuridine (BrdU) [5].

Stage 5. After the three stages above, cells are induced eventually to exodus from the cell cycle and enter an ephemeral postmitotic stage entering the early neuronal development

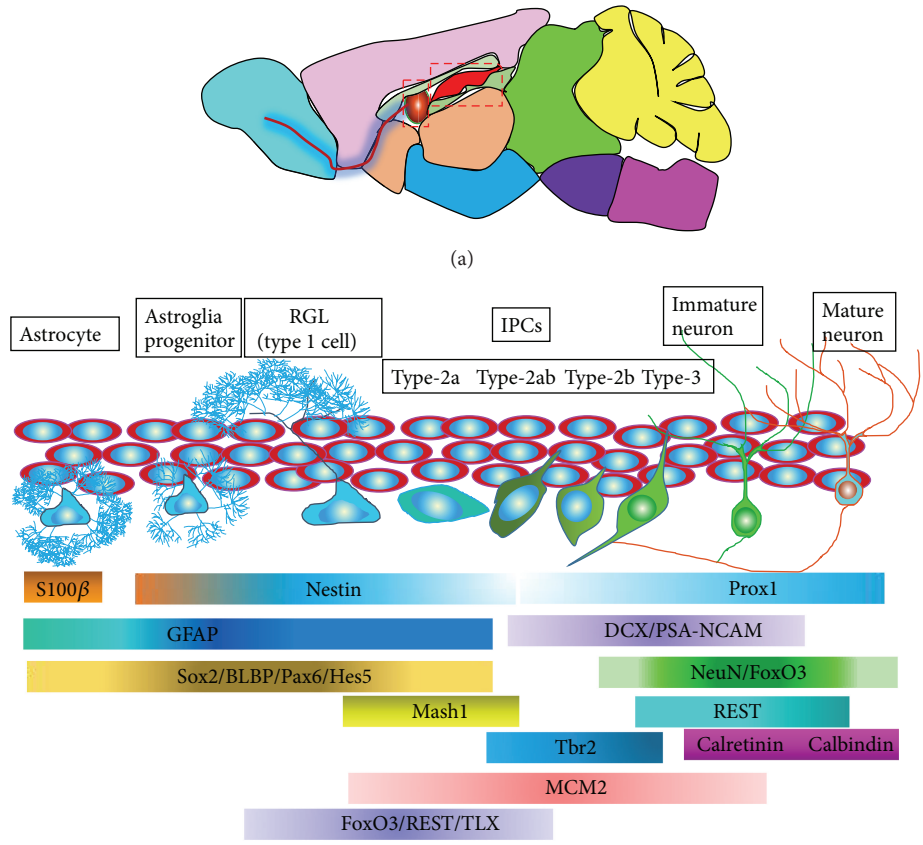

FIGURE 2: The schematic of adult neurogenesis and specific markers for specific cell types in different time-courses. (a) A model of the two major NSCs niches (labeled by the red panes) in the adult brain. (b) The process of adult neurogenesis originates from the active radial glial cells RGCs, (type-1 cells), generating intermediate progenitor cells (IPCs, type-2a, type-2ab, and type-2b cells), subsequently immature neurons, and finally mature neurons. The specific cell types emerging in the certain strategies are traced by various special markers [17]. GCL, granular cell layer; IPCs, intermediate progenitor cells; SGZ, subgranular zone.

and formatting immature neurons which can be marked by DCX, NeuN, and Ca^{2+}-binding protein calretinin [62].

Stage 6. This is the stage of the ultimately mature new granule cells expressing calbindin. Thereabout 2-3 weeks after the postmitotic stage 5, the new cells transform the calretinin-positive cells to calbindin-positive cells [63].

During the process of neurogenesis, a number of diverse biomarkers can be utilized by immunohistochemical means labeling the specific cell types in diverse states. Following statements will delineate the developmental procedures of neurogenesis with the key identifications, accompanied with generally utilized stage-specific markers.

3.2. Molecular Biomarkers in Hippocampal Neurogenesis. With the progress of adult neurogenesis, a series of peculiar cell lineages emerge in turn. Here, we particularize the major biomarkers according to the following capabilities: proliferation, neurogenesis, and gliogenesis.

3.2.1. PCNA. PCNA, proliferating cell nuclear antigen, is important in both the repair and the replication of DNA. The expression of PCNA is increased during the G_1 and S phases and decreased upon the cell converting into G_2 and M phases. Nevertheless, this marker can also be detected in the early G_0 phase, which is caused by the long half-life period of eight to twenty hours [64]. Therefore, it refers to the fact that PCNA is expressed in the whole process of cell cycle. As a proliferation marker, it is usually applied to mark a subgroup of actively dividing cells, which is an indicator of proliferating NSCs (PCNA-positive cells) in SVZ, SGZ, tracing for the elusive adult NSCs [64, 65].

3.2.2. Ki67. Ki67, also known as MKI67, is a nuclear protein, which can be used as a marker for dividing cells. It can be found in all time-courses of cell cycle but G_0 and early G_1 phases and the same to quiescent cells [64]. According to the above investigation, both PCNA and Ki-67 can be used to label dividing cells, but PCNA is broader than Ki67 [66].

3.2.3. PH3. PH3, phosphohistone H3, is expressed at the late stage of G_2 phase and the entire course of M phase during cell division [67]. Given the property of PH3, it is usually applied to seek the cell subgroups in proliferating and mitotic states [68].

3.2.4. BrdU. BrdU (5′-bromo-2′-deoxyuridine), thymidine analog, is usually used to label cells being in the cell cycle of S phase in both embryonic and adult dividing cells. However, BrdU uniquely labeling, without additional markers, is only a prevalent symbolization for neurogenesis. BrdU-positive cells may indicate a subtype of progenitors for new neurons but not progenitors for neuronal cells [69–71].

3.2.5. MCM2. MCM2, minichromosome maintenance protein 2, is associated with the DNA replication. It is expressed at the early stage of G_1 phase and is sustained throughout cell cycle. Besides, it can be detected in proliferating cells without DNA synthesis too. Its expression level is thus higher than Ki67 which is the short-lived cell proliferation marker [72]. Furthermore, MCM2 has been confirmed to unfold a better tool for the labeling of cell proliferation than Ki67 and has been identified as a more useful marker in adult neurogenesis [73].

3.2.6. GFAP. GFAP, glial fibrillary acidic protein, is an intermediate filament (IF) protein which works as a holder of astrocyte mechanical strength. It is a well-known marker for astrocytes [74]. It has been reported that cells with astrocytic property can serve as an origination of new neurons during adult neurogenesis [75]. Rising proof suggests that GFAP-positive progenitor cells can generate specific cell types of neurons during neurogenesis [76]. Radial astrocytes stretching across the granule cell layer are assumed as potential DG NSCs [55].

3.2.7. BLBP. BLBP, brain lipid binding protein (BLBP), also called B-FABP or FABP7, is subjected to a member of fatty acid-binding proteins (FABPs) family, which are cytoplasmic proteins undertaking fatty acid intake, transportation, and targeting [77]. BLBP extensively serves as a radial-glia cell marker in both embryonic and adult brain developments and is expressed in the astrocyte lineage [78, 79]. It also presents in type-1 cells and a handful of type-2 cells in SGZ [80, 81]. The advent of BLBP in activated astrocytes is related to the expression of oligodendrocyte progenitor cells [50, 82].

3.2.8. Sox2. Sox2, known as SRY (sex determining region Y)box 2, is a member of Sox family of transcription factors. It encodes a highly conserved DNA-binding motif identified as HMG (high-mobility group) box, playing vital roles in distinct stages of mammalian development. Sox2, presenting a high expression in embryonic stem cells and adult NSCs during development [83–85], is a frequency marker for NSCs and is thought to be critical for NSCs proliferation and differentiation. Sox2-positive cells proliferate a subpopulation of undifferentiated, dividing cells in the subgranular zone (SGZ) of adult dentate gyrus. They are capable of generating differentiated cells and identical Sox2-positive cells, indicating their multipotent properties and capacities of self-renewal in the adult brain [86].

On the other hand, Sox1 is also expressed in adult neural progenitor cells and multipotent neural stem cells *in vitro* [87].

3.2.9. PSA-NCAM. PSA-NCAM, polysialylated neural cell adhesion molecule, is highly expressed in neural progenitor cells or mostly glial progenitor cells during brain development [88]. As for the adult brain, PSA-NCAM-positive cells can be focused on the granule cells that are newly generated or in the developing process in the adult brain [89, 90]. It has also been identified as a migrating neuroblasts marker that became neurons in the olfactory bulb (OB) in the SVZ *in vivo* [91]. Additionally, most of PSA-NCAM-positive cells is also NeuroD-positive, doublecortin-positive, NeuN-positive but GFAP-negative. Therefore, PSA-NCAM can be considered as a marker that arrives at the late strategy of adult neurogenesis [89, 90].

3.2.10. NeuroD. NeuroD (neurogenic differentiation) is a transcription factor belonging to the family of basic helix-loop-helix protein. It is presented in later strategies of neuronal progression and is classified as a differentiation indicator for neurogenesis, which may serve as a neuronal determination gene. It can also serve as a specific marker of adult cells in SGZ and inner granule layer [92, 93]. It is basilic for the proliferation of neurons in the adult brain [94]. Meanwhile, the expression of NeuroD can also be detected in PSA-NCAM-positive cells and it is colabeled with about 50% of Pax6-positive cells [95].

3.2.11. Pax6. PAX6, paired box 6, is a member of the paired box (Pax) family. As a conserved transcription factor with different DNA-binding domains (PD, a paired domain, and HD, a paired-type homeodomain), Pax6 is intensely expressed in the cells originating from the embryonic neural development and adult neurogenic niches [96]. It is multifunctional in regulating NSCs proliferation and differentiation by the modulation of various downstream molecules expression. It possesses the capacity of fate specification which sustains the survival of the distinct neuronal subtypes in the adulthood [97]. And its expression in progenitor cells is arrested at the early postnatal periods and is maintained only in adult neural progenitor cells in the restrict regions of SGZ and SVZ [98].

As a transcription factor, Pax6 emerges in embryonic progenitor cells and participates in the cell proliferation and the determination of neuronal fate as a pivotal regulator [99]. Nacher's investigation showed that Pax6 also turns up in the resident cells of adult SVZ and SGZ [95]. In the SGZ, Pax6 can be found in early progenitor cells with radial-glia-like appearance and GFAP/nestin-positive [93, 96]. Yet, there is a small bunch of cells exhibiting both Pax6 and PSA-NCAM or DCX or even NeuroD [100–102]. Pax6, collaborating with Dlx2, is required to specify and maintain neuronal subtype peculiarity in the adult and developing brain [103, 104]. Taking together, Pax6 might be used to classify the newly born cells from the differentiation state in SGZ.

3.2.12. FoxO3. FoxO3 (forkhead box O3) is a transcription factor belonging to the O subclass of the forkhead family which are identified by an evident fork head DNA-binding domain. FoxO factors can lure a series of cellular responses, involving the arrest of cell cycle, cell differentiation, apoptosis, and the opposition to oxidative stress [105]. FoxO3 protein

can be detected in adult NSCs/progenitor cells in the adult mouse brain [106]. And FoxO3 probably acts as an activator of apoptosis through upregulating the genes necessary for cell death and downregulating antiapoptotic proteins [107] and as a key player in Notch signaling pathway which is essential for sustaining the adult NSCs quiescent state [108]. The gene expression profile of FoxO3 in NSCs indicates that FoxO3 maintains the homeostasis of mouse NSC pool by provoking the genes that sustains quiescence, prohibits premature differentiation, and regulates oxygen metabolism [106].

3.2.13. Nestin. Nestin, neuroepithelial stem cell protein, is a sort of intermediate filament protein involved in classes VI and IV, which is expressed transiently in adult NSCs, immature neural progenitor cells, and vanishes upon the cells converting into differentiation [109]. It has been frequently utilized as a marker of NSCs both in embryo and in adult brain [110]. Park's data also suggests that nestin is basilic for the survival and self-renewal of NSCs [111].

In the adult mouse brain, nestin-positive cells can be observed extensively in restricted regions, where they might serve as a niche of stem/progenitor cells with the capacity of proliferation and differentiation [112]. During embryogenesis, most nestin-positive cells in early developmental stage indicate a cohort of stem/progenitor cells encompassed in active proliferation [113]. Upon these cells halting to divide and engaging into differentiation, nestin expression will be downregulated [113]. In the adult mouse brain, nestin-positive cells can be observed extensively in restricted regions, where they might serve as a niche of stem/progenitor cells with the capacity of proliferation and differentiation [112].

3.2.14. TLX. TLX, an orphan nuclear receptor (also called NR2E1), is encoded by the tailless (TLX) gene. It can be found in both neural stem/progenitor cells (quiescent NSCs) and transit-amplifying neural progenitors (active NSCs) in the SVZ (subventricular zone) and SGZ (subgranular zone) of adult mouse brain [114–116]. It is important in regulating NSCs self-renewal and proliferation during embryonic development and adulthood via a cell-autonomous mode [117]. And the adult neural stem cell pool consists of TLX-positive cells [116].

TLX is uniquely expressed by astrocyte-like B cells of SVZ. And the deletion of TLX gene may result in an absolute loss of SVZ neurogenesis and the deprivation of NSC property of GFAP-positive cells [115]. Further analysis of TLX indicates an essential role during the identified transition from radial glial cells to astrocyte-like B cells, which suggests that TLX should play as a crucial role in the process of the adult NSCs generation and maintenance in the SVZ [114].

3.2.15. bHLH. The bHLH is a basic helix-loop-helix protein transcription factor family, which regulates vertebrate neurogenesis, showing the capacity of transforming nonneuronal fate to neuronal fate when it is expressed ectopically [118].

3.2.16. Hes5. Hes5 is a member of Hes genes (mammalian homologues of Drosophila hairy and Enhancer of split genes) which can encode a series of basic helix-loop-helix (bHLH) transcriptional repressors. There are three conserved domains (bHLH, Orange, and WRPW domains) involved in Hes5 factor, through which Hes5 factor can set up transcriptional activities [9]. Studies have shown that, during embryogenesis, cells expressing Hes5 are maintained as neural stem cells. Hes5 habituates specifically in the SGZ, being in line with property of progenitor cells in the neurogenic niche [119, 120]. And the Hes5::GFP can mark more restricted and undifferentiated cohorts than Sox2 and BLBP [120].

3.2.17. Mash1. Mash1, mammalian achaete-scute homolog (also called Ascl1), is a bHLH transcription factor, which is essential for embryonic neural differentiation [121]. It is dynamically expressed not only in the intermediate progenitor cells (type C cells) but also in a subpopulation of NSCs potential for long-term neurogenesis in SVZ and SGZ of adult brain [115, 122].

3.2.18. REST. REST, RE1-silencing transcription factor (also known as NRSF), is the GLI-Kruppel class C2H2 zinc finger protein expressed in various neuronal genes [123]. It can silence the gene expression via recruiting mSin3A/B and CoREST [124, 125]. It can be found in nonneural cells and embryonic stem cells at high levels but declines when embryonic stem cells transfer to NSCs and cortical progenitor cells [125]. Conversely, REST highlights obvious levels in granular and pyramidal neurons in adult brain [126]. There is a putative implication that REST shows distinct functions when it arrives at embryonic and adult timelines. The deletion of REST may result in the functional depletion of adult NSC pool, which implies the crucial role of REST in sustaining the quiescent state of adult NSCs [127].

3.2.19. DCX. DCX, doublecortin, a protein facilitating microtubule polymerization, is expressed in migrating neuroblasts and immature neurons, which can be classified as a marker for adult neurogenesis in SGZ. However, not all newly born neurons express DCX. It can be found in newly generated hippocampal, striatal, and olfactory neurons, but not in newly generated neurons in the neocortex [128]. In a word, DCX can be utilized to label the postmitotic neuronal progenitor cells and early immature neurons [60]. And a tiny episode of overlap can be seen between the DCX-positive and nestin-positive cells [129].

3.2.20. Vimentin. Vimentin and GFAP are the two main intermediate filament proteins which imply the property of glial cells. And vimentin is mainly exhibited in the radial-glia and immature astrocytes of the early brain development and vanishes at the terminal of gestation. Simultaneously, GFAP presents in the astroglia cells instead of vimentin. However, Seri's research also suggests that vimentin is expressed in both radial-glia and horizontal cells in SGZ [68, 130].

3.2.21. S100β. S100β, also called calcium binding protein β, is a member of the S100 family, which is anchored at the cytoplasm and nucleus and participates in the procedure of cell cycle and differentiation. It can be detected in a subgroup of specific postmitotic astrocytes [131]. The expression of S100β discriminates a cohort of cells losing their NSCs potential from the GFAP-positive cells and indicates a more mature stage [132]. Given the above messages, we can conclude that $GFAP^+$ and $nestin^+$ progenitor cells are negative for S100β [55]. It has been reported that S100β could be reflected by immunofluorescent staining in horizontal zone but not radial astrocytes in SGZ [133].

3.2.22. GLAST and GLT1. GLAST (also known as EAAT1) is astrocyte-specific glutamate transporter and GLT1 (also known as EAAT2) is glutamate transporter; both are defined as markers of glial group [134]. GLAST has been found presenting in most of S100β-positive cells in SGZ [135]. It initially presents at mouse embryonic days 13/14 (E13/14) and keeps on throughout adulthood [136]. Nevertheless, the results derived from the adult NSCs culture *in vitro* showed that both GLAST and GLT could be detected in neuronal subgroups. Otherwise, investigations also unfolded that nestin-positive and Sox2-positive NSCs could be found expressing GLAST and GFAP [137, 138].

3.2.23. Tbr2. Tbr2, T-box brain gene 2, is a member of the mammalian brain-specific T-box gene family, which was expressed in a couple of regions in the developing brain. Yet, it is absent in most regions of adult brain but hippocampus and OB [139]. Increasing proofs have shown that Tbr2 is involved in adult neurogenesis in SGZ. It is present in a small bunch of Sox2 and Pax6-positive cells but absent in the S100β-positive cells. It overlaps with NeuroD-positive cells, as well as DCX^+ and PSA-$NCAM^+$ cells. And Tbr2 gradually disappeared when the cells are predestined to convert into neurons and exit mitotic cycle. Thus, it is not detectable either in calretinin/calbindin-positive immature neurons or in NeuN-positive mature cells. Together, we can conclude that Tbr2 is restrictedly expressed in type-2 and a handful of type-3 progenitor cells [68, 93, 140].

3.2.24. NeuroD. NeuroD, the basic helix-loop-helix protein, is a transcription factor, which has been parted into the group of markers for differentiated cells during neurogenesis in the SGZ [92]. It can be observed in inner granule cell layer and in a half of Pax6 and NeuroD-positive cells as well as PSA-NCAM-positive ones [93, 95, 133]. Gathered together, NeuroD can be defined as a marker for the early neuronal lineage and for the identification of mitotic neuronal cells [68].

3.2.25. Tuj1. Tuj1, neuron-specific class III β-tubulin, can be detected in immature neurons starting up at mouse early embryonic 8.5 day and persisting throughout the adulthood. The Tuj1-positive cells can be colabeled with DCX-positive and PSA-NCA-positive cells [141, 142]. Furthermore, it has been reported that Tuj1 can also be detected in basket cells in SGZ [133].

3.2.26. Prox1. Prox1, prosperorelated homeobox gene 1, is necessary for the preservation of IPCs (intermediate progenitor cells) and is needed to promote granule cells to maturate during the procedure of adult neurogenesis [143]. It is absent in $nestin^+$ or $Sox2^+$ cells but can be found in DCX^+ cells and $calretinin^+$ cells in the adult granule cells [144]. It can be applied to trace the neuronal lineage and mature neurons in the SGZ [53, 144].

3.2.27. CNPase. CNPase, 2′,3′-cyclic-nucleotide 3′-phosphodiesterase, presents specifically in oligodendrocytes in SVZ and SGZ, whose morphology reflected by the immunostaining refers to the beginning of oligodendrocyte differentiation. Furthermore, it is considered to play a leading role in the formation of myelination [145, 146].

3.3. Molecular Biomarkers in Adult SVZ. Subventricular zone (SVZ) is the other NSCs pool of the two restricted regions. The SVZ mainly consists of four main cell types: SVZ astrocytes/NSCs (type B cells), intermediate progenitor cells (type C cells), neuroblasts (type A cells), and ependymal cells [75, 147]. The adult SVZ functions as a neurogenesis pool through a surprising resemblance to the embryonic SVZ [148]. Experiencing the embryogenesis, the neonatal radial-glia (RG) cells persist to produce neurons and oligodendrocytes which originate from the intermediate progenitor cells (IPCs). One group of these cells transforms into ependymal cells, and most of the left cells convert into astrocytes (called type B cells) locating at adult SVZ, which continue to serve as NSCs throughout the adulthood. B cells preserve the epithelial formation which fix the apical into the ventricle zone and terminate the basal layer in blood vessels. Type B cells express markers tracing for astroglia, such as GFAP, glial fibrillary acidic protein; GLAST, astrocyte-specific glutamate transporter; BLBP, brain-lipid-binding protein; and nestin [148, 149].

And the slowly dividing astrocytes (B cells) continue to produce precursor C cells (intermediate progenitor cells), and C cells can produce the specific lineage A cells (neuroblasts) which will migrate along the RMS (rostral migratory stream) to the OB (olfactory bulb) where they finish their destined mission and convert into granule neurons [150].

GFAP specifically marks the NSCs and astrocytes residing in the SVZ but does not mark the subgroup of TAPs (transient amplifying progenitor cells) [78]. Meanwhile, Ki67, MCM2 (minichromosome maintenance 2), and PH3 (phosphohistone H3) can be used to mark the nuclei of proliferating cells, which make NSC nuclei visual in single one.

Sox2 marks the active astrocytes (NSCs) and neural progenitors (TAPs) of SVZ [75, 84]. PSA-NCAM marks the neuroblasts. NG2 and Mash1 exclusively mark the TAPs and a subgroup of migrating neuroblasts [151]. S100β marks the astrocytes and ependymal cells [152]. CD24 marks the migrating immature neurons and ependymal cells. CD31 (PECAM-1) marks the vascular endothelial cells [153]. In the

SVZ, cells that transform into another morphology through a series of time-courses can be marked by Tuj1 for neurons, GFAP for astrocytes, and O4/CNPase for oligodendrocytes (O4 and CNPase) [154].

Besides the markers mentioned above, a number of biomarkers reported in abundant investigations are remaining. Here, we enumerate some of them that were not illustrated in this review.

Astrocytes Markers. These include Aldh1L1, aldehyde dehydrogenase family 1 member L1; Bysl, bystin; GjA1, connexin 43; Glul, glutamine synthetase; PygB, glycogen phosphorylase; Slc1A2 GLT-1, excitatory amino acid transporter 2; Slc1A3, Glast-1, excitatory amino acid transporter 1.

Radial-Glia Markers. These include Aqp4, aquaporin-4; Slc1A2 GLT-1, excitatory amino acid transporter 2.

Oligodendrocyte Markers. These include Olig2, oligodendrocyte transcription factor; Car2, carbonic anhydrase 2; NFIA, nuclear factor 1 A-type; NFIB, nuclear factor 1 B-type; NFIX, nuclear factor 1 X-type; NSCs: NFIA, nuclear factor 1 A-type; NFIB, nuclear factor 1 B-type; Slc1A2 GLT-1, excitatory amino acid transporter 2.

4. Concluding Remarks

Given so abundant investigations and reviews by so many prominent scientists, we can now sketch the outline of various biomarker functional characteristics and latent application in multiple aspects. Gathering all of the formulations above, we catch a sight of many milestones established in the development of neurogenesis as well as obstacles being unfathomed.

Neural stem cells (NSCs) are the fundamental source of all cell types in the CNS. To grasp the nature of niche components in the mouse brain, we need to understand the major characteristics and functions of each element in the niche, to comprehend what role each cellular member plays in the procedure of NSCs maintenance, proliferation, and differentiation. However, it is difficult, using a single marker, to identify a single cell lineage exclusively. And thus it is necessary to apply multiple markers to the analysis of one peculiar cell type. Recently, numerous methods and technologies have been emerging to classify and identify the specific cell types during the neurogenesis of both embryonic and adult brains. Nevertheless, each approach possesses shining points and flaws. We need more concerns to consummate them.

Conflict of Interests

The authors declare that there is no actual or potential conflict of interests to this work, including any financial, personal, or other relationships with relevant people or organizations.

Acknowledgments

This work was supported by the Ministry of Science and Technology of China (2014CB964903) and Strategic Priority Research Program (XDA01020301). The work submitted has not been published previously, and it is not under consideration for publication elsewhere.

References

[1] F. H. Gage, "Mammalian neural stem cells," *Science*, vol. 287, no. 5457, pp. 1433–1438, 2000.

[2] F. H. Gage and S. Temple, "Neural stem cells: generating and regenerating the brain," *Neuron*, vol. 80, no. 3, pp. 588–601, 2013.

[3] P. Taupin, "Adult neurogenesis and neuroplasticity," *Restorative Neurology and Neuroscience*, vol. 24, no. 1, pp. 9–15, 2006.

[4] G.-L. Ming and H. Song, "Adult neurogenesis in the mammalian central nervous system," *Annual Review of Neuroscience*, vol. 28, pp. 223–250, 2005.

[5] G. Kempermann, S. Jessberger, B. Steiner, and G. Kronenberg, "Milestones of neuronal development in the adult hippocampus," *Trends in Neurosciences*, vol. 27, no. 8, pp. 447–452, 2004.

[6] I. Imayoshi, M. Sakamoto, T. Ohtsuka, and R. Kageyama, "Continuous neurogenesis in the adult brain," *Development Growth & Differentiation*, vol. 51, no. 3, pp. 379–386, 2009.

[7] L. de Filippis, G. Lamorte, E. Y. Snyder, A. Malgaroli, and A. L. Vescovi, "A novel, immortal, and multipotent human neural stem cell line generating functional neurons and oligodendrocytes," *Stem Cells*, vol. 25, no. 9, pp. 2312–2321, 2007.

[8] L. Pevny and M. S. Rao, "The stem-cell menagerie," *Trends in Neurosciences*, vol. 26, no. 7, pp. 351–359, 2003.

[9] R. Kageyama, J. Hatakeyama, and T. Ohtsuka, "Roles of Hes bHLH factors in neural development," in *Transcription Factors in the Nervous System: Development, Brain Function, and Diseases*, pp. 3–22, Wiley, 2006.

[10] F. Guillemot, "Cellular and molecular control of neurogenesis in the mammalian telencephalon," *Current Opinion in Cell Biology*, vol. 17, no. 6, pp. 639–647, 2005.

[11] K. Campbell, "Cortical neuron specification: it has its time and place," *Neuron*, vol. 46, no. 3, pp. 373–376, 2005.

[12] A. Alvarez-Buylla, J. M. García-Verdugo, and A. D. Tramontin, "A unified hypothesis on the lineage of neural stem cells," *Nature Reviews Neuroscience*, vol. 2, no. 4, pp. 287–293, 2001.

[13] S. Fujita, "The discovery of the matrix cell, the identification of the multipotent neural stem cell and the development of the central nervous system," *Cell Structure and Function*, vol. 28, no. 4, pp. 205–228, 2003.

[14] D. Gleason, J. H. Fallon, M. Guerra, J.-C. Liu, and P. J. Bryant, "Ependymal stem cells divide asymmetrically and transfer progeny into the subventricular zone when activated by injury," *Neuroscience*, vol. 156, no. 1, pp. 81–88, 2008.

[15] K. Y. Kwan, N. Šestan, and E. S. Anton, "Transcriptional co-regulation of neuronal migration and laminar identity in the neocortex," *Development*, vol. 139, no. 9, pp. 1535–1546, 2012.

[16] M. B. Woodworth, L. Custo Greig, A. R. Kriegstein, and J. D. MacKlis, "SnapShot: cortical development," *Cell*, vol. 151, no. 4, pp. 918–e1, 2012.

[17] K. C. Vadodaria and F. H. Gage, "SnapShot: adult hippocampal neurogenesis," *Cell*, vol. 156, no. 5, pp. 1114–1114.e1, 2014.

[18] A. Mallamaci, R. Iannone, P. Briata et al., "EMX2 protein in the developing mouse brain and olfactory area," *Mechanisms of Development*, vol. 77, no. 2, pp. 165–172, 1998.

[19] C. Cecchi, A. Mallamaci, and E. Boncinelli, "Mouse forebrain development. The role of *Emx2* homeobox gene," *Comptes*

Rendus de l'Académie des Sciences, vol. 322, no. 10, pp. 837–842, 1999.

[20] C. Cecchi, "Emx2: a gene responsible for cortical development, regionalization and area specification," *Gene*, vol. 291, no. 1-2, pp. 1–9, 2002.

[21] K. Y. Kwan, M. M. S. Lam, M. B. Johnson et al., "Species-dependent posttranscriptional regulation of *NOS1* by FMRP in the developing cerebral cortex," *Cell*, vol. 149, no. 4, pp. 899–911, 2012.

[22] T. Lai, D. Jabaudon, B. J. Molyneaux et al., "SOX5 controls the sequential generation of distinct corticofugal neuron subtypes," *Neuron*, vol. 57, no. 2, pp. 232–247, 2008.

[23] K. Y. Kwan, M. M. S. Lam, Ž. Krsnik, Y. I. Kawasawa, V. Lefebvre, and N. Šestan, "SOX5 postmitotically regulates migration, postmigratory differentiation, and projections of subplate and deep-layer neocortical neurons," *Proceedings of the National Academy of Sciences of the United States of America*, vol. 105, no. 41, pp. 16021–16026, 2008.

[24] P. Arlotta, B. J. Molyneaux, J. Chen, J. Inoue, R. Kominami, and J. D. MacKlis, "Neuronal subtype-specific genes that control corticospinal motor neuron development in vivo," *Neuron*, vol. 45, no. 2, pp. 207–221, 2005.

[25] R. Simon, H. Brylka, H. Schwegler et al., "A dual function of Bcl11b/Ctip2 in hippocampal neurogenesis," *The EMBO Journal*, vol. 31, no. 13, pp. 2922–2936, 2012.

[26] R. F. Hevner, L. Shi, N. Justice et al., "Tbr1 regulates differentiation of the preplate and layer 6," *Neuron*, vol. 29, no. 2, pp. 353–366, 2001.

[27] W. Han, K. Y. Kwan, S. Shim et al., "TBR1 directly represses *Fezf2*to control the laminar origin and development of the corticospinal tract," *Proceedings of the National Academy of Sciences of the United States of America*, vol. 108, no. 7, pp. 3041–3046, 2011.

[28] W. L. McKenna, J. Betancourt, K. A. Larkin et al., "Tbr1 and Fezf2 regulate alternate corticofugal neuronal identities during neocortical development," *Journal of Neuroscience*, vol. 31, no. 2, pp. 549–564, 2011.

[29] F. Bedogni, R. D. Hodge, G. E. Elsen et al., "Tbr1 regulates regional and laminar identity of postmitotic neurons in developing neocortex," *Proceedings of the National Academy of Sciences of the United States of America*, vol. 107, no. 29, pp. 13129–13134, 2010.

[30] O. Britanova, C. D. J. Romero, A. Cheung et al., "Satb2 is a postmitotic determinant for upper-layer neuron specification in the neocortex," *Neuron*, vol. 57, no. 3, pp. 378–392, 2008.

[31] E. A. Alcamo, L. Chirivella, M. Dautzenberg et al., "Satb2 regulates callosal projection neuron identity in the developing cerebral cortex," *Neuron*, vol. 57, no. 3, pp. 364–377, 2008.

[32] L. Zhang, N.-N. Song, J.-Y. Chen, Y. Huang, H. Li, and Y.-Q. Ding, "Satb2 is required for dendritic arborization and soma spacing in mouse cerebral cortex," *Cerebral Cortex*, vol. 22, no. 7, pp. 1510–1519, 2012.

[33] B. Cubelos, A. Sebastián-Serrano, L. Beccari et al., "Cux1 and Cux2 regulate dendritic branching, spine morphology, and synapses of the upper layer neurons of the cortex," *Neuron*, vol. 66, no. 4, pp. 523–535, 2010.

[34] R. Benavides-Piccione, F. Hamzei-Sichani, I. Ballesteros-Yáñez, J. Defelipe, and R. Yuste, "Dendritic size of pyramidal neurons differs among mouse cortical regions," *Cerebral Cortex*, vol. 16, no. 7, pp. 990–1001, 2006.

[35] K. Sumiyama, K. Washio-Watanabe, N. Saitou, T. Hayakawa, and S. Ueda, "Class III POU genes: generation of homopolymeric amino acid repeats under GC pressure in mammals," *Journal of Molecular Evolution*, vol. 43, no. 3, pp. 170–178, 1996.

[36] R. J. McEvilly, M. O. de Diaz, M. D. Schonemann, F. Hooshmand, and M. G. Rosenfeld, "Transcriptional regulation of cortical neuron migration by POU domain factors," *Science*, vol. 295, no. 5559, pp. 1528–1532, 2002.

[37] Y. Sugitani, S. Nakai, O. Minowa et al., "Brn-1 and Brn-2 share crucial roles in the production and positioning of mouse neocortical neurons," *Genes and Development*, vol. 16, no. 14, pp. 1760–1765, 2002.

[38] M. H. Dominguez, A. E. Ayoub, and P. Rakic, "POU-III transcription factors (Brn1, Brn2, and Oct6) influence neurogenesis, molecular identity, and migratory destination of upper-layer cells of the cerebral cortex," *Cerebral Cortex*, vol. 23, no. 11, pp. 2632–2643, 2013.

[39] V. Tarabykin, A. Stoykova, N. Usman, and P. Gruss, "Cortical upper layer neurons derive from the subventricular zone as indicated by Svet1 gene expression," *Development*, vol. 128, no. 11, pp. 1983–1993, 2001.

[40] P. W. Land and A. P. Monaghan, "Expression of the transcription factor, tailless, is required for formation of superficial cortical layers," *Cerebral Cortex*, vol. 13, no. 9, pp. 921–931, 2003.

[41] J. Wen, Q. Hu, M. Li et al., "Pax6 directly modulate Sox2 expression in the neural progenitor cells," *Neuroreport*, vol. 19, no. 4, pp. 413–417, 2008.

[42] C. Alfano, L. Viola, J. I. Heng et al., "COUP-TFI promotes radial migration and proper morphology of callosal projection neurons by repressing Rnd2 expression," *Development*, vol. 138, no. 21, pp. 4685–4697, 2011.

[43] D. O'Leary and S. Sahara, "Genetic regulation of arealization of the neocortex," *Current Opinion in Neurobiology*, vol. 18, no. 1, pp. 90–100, 2008.

[44] J. Aubert, M. P. Stavridis, S. Tweedie et al., "Screening for mammalian neural genes via fluorescence-activated cell sorter purification of neural precursors from Sox1-gfp knock-in mice," *Proceedings of the National Academy of Sciences of the United States of America*, vol. 100, no. 1, pp. 11836–11841, 2003.

[45] C. Zhao, W. Deng, and F. H. Gage, "Mechanisms and functional implications of adult neurogenesis," *Cell*, vol. 132, no. 4, pp. 645–660, 2008.

[46] O. V. B. U. Halbach, "Immunohistological markers for staging neurogenesis in adult hippocampus," *Cell and Tissue Research*, vol. 329, no. 3, pp. 409–420, 2007.

[47] E. Bazán, F. J. M. Alonso, C. Redondo et al., "In vitro and in vivo characterization of neural stem cells," *Histology and Histopathology*, vol. 19, no. 4, pp. 1261–1275, 2004.

[48] X. Duan, E. Kang, C. Y. Liu et al., "Development of neural stem cell in the adult brain," *Current Opinion in Neurobiology*, vol. 18, no. 1, pp. 108–115, 2008.

[49] F. A. Siebzehnrubl, V. Vedam-Mai, H. Azari, B. A. Reynolds, and L. P. Deleyrolle, "Isolation and characterization of adult neural stem cells," *Methods in Molecular Biology*, vol. 750, pp. 61–77, 2011.

[50] T. E. Anthony, C. Klein, G. Fishell, and N. Heintz, "Radial glia serve as neuronal progenitors in all regions of the central nervous system," *Neuron*, vol. 41, no. 6, pp. 881–890, 2004.

[51] D. K. Ma, M. A. Bonaguidi, G.-L. Ming, and H. Song, "Adult neural stem cells in the mammalian central nervous system," *Cell Research*, vol. 19, no. 6, pp. 672–682, 2009.

[52] G. Kempermann, H. G. Kuhn, and F. H. Gage, "Experience-induced neurogenesis in the senescent dentate gyrus," *The Journal of Neuroscience*, vol. 18, no. 9, pp. 3206–3212, 1998.

[53] B. Steiner, S. Zurborg, H. Hörster, K. Fabel, and G. Kempermann, "Differential 24 h responsiveness of Prox1-expressing precursor cells in adult hippocampal neurogenesis to physical activity, environmental enrichment, and kainic acid-induced seizures," *Neuroscience*, vol. 154, no. 2, pp. 521–529, 2008.

[54] G. L. Ming and H. Song, "Adult neurogenesis in the mammalian central nervous system," *Annual Review of Neuroscience*, vol. 28, pp. 223–250, 2005.

[55] V. Filippov, G. Kronenberg, T. Pivneva et al., "Subpopulation of nestin-expressing progenitor cells in the adult murine hippocampus shows electrophysiological and morphological characteristics of astrocytes," *Molecular and Cellular Neuroscience*, vol. 23, no. 3, pp. 373–382, 2003.

[56] S. Fukuda, F. Kato, Y. Tozuka, M. Yamaguchi, Y. Miyamoto, and T. Hisatsune, "Two distinct subpopulations of nestin-positive cells in adult mouse dentate gyrus," *The Journal of Neuroscience*, vol. 23, no. 28, pp. 9357–9366, 2003.

[57] J. M. Parent, T. W. Yu, R. T. Leibowitz, D. H. Geschwind, R. S. Sloviter, and D. H. Lowenstein, "Dentate granule cell neurogenesis is increased by seizures and contributes to aberrant network reorganization in the adult rat hippocampus," *The Journal of Neuroscience*, vol. 17, no. 10, pp. 3727–3738, 1997.

[58] E. Gould, H. A. Cameron, D. C. Daniels, C. S. Woolley, and B. S. McEwen, "Adrenal hormones suppress cell division in the adult rat dentate gyrus," *The Journal of Neuroscience*, vol. 12, no. 9, pp. 3642–3650, 1992.

[59] G. Kronenberg, K. Reuter, B. Steiner et al., "Subpopulations of proliferating cells of the adult hippocampus respond differently to physiologic neurogenic stimuli," *Journal of Comparative Neurology*, vol. 467, no. 4, pp. 455–463, 2003.

[60] J. P. Brown, S. Couillard-Després, C. M. Cooper-Kuhn, J. Winkler, L. Aigner, and H. G. Kuhn, "Transient expression of doublecortin during adult neurogenesis," *Journal of Comparative Neurology*, vol. 467, no. 1, pp. 1–10, 2003.

[61] M. D. Brandt, S. Jessberger, B. Steiner et al., "Transient calretinin expression defines early postmitotic step of neuronal differentiation in adult hippocampal neurogenesis of mice," *Molecular and Cellular Neuroscience*, vol. 24, no. 3, pp. 603–613, 2003.

[62] Z. Li, T. Kato, K. Kawagishi, N. Fukushima, K. Yokouchi, and T. Moriizumi, "Cell dynamics of calretinin-immunoreactive neurons in the rostral migratory stream after ibotenate-induced lesions in the forebrain," *Neuroscience Research*, vol. 42, no. 2, pp. 123–132, 2002.

[63] S. Jessberger and G. Kempermann, "Adult-born hippocampal neurons mature into activity-dependent responsiveness," *European Journal of Neuroscience*, vol. 18, no. 10, pp. 2707–2712, 2003.

[64] A. Zacchetti, E. Van Garderen, E. Teske, H. Nederbragt, J. H. Dierendonck, and G. R. Rutteman, "Validation of the use of proliferation markers in canine neoplastic and non-neoplastic tissues: comparison of KI-67 and proliferating cell nuclear antigen (PCNA) expression versus in vivo bromodeoxyuridine labelling by immunohistochemistry," *APMIS*, vol. 111, no. 3, pp. 430–438, 2003.

[65] T. L. Limke, J. Cai, T. Miura, M. S. Rao, and M. P. Mattson, "Distinguishing features of progenitor cells in the late embryonic and adult hippocampus," *Developmental Neuroscience*, vol. 25, no. 2–4, pp. 257–272, 2003.

[66] S. Jinno, "Topographic differences in adult neurogenesis in the mouse hippocampus: a stereology-based study using endogenous markers," *Hippocampus*, vol. 21, no. 5, pp. 467–480, 2011.

[67] P. Taupin, "BrdU immunohistochemistry for studying adult neurogenesis: paradigms, pitfalls, limitations, and validation," *Brain Research Reviews*, vol. 53, no. 1, pp. 198–214, 2007.

[68] O. Von Bohlen Und Halbach, "Immunohistological markers for proliferative events, gliogenesis, and neurogenesis within the adult hippocampus," *Cell and Tissue Research*, vol. 345, no. 1, pp. 1–19, 2011.

[69] H. G. Kuhn, H. Dickinson-Anson, and F. H. Gage, "Neurogenesis in the dentate gyrus of the adult rat: age-related decrease of neuronal progenitor proliferation," *The Journal of Neuroscience*, vol. 16, no. 6, pp. 2027–2033, 1996.

[70] G. Kempermann, H. G. Kuhn, and F. H. Gage, "More hippocampal neurons in adult mice living in an enriched environment," *Nature*, vol. 386, no. 6624, pp. 493–495, 1997.

[71] G. Kempermann, D. Gast, G. Kronenberg, M. Yamaguchi, and F. H. Gage, "Early determination and long-term persistence of adult-generated new neurons in the hippocampus of mice," *Development*, vol. 130, no. 2, pp. 391–399, 2003.

[72] P. J. Lucassen, M. W. Stumpel, Q. Wang, and E. Aronica, "Decreased numbers of progenitor cells but no response to antidepressant drugs in the hippocampus of elderly depressed patients," *Neuropharmacology*, vol. 58, no. 6, pp. 940–949, 2010.

[73] A. Hanna-Morris, S. Badvie, P. Cohen, T. McCullough, H. J. N. Andreyev, and T. G. Allen-Marsh, "Minichromosome maintenance protein 2 (MCM2) is a stronger discriminator of increased proliferation in mucosa adjacent to colorectal cancer than Ki-67," *Journal of Clinical Pathology*, vol. 62, no. 4, pp. 325–330, 2009.

[74] J. Szymas and F. Tokarz, "Determination of the glial fibrillary acidic protein in human cerebrospinal fluid and in cyst fluid of brain tumors," *Acta Neurochirurgica*, vol. 83, no. 3-4, pp. 144–150, 1986.

[75] F. Doetsch, J. M. García-Verdugo, and A. Alvarez-Buylla, "Cellular composition and three-dimensional organization of the subventricular germinal zone in the adult mammalian brain," *Journal of Neuroscience*, vol. 17, no. 13, pp. 5046–5061, 1997.

[76] A. R. Kriegstein and M. Götz, "Radial glia diversity: a matter of cell fate," *GLIA*, vol. 43, no. 1, pp. 37–43, 2003.

[77] J. H. Veerkamp and A. W. Zimmerman, "Fatty acid-binding proteins of nervous tissue," *Journal of Molecular Neuroscience*, vol. 16, no. 2-3, pp. 133–142, 2001.

[78] M. Sibbe, E. Förster, O. Basak, V. Taylor, and M. Frotscher, "Reelin and Notch1 cooperate in the development of the dentate gyrus," *The Journal of Neuroscience*, vol. 29, no. 26, pp. 8578–8585, 2009.

[79] L. Pinto and M. Götz, "Radial glial cell heterogeneity—the source of diverse progeny in the CNS," *Progress in Neurobiology*, vol. 83, no. 1, pp. 2–23, 2007.

[80] B. Steiner, F. Klempin, L. Wang, M. Kott, H. Kettenmann, and G. Kempermann, "Type-2 cells as link between glial and neuronal lineage in adult hippocampal neurogenesis," *GLIA*, vol. 54, no. 8, pp. 805–814, 2006.

[81] B. Brunne, S. Zhao, A. Derouiche et al., "Origin, maturation, and astroglial transformation of secondary radial glial cells in the developing dentate gyrus," *Glia*, vol. 58, no. 13, pp. 1553–1569, 2010.

[82] M. Kipp, S. Gingele, F. Pott et al., "BLBP-expression in astrocytes during experimental demyelination and in human multiple

sclerosis lesions," *Brain, Behavior, and Immunity*, vol. 25, no. 8, pp. 1554–1568, 2011.

[83] A. A. Avilion, S. K. Nicolis, L. H. Pevny, L. Perez, N. Vivian, and R. Lovell-Badge, "Multipotent cell lineages in early mouse development depend on SOX2 function," *Genes and Development*, vol. 17, no. 1, pp. 126–140, 2003.

[84] A. L. M. Ferri, M. Cavallaro, D. Braida et al., "Sox2 deficiency causes neurodegeneration and impaired neurogenesis in the adult mouse brain," *Development*, vol. 131, no. 15, pp. 3805–3819, 2004.

[85] A. Rizzino, "Sox2 and Oct-3/4: a versatile pair of master regulators that orchestrate the self-renewal and pluripotency of embryonic stem cells," *Wiley Interdisciplinary Reviews: Systems Biology and Medicine*, vol. 1, no. 2, pp. 228–236, 2009.

[86] H. Suh, A. Consiglio, J. Ray, T. Sawai, K. A. D'Amour, and F. Gage, "In vivo fate analysis reveals the multipotent and self-renewal capacities of Sox^{2+} neural stem cells in the adult hippocampus," *Cell Stem Cell*, vol. 1, no. 5, pp. 515–528, 2007.

[87] J. Cai, A. Cheng, Y. Luo et al., "Membrane properties of rat embryonic multipotent neural stem cells," *Journal of Neurochemistry*, vol. 88, no. 1, pp. 212–226, 2003.

[88] R. Marmur, P. C. Mabie, S. Gokhan, Q. Song, J. A. Kessler, and M. F. Mehler, "Isolation and developmental characterization of cerebral cortical multipotent progenitors," *Developmental Biology*, vol. 204, no. 2, pp. 577–591, 1998.

[89] T. Seki, "Expression patterns of immature neuronal markers PSA-NCAM, CRMP-4 and NeuroD in the hippocampus of young adult and aged rodents," *Journal of Neuroscience Research*, vol. 70, no. 3, pp. 327–334, 2002.

[90] T. Seki, "Hippocampal adult neurogenesis occurs in a microenvironment provided by PSA-NCAM-expressing immature neurons," *Journal of Neuroscience Research*, vol. 69, no. 6, pp. 772–783, 2002.

[91] F. Doetsch, I. Caillé, D. A. Lim, J. M. Garcia-Verdugo, and A. Alvarez-Buylla, "Subventricular zone astrocytes are neural stem cells in the adult mammalian brain," *Cell*, vol. 97, no. 6, pp. 703–716, 1999.

[92] T. Kawai, N. Takagi, K. Miyake-Takagi, N. Okuyama, N. Mochizuki, and S. Takeo, "Characterization of BrdU-Positive Neurons Induced by Transient Global Ischemia in Adult Hippocampus," *Journal of Cerebral Blood Flow and Metabolism*, vol. 24, no. 5, pp. 548–555, 2004.

[93] R. F. Hevner, R. D. Hodge, R. A. M. Daza, and C. Englund, "Transcription factors in glutamatergic neurogenesis: conserved programs in neocortex, cerebellum, and adult hippocampus," *Neuroscience Research*, vol. 55, no. 3, pp. 223–233, 2006.

[94] M. Liu, S. J. Pleasure, A. E. Collins et al., "Loss of BETA2/NeuroD leads to malformation of the dentate gyrus and epilepsy," *Proceedings of the National Academy of Sciences of the United States of America*, vol. 97, no. 2, pp. 865–870, 2000.

[95] J. Nacher, E. Varea, J. M. Blasco-Ibañez et al., "Expression of the transcription factor Pax6 in the adult rat dentate gyrus," *Journal of Neuroscience Research*, vol. 81, no. 6, pp. 753–761, 2005.

[96] N. Osumi, H. Shinohara, K. Numayama-Tsuruta, and M. Maekawa, "Concise review: Pax6 transcription factor contributes to both embryonic and adult neurogenesis as a multifunctional regulator," *Stem Cells*, vol. 26, no. 7, pp. 1663–1672, 2008.

[97] J. Ninkovic, L. Pinto, S. Petricca et al., "The transcription factor Pax6 regulates survival of dopaminergic olfactory bulb neurons via crystallin αA," *Neuron*, vol. 68, no. 4, pp. 682–694, 2010.

[98] M. S. Brill, J. Ninkovic, E. Winpenny et al., "Adult generation of glutamatergic olfactory bulb interneurons," *Nature Neuroscience*, vol. 12, no. 12, pp. 1524–1533, 2009.

[99] C. Englund, A. Fink, C. Lau et al., "Pax6, Tbr2, and Tbr1 are expressed sequentially by radial glia, intermediate progenitor cells, and postmitotic neurons in developing neocortex," *Journal of Neuroscience*, vol. 25, no. 1, pp. 247–251, 2005.

[100] M. Maekawa, N. Takashima, Y. Arai et al., "Pax6 is required for production and maintenance of progenitor cells in postnatal hippocampal neurogenesis," *Genes to Cells*, vol. 10, no. 10, pp. 1001–1014, 2005.

[101] J. C. Quinn, M. Molinek, B. S. Martynoga et al., "Pax6 controls cerebral cortical cell number by regulating exit from the cell cycle and specifies cortical cell identity by a cell autonomous mechanism," *Developmental Biology*, vol. 302, no. 1, pp. 50–65, 2007.

[102] Z. Molnár and A. F. P. Cheung, "Towards the classification of subpopulations of layer V pyramidal projection neurons," *Neuroscience Research*, vol. 55, no. 2, pp. 105–115, 2006.

[103] J. Ninkovic, T. Mori, and M. Götz, "Distinct modes of neuron addition in adult mouse neurogenesis," *Journal of Neuroscience*, vol. 27, no. 40, pp. 10906–10911, 2007.

[104] T. C. Tuoc and A. Stoykova, "Trim11 modulates the function of neurogenic transcription factor Pax6 through ubiquitin-proteosome system," *Genes and Development*, vol. 22, no. 14, pp. 1972–1986, 2008.

[105] D. A. Salih and A. Brunet, "FoxO transcription factors in the maintenance of cellular homeostasis during aging," *Current Opinion in Cell Biology*, vol. 20, no. 2, pp. 126–136, 2008.

[106] V. M. Renault, V. A. Rafalski, A. A. Morgan et al., "FoxO3 regulates neural stem cell homeostasis," *Cell Stem Cell*, vol. 5, no. 5, pp. 527–539, 2009.

[107] C. Skurk, H. Maatz, H.-S. Kim et al., "The Akt-regulated forkhead transcription factor FOXO3a controls endothelial cell viability through modulation of the caspase-8 inhibitor FLIP," *Journal of Biological Chemistry*, vol. 279, no. 2, pp. 1513–1525, 2004.

[108] S. D. Gopinath, A. E. Webb, A. Brunet, and T. A. Rando, "FOXO3 promotes quiescence in adult muscle stem cells during the process of self-renewal," *Stem Cell Reports*, vol. 2, no. 4, pp. 414–426, 2014.

[109] U. Lendahl, L. B. Zimmerman, and R. D. G. McKay, "CNS stem cells express a new class of intermediate filament protein," *Cell*, vol. 60, no. 4, pp. 585–595, 1990.

[110] A. V. Gilyarov, "Nestin in central nervous system cells," *Neuroscience and Behavioral Physiology*, vol. 38, no. 2, pp. 165–169, 2008.

[111] D. Park, A. P. Xiang, F. F. Mao et al., "Nestin is required for the proper self-renewal of neural stem cells," *Stem Cells*, vol. 28, no. 12, pp. 2162–2171, 2010.

[112] J. Namiki, S. Suzuki, T. Masuda, Y. Ishihama, and H. Okano, "Nestin protein is phosphorylated in adult neural stem/progenitor cells and not endothelial progenitor cells," *Stem Cells International*, vol. 2012, Article ID 430138, 5 pages, 2012.

[113] C. Wiese, A. Rolletschek, G. Kania et al., "Nestin expression—a property of multi-lineage progenitor cells?" *Cellular and Molecular Life Sciences*, vol. 61, no. 19-20, pp. 2510–2522, 2004.

[114] H.-K. Liu, T. Belz, D. Bock et al., "The nuclear receptor tailless is required for neurogenesis in the adult subventricular zone," *Genes and Development*, vol. 22, no. 18, pp. 2473–2478, 2008.

[115] S. Li, G. Sun, K. Murai, P. Ye, and Y. Shi, "Characterization of TLX expression in neural stem cells and progenitor cells in adult brains," *PLoS ONE*, vol. 7, no. 8, Article ID e43324, 2012.

[116] Y. Shi, D. C. Lie, P. Taupin et al., "Expression and function of orphan nuclear receptor TLX in adult neural stem cells," *Nature*, vol. 427, no. 6969, pp. 78–83, 2004.

[117] C.-L. Zhang, Y. Zou, W. He, F. H. Gage, and R. M. Evans, "A role for adult TLX-positive neural stem cells in learning and behaviour," *Nature*, vol. 451, no. 7181, pp. 1004–1007, 2008.

[118] J. E. Lee, "Basic helix-loop-helix genes in neural development," *Current Opinion in Neurobiology*, vol. 7, no. 1, pp. 13–20, 1997.

[119] G. Stump, A. Durrer, A.-L. Klein, S. Lütolf, U. Suter, and V. Taylor, "Notch1 and its ligands Delta-like and Jagged are expressed and active in distinct cell populations in the postnatal mouse brain," *Mechanisms of Development*, vol. 114, no. 1-2, pp. 153–159, 2002.

[120] S. Lugert, O. Basak, P. Knuckles et al., "Quiescent and active hippocampal neural stem cells with distinct morphologies respond selectively to physiological and pathological stimuli and aging," *Cell Stem Cell*, vol. 6, no. 5, pp. 445–456, 2010.

[121] N. Bertrand, D. S. Castro, and F. Guillemot, "Proneural genes and the specification of neural cell types," *Nature Reviews Neuroscience*, vol. 3, no. 7, pp. 517–530, 2002.

[122] E. J. Kim, J. L. Ables, L. K. Dickel, A. J. Eisch, and J. E. Johnson, "Ascl1 (Mash1) defines cells with long-term neurogenic potential in subgranular and subventricular zones in adult mouse brain," *PLoS ONE*, vol. 6, no. 3, Article ID e18472, 2011.

[123] J. A. Chong, J. Tapia-Ramírez, S. Kim et al., "REST: a mammalian silencer protein that restricts sodium channel gene expression to neurons," *Cell*, vol. 80, no. 6, pp. 949–957, 1995.

[124] L. Sharling, A. Roopra, I. C. Wood et al., "Transcriptional repression by neuron-restrictive silencer factor is mediated via the Sin3-histone deacetylase complex," *Molecular & Cellular Biology*, vol. 20, no. 6, pp. 2147–2157, 2000.

[125] N. Ballas, E. Battaglioli, F. Atouf et al., "Regulation of neuronal traits by a novel transcriptional complex," *Neuron*, vol. 31, no. 3, pp. 353–365, 2001.

[126] Y.-M. Sun, D. J. Greenway, R. Johnson et al., "Distinct profiles of REST interactions with its target genes at different stages of neuronal development," *Molecular Biology of the Cell*, vol. 16, no. 12, pp. 5630–5638, 2005.

[127] Z. Gao, K. Ure, P. Ding et al., "The master negative regulator REST/NRSF controls adult neurogenesis by restraining the neurogenic program in quiescent stem cells," *Journal of Neuroscience*, vol. 31, no. 26, pp. 9772–9786, 2011.

[128] A. G. Dayer, K. M. Cleaver, T. Abouantoun, and H. A. Cameron, "New GABAergic interneurons in the adult neocortex and striatum are generated from different precursors," *The Journal of Cell Biology*, vol. 168, no. 3, pp. 415–427, 2005.

[129] S. Couillard-Despres, B. Winner, C. Karl et al., "Targeted transgene expression in neuronal precursors: watching young neurons in the old brain," *European Journal of Neuroscience*, vol. 24, no. 6, pp. 1535–1545, 2006.

[130] B. Seri, J. M. García-Verdugo, B. S. McEwen, and A. Alvarez-Buylla, "Astrocytes give rise to new neurons in the adult mammalian hippocampus," *Journal of Neuroscience*, vol. 21, no. 18, pp. 7153–7160, 2001.

[131] D. Ehninger and G. Kempermann, "Neurogenesis in the adult hippocampus," *Cell and Tissue Research*, vol. 331, no. 1, pp. 243–250, 2008.

[132] E. Raponi, F. Agenes, C. Delphin et al., "S100B expression defines a state in which GFAP-expressing cells lose their neural stem cell potential and acquire a more mature developmental stage," *Glia*, vol. 55, no. 2, pp. 165–177, 2007.

[133] B. Seri, J. M. García-Verdugo, L. Collado-Morente, B. S. McEwen, and A. Alvarez-Buylla, "Cell types, lineage, and architecture of the germinal zone in the adult dentate gyrus," *Journal of Comparative Neurology*, vol. 478, no. 4, pp. 359–378, 2004.

[134] P. Kugler and V. Schleyer, "Developmental expression of glutamate transporters and glutamate dehydrogenase in astrocytes of the postnatal rat hippocampus," *Hippocampus*, vol. 14, no. 8, pp. 975–985, 2004.

[135] T. Namba, H. Mochizuki, M. Onodera, Y. Mizuno, H. Namiki, and T. Seki, "The fate of neural progenitor cells expressing astrocytic and radial glial markers in the postnatal rat dentate gyrus," *European Journal of Neuroscience*, vol. 22, no. 8, pp. 1928–1941, 2005.

[136] G. Barry, M. Piper, C. Lindwall et al., "Specific glial populations regulate hippocampal morphogenesis," *Journal of Neuroscience*, vol. 28, no. 47, pp. 12328–12340, 2008.

[137] D. N. Plachez and M. Récasens, "Transient expression of the glial glutamate transporters GLAST and GLT in hippocampal neurons in primary culture," *Journal of Neuroscience Research*, vol. 59, no. 5, pp. 587–593, 2000.

[138] A. Lee and D. V. Pow, "Astrocytes: glutamate transport and alternate splicing of transporters," *International Journal of Biochemistry and Cell Biology*, vol. 42, no. 12, pp. 1901–1906, 2010.

[139] N. Kimura, K. Nakashima, M. Ueno, H. Kiyama, and T. Taga, "A novel mammalian T-box-containing gene, *Tbr2*, expressed in mouse developing brain," *Developmental Brain Research*, vol. 115, no. 2, pp. 183–193, 1999.

[140] R. D. Hodge, T. D. Kowalczyk, S. A. Wolf et al., "Intermediate progenitors in adult hippocampal neurogenesis: Tbr2 expression and coordinate regulation of neuronal output," *Journal of Neuroscience*, vol. 28, no. 14, pp. 3707–3717, 2008.

[141] P. Ambrogini, D. Lattanzi, S. Ciuffoli et al., "Morpho-functional characterization of neuronal cells at different stages of maturation in granule cell layer of adult rat dentate gyrus," *Brain Research*, vol. 1017, no. 1-2, pp. 21–31, 2004.

[142] H. K. C. Yang, N. L. Sundholm-Peters, G. E. Goings, A. S. Walker, K. Hyland, and F. G. Szele, "Distribution of doublecortin expressing cells near the lateral ventricles in the adult mouse brain," *Journal of Neuroscience Research*, vol. 76, no. 3, pp. 282–295, 2004.

[143] A. Lavado, O. V. Lagutin, L. M. L. Chow, S. J. Baker, and G. Oliver, "Prox1 is required for granule cell maturation and intermediate progenitor maintenance during brain neurogenesis," *PLoS Biology*, vol. 8, no. 8, pp. 43–44, 2010.

[144] I. Navaero-Quiroga, M. Fernandez-Valdes, S. L. Lin, and J. R. Naegele, "Postnatal cellular contributions of the hippocampus subventricular zone to the dentate gyrus, corpus callosum, fimbria, and cerebral cortex," *Journal of Comparative Neurology*, vol. 497, no. 5, pp. 833–845, 2006.

[145] H. Kasama-Yoshida, Y. Tohyama, T. Kurihara, M. Sakuma, H. Kojima, and Y. Tamai, "A comparative study of 2',3'-cyclic-nucleotide 3'-phosphodiesterase in vertebrates: cDNA cloning and amino acid sequences for chicken and bullfrog enzymes," *Journal of Neurochemistry*, vol. 69, no. 4, pp. 1335–1342, 1997.

[146] M. S. Davidoff, R. Middendorff, E. Köfüncü, D. Müller, D. Ježek, and A.-F. Holstein, "Leydig cells of the human testis

possess astrocyte and oligodendrocyte marker molecules," *Acta Histochemica*, vol. 104, no. 1, pp. 39–49, 2002.

[147] C. K. Tong and A. Alvarez-Buylla, "SnapShot: adult Neurogenesis in the V-SVZ," *Neuron*, vol. 81, no. 1, pp. 220–220.e1, 2014.

[148] X. Liu, A. J. Bolteus, D. M. Balkin, O. Henschel, and A. Bordey, "GFAP-expressing cells in the postnatal subventricular zone display a unique glial phenotype intermediate between radial glia and astrocytes," *Glia*, vol. 54, no. 5, pp. 394–410, 2006.

[149] T. Nomura, C. Göritz, T. Catchpole, M. Henkemeyer, and J. Frisén, "EphB signaling controls lineage plasticity of adult neural stem cell niche cells," *Cell Stem Cell*, vol. 7, no. 6, pp. 730–743, 2010.

[150] S. Bovetti, P. Bovolin, I. Perroteau, and A. C. Puche, "Subventricular zone-derived neuroblast migration to the olfactory bulb is modulated by matrix remodelling," *European Journal of Neuroscience*, vol. 25, no. 7, pp. 2021–2033, 2007.

[151] C. M. Parras, R. Galli, O. Britz et al., "*Mash1* specifies neurons and oligodendrocytes in the postnatal brain," *The EMBO Journal*, vol. 23, no. 22, pp. 4495–4505, 2004.

[152] B. V. Jacquet, R. Salinas-Mondragon, H. Liang et al., "FoxJ1-dependent gene expression is required for differentiation of radial glia into ependymal cells and a subset of astrocytes in the postnatal brain," *Development*, vol. 136, no. 23, pp. 4021–4031, 2009.

[153] M. Tavazoie, L. Van der Veken, V. Silva-Vargas et al., "A specialized vascular niche for adult neural stem cells,," *Cell Stem Cell*, vol. 3, no. 3, pp. 279–288, 2008.

[154] S. Pennartz, R. Belvindrah, S. Tomiuk et al., "Purification of neuronal precursors from the adult mouse brain: comprehensive gene expression analysis provides new insights into the control of cell migration, differentiation, and homeostasis," *Molecular and Cellular Neuroscience*, vol. 25, no. 4, pp. 692–706, 2004.

Hindawi Publishing Corporation
BioMed Research International
Volume 2015, Article ID 923861, 10 pages
http://dx.doi.org/10.1155/2015/923861

Research Article

Gray and White Matter Volumes and Cognitive Dysfunction in Drug-Naïve Newly Diagnosed Pediatric Epilepsy

Jung Hwa Lee,[1,2] Song E. Kim,[1] Chang-hyun Park,[1] Jeong Hyun Yoo,[3] and Hyang Woon Lee[1]

[1]*Department of Neurology, Ewha Womans University School of Medicine and Ewha Medical Research Institute, Seoul 158-710, Republic of Korea*
[2]*Department of Neurology, Samsung Changwon Hospital, Sungkyunkwan University School of Medicine, Changwon 630-723, Republic of Korea*
[3]*Department of Radiology, Ewha Womans University School of Medicine and Ewha Medical Research Institute, Seoul 158-710, Republic of Korea*

Correspondence should be addressed to Hyang Woon Lee; leeh@ewha.ac.kr

Received 27 June 2014; Revised 20 April 2015; Accepted 21 June 2015

Academic Editor: Marco Giannelli

Epilepsy patients often have cognitive dysfunction even at early stages of disease. We investigated the relationship between structural findings and neuropsychological status in drug-naïve newly diagnosed pediatric epilepsy patients. Thirty newly diagnosed pediatric epilepsy patients and 25 healthy control subjects aged 7~16 years were enrolled, who were assessed by the Korean version of the Wechsler Intelligence Scale for Children (K-WISC-III), the Stroop test, and the trail making test (TMT). Optimized voxel-based morphometry (VBM) was performed for both Gray Matter (GM) and White Matter (WM) volumes. Lower performance levels of verbal intelligence quotient, freedom from distractibility, and executive function were observed in epilepsy group. Interestingly, poor performance in these cognitive subdomains was correlated with regional VBM findings involving both GM and WM volumes, but with different patterns between groups. GM volumes revealed clear differences predominantly in the bilateral frontal regions. These findings indicate that certain cognitive functions may be affected in the early stage of epilepsy, not related to the long-standing epilepsy or medication, but more related to the neurocognitive developmental process in this age. Epilepsy can lead to neuroanatomical alterations in both GM and WM, which may affect cognitive functions, during early stages even before commencement of AED medication.

1. Introduction

Cognitive or intellectual function is an important issue in childhood epilepsy since epilepsy can have significant effects on the development and function of the immature brain. It has been reported that cognitive abilities, particularly verbal and nonverbal intelligence quotients (IQ) and executive function, are impaired in childhood epilepsy [1, 2]. Previous studies reported that cognitive impairments in epilepsy patients are related to various clinical factors such as the age at onset [1], longer duration or type of seizures [2], epileptic syndrome [3], and use of antiepileptic drugs (AEDs) [4]. However, a small number of studies showed that children with newly diagnosed epilepsy also have neuropsychological dysfunctions [5–8]. To obtain a clear perspective of the potential progressive and lifetime neuropsychological consequences of epilepsy, it is important to characterize cognitive impairments in pediatric patients with new-onset epilepsy before the AED medication. Interestingly, each epileptic syndrome tends to be associated with specific cognitive dysfunctions in children with new-onset epilepsy [7], for example, language dysfunction in benign childhood epilepsy with centrotemporal spikes (BECTS) [9], memory impairment in temporal lobe epilepsy [10], attention deficit disorder in absence epilepsy [11], and executive dysfunction in juvenile myoclonic epilepsy [12].

Many studies using quantitative analyses of structural magnetic resonance imaging (MRI), such as volumetry,

cortical thickness, and/or diffusion tensor imaging (DTI), have suggested structural brain abnormalities as the etiology of cognitive impairment in childhood epilepsy. Volumetric studies on pediatric epilepsy revealed abnormalities in the cerebrum [13], cerebellum, and hippocampus [14, 15] as well as temporal and extratemporal Gray Matter (GM) [16, 17]. In children and adolescents with epilepsy, cognitive and behavioral problems are significantly correlated with decreased cortical thickness in specific brain regions [18]. A recent study using DTI showed that White Matter (WM) abnormalities in the dominant frontal and temporal regions were related to language, executive function, and intelligence in BECTS [9]. Quantitative MR volumetry has been used to characterize the nature and pattern of brain abnormalities in adults with epilepsy, especially temporal lobe epilepsy, and volumetric abnormalities are one of the clinical consequences, as demonstrated by their relationship with impaired cognition [19–24]. However, there have been only a few volumetric studies conducted in children [6, 14, 15, 25]. Although there have been several studies in children and adolescents with epilepsy associated with neuropsychological abnormalities [6], the neuroanatomical basis is not fully understood yet. Examination of children at the time of epilepsy onset would help elucidate the neuroanatomical correlates of cognitive dysfunction in pediatric epilepsy. This study was performed to further extend this line of research by investigating (i) the neuropsychological status, especially intellectual ability and executive function before AED medication, (ii) regional GM and WM volumes in the epileptic brains, and (iii) association patterns between regional GM/WM volumes and cognitive function in patients with newly diagnosed pediatric epilepsy before AED administration.

2. Materials and Methods

2.1. Subjects. The study population consisted of 30 children and adolescents with drug-naïve newly diagnosed pediatric epilepsy. The inclusion criteria were (1) newly diagnosed epilepsy with no AED administration prior to participation; (2) seizure onset within 12 months based on history; (3) age between 7 and 16 years; and (4) attendance at standard schools. Diagnosis of epilepsy was made by expert neurologists (Jung Hwa Lee and Hyang Woon Lee) based on clinical, electroencephalographic (EEG), and MRI findings. The diagnosis of epileptic syndrome was based on the International League Against Epilepsy criteria [26]. Exclusion criteria were (1) developmental disabilities; (2) IQ < 70; and (3) any history of usage of medications acting on the central nervous system.

The control group included 25 normal children who were close friends of the index patients and were similar in age, gender, socioeconomic status, and educational level. Children with IQ < 70, a history of usage of medications acting on the central nervous system, no attendance at standard schools, a past or current history of neuropsychiatric disorders or head injury, or a first-degree relative with a history of epilepsy or febrile convulsions were excluded.

The patients with drug-naïve newly diagnosed epilepsy included 16 males and 14 females, with a mean age of 10.5 ± 2.9 years (Table 1). Of the 25 control subjects, 13 were male and 12 female, with a mean age of 11.1 ± 3.0 years. The average durations of education were 4.6 ± 3.1 and 4.9 ± 3.2 years in the patient and control groups, respectively. Twenty-one patients (21/30, 70%) were diagnosed as focal epilepsy, and the remaining nine patients (30%) were diagnosed as generalized epilepsy.

Table 1: Demographic data of the epilepsy and control groups.

Patient number	Epilepsy group		Control group
	Focal epilepsy	Generalized epilepsy	
Number of patients	21	9	25
Age (years)	10.5 ± 2.9		11.1 ± 3.0
Gender (M : F)	16 : 14		13 : 12
Education duration	4.6 ± 3.1 years		4.9 ± 3.2 years
Duration of epilepsy	3.4 ± 2.5 months		
Epileptic syndromes	BECTS 13 BCEOP 2 FLE 4 TLE 2	JME 5 CAE 2 JAE 1 IGE 1	

M: male; F: female; BECTS: benign childhood epilepsy with centrotemporal spikes, BCEOP: benign childhood epilepsy with occipital paroxysm, FLE: frontal lobe epilepsy, TLE: temporal lobe epilepsy, JME: juvenile myoclonic epilepsy, CAE: childhood absence epilepsy; JAE, juvenile absence epilepsy, IGE: idiopathic generalized epilepsy. Data are shown as means ± standard deviation.

Structural MRI and neuropsychological evaluations were performed in the patients at the time of diagnosis before commencement of AED medication. Signed informed consent was obtained for all participants from their parents or guardians. This study was approved by the Human Investigation Committee of the Ewha Womans University Medical Center.

2.2. Neuropsychological Assessment. All subjects underwent a comprehensive neuropsychological testing battery including (1) the Korean version of Wechsler Intelligence Scale for Children-III (K-WISC-III) standardized for Korean children and adolescents, consisting of 10 standard and 3 supplementary subsets, including full scale IQ, verbal IQ, and performance IQ, verbal comprehension (information, similarities, vocabulary, and comprehension), perceptual organization (picture completion, picture arrangement, block design, and object assembly), freedom from distractibility (coding, symbol search), and processing speed (coding and symbol search) [27, 28]; (2) the Stroop-color-word association test [29]; and (3) the trail making test (TMT) A and TMT B for Children [30]. Raw test scores were converted to age-adjusted scores. The reliability of the K-WISC-III was reported with Cronbach's alpha coefficients of 0.84, 0.92, and 0.68 for full scale IQ, verbal IQ, and performance IQ, respectively [28].

2.3. MRI Acquisition. MRI examinations were performed using a 3 T scanner (Philips Achieva v2.6, Best, Netherlands) in all subjects. Whole-brain 3D T1-weighted gradient echo images were acquired for each subject using the magnetization-prepared rapid acquisition with gradient echo (MPRAGE) sequence (TR = 1160 ms, TE = 4.19 ms,

TI = 600 ms, field of view = 140 × 250 mm^2, matrix size = 256 × 192, slice thickness = 1.2 mm, and flip angle = 15°), yielding 130~140 contiguous coronal slices depending on the head size with a defined voxel size of 0.94 × 0.94 × 1.2 mm^3. Together with the volumetric data, T1-weighted axial, T2-weighted axial/oblique coronal, and FLAIR axial/oblique coronal images were also acquired as part of an epilepsy MRI protocol (5 mm thickness for each sequence).

2.4. Voxel-Based Morphometry. Optimized voxel-based morphometry (VBM) was used for quantitative analysis of MRI, similarly to previous studies [31, 32] using SPM8 (Wellcome Trust Centre for Neuroimaging, http://www.fil.ion.ucl.ac.uk) implemented in MATLAB 7.3 (The MathWorks, Natick, MA, USA). Following the standard protocol, VBM analysis was performed in the following order [33–35].

Since we included subjects with wide range of age, we created a customized template appropriate to the population samples [34, 35]. Each image was spatially normalized to the standard MNI template included in SPM8. The normalized image was then smoothed with a 6-mm full width at half maximum (FWHM) Gaussian kernel, and a mean image was created as the study-specific template.

For spatial normalization, all images in native space were transformed to the same stereotactic space by registering each to the template image. We followed the normalization procedure in SPM8 using default options. That is, the affine registration that determined the optimum 12 parameters was followed by estimating nonlinear deformations defined by a linear combination of three-dimensional discrete cosine transform [36]. According to the default options, each of the deformation fields was described by 1176 parameters that represented coefficients of the deformations in three orthogonal directions. The spatially normalized images were resliced to a final voxel size of 1 mm^3 to yield more accurate subsequent tissue segmentation [37].

The normalized images were then segmented into GM, WM, and CSF. With a mixture model clustering algorithm, voxel intensities matching particular tissue types were identified. The segmentation step also incorporated correction for image intensity nonuniformity [38].

Finally, the normalized, segmented images were smoothed using a 10-mm FWHM Gaussian kernel. This made the images conform more closely to the Gaussian random field model [38], which supported inferences about regionally specific effects in subsequent statistical analysis.

2.5. Statistical Analysis. The neuropsychological test scores were compared between the patient and control groups after adjustment for age and gender using multivariate analysis of covariance (MANCOVA). Education level was not adjusted since all of the subjects in both patient and control groups were enrolled for Korean standard education system and the duration of education years did not show any difference between the groups. Wilcoxon's signed rank test was used for comparison of the focal and generalized epilepsy groups. We also examined other clinical factors including EEG focus/lateralization, age at onset, type of seizures, and seizure frequency for their effects on cognitive functions using ANOVA. Statistical analyses were performed using SPSS version 12.0 (SPSS Inc., Chicago, IL, USA). In all analyses, $P < 0.05$ was taken to indicate statistical significance, and F values with Cohen's d distributions were presented for each cognitive domain.

For statistical analysis of VBM, analysis of covariance (ANCOVA) was applied for voxelwise comparison of GM and WM volumes between the epilepsy and control groups, with age and gender as confounding covariates. The false discovery rate (FDR) was applied to correct for multiple comparisons at $P < 0.05$ [39] and the contiguous voxel extent threshold was set to 100 voxels. The anatomical localization of significant clusters was identified using Talairach coordinates [40].

To investigate the relationship between VBM GM/WM volumes and psychological performance scores, a general linear model was applied. First, the values of each voxel in GM and WM were extracted separately as the "volume of interest" (VOI), without designating a priori assumption by choosing specific brain regions, and then correlated with cognitive test scores, using partial correlation coefficients with correction for age and gender, in the epilepsy and control groups, respectively. For group differences from VBM, age and gender were adjusted as covariates of no interest, and FDR correction with the same extent threshold of 100 contiguous voxels was used for statistical significance ($P < 0.05$).

3. Results

3.1. Analysis of Neuropsychological Tests. Table 2 provides a comparison of neuropsychological performance between the control and epilepsy groups. The epilepsy group had lower verbal IQ and freedom from distractibility mean scores, as well as longer response times in the Stroop-color and Stroop-color-word tests compared with controls ($P < 0.05$). There were similar trends of decreased scores in most cognitive subdomains especially verbal comprehension, perceptual organization, or processing speed. To determine whether there were distinctive neuropsychological performance patterns between the different epileptic syndromes, focal and generalized epilepsy groups were also compared. Patients with focal epilepsy showed lower verbal IQ scores compared with generalized epilepsy patients. Similarly, perceptual organization tended to be lower in focal epilepsy than generalized epilepsy group. There were no other significant differences in each cognitive domain between the different epileptic syndromes (Table 3). There were no significant associations in other clinical factors including EEG focus/lateralization, age at onset, type of seizures, and epileptic syndrome.

3.2. Analysis of Voxel-Based Morphometry. Optimized VBM analysis was performed in 30 epilepsy patients and 25 control subjects to compare cerebral GM and WM volumes. Most prominently, GM volume was decreased in the left inferior frontal and right middle frontal gyri of the patients compared with the controls (corrected $P < 0.001$) (Figures 1(a) and 1(b)). Detailed x, y, z coordinates and more information were summarized in Table 4.

Table 2: Comparison of neuropsychological performance between control and epilepsy patient groups.

Cognitive test domain	Control	Epilepsy	F	Cohen's d	P value
Full scale IQ	110.05 ± 18.3	106.82 ± 16.72	2.038	0.184	0.160
Verbal IQ	106.1 ± 15.77	101.39 ± 15.57	4.138	0.301	0.048*
Performance IQ	109.38 ± 18.27	105.12 ± 16.93	3.286	0.242	0.076
Verbal comprehension	109.05 ± 18.15	105.27 ± 16.78	3.183	0.216	0.081
Perceptual organization	108.1 ± 14.76	104.06 ± 15.07	3.602	0.271	0.064
Freedom from distractibility	112.1 ± 18.92	107.57 ± 17.2	3.946	0.249	0.047*
Processing speed	99.05 ± 15.96	94.27 ± 14.8	3.434	0.311	0.070
Stroop-color (RT, s)	13.7 ± 9.6	27.4 ± 17.5	6.071	0.947	0.018*
Stroop-color (no. of errors)	0.35 ± 0.59	0.48 ± 0.77	0.534	0.190	0.469
Stroop-cw (RT, s)	24.4 ± 15.13	27.38 ± 17.47	0.033	0.182	0.857
Stroop-cw (no. of errors)	0.59 ± 0.83	1.21 ± 1.77	3.205	0.513	0.081
TMT-A (RT, s)	24.85 ± 10.11	30.02 ± 14.17	1.224	0.420	0.276
TMT-B (RT, s)	71.85 ± 32.43	92.79 ± 60.81	1.166	0.430	0.287

IQ: intelligence quotient, Stroop-cw: Stroop-color-word test, RT: response time, s: seconds, no.: number, and TMT: trail making test, data shown as mean ± standard deviation, * $P < 0.05$ by MANCOVA.

Table 3: Comparison of neuropsychological performance between generalized and focal epilepsy groups.

Cognitive test domain	Generalized epilepsy	Focal epilepsy	F	Cohen's d	P value
Full scale IQ	103.78 ± 17.97	104.57 ± 15.44	0.004	0.047	0.952
Verbal IQ	105.89 ± 17.05	98.1 ± 14.81	4.593	0.488	0.042*
Performance IQ	105.22 ± 19.04	102.13 ± 15.54	0.753	0.178	0.394
Verbal comprehension	100.89 ± 19.37	102.63 ± 15.51	0.079	0.099	0.781
Perceptual organization	108.11 ± 16.68	101.23 ± 14.88	3.945	0.435	0.058
Freedom from distractibility	101 ± 14.07	104.4 ± 15.44	0.348	0.230	0.561
Processing speed	95.11 ± 10.87	90.93 ± 13.19	0.968	0.346	0.334
Stroop-color (RT, s)	16.2 ± 6.16	15.98 ± 5.43	2.584	0.038	0.125
Stroop-color (errors)	0.35 ± 0.59	0.48 ± 0.77	0.294	0.190	0.594
Stroop-cw (RT, s)	24.4 ± 15.13	27.38 ± 17.47	1.022	0.182	0.325
Stroop-cw (errors)	0.5 ± 0.83	1.21 ± 1.77	1.753	0.514	0.202
TMT-A (RT, s)	24.85 ± 10.11	30.02 ± 14.17	0.054	0.420	0.818
TMT-B (RT, s)	71.85 ± 32.43	92.79 ± 60.81	2.277	0.430	0.149

IQ: intelligence quotient, Stroop-cw: Stroop-color-word test, RT: response time, s: seconds, no.: number, and TMT: trail making test, data shown as mean ± standard deviation, * $P < 0.05$ by MANCOVA.

3.3. Relationships between Cognition and VBM Findings. In whole-brain voxel correlation analysis using three cognitive variables with significant group differences, lower verbal IQ scores were correlated with decreased GM volumes in the left superior temporal and anterior cingulate gyri and decreased WM volumes in the left superior temporal and the right parahippocampal gyri in the control group (corrected $P < 0.001$) (Figure 1(c)). However, no correlations were found between the verbal IQ score and GM/WM volumes in the epilepsy group. Detailed x, y, z coordinates and more information were summarized in Table 5.

In addition, lower scores in freedom from distractibility were correlated with decreased WM volumes in the left frontal subgyral area, precuneus, and the superior parietal lobule as well as the right parahippocampal and middle temporal gyri in the control group (corrected $P < 0.05$) (Figure 2(a) and Table 5). However, lower scores in freedom from distractibility were correlated with decreased GM volumes in the left postcentral gyrus in the epilepsy group (corrected $P = 0.033$) (Figures 2(b), 2(c) and Table 5).

A longer response time in the Stroop-color test was correlated with decreased GM volume of the right posterior lobe and decreased WM volumes of the right frontal subgyral and insular areas and part of the left sublobar region in the control group (corrected $P < 0.01$) (Figure 3(a) and Table 5). In contrast, a correlation between Stroop-color test response time and GM volume was observed only in the right superior temporal gyrus in the epilepsy group (corrected $P = 0.033$) (Figures 3(b), 3(c) and Table 5). No significant correlations were observed for other cognitive variables in either the control or the epilepsy group.

4. Discussion

Using neuropsychological tests and VBM, we investigated the neuropsychological status and structural brain alterations

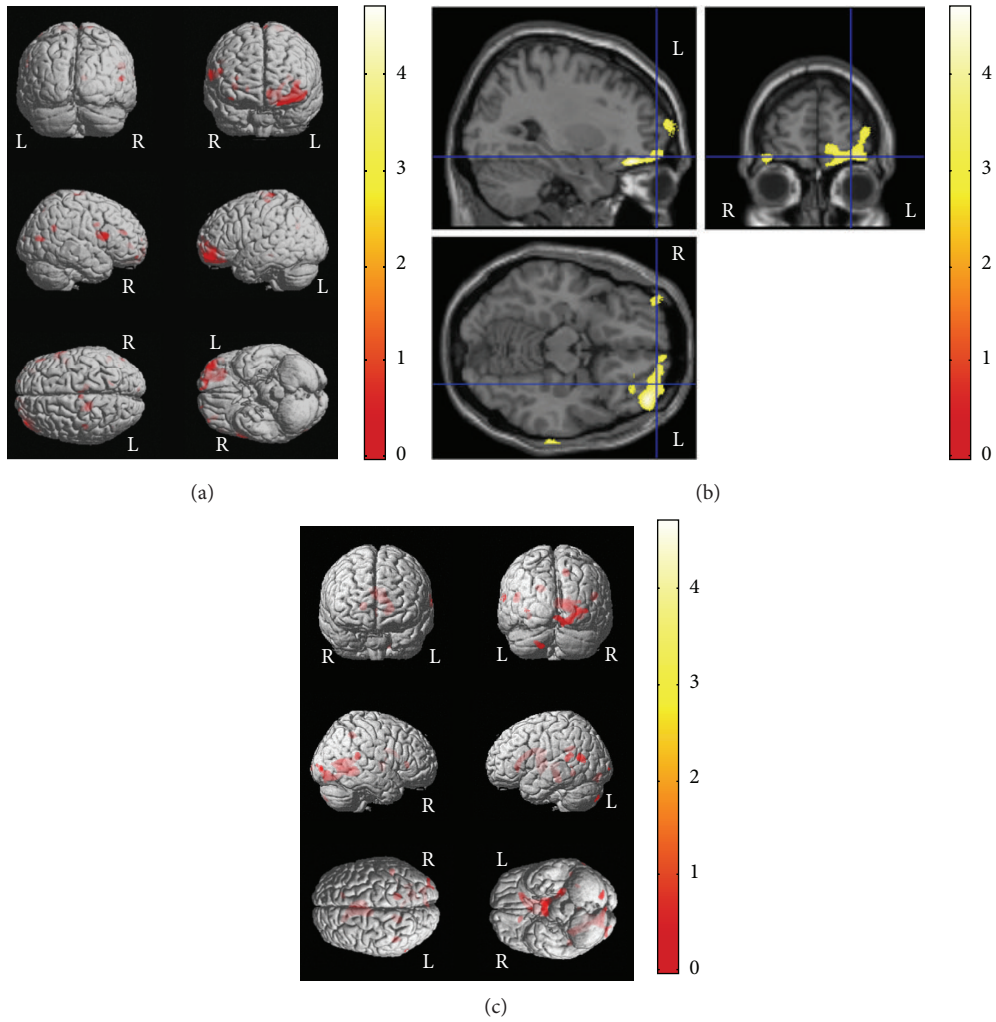

Figure 1: VBM results of brain regional differences between patients with newly diagnosed pediatric epilepsy and control subjects and correlations between VBM results and cognitive functions in control subjects. Patients with newly diagnosed pediatric epilepsy showed VBM abnormalities in both GM and WM areas compared with control subjects at the time of diagnosis, which suggests these could be more related to the epilepsy itself rather than long-standing seizures or medication effects. GM volumes were decreased in the left inferior frontal and right middle frontal gyri in epilepsy patients compared with control subjects ((a) and (b)). In addition, association patterns between structural findings and cognitive functions showed clear difference between groups; that is, decreased verbal IQ scores were correlated with decreased GM volumes in the left superior temporal and anterior cingulate gyri and decreased WM volumes in the left superior temporal and the right parahippocampal gyri in control subjects (c), but no correlation was observed in epilepsy patients. Please also note Tables 4 and 5 for x, y, z coordinates and more detailed information. L, left; R, right.

Table 4: Brain regions that showed group differences between the control and epilepsy groups for Figures 1(a) and 1(b).

Group difference	Anatomical regions	Coordinate			Cluster size	Cluster-level corrected P value
		(x	y	z)		
Control > Epilepsy	Left inferior frontal gyrus, Gray Matter	−17	13	21	5261	<0.001
	Right middle frontal gyrus, Gray Matter	26	40	−19	2191	<0.001

Control > Epilepsy means the brain areas that showed more decreased VBM values in the epilepsy group compared with those in the control group.

in children and adolescents with drug-naïve newly diagnosed epilepsy. In addition, we characterized the relationship between each cognitive domain and specific brain region. Patients with newly diagnosed pediatric epilepsy showed (i) poor performance in several cognitive domains, verbal IQ, freedom from distractibility scores, and response time of the Stroop-color test; (ii) decreased GM volume in the left inferior frontal and right middle frontal gyri; and (iii) distinct association patterns between structural findings and cognitive functions for freedom from distractibility and Stroop test

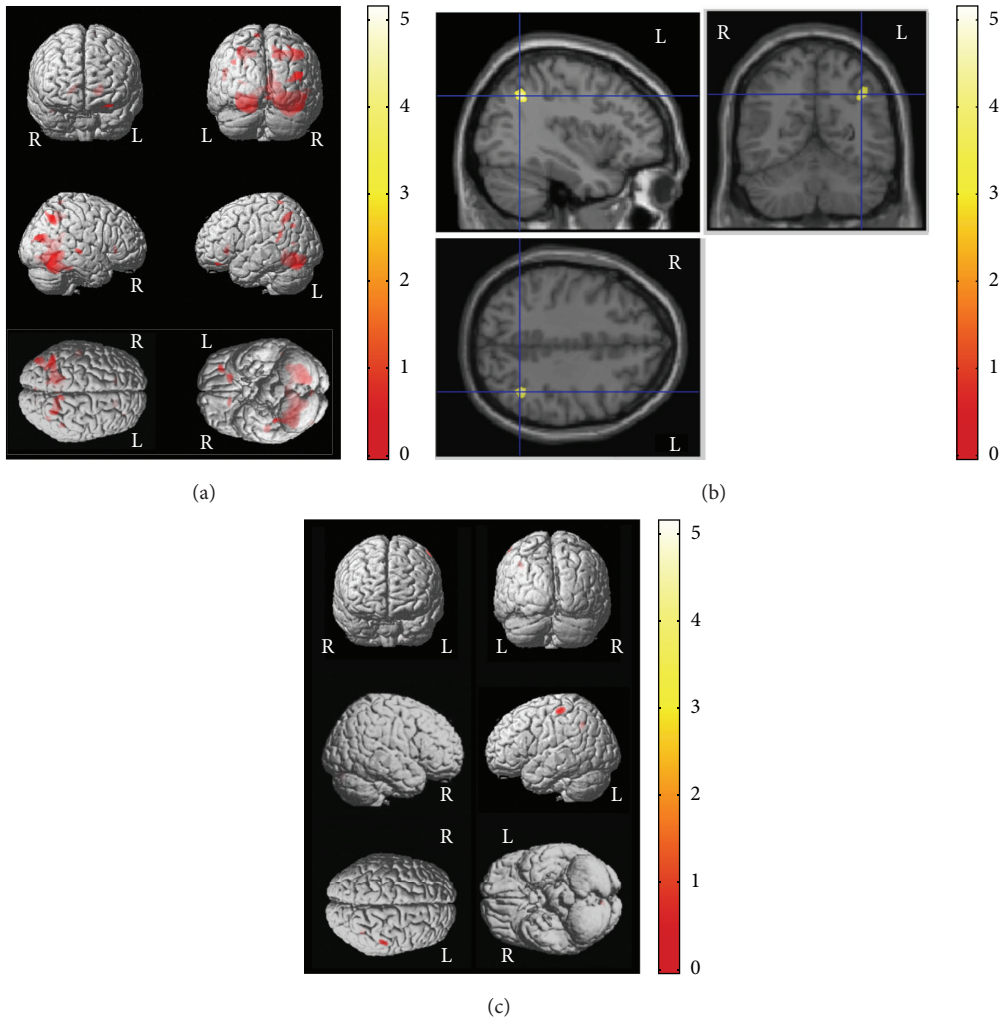

Figure 2: Correlations between VBM results and cognitive functions in patients with newly diagnosed pediatric epilepsy and control subjects. Association patterns between structural findings and cognitive functions showed some differences between the groups. Lower scores in freedom from distractibility were correlated with decreased WM volumes in the right parahippocampal and the middle temporal gyri and the left frontal subgyral, precuneus, and the superior parietal lobule areas in the control group (corrected $P < 0.001$) (a). However, lower scores in freedom from distractibility were correlated with decreased GM volumes in the left postcentral gyrus in the epilepsy group (corrected $P = 0.033$) ((b) and (c)). Please also note Table 5 for x, y, z coordinates and more detailed information. L, left; R, right.

performance compared with those in control subjects. These findings suggest that cognitive functions, especially verbal IQ, freedom from distractibility, and executive function, could be affected in pediatric epilepsy patients at the time of diagnosis, not related to the long-standing epilepsy and/or AED medication effects but more related to the early insult from epilepsy itself in the rapidly growing young brain, especially in the frontal regions.

As we mentioned already, this study was performed in drug-naïve childhood and adolescents with newly diagnosed epilepsy before they started AED medication. Similar to previous studies in new-onset epilepsy [6, 8], neuropsychological dysfunction in several cognitive subdomains and executive function in newly diagnosed epilepsy patients in the present study cannot be explained by disease duration or AEDs, as all evaluations were performed before commencement of AED administration. These findings support previous reports that the neuropsychological status in children and adolescents with epilepsy seems to be affected at a very early stage of the disease, even before AED treatment. In fact, most cognitive domains showed similar tendency of impairment in epilepsy patients compared with control subjects, including significant differences in verbal IQ, freedom from distractibility, Stroop test, and marginal significance in verbal comprehension, perceptual organization, and processing speed. In subgroup analyses, patients with focal epilepsy showed lower verbal IQ scores and similar trend of lower perceptual organization score compared with those with generalized epilepsy. One possible reason for this may be that the majority of focal epilepsy was BECTS, which is reportedly related to early involvement of language dysfunction mainly affecting the dominant hemisphere [9, 41].

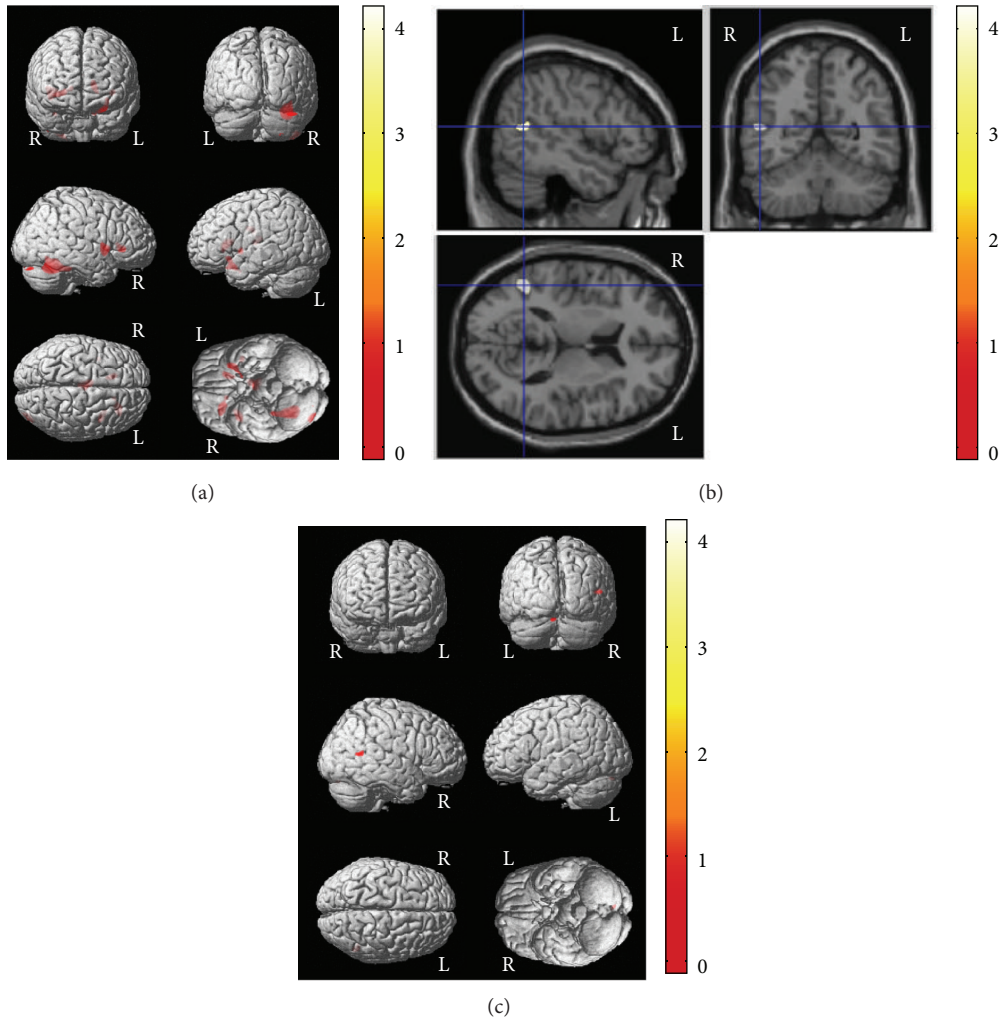

Figure 3: Correlations between VBM results and cognitive functions in patients with newly diagnosed pediatric epilepsy and control subjects. Association patterns between structural findings and cognitive functions showed clear differences between the groups. In the control group, poor performance in the Stroop-color test (longer response time) was correlated with decreased GM volume in the right posterior lobe and decreased WM volumes of the right frontal subgyral and insular areas and the left sublobar region (a). In contrast, in the epilepsy group, a longer response time in the Stroop-color test was correlated with decreased GM volume only of the right superior temporal gyrus in the epilepsy group ((b) and (c)). Please also note Table 5 for x, y, z coordinates and more detailed information. L, left; R, right.

In this study, we also investigated the possible associations between cognitive dysfunctions and regional GM/WM volumes in patients with newly diagnosed pediatric epilepsy. In the present study, the most prominent structural abnormalities observed in newly diagnosed pediatric epilepsy were decreased GM volumes in the bilateral frontal areas, especially the left inferior frontal and right middle frontal gyri. Based on the results of this study and previous VBM studies in pediatric epilepsy, predominant frontal structural abnormalities may be a common pattern of pediatric epilepsy across various epileptic syndromes. Several possible mechanisms may account for why these abnormalities are observed mainly in the frontal area. First, direct tissue damage due to recurrent epileptic discharges may be possible since the frontal lobe occupies the largest volume of the brain. Second, cortical damage may result from an interaction between brain development and seizures. The areas most vulnerable to damage could be those that are not only connected to an epileptogenic region, but also undergoing a period of rapid development [42]. Different brain areas undergo peaks in growth and maturation at different stages [43], and frontal regions are also known to undergo marked structural changes, especially in cortical thickness during adolescence as a result of pruning. As this study included adolescents, the frontal lobe may be the most vulnerable area affected by seizures. This would require further validation, possibly via longitudinal studies in patients of a more restricted age range.

Several studies indicated significant correlations between general intelligence and regional GM density or volume [44, 45]. In the present study, poor performance in several cognitive subdomains was correlated with regional VBM abnormalities with clear differences between the control and

Table 5: Brain regions correlated with intelligence scores in the control and epilepsy groups for Figures 1(c), 2, and 3.

Group	Cognitive subdomain	Anatomical regions	Coordinate (x y z)			Cluster size	Cluster-level corrected P value
Control	Verbal IQ	Left superior temporal gyrus, Gray Matter	−67	−62	14	1983	<0.001
		Left anterior cingulate gyrus, Gray Matter	−46	−44	15	721	<0.001
		Left superior temporal gyrus, White Matter	−16	−44	26	934	<0.001
		Right parahippocampal gyrus, White Matter	32	−48	−3	13973	<0.001
Control	Freedom from distractibility	Left frontal lobe, Subgyral, White Matter	−17	28	−2	851	<0.001
		Left parietal lobe, precuneus, White Matter	17	−58	42	4952	0.016
		Left superior parietal lobule, White Matter	−28	−55	45	2208	<0.001
		Right parahippocampal gyrus, White Matter	32	−51	−6	36365	<0.001
		Right middle temporal gyrus, White Matter	38	−72	19	2015	<0.001
Control	Stroop-color	Right posterior lobe, Gray Matter	33	−59	−27	4779	<0.001
		Right frontal lobe, Subgyral, White Matter	23	30	0	1034	0.005
		Right insular, White Matter	40	8	−2	1360	0.001
		Left cerebrum, Sublobar, White Matter	−2	−13	15	2472	<0.001
Epilepsy	Freedom from distractibility	Left postcentral gyrus, Gray Matter	−53	−28	60	766	0.033
Epilepsy	Stroop-color	Right superior temporal gyrus, Gray Matter	19	−54	12	475	0.033

IQ: intelligence quotient.

epilepsy groups. Lower scores in freedom from distractibility were correlated with decreased WM volumes of the left frontal subgyral area, precuneus, and superior parietal lobule and the right parahippocampal and middle temporal gyri in the control group, whereas the correlation was only observed in the GM volume of the left postcentral gyrus in the epilepsy group. In addition, longer response time in the Stroop-color test was correlated with decreased GM volume in the right posterior lobe and decreased WM volumes especially in the right frontal subgyral and insular regions in the control group. In contrast, this kind of correlation was observed only in GM volume of the right superior temporal gyrus in the epilepsy patients. These findings suggested potential early involvement of their cognitive dysfunction associated with neuroanatomical abnormalities developing early in the course of disease progression in newly diagnosed pediatric epilepsy.

The present study had several limitations. Differences in various epileptic syndromes could not be detected as the numbers of patients with each syndrome were insufficient for separate analyses. Future long-term prospective investigations with larger patient populations and individualized studies in each epileptic syndrome are required. This study focused mainly on intellectual ability and executive function due to time restrictions, since we aimed to perform all investigations before commencement of AEDs. All patients in the epilepsy group were attending standard schools in order to compare them with control subjects of similar educational levels. Patients who are not attending school are also worth evaluating, as they may have higher rates of various behavioral and academic problems and/or learning disabilities. Further investigations of newly diagnosed epilepsy patients with distinct epilepsy syndromes including careful prospective study designs with longitudinal follow-up of the same patient groups would be beneficial to identify more clear understanding of neuropsychological, behavioral, academic/learning problems of these patients. Another promising approach could be more advanced imaging methods accompanied by technical improvement by means of the advanced image registration algorithm, for instance, tensor-based morphometry using DARTEL algorithm [46] for more sensitive detection of subtle and early neuroanatomical alterations in future longitudinal studies.

5. Conclusion

In summary, we evaluated neuropsychological performance and relationships with respect to GM and WM volumes demonstrated by optimized VBM analysis in children and adolescents with newly diagnosed epilepsy. Pediatric epilepsy patients showed poorer performance in verbal IQ, freedom from distractibility, and executive function at the time of epilepsy diagnosis before commencement of AEDs. GM volumes revealed clear differences predominantly in the bilateral frontal regions. These findings indicate that cognitive functions, especially verbal IQ and executive function, may be affected in the early stage of epilepsy, not related to the long-standing epilepsy or AED medication but more related to the neurocognitive developmental process in these young pediatric age groups.

Disclosure

The authors confirm that they have read the journal's position on issues involved in ethical publication and affirm that this report is consistent with those guidelines.

Conflict of Interests

The authors declare that there is no conflict of interests regarding the publication of this paper.

Acknowledgments

This study was supported by the grant of the Korea Healthcare Technology R&D Project, Ministry for Health, Welfare & Family Affairs, Republic of Korea (hpeb 2009 A091183) and Samsung Biomedical Research Institute grant to J. H. Lee, and supported by grants of the Korea Health Technology R&D Project through the Korea Health Industry Development Institute (KHIDI), funded by the Ministry of Health & Welfare (HI14C1989), and the Basic Science Research Program through the National Research Foundation of Korea (NRF) funded by the Ministry of Education, Science and Technology (NRF-R01-2011-0015788 and NRF-2014R1A2A1A11052103) to H. W. Lee.

References

[1] C. E. Elger, C. Helmstaedter, and M. Kurthen, "Chronic epilepsy and cognition," *The Lancet Neurology*, vol. 3, no. 11, pp. 663–672, 2004.

[2] G. Vingerhoets, "Cognitive effects of seizures," *Seizure*, vol. 15, no. 4, pp. 221–226, 2006.

[3] S. C. Tromp, J. W. Weber, A. P. Aldenkamp, J. Arends, I. vander Linden, and L. Diepman, "Relative influence of epileptic seizures and of epilepsy syndrome on cognitive function," *Journal of Child Neurology*, vol. 18, no. 6, pp. 407–412, 2003.

[4] P. Rzezak, D. Fuentes, C. A. Guimarães et al., "Frontal lobe dysfunction in children with temporal lobe epilepsy," *Pediatric Neurology*, vol. 37, no. 3, pp. 176–185, 2007.

[5] P. S. Fastenau, C. S. Johnson, S. M. Perkins et al., "Neuropsychological status at seizure onset in children: risk factors for early cognitive deficits," *Neurology*, vol. 73, no. 7, pp. 526–534, 2009.

[6] B. Hermann, J. Jones, R. Sheth, C. Dow, M. Koehn, and M. Seidenberg, "Children with new-onset epilepsy: neuropsychological status and brain structure," *Brain*, vol. 129, part 10, pp. 2609–2619, 2006.

[7] B. P. Hermann, J. E. Jones, D. C. Jackson, and M. Seidenberg, "Starting at the beginning: the neuropsychological status of children with new-onset epilepsies," *Epileptic Disorders*, vol. 14, no. 1, pp. 12–21, 2012.

[8] K. J. Oostrom, A. Smeets-Schouten, C. L. J. J. Kruitwagen, A. C. B. Peters, and A. Jennekens-Schinkel, "Not only a matter of epilepsy: early problems of cognition and behavior in children with 'epilepsy only'—a prospective, longitudinal, controlled study starting at diagnosis," *Pediatrics*, vol. 112, no. 6 I, pp. 1338–1344, 2003.

[9] S. E. Kim, J. H. Lee, H. K. Chung, S. M. Lim, and H. W. Lee, "Alterations in white matter microstructures and cognitive dysfunctions in benign childhood epilepsy with centrotemporal spikes," *European Journal of Neurology*, vol. 21, no. 5, pp. 708–717, 2014.

[10] B. Bell, J. J. Lin, M. Seidenberg, and B. Hermann, "The neurobiology of cognitive disorders in temporal lobe epilepsy," *Nature Reviews Neurology*, vol. 7, no. 3, pp. 154–164, 2011.

[11] R. Caplan, P. Siddarth, L. Stahl et al., "Childhood absence epilepsy: behavioral, cognitive, and linguistic comorbidities," *Epilepsia*, vol. 49, no. 11, pp. 1838–1846, 2008.

[12] T. F. Pascalicchio, G. M. D. A. Filho, M. H. D. S. Noffs et al., "Neuropsychological profile of patients with juvenile myoclonic epilepsy: a controlled study of 50 patients," *Epilepsy & Behavior*, vol. 10, no. 2, pp. 263–267, 2007.

[13] B. P. Hermann, K. Dabbs, T. Becker et al., "Brain development in children with new onset epilepsy: a prospective controlled cohort investigation," *Epilepsia*, vol. 51, no. 10, pp. 2038–2046, 2010.

[14] J. A. Lawson, S. Vogrin, A. F. Bleasel et al., "Predictors of hippocampal, cerebral, and cerebellar volume reduction in childhood epilepsy," *Epilepsia*, vol. 41, no. 12, pp. 1540–1545, 2000.

[15] J. A. Lawson, M. J. Cook, S. Vogrin et al., "Clinical, EEG, and quantitative MRI differences in pediatric frontal and temporal lobe epilepsy," *Neurology*, vol. 58, no. 5, pp. 723–729, 2002.

[16] F. Cormack, D. G. Gadian, F. Vargha-Khadem, J. H. Cross, A. Connelly, and T. Baldeweg, "Extra-hippocampal grey matter density abnormalities in paediatric mesial temporal sclerosis," *NeuroImage*, vol. 27, no. 3, pp. 635–643, 2005.

[17] K. Dabbs, J. E. Jones, D. C. Jackson, M. Seidenberg, and B. P. Hermann, "Patterns of cortical thickness and the Child Behavior Checklist in childhood epilepsy," *Epilepsy and Behavior*, vol. 29, no. 1, pp. 198–204, 2013.

[18] S. A. Baxendale, W. van Paesschen, P. J. Thompson et al., "The relationship between quantitative MRI and neuropsychological functioning in temporal lobe epilepsy," *Epilepsia*, vol. 39, no. 2, pp. 158–166, 1998.

[19] N. Bernasconi, S. Duchesne, A. Janke, J. Lerch, D. L. Collins, and A. Bernasconi, "Whole-brain voxel-based statistical analysis of gray matter and white matter in temporal lobe epilepsy," *NeuroImage*, vol. 23, no. 2, pp. 717–723, 2004.

[20] C. Dow, M. Seidenberg, and B. Hermann, "Relationship between information processing speed in temporal lobe epilepsy and white matter volume," *Epilepsy and Behavior*, vol. 5, no. 6, pp. 919–925, 2004.

[21] H. R. Griffith, R. W. Pyzalski, M. Seidenberg, and B. P. Hermann, "Memory relationships between MRI volumes and resting PET metabolism of medial temporal lobe structures," *Epilepsy and Behavior*, vol. 5, no. 5, pp. 669–676, 2004.

[22] B. Hermann, M. Seidenberg, L. Sears et al., "Cerebellar atrophy in temporal lobe epilepsy affects procedural memory," *Neurology*, vol. 63, no. 11, pp. 2129–2131, 2004.

[23] R. C. Martin, J. W. Hugg, D. L. Roth et al., "MRI extrahippocampal volumes and visual memory: correlations independent of MRI hippocampal volumes in temporal lobe epilepsy patients," *Journal of the International Neuropsychological Society*, vol. 5, no. 6, pp. 540–548, 1999.

[24] M. Seidenberg, K. G. Kelly, J. Parrish et al., "Ipsilateral and contralateral MRI volumetric abnormalities in chronic unilateral temporal lobe epilepsy and their clinical correlates," *Epilepsia*, vol. 46, no. 3, pp. 420–430, 2005.

[25] J. A. Lawson, M. J. Cook, A. F. Bleasel, V. Nayanar, K. F. Morris, and A. M. E. Bye, "Quantitative MRI in outpatient childhood epilepsy," *Epilepsia*, vol. 38, no. 12, pp. 1289–1293, 1997.

[26] J. Engel Jr., "A proposed diagnostic scheme for people with epileptic seizures and with epilepsy: report of the ILAE task force on classification and terminology," *Epilepsia*, vol. 42, no. 6, pp. 796–803, 2001.

[27] K. W. Park, J. R. Yoon, H. J. Park, and K. W. Kim, *Manual for the Korean Education Development Institute-Wechsler Intelligence Scale for Children*, Korean Education Development Institute, Seoul, Republic of Korea, 1991.

[28] K. J. Kwak, H. W. Park, and C. T. Kim, "The standardization study for the Korean Wechsler intelligence scale for children—third edition (1): reliability and validity," *Korean Journal of Developmental Psychology*, vol. 15, no. 1, pp. 19–33, 2002.

[29] M. S. Shin, M. Park, and J. Stroop, *Stroop Color and Word Test: A Manual for Clinical and Experimental Uses*, Hakjisa, Seoul, Republic of Korea, 2007.

[30] J. B. Lee, J. S. Kim, W. S. Seo, H. J. Shin, D. S. Bai, and H. L. Lee, "The validity and reliability of computerized neurocognitive function test in the elementary school child," *Korean Journal of Psychosomatic Medicine*, vol. 11, pp. 97–117, 2003.

[31] C. D. Good, I. S. Johnsrude, J. Ashburner, R. N. A. Henson, K. J. Friston, and R. S. J. Frackowiak, "A voxel-based morphometric study of ageing in 465 normal adult human brains," *NeuroImage*, vol. 14, no. 1, part 1, pp. 21–36, 2001.

[32] G. R. Ridgway, S. M. D. Henley, J. D. Rohrer, R. I. Scahill, J. D. Warren, and N. C. Fox, "Ten simple rules for reporting voxel-based morphometry studies," *NeuroImage*, vol. 40, no. 4, pp. 1429–1435, 2008.

[33] S. S. Keller, M. Wilke, U. C. Wieshmann, V. A. Sluming, and N. Roberts, "Comparison of standard and optimized voxel-based morphometry for analysis of brain changes associated with temporal lobe epilepsy," *NeuroImage*, vol. 23, no. 3, pp. 860–868, 2004.

[34] U. Yoon, V. S. Fonov, D. Perusse, and A. C. Evans, "The effect of template choice on morphometric analysis of pediatric brain data," *NeuroImage*, vol. 45, no. 3, pp. 769–777, 2009.

[35] M. Wilke, V. J. Schmithorst, and S. K. Holland, "Assessment of spatial normalization of whole-brain magnetic resonance images in children," *Human Brain Mapping*, vol. 17, no. 1, pp. 48–60, 2002.

[36] J. Ashburner and K. J. Friston, "Voxel-based morphometry—the methods," *NeuroImage*, vol. 11, no. 6, pp. 805–821, 2000.

[37] J. H. Kim, J. K. Lee, S.-B. Koh et al., "Regional grey matter abnormalities in juvenile myoclonic epilepsy: a voxel-based morphometry study," *NeuroImage*, vol. 37, no. 4, pp. 1132–1137, 2007.

[38] K. J. Worsley, M. Andermann, T. Koulis, D. MacDonald, and A. C. Evans, "Detecting changes in nonisotropic images," *Human Brain Mapping*, vol. 8, no. 2-3, pp. 98–101, 1999.

[39] C. R. Genovese, N. A. Lazar, and T. Nichols, "Thresholding of statistical maps in functional neuroimaging using the false discovery rate," *NeuroImage*, vol. 15, no. 4, pp. 870–878, 2002.

[40] J. L. Lancaster, M. G. Woldorff, L. M. Parsons et al., "Automated Talairach atlas labels for functional brain mapping," *Human Brain Mapping*, vol. 10, no. 3, pp. 120–131, 2000.

[41] A. Verrotti, C. D'Egidio, S. Agostinelli, P. Parisi, F. Chiarelli, and G. Coppola, "Cognitive and linguistic abnormalities in benign childhood epilepsy with centrotemporal spikes," *Acta Paediatrica, International Journal of Paediatrics*, vol. 100, no. 5, pp. 768–772, 2011.

[42] G. L. Holmes, Y. Ben-Ari, and A. Zipursky, "The neurobiology and consequences of epilepsy in the developing brain," *Pediatric Research*, vol. 49, no. 3, pp. 320–325, 2001.

[43] N. Gogtay, J. N. Giedd, L. Lusk et al., "Dynamic mapping of human cortical development during childhood through early adulthood," *Proceedings of the National Academy of Sciences of the United States of America*, vol. 101, no. 21, pp. 8174–8179, 2004.

[44] S. Frangou, X. Chitins, and S. C. R. Williams, "Mapping IQ and gray matter density in healthy young people," *NeuroImage*, vol. 23, no. 3, pp. 800–805, 2004.

[45] M. Wilke, J.-H. Sohn, A. W. Byars, and S. K. Holland, "Bright spots: correlations of gray matter volume with IQ in a normal pediatric population," *NeuroImage*, vol. 20, no. 1, pp. 202–215, 2003.

[46] J. Ashburner, "A fast diffeomorphic image registration algorithm," *NeuroImage*, vol. 38, no. 1, pp. 95–113, 2007.

Hindawi Publishing Corporation
BioMed Research International
Volume 2015, Article ID 709230, 6 pages
http://dx.doi.org/10.1155/2015/709230

Research Article

The Cortisol Awakening Response in Patients with Poststroke Depression Is Blunted and Negatively Correlated with Depressive Mood

Oh Jeong Kwon,[1] Munsoo Kim,[2] Ho Sub Lee,[1] Kang-keyng Sung,[3] and Sangkwan Lee[1,3]

[1]*Hanbang Body-Fluid Research Center, Wonkwang University, Shinyong-dong, Iksan, Jeonbuk 570-749, Republic of Korea*
[2]*Department of Psychology, College of Social Sciences, Chonnam National University, Yongbong-dong 300, Buk-gu, Gwangju 500-757, Republic of Korea*
[3]*Department of Internal Medicine and Neuroscience, College of Oriental Medicine, Wonkwang University, 344-2 Shinyong-dong, Iksan, Chonbuk 570-749, Republic of Korea*

Correspondence should be addressed to Sangkwan Lee; sklee@wonkwang.ac.kr

Received 18 June 2014; Accepted 12 January 2015

Academic Editor: Diego Gazzolo

It is important to reduce poststroke depression (PSD) to improve the stroke outcomes and quality of life in stroke patients, but the underlying mechanisms of PSD are not completely understood. As many studies implicate dysregulation of hypothalamic-pituitary-adrenal axis in the etiology of major depression and stroke, we compared the cortisol awakening response (CAR) of 28 admitted PSD patients with that of 23 age-matched caregiver controls. Saliva samples for cortisol measurement were collected immediately, 15, 30, and 45 min after awakening for two consecutive days. Depressive mood status in PSD patients was determined with Beck Depression Inventory and Hamilton Depression Rating Scale. Salivary cortisol levels of PSD patients did not rise significantly at any sampling time, showing a somewhat flat curve. Caregiver controls showed significantly higher CAR at 15 and 30 min after awakening compared to PSD patients even though the two groups did not differ at awakening or 45 min after awakening. Area-under-the-curve analysis revealed a significant negative correlation between the CAR and the degree of depression in PSD patients. Thus, our findings suggest that poststroke depression is closely related with dysfunctional HPA axis indicated by blunted CAR.

1. Introduction

A stroke is the rapid loss of brain function due to disturbance in blood supply to the brain. This can be due to ischemia caused by blockage or hemorrhage [1]. Stroke patients suffer from deterioration of physical ability, but in many cases emotional problems such as depression also accompany the physical symptoms. Although prevalence of poststroke depression (PSD) varies depending on the patient population, the pooled prevalence of all types of PSD is estimated to be 25–47 and 35–72% from studies carried out in patients of acute and rehabilitation stages, respectively [2]. PSD has negative impact on rehabilitation processes, but the underlying mechanisms of PSD are not completely understood [3–5]. Several epidemiological studies have shown that PSD is associated with increased disability, and poor function and cognitive outcomes in stroke survivors [6, 7]. It is observed not only in disabled stroke patients but also in those who seem to be functionally independent in their activities of daily living [8]. Thus, it is important to reduce PSD to improve the stroke outcomes and quality of life in stroke patients.

Many studies implicate dysregulation of hypothalamic-pituitary-adrenal (HPA) axis in the etiology of major depression [9]. There is accumulating evidence that dysfunction of HPA axis is not just an epiphenomenon of depression, but instead endophenotype playing a key role in its pathophysiology [10, 11]. Recent investigations have looked at associations between depression and cortisol secretion, especially, the cortisol awakening response (CAR), defined as the period of cortisol secretory activity in the first 60 minutes after awakening [12]. Some studies found significantly lower CAR in individuals with major depression [13, 14] while others

found higher CAR [15, 16]. A prospective study suggests that the CAR is a better predictor of future depressive episodes when compared with other predictors [9]. Some studies suggested that an attenuated CAR may be present prior to the development of a formal diagnosis and is a biological risk factor playing a role in the pathophysiology of depression [17, 18].

Extensive studies on the relationship between cortisol secretion and stroke have found dysregulation of HPA axis function in stroke patients (e.g., [19, 20]). Also, in a recent study, we found that evening, but not morning, cortisol levels (at 8 pm) were higher in stroke patients compared to caregiver controls [21]. However, studies examining CAR in stroke patients are almost nonexistent.

Considering the involvement of HPA axis in depression and stroke, it would be interesting to see if PSD patients have altered HPA axis function. More specifically, PSD patients may show exaggerated CAR according to the general finding of hypercortisolemia in acute stroke patients, or reduced CAR according to some studies mentioned above. Thus, the present study investigated whether the CAR of PSD patients differs from a selected group of control subjects, and if so, how. Furthermore, we examined whether the magnitude of the CAR in PSD patients correlates with their depressive mood status.

2. Materials and Methods

2.1. Subjects. Participants whose stroke had happened at least 2 months before the present study were recruited from the Stroke Clinic of Wonkwang Gwangju Medical Center. Forty-nine PSD patients showing scores higher than 14 on Beck Depression Inventory II (BDI) or 7 on the Hamilton Depression Rating Scale (HDRS) were selected. Stroke was diagnosed with brain MRI. Additionally, we obtained records of neurological examinations and blood tests from all subjects. Four of these 49 patients had to be excluded because they were taking antidepressants or steroid drugs. Seventeen additional patients were excluded because of nonadherence to the sampling method or insufficient amount of saliva. Thus, the final study population consisted of 28 hospitalized stroke patients (15 males and 13 females; mean age 62.5 ± 7.9 y).

Twenty-eight age-matched patients' caregivers were initially recruited as control subjects from the same medical center. Five of these caregivers had to be excluded because of nonadherence to the sampling method (i.e., eating food or brushing teeth during sampling) or their saliva samples being reddish and contaminated with sputum. Thus, the final control population consisted of 23 caregivers (6 males and 17 females; mean age 58.2 ± 6.7 y). They lived together with their patients in our hospital. Our hospital provides space and instruments for caregivers to care for their patients closely. Thus, caregivers had schedules of daily activities similar to those of stroke patients, including sleep-awakening time, mealtime, and exercise. Caregiver controls were free of medication and did not have any neurological or psychiatric disorder at the time of testing. All participants gave informed consent. The study was approved by the Institutional Review Board of Wonkwang Gwangju Medical Center.

2.2. Measures

2.2.1. Salivary Cortisol Collection and Assay. Since all PSD patients were hospitalized in our stroke clinic, they had very similar daily schedules for care, including the duration of rehabilitation, mealtime, and sleep-awakening schedule. They were asked to go to bed before midnight and wake up at 06:00 h. If a patient was not awake at 06:00 h on the sampling day, he or she was awakened by his or her physician or caregiver and saliva was collected according to a fixed sampling protocol [22]. Each patient provided four saliva samples: the first immediately after awakening, the second 15 min, the third 30 min, and the fourth 45 min after awakening. Patients were asked to stay in bed for the duration of saliva sampling and refrain from eating and drinking.

Caregiver controls were instructed to follow the same sampling procedures as those described above for the stroke patients. They performed the saliva sampling in the same clinic under supervision. They were also instructed to keep the same sleep-awakening schedule for several days before the sampling day and to stay in bed and refrain from eating and drinking until sampling was completed. Samples were collected by the research staff or caregivers. For both patients and controls, saliva sampling was performed on two consecutive days.

For each sample, a minimum volume of 2 mL of saliva was collected. Samples were frozen at −80°C until assay. Free cortisol in saliva samples was determined using a competitive solid-phase radioimmunoassay (Coat-A-Count, Siemens, Medical Solutions Diagnostics, Los Angeles, CA) as previously described [23]. The intra- and interassay variability were below 7 and 8%, respectively. This solid phase RIA had analytical sensitivity of 5.5 nmol/L.

2.2.2. Evaluation of Depression. The Korean version of the BDI is a 21-item self-report test, one of the most widely used tools for measuring severity of depression. When presented with the BDI, subjects were asked to consider each statement as it relates to the way they have felt for the past two weeks. There is a four-point scale for each item, ranging from 0 to 3 [24]. Thus, a higher total score reflects more severe depressive mood status.

The Korean version of the HDRS is a clinician-administered 17-item multiple-choice questionnaire for rating severity of depression. It is currently one of the most commonly used scales for rating depression in medical research. Nine of the items are scored on a five-point scale, ranging from 0 to 4. The other eight items are scored on a three-point scale, from 0 to 2. A score of zero represents absence of depressive symptoms [25]. Thus, a higher total score reflects more severe depressive mood status.

BDI and HDRS were assessed on the first day saliva sampling took place.

2.3. Data Analysis. For each sampling point, cortisol levels were averaged for the two consecutive sampling days and

analyzed using a repeated-measures ANOVA with Group as between-subject and Sampling Time as within-subject factors. Additional analysis used Scheffé test to determine the source of the detected significance. In order to obtain indices for the CAR, the global area under the curve (AUCg) for total cortisol output and the area under the response (or increase) curve (AUCi) for the responsivity of the system were computed [26]. Pearson correlation coefficients were calculated to examine whether depressive mood status (i.e., BDI and HDRS scores) was linked to the AUCg or AUCi measures of the CAR. $P < 0.05$ was considered statistically significant for all comparisons.

3. Results

3.1. PSD Patients Show a Blunted Cortisol Awakening Response. Figure 1 shows salivary cortisol levels of PSD patients and caregiver controls after awakening. A repeated-measures ANOVA revealed significant main effects of Group ($F_{1,49} = 17.095$, $P < 0.001$) and Sampling Time ($F_{3,49} = 18.775$, $P < 0.001$), indicating that overall cortisol levels differed between the two groups and changed during the first 45 min after awakening. Also the Group × Sampling Time interaction was significant ($F_{3,47} = 13.098$, $P < 0.001$), indicating that the pattern of cortisol change across time differed between the groups.

At awakening, cortisol levels of PSD patients and caregiver controls did not differ. The amount of saliva cortisol of caregiver controls rose to a significantly higher level at 15 and 30 min after awakening compared to that immediately after awakening ($P < 0.001$ for both) and subsided to a marginally significant level at 45 min after awakening ($P < 0.07$). In contrast, cortisol level of PSD patients did not rise significantly at any sampling time, showing a somewhat flat curve. Increase in cortisol level only approached significance at 30 min after awakening ($P < 0.07$) in this group. Thus, while caregiver controls showed a normal CAR, the PSD patients did not.

The difference between cortisol levels of PSD patients and caregiver controls was significant at all sampling time points except for immediate postawakening ($t = 4.148$, $P < 0.001$; $t = 4.212$, $P < 0.001$; $t = 2.333$, $P < 0.03$, for 15, 30, and 45 min after awakening, resp.). Overall, this pattern of results indicates that PSD patients show a greatly blunted CAR.

Accordingly, the AUCi, reflecting the increase in cortisol level after awakening, of PSD patients was significantly smaller than that of the caregiver controls (PSD patients: 73.2 ± 21.8; caregiver controls: 311.4 ± 35.9; $t = 5.88$, $P < 0.001$). The AUCg, reflecting total cortisol output during the first 45 min after awakening, of PSD patients was also significantly smaller than that of the caregiver controls (PSD patients: 545.2 ± 22.3; caregiver controls: 782.4 ± 49.8; $t = 4.61$, $P < 0.001$).

3.2. The Cortisol Awakening Response of PSD Patients Correlates with Depressive Status. As shown in Figure 2, the AUCi for the cortisol response after awakening correlated significantly with both the BDI and HDRS scores of depressive mood status (for BDI, $r = -0.747$, $P < 0.001$; for HDRS, $r = -0.713$, $P < 0.001$), indicating that smaller AUCi values were associated with higher BDI or HDRS scores (i.e., more severe depressive status). Addition of the factors age or gender as a covariate into the analysis did not significantly alter the results.

The AUCg also correlated significantly with HDRS scores ($r = -0.448$, $P < 0.02$), although the correlation between AUCg and BDI scores did not reach significance ($r = -0.336$, $P < 0.1$) (Figure 3).

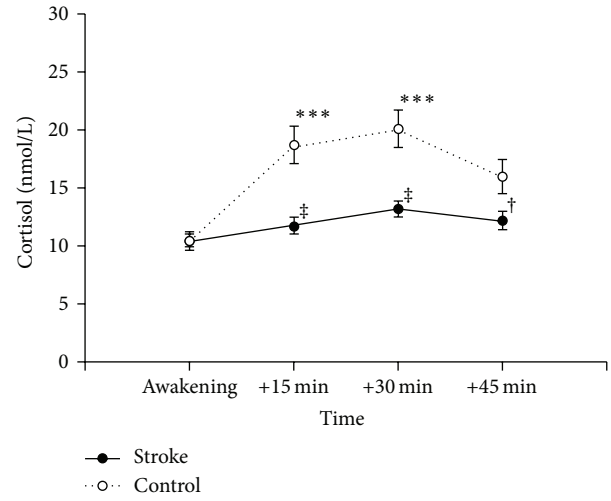

Figure 1: Cortisol awakening response of poststroke depression patients (stroke) and caregiver controls (control). Data points represent mean ± SEM. $^{***}P < 0.001$, different from Awakening. $^{‡}P < 0.001$ and $^{†}P < 0.03$, different from caregiver controls.

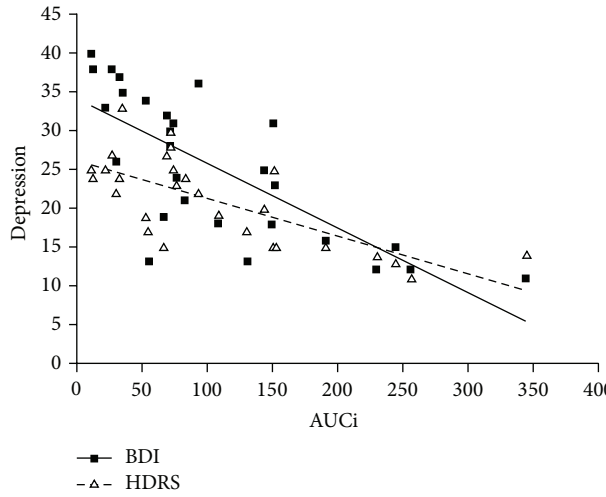

Figure 2: Association between the area under the response (or increase) curve (AUCi) and Beck Depression Inventory (BDI) or Hamilton Depression Rating Scale (HDRS) in poststroke depression patients ($r = -0.747$, $P < 0.001$ for BDI; $r = -0.713$, $P < 0.001$ for HDRS).

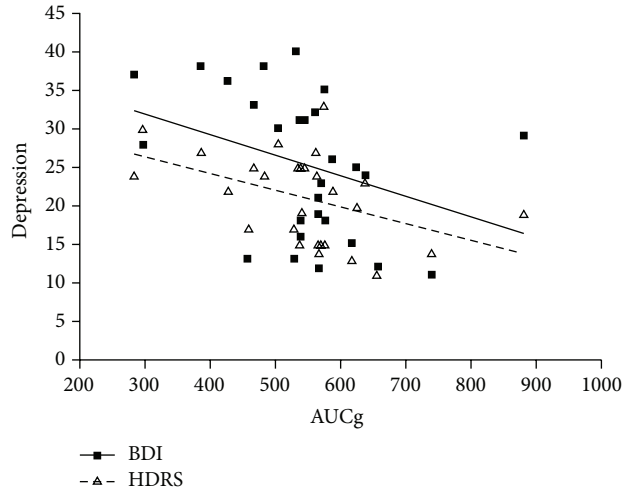

Figure 3: Association between the global area under the curve (AUCg) and Beck Depression Inventory (BDI) or Hamilton Depression Rating Scale (HDRS) in poststroke depression patients ($r = -0.336$, $P < 0.1$ for BDI; $r = -0.448$, $P < 0.02$ for HDRS).

4. Discussion

The main findings of the present study are that PSD patients show a blunted CAR as compared to caregiver controls and that magnitude of the CAR is negatively correlated with severity of depression in PSD patients.

The blunted CAR in PSD patients is a novel finding, consistent with other studies showing dysfunction of HPA axis following stroke. Although cortisol secretion has been reported to be increased acutely after stroke [19, 27], our results show that, in chronic PSD patients (2 months after stroke or longer in the present study), cortisol secretion after awakening is decreased. In a previous study, we found increased evening cortisol secretion (at 20:00 h) in chronic stroke patients whose mood status was not measured [21]. Because little is known about the diurnal variation of cortisol following stroke [28], further investigations regarding this issue are needed.

The CAR is considered to be a reliable indicator of HPA axis function and has been studied extensively, not only in healthy populations, but also in relation to many disorders [22]. For example, blunted CAR has been found in chronically ill patients [29], patients with severe global amnesia [30], posttraumatic stress disorder [31], amyotrophic lateral sclerosis [32], and chronic fatigue syndrome [33]. Also, depression and emotional distress are associated with a flatter cortisol diurnal rhythm [34, 35]. Thus, the blunted CAR found in our study is indicative of dysfunctional HPA axis in PSD patients and may be related to the emotional or physical distress and PSD-associated symptoms such as fatigue, vegetative symptoms (e.g., disturbances in sleep, appetite, sexual drive, or energy metabolism), or depressive mood.

The HPA axis plays a key role in mobilizing energy resources in conditions of reduced energy supply [36]. The early morning rise in HPA axis activity originates, in part, from a negative energy balance and increases in cerebral glucose demands [37]. Stroke causes changes in the energy-dependent processes [38]. Vegetative symptoms including disturbance in energy metabolism are common in both stroke and depression patients and become worse in depressed than nondepressed stroke patients [39]. Exercise, including ambulation, is known to stimulate HPA axis activity, increasing the production of cortisol and catecholamines [40]. Thus, lack of exercise such as ambulation may induce dysfunction of the HPA axis in stroke patients, which in turn would cause the blunted CAR in PSD patients.

Although physical disability may cause reactive depressive processes in the early stages after stroke, it does not mediate the development of PSD in the long run [41]. In the present study, we recruited PSD patients 2 months after stroke or longer. The correlation between depressive mood status of our patients and AUCi and AUCg of their CAR remained significant after controlling for motor impairments (data not shown). Thus, it is not likely that the strong correlation between the blunted CAR and depressive mood status in our PSD patients is a direct consequence of physical disability.

The CAR is known to be related with depression in nonstroke patients. Participants who were currently or previously depressed [15, 42] or had higher depressive symptoms [16] exhibit higher CAR. In contrast, another study showed a blunted CAR in depressed participants [14]. The inconsistent findings may be due to differences in illness stages, as well as methodological differences in cortisol sampling [15]. A recent meta-analysis study specifically looking at the AUCi or absolute increase of cortisol secretion found a negative relationship between the CAR and severity of depression [43], which is consistent with our finding.

Experiencing a stroke can be a traumatic event. Stroke patients face enormous emotional challenge due to physical disability, profound changes in social and professional roles, and often financial insecurity. Thus, it is worth noting that many studies reported blunted CAR in posttraumatic stress disorder patients (see [43]), which is consistent with our finding.

The treatment of PSD usually involves administration of selective serotonin reuptake inhibitors or tricyclic antidepressants. However, antidepressants have not been shown to have a positive impact on neurological disturbances including cognitive deficits [44–46]. The present finding of reduced responsivity of the HPA axis correlated with depressive mood in PSD patients may provide interesting and novel information toward successful treatments of PSD. Because cortisol is related to a wide variety of functions including energy metabolism, immune function, cognition, and neuronal degeneration, restoring HPA axis function may have desirable effects on the quality of life of PSD patients.

Limitations of the present study include its cross-sectional nature and lack of comparison group without PSD.

In sum, the findings of the present study show a blunted CAR in PSD patients. The magnitude of the CAR was significantly associated with depressive mood. Future studies are needed to investigate the neurological or pathological mechanisms underlying this alteration in HPA responsivity in PSD patients.

Conflict of Interests

The authors declare that there is no conflict of interests regarding the publication of this paper.

Authors' Contribution

Oh Jeong Kwon and Munsoo Kim contributed equally to this research as first authors.

Acknowledgments

This research was supported by Basic Science Research Program through the National Research Foundation of Korea (NRF) funded by the Ministry of Education, Science and Technology (MEST) (2010-0029468) and a grant of the Traditional Korean Medicine R&D Project, Ministry for Health & Welfare & Family Affairs, Republic of Korea (B110010). All authors acknowledge and approve this paper as their own work.

References

[1] N. R. Sims and H. Muyderman, "Mitochondria, oxidative metabolism and cell death in stroke," *Biochimica et Biophysica Acta—Molecular Basis of Disease*, vol. 1802, no. 1, pp. 80–91, 2010.

[2] R. G. Robinson, "Poststroke depression: prevalence, diagnosis, treatment, and disease progression," *Biological Psychiatry*, vol. 54, no. 3, pp. 376–387, 2003.

[3] S. Paolucci, G. Antonucci, M. G. Grasso et al., "Post-stroke depression, antidepressant treatment and rehabilitation results: a case-control study," *Cerebrovascular Diseases*, vol. 12, no. 3, pp. 264–271, 2001.

[4] R. Gillen, H. Tennen, T. E. McKee, P. Gernert-Dott, and G. Affleck, "Depressive symptoms and history of depression predict rehabilitation efficiency in stroke patients," *Archives of Physical Medicine and Rehabilitation*, vol. 82, no. 12, pp. 1645–1649, 2001.

[5] N. Herrmann, S. E. Black, J. Lawrence, C. Szekely, and J. P. Szalai, "The Sunnybrook stroke study a prospective study of depressive symptoms and functional outcome," *Stroke*, vol. 29, no. 3, pp. 618–624, 1998.

[6] T. Pohjasvaara, R. Vataja, A. Leppävuori, M. Kaste, and T. Erkinjuntti, "Depression is an independent predictor of poor long-term functional outcome post-stroke," *European Journal of Neurology*, vol. 8, no. 4, pp. 315–319, 2001.

[7] A. Berg, H. Palomäki, M. Lehtihalmes, J. J. Lönnqvist, and M. Kaste, "Poststroke depression: an 18-month follow-up," *Stroke*, vol. 34, no. 1, pp. 138–143, 2003.

[8] S.-M. Lai, S. Studenski, P. W. Duncan, and S. Perera, "Persisting consequences of stroke measured by the stroke impact scale," *Stroke*, vol. 33, no. 7, pp. 1840–1844, 2002.

[9] E. K. Adam, L. D. Doane, R. E. Zinbarg, S. Mineka, M. G. Craske, and J. W. Griffith, "Prospective prediction of major depressive disorder from cortisol awakening responses in adolescence," *Psychoneuroendocrinology*, vol. 35, no. 6, pp. 921–931, 2010.

[10] G. Hasler and G. Northoff, "Discovering imaging endophenotypes for major depression," *Molecular Psychiatry*, vol. 16, no. 6, pp. 604–619, 2011.

[11] L. M. Oswald, P. Zandi, G. Nestadt, J. B. Potash, A. E. Kalaydjian, and G. S. Wand, "Relationship between cortisol responses to stress and personality," *Neuropsychopharmacology*, vol. 31, no. 7, pp. 1583–1591, 2006.

[12] I. Wilhelm, J. Born, B. M. Kudielka, W. Schlotz, and S. Wüst, "Is the cortisol awakening rise a response to awakening?" *Psychoneuroendocrinology*, vol. 32, no. 4, pp. 358–366, 2007.

[13] T. J. Huber, K. Issa, G. Schik, and O. T. Wolf, "The cortisol awakening response is blunted in psychotherapy inpatients suffering from depression," *Psychoneuroendocrinology*, vol. 31, no. 7, pp. 900–904, 2006.

[14] C. Stetler and G. E. Miller, "Blunted cortisol response to awakening in mild to moderate depression: regulatory influences of sleep patterns and social contacts," *Journal of Abnormal Psychology*, vol. 114, no. 4, pp. 697–705, 2005.

[15] Z. Bhagwagar, S. Hafizi, and P. J. Cowen, "Increased salivary cortisol after waking in depression," *Psychopharmacology*, vol. 182, no. 1, pp. 54–57, 2005.

[16] M. Pruessner, D. H. Hellhammer, J. C. Pruessner, and S. J. Lupien, "Self-reported depressive symptoms and stress levels in healthy young men: associations with the cortisol response to awakening," *Psychosomatic Medicine*, vol. 65, no. 1, pp. 92–99, 2003.

[17] K. Dedovic, V. Engert, A. Duchesne et al., "Cortisol awakening response and hippocampal volume: vulnerability for major depressive disorder?" *Biological Psychiatry*, vol. 68, no. 9, pp. 847–853, 2010.

[18] H. M. van Praag, "Can stress cause depression?" *Progress in Neuro-Psychopharmacology & Biological Psychiatry*, vol. 28, no. 5, pp. 891–907, 2004.

[19] T. Olsson, "Urinary free cortisol excretion shortly after ischaemic stroke," *Journal of Internal Medicine*, vol. 228, no. 2, pp. 177–181, 1990.

[20] A. Slowik, W. Turaj, J. Pankiewicz, T. Dziedzic, P. Szermer, and A. Szczudlik, "Hypercortisolemia in acute stroke is related to the inflammatory response," *Journal of the Neurological Sciences*, vol. 196, no. 1-2, pp. 27–32, 2002.

[21] S. Lee, M. Kim, J.-I. Youn, B.-K. Song, and K.-K. Sung, "Increase in salivary cortisol in the evening correlates with sleep duration and quality in stroke patients," *International Journal of Cardiology*, vol. 152, supplement 1, article S14, 2011.

[22] S. Wust, J. Wolf, D. H. Hellhammer, I. Federenko, N. Schommer, and C. Kirschbaum, "The cortisol awakening response-normal values and confounds," *Noise and Health*, vol. 2, no. 7, p. 79, 2000.

[23] D. Pravettoni, K. Doll, M. Hummel, E. Cavallone, M. Re, and A. G. Belloli, "Insulin resistance and abomasal motility disorders in cows detected by use of abomasoduodenal electromyography after surgical correction of left displaced abomasum," *American Journal of Veterinary Research*, vol. 65, no. 10, pp. 1319–1324, 2004.

[24] H. Sung, J. Kim, Y. Park, D. Bai, S. Lee, and H. Ahn, "A study on the reliability and the validity of Korean version of the Beck Depression Inventory-II (BDI-II)," *Journal of the Korean Society of Biological Therapies in Psychiatry*, vol. 14, no. 2, pp. 201–212, 2008.

[25] J. S. Yi, S. O. Bae, Y. M. Ahn et al., "Validity and reliability of the korean version of the hamilton depression rating scale (K-HDRS)," *Journal of Korean Neuropsychiatric Association*, vol. 44, no. 4, pp. 456–465, 2005.

[26] J. C. Pruessner, C. Kirschbaum, G. Meinlschmid, and D. H. Hellhammer, "Two formulas for computation of the area under

the curve represent measures of total hormone concentration versus time-dependent change," *Psychoneuroendocrinology*, vol. 28, no. 7, pp. 916–931, 2003.

[27] J. H. Feibel, P. M. Hardy, R. G. Campbell, M. N. Goldstein, and R. J. Joynt, "Prognostic value of the stress response following stroke," *The Journal of the American Medical Association*, vol. 238, no. 13, pp. 1374–1376, 1977.

[28] B. M. Tchiteya, A. R. Lecours, R. Élie, and S. J. Lupien, "Impact of a unilateral brain lesion on cortisol secretion and emotional state: anterior/posterior dissociation in humans," *Psychoneuroendocrinology*, vol. 28, no. 5, pp. 674–686, 2003.

[29] B. M. Kudielka and C. Kirschbaum, "Awakening cortisol responses are influenced by health status and awakening time but not by menstrual cycle phase," *Psychoneuroendocrinology*, vol. 28, no. 1, pp. 35–47, 2003.

[30] O. T. Wolf, E. Fujiwara, G. Luwinski, C. Kirschbaum, and H. J. Markowitsch, "No morning cortisol response in patients with severe global amnesia," *Psychoneuroendocrinology*, vol. 30, no. 1, pp. 101–105, 2005.

[31] M. Wessa, N. Rohleder, C. Kirschbaum, and H. Flor, "Altered cortisol awakening response in posttraumatic stress disorder," *Psychoneuroendocrinology*, vol. 31, no. 2, pp. 209–215, 2006.

[32] B. Roozendaal, S. Kim, O. T. Wolf, M. S. Kim, K.-K. Sung, and S. Lee, "The cortisol awakening response in amyotrophic lateral sclerosis is blunted and correlates with clinical status and depressive mood," *Psychoneuroendocrinology*, vol. 37, no. 1, pp. 20–26, 2012.

[33] A. D. L. Roberts, S. Wessely, T. Chalder, A. Papadopoulos, and A. J. Cleare, "Salivary cortisol response to awakening in chronic fatigue syndrome," *The British Journal of Psychiatry*, vol. 184, no. 2, pp. 136–141, 2004.

[34] E. Sjögren, P. Leanderson, and M. Kristenson, "Diurnal saliva cortisol levels and relations to psychosocial factors in a population sample of middle-aged Swedish men and women," *International Journal of Behavioral Medicine*, vol. 13, no. 3, pp. 193–200, 2006.

[35] G. E. Miller, E. Chen, and E. S. Zhou, "If it goes up, must it come down? Chronic stress and the hypothalamic-pituitary-adrenocortical axis in humans," *Psychological Bulletin*, vol. 133, no. 1, pp. 25–45, 2007.

[36] A. Peters, U. Schweiger, L. Pellerin et al., "The selfish brain: competition for energy resources," *Neuroscience & Biobehavioral Reviews*, vol. 28, no. 2, pp. 143–180, 2004.

[37] C. Benedict, W. Kern, S. M. Schmid, B. Schultes, J. Born, and M. Hallschmid, "Early morning rise in hypothalamic-pituitary-adrenal activity: a role for maintaining the brain's energy balance," *Psychoneuroendocrinology*, vol. 34, no. 3, pp. 455–462, 2009.

[38] K. Katsura, T. Kristian, and B. K. Siesjo, "Energy metabolism, ion homeostasis, and cell damage in the brain," *Biochemical Society Transactions*, vol. 22, no. 4, pp. 991–996, 1994.

[39] J. P. Fedoroff, S. E. Starkstein, R. M. Parikh, T. R. Price, and R. G. Robinson, "Are depressive symptoms nonspecific in patients with acute stroke?" *The American Journal of Psychiatry*, vol. 148, no. 9, pp. 1172–1176, 1991.

[40] A. Leal-Cerro, A. Gippini, M. J. Amaya et al., "Mechanisms underlying the neuroendocrine response to physical exercise," *Journal of Endocrinological Investigation*, vol. 26, no. 9, pp. 879–885, 2003.

[41] J. E. Downhill Jr. and R. G. Robinson, "Longitudinal assessment of depression and cognitive impairment following stroke," *The Journal of Nervous and Mental Disease*, vol. 182, no. 8, pp. 425–431, 1994.

[42] S. A. Vreeburg, W. J. G. Hoogendijk, J. van Pelt et al., "Major depressive disorder and hypothalamic-pituitary-adrenal axis activity: results from a large cohort study," *Archives of General Psychiatry*, vol. 66, no. 6, pp. 617–626, 2009.

[43] Y. Chida and A. Steptoe, "Cortisol awakening response and psychosocial factors: a systematic review and meta-analysis," *Biological Psychology*, vol. 80, no. 3, pp. 265–278, 2009.

[44] J. R. Lipsey, R. G. Robinson, G. D. Pearlson, K. Rao, and T. R. Price, "Nortriptyline treatment of post-stroke depression: a double-blind study," *The Lancet*, vol. 1, no. 8372, pp. 297–300, 1984.

[45] R. G. Robinson, S. K. Schultz, C. Castillo et al., "Nortriptyline versus fluoxetine in the treatment of depression and in short-term recovery after stroke: a placebo-controlled, double-blind study," *The American Journal of Psychiatry*, vol. 157, no. 3, pp. 351–359, 2000.

[46] L. Wiart, H. Petit, P. A. Joseph, J. M. Mazaux, and M. Barat, "Fluoxetine in early poststroke depression: a double-blind placebo-controlled study," *Stroke*, vol. 31, no. 8, pp. 1829–1832, 2000.

Hindawi Publishing Corporation
BioMed Research International
Volume 2015, Article ID 402959, 16 pages
http://dx.doi.org/10.1155/2015/402959

Review Article

Biomarkers of Brain Damage and Postoperative Cognitive Disorders in Orthopedic Patients: An Update

Dariusz Tomaszewski

Department of Anesthesiology and Intensive Therapy, Military Institute of Medicine, Szaserow 128 Street, 04-141 Warsaw, Poland

Correspondence should be addressed to Dariusz Tomaszewski; dtomaszewski@wim.mil.pl

Received 26 June 2014; Accepted 24 November 2014

Academic Editor: Giovanni Scapagnini

The incidence of postoperative cognitive dysfunction (POCD) in orthopedic patients varies from 16% to 45%, although it can be as high as 72%. As a consequence, the hospitalization time of patients who developed POCD was longer, the outcome and quality of life were worsened, and prolonged medical and social assistance were necessary. In this review the short description of such biomarkers of brain damage as the S100B protein, NSE, GFAP, Tau protein, metalloproteinases, ubiquitin C terminal hydrolase, microtubule-associated protein, myelin basic protein, α-II spectrin breakdown products, and microRNA was made. The role of thromboembolic material in the development of cognitive decline was also discussed. Special attention was paid to optimization of surgical and anesthetic procedures in the prevention of postoperative cognitive decline.

1. Postoperative Cognitive Disorders: Terminology, Clinical Spectrum, Incidence, and Risk Factors

Postoperative cognitive disorders are common in elderly (>65-year-old) patients. Cognitive dysfunction is present more often in orthopedic patients than in any other hospitalized group. It includes the deterioration of perception, memory, information analysis, attentional focus, concentration, and patients' response [1]. Those disorders are divided into postoperative delirium, postoperative cognitive dysfunction (POCD), and dementia [2]. Delirium and dementia are reported in the literature as parts of the continuum of postoperative cognitive impairment [3].

Delirium characterizes the following: (1) a disturbance of consciousness with inattention; (2) acute changes in cognition (i.e., memory deficits, disorientation, language disturbances, and perceptual disturbances); (3) the disturbances that develop over a short period of time and fluctuate over time; and (4) the disturbance is not caused by a general medical condition [4].

In the terminology relating to time course, delirium can be prevalent, incident, or persisting. Motor subtypes are classified into hyperactive delirium (characterized by increased psychomotor activity with agitation), hypoactive or "quiet" delirium (with reduced psychomotor behavior and lethargy), and mixed delirium, which alternates between a hyperactive and hypoactive manifestation. Additional definitions include subsyndromal delirium or delirium superimposed on dementia [2, 4, 5]. POCD is the subtle impairment of memory, concentration, and information processing [2, 4]. The symptoms of POCD vary from mild memory loss to the inability to concentrate or process information [2]. The nature of postoperative cognitive disorders is frequently subclinical and no changes in diagnostic imaging are present [6]. Therefore, in many cases, only the patient and/or partner can recognize the onset of the pathology [2].

In clinical practice, postoperative delirium is diagnosed by the Confusion Assessment Method (CAM). This method assesses four features: (1) acute onset and fluctuating course, (2) inattention, (3) disorganized thinking, and (4) altered level of consciousness [2]. The diagnosis of delirium requires

the presence of the first two features and either third or fourth [2, 5]. In the diagnosis and grading of delirium, several tests are validated, including the CAM, the Delirium Rating Scale Revised-98, the Delirium Symptom Interview, the NEECHAM Confusion Scale, and the Estimation of Psychologic Ability and Surgical Stress (E-PASS) [5]. However, there are no approved criteria for the assessment and diagnosis of POCD [2, 5]. Therefore, POCD is much more difficult to define. There are three types of POCD through which patients can suffer from isolated learning/memory decline, difficulties in executive functions, or combined cognitive decline [7]. The diagnosis of POCD requires perioperative neuropsychological testing. Several tests are used, such as the Logical Memory Test, the CERAD word list memory, the Boston Naming Test, the Category Fluency Test, the Digit Span Test, the Trail Making test, and the Digit Symbol Substitution test [5]. Common diagnostic criteria include a 20% change from the baseline evaluation and a predefined (usually two or more) number of tests or an absolute decline (>1 SD) from baseline scores in two or more psychological tests [4].

Variability in the incidence of POCD can be caused by variable test batteries, the nonstandardization of neuropsychological tests performed at different times of the day, the lack of a control group, differences in significance levels between studies, significant loss of patients during follow-up as well, and the so-called "learning effect," which occurs when the same test is applied to the same person many times [2, 27]. Another question concerns the time at which the diagnosis of POCD was made. Different drugs administered in the perioperative period can affect patients' cognition. Thus, some authors believe that the diagnosis of POCD should be made no earlier than two weeks after the surgery [27].

Delirium is the manifestation of cortical dysfunction resulting from disturbances in neurotransmitter systems. Abnormal serum anticholinergic activity as well as melatonin, norepinephrine, and lymphokines was described in the etiology of delirium. A relationship with surgical stress and inflammatory response was also suggested [5]. The risk factors of postoperative delirium include advancing age (>70), sensory deprivation (visual or hearing impairment), sleep deprivation, social isolation, physical restraint, use of urinary bladder catheter, iatrogenic adverse events, polypharmacy, preoperative use of opioids or benzodiazepines, severe illness (especially infection, fracture, or stroke), cognitive impairment, previous history of delirium or cognitive impairment, decreased cerebral perfusion pressure, fever or hypothermia, dehydration, malnutrition, low serum albumin, and a serum urea nitrogen/creatinine ratio of 18 or greater. Significant blood loss during surgery, blood transfusion, postoperative hematocrit <30%, and severe postoperative pain also were identified as a risk factors of postoperative delirium [2, 5].

According to Monk and Price [2], increasing age, lower education level, a history of a previous cerebral vascular accident with no residual impairment, and POCD at hospital discharge are identified as independent risk factors for POCD three months after surgery. Other studies included the following factors for the risk postoperative cognitive impairment: a general anesthesia rather than a regional one (although some authors [5] did not found it to be significant), increasing duration of anesthesia, reoperation, postoperative infections, postoperative respiratory complications, lower preoperative level of consciousness, and treatment with cholinergic drugs and benzodiazepines. Additional risk factors are noise, bright light, and physiologic disturbances, such as hyponatremia or hypoalbuminemia, as well as male sex, depression, and reduced activity in daily life [27–32]. Surprisingly, there was no evidence that hypoxemia is associated with the development of POCD [30, 33]. Some studies found that hypotension was the only intraoperative risk factor responsible for postoperative delirium [31]. However, other authors did not support that observation [30].

The incidence of postoperative delirium varies from 5% to 15%. In some patients, such as those with hip fracture, the problem is common and varies from 16% to 62% [5]. The incidence of POCD is difficult to describe. According to Deiner and Silverstein [5], it should be described at specific intervals after surgery; between the second and tenth day after surgery, the incidence is as much as 25%. The incidence then decreases as follows: to 10% at three months, 5% at six months, and 1% at one year [5]. According to Coburn et al., the incidence of POCD one week after surgery in patients older than 18 years varies from 19% to 41%, and a rate of 10% three months after surgery is detected in patients older than 60 years [34]. In 60-year-old patients who underwent major surgical procedures under general anesthesia lasting over two hours, 10% suffered memory impairment and concentration problems for more than three months after the surgery. The disorder occurred twice as often in patients between 70 and 80 years than in patients between 60 and 70 years [35]. According to statistical data, about 70% of patients with POCD die within five years, compared to about 35% of patients without postoperative delirium [36].

2. Surgery-Induced Stress Response and the Role of Anesthetic Agents in Neuroinflammation

Surgery-induced stress response leads to the following: (1) the cardiovascular effects of tachycardia and hypertension resulting from the increased secretion of catecholamines from the adrenal medulla and norepinephrine from the presynaptic nerve terminals because of the activation of the sympathetic nervous system; (2) changes in hormone secretion in hypothalamic-pituitary-adrenal axis, which influences the metabolism of carbohydrates, proteins, fat, salt, and water; and (3) immunological and hematological changes [37]. Immunological and hematological changes include cytokine production, acute phase reaction, neutrophil leukocytosis, and lymphocyte proliferation. Cytokines—mainly interleukin-1 (IL-1), tumor necrosis factor-α (TNF-α), and IL-6, which are released from activated leukocytes, fibroblasts, and endothelial cells—play an important role in systemic inflammatory reaction [37]. Some authors [5, 15, 27, 32, 38–41] suggest that inflammation plays a substantial role in the pathogenesis of POCD. Rudolph et al. [42] found

that the chemokine concentration in the early postoperative period was more elevated in patients who developed delirium, compared to the matched controls. However, Lemstra et al. [38], in comparison to 18 patients who developed postoperative delirium with 50 controls, found no differences in preoperative concentrations of C-reactive protein, IL-6, and insulin growth factor 1 (IGF-1) between groups. Animal studies also showed that the development of POCD in rats was associated with glial activation and the expression of proinflammatory cytokines within the hippocampal region [27]. Some studies revealed the role of interleukin-18 (IL-18) in the neuroinflammation and neurodegeneration of the central nervous system. Patients with a defect in the IL-18 cytokine promoter gene had higher concentrations of serum amyloid peptides [36].

The increased production of TNF-α, IL-β, and IL-6 in mice neurons after isoflurane anesthesia was described by Wu et al. [43]. However, Schilling et al. found that volatile anesthetics (especially sevoflurane and desflurane) reduced proinflammatory cytokine release [44]. The exact mechanism by which volatile anesthetics increase proinflammatory cytokines remains unknown. It was suggested that nuclear factor kappa B-dependent (NF-κB-dependent) pathways and the receptor for advanced glycation end products (RAGE) play a role in this mechanism [39].

The amyloid-β peptide concentration was related to learning, memory deficiencies, and neurodegeneration. The continuous infusion of amyloid-β peptide in rats resulted in impairments in learning and memory. Higher levels of amyloid-β peptide in the hippocampus were observed in older rats, compared to younger rats [36].

The literature includes a discussion on the role of anesthesia in the development of postoperative cognitive decline. However, the mechanism of the association of POCD with surgery and anesthesia remains unclear. However, some theories consider these effects of anesthetics, which include direct toxicity, alterations in calcium homeostasis, the systemic inflammatory effect, the age-sensitive suppression of neuronal stem cell function, and the acceleration of endogenous neurodegenerative processes, as well as caspase activation and apoptosis [45, 46]. Cell culture studies have shown that volatile anesthetics (isoflurane, sevoflurane, and desflurane, the latter in the presence of hypoxia) induce apoptosis and increase amyloid-β formation [36, 45]. It was shown that isoflurane is an agent promoting β-site amyloid precursor protein-cleaving enzyme (BACE) activity and amyloid-β deposition [39]. In an animal model, Dong et al. found that that sevoflurane increased BACE concentration and amyloid-β [47]. In addition, halothane produced the concentration-dependent enhancement of amyloid-β oligomerization [39]. Moreover, many anesthetics can promote the hyperphosphorylation of the microtubule-associated protein Tau, which was observed in hypothermic conditions, but not normothermic conditions [36, 45]. Propofol increased Tau phosphorylation, even with normothermia [48]. Fodale et al. [36] found that intravenous anesthetics, such as propofol and thiopental, did not significantly change the amyloid precursor protein [36].

Some authors discussed the role of genetic factors in the pathogenesis of neurodegenerative disorders. They found an association between the apolipoprotein ε4 (APO-ε4) allele and Alzheimer's disease [27]. Hence, the APO-ε4 gene could be a predictor of postoperative cognitive disorders [36]. However, in Abildstrom et al.'s study of 976 patients aged 40 years and older and undergoing noncardiac surgery, the ε4 allele was found in 272 patients. No significant association was found between the ε4 genotype and POCD [49].

3. POCD in Orthopedic Patients

According to Scott et al. [50], the incidence of POCD after big joint arthroplasty varies from 16% to 45%, although it was reported [51] as high as 72% at six days and 30% at six months, postoperatively. The etiology of POCD in orthopedic patients is unclear. Many factors are posited, including thromboembolic complications, the influence of anesthesia, and the influence of pain therapy in the postoperative period [50]. The high incidence of cognitive dysfunction in orthopedic patients can result (in addition to the above-mentioned risk factors) from long bone fractures, from prolonged immobilization, and partially from perioperative stress [6] or a surgery technique. Colonna et al. concluded that the incidence of cerebral embolization after lower extremity arthroplasty was between 40 and 60% [52]. Fatal cerebral embolization constituted complications accompanying long bone fractures [53], total knee replacements [54], hip arthroplasty [55], and vertebroplasty [56], in which the embolic material passed into the brain through an open foramen ovale [57], although postmortem examinations did not reveal it [52].

4. Biomarkers of Brain Damage

Biochemical tests are useful diagnostic tools in the examination of functional brain disorders. Elevated serum concentrations of the markers of brain damage indicate a neuronal and/or glial injury. The biomarkers are released because of either transient ischemia or ultimate cell degradation. Their serum concentration depends on the localization of pathological changes, the degree of tissue damage, and the time that has passed since the onset of changes. The ideal marker of brain damage should have the following characteristics: (1) highly specific; (2) highly sensitive; (3) released in only cases of irreversible damage to cerebral neurons; (4) detectable in the blood and/or cerebrospinal fluid within a short period of time after the injury; and (5) released in well-known time sequences after the injury. Furthermore, the marker should be (6) age- and sex-independent and (7) easily detectable in the blood because frequent drawing of cerebrospinal fluid samples is impractical; and (8) its concentration should be easily measureable in laboratory tests [58].

The following substances have been investigated as relevant neurological biomarkers in the postoperative period.

4.1. S100B Protein. The S100B protein has a molecular weight of 21 kDa. It belongs to the calcium-mediated proteins in

the S100 proteins family, which consists of 24 members that have similar structures and functions [59]. Some members of the S100 protein family are specific for certain localizations [60]. High S100B protein concentrations are present inside the brain, mainly in astroglial and Schwann cells, as well as in adipocytes, chondrocytes, and melanocytes [10, 61, 62]. The S100B protein plays different roles in the human body and is present in many types of cells and tissues [63]. It has intra- and extracellular targets, and it has autocrine and paracrine effects on glia, neurons, and microglia [64]. Although the exact functions of the S100B protein are still unclear, it may be involved in neuronal and glial growth, proliferation, and activation [64].

Increased S100B concentrations in serum and cerebrospinal fluid were observed after brain infarction, trauma, and toxic injury [64]. The highest S100B protein serum level was observed just after an injury [58] and was then normalized within 24 hours, even in patients with poor outcomes [65]. An increased concentration of the S100B protein was shown on the sixth day after head trauma, which was probably the result of a secondary injury [65]. Elevated concentrations of S100B protein were also demonstrated in a posttraumatic animal model [65]. The results of animal studies suggested that S100B protein levels correlated with the degree of shock: in moderate shock, they were higher than in severe shock [66]. The concentration of S100B protein increased immediately after bilateral long bone fractures, as well as after local ischemia and the reperfusion of the liver, gut, and kidneys [10, 66]. In rabbits with femur fracture and no evidence of neurological injury, S100B protein concentration increased within minutes after bone trauma, suggesting that the S100B protein was released from nonneuronal sources [64]. This finding supports observations that elevated levels of the S100B protein can be caused by increased permeability of the blood-brain barrier, regardless of cerebral damage [65].

Elevated levels of S100B protein were shown in basketball and hockey players after competition, as well as in runners, boxers [67], swimmers, and soccer players. In the latter, however, latter there was a correlation between increased protein concentration and frequency of head injury [13]. Intense physical exercise can remarkably increase serum S100B concentration. It was shown that, after acute muscle injury, S100B expressed in mature muscle myofibrils was released from injured muscle tissue and could penetrate the bloodstream [68]. Another possible cause of increased serum S100B level is the catecholamine-dependent activation of adipocytes [68].

A raised plasma level of the S100B protein also occurred in melanoma patients [69] and in sepsis-associated encephalopathy [70].

The possibility that the S100B protein could be released from extracerebral localization restricts its utility as a marker of brain damage, which, nonetheless, still ranges from 70 to 80% [62]. The S100B protein is a very useful biochemical tool because of its short (25 minutes) half-life [58, 62, 64], as well as the fact that its serum concentrations are not affected by age or sex [58]. Moreover, serum concentrations are not altered by alcohol overdose, moderate renal dysfunction, or hemolysis [62, 64].

4.2. Neuron Specific Enolase (NSE). Neuron specific enolase (NSE) is an enzyme that catalyzes the conversion of 2-phospho-D-glycerate to phosphoenolpyruvate in a glycolytic pathway. It is found in the cytoplasm of neurons and neuroendocrine cells and its subunits, and α and γ are specific for neurons. NSE is also found in red cells and platelets [64, 71]. The molecular weight of NSE is 78 kDa, and its half-life is 24 hours [64]. The normal serum concentration of NSE varies between 2 and 20 mg/L; values >30 mg/L are pathological, and ≥115 mg/L are related to poor prognosis [64]. Increased levels of NSE were observed after cortical brain injury and severe head trauma and in patients with temporal lobe epilepsy as well as in the patients with internal cardiac defibrillators, where correlations were found between NSE levels and the number of shocks and the cumulative time of cardiac arrest [64].

This protein is effective in predicting neurological outcomes after cardiac arrest and in patients with ischemic stroke [64]. The results of a study on cardiac surgery patients were ambiguous. In some studies, the correlation of NSE with POCD was observed [12, 20], but not in others [11]. The NSE concentration in the cerebrospinal fluid in patients after aortic aneurysm repair surgery was increased regardless of the presence or absence of neurological symptoms [64]. Gempp et al.'s study of recreational divers found that NSE levels >15.9 μg/L predicted the development of neurological decompression sickness with a specificity of 100% [26]. Observations of patients undergoing liver transplantation revealed that the postreperfusion concentration of NSE correlated with decreased regional oxygen saturation [64].

Similarly, the results of studies analyzing the correlation between the APOE4 genotype and cognition with NSE serum levels in the postoperative period were inconclusive [64].

4.3. Glial Fibrillary Acidic Protein (GFAP). The glial fibrillary acidic protein (GFAP) is a monomeric filament protein found in the astroglial skeleton [71]. It is a specific marker of brain damage and is potentially useful in predicting clinical outcomes [71]. It was shown that the serum GFAP levels were higher in patients with mass lesions than in those with diffuse brain injury [71]. Pelinka et al. [72, 73] found that serum GFAP levels were increased in patients with intracranial pressure (ICP) above 25 mmHg. However, the cutoff value of GFAP for detection ICP elevation was not defined.

Clinical data suggests that GFAP provides important information for the prognosis of traumatic brain injury as well as for differential diagnosis and prognosis in various types of stroke [74]. The most recent data showed that, in intracerebral hemorrhage, GFAP sensitivity is 0.8 and specificity is 0.97 [75].

4.4. Tau Protein. The Tau protein is a microtubule-associated protein that stabilizes the axonal microtubules [64]. It is found in the brain and the spinal cord [64]. The tau protein has different isoforms, with molecular weight varying from

45 to 68 kDa [64]. The phosphorylation of the Tau protein is associated with neuronal death, and it is observed in neurodegenerative diseases [64]. Increased concentrations of the tau protein were observed in patients who developed postoperative cognitive decline [64]. A correlation between increased serum levels of the tau protein and the size of brain infarction was observed in noncardiac surgery patients [64].

4.5. Metalloproteinases (MMP). Metalloproteinases (MMP) are zinc-dependent endopeptidases that degrade most extracellular matrix proteins [64]. MMPs are secreted as cells in blood vessel walls as myocytes, endothelial cells, and macrophages [64].

MMPs are divided into the following: (a) gelatinases (MMP-2, MMP-9); (b) collagenases (MMP-1, MMP-8, and MMP-13); (c) matrilysins (MMP-7); (d) membrane-type MMPs (MMP-14, MMP-15, MMP-16, and MMP-17); and (e) others (MMP-11, MMP-12) [64].

MMP-9 was observed to be a marker of blood-brain barrier dysfunction, and elevated concentrations of this protein were noted in patients with stroke [64]. Gaudet et al. [16], in their study of 73 patients undergoing carotid surgery, found elevated serum concentrations of MMP-9 in patients who developed postoperative cognitive decline. This finding is supported by Taurino et al., who found that, in patients undergoing carotid surgery, MMP-9 levels were significantly higher in those with cerebral lesions at neuroimaging, compared to the healthy controls [14].

4.6. Ubiquitin C Terminal Hydrolase-L1 (UCH-L1). Ubiquitin C terminal hydrolase-L1 (UCH-L1), also called neuronal-specific gene product (PGP 9.3), is a highly specific neuronal protein with a molecular weight of 24 kDa. It is found in perikarya in gray matter. Its role is removing excessive, oxidized, or misfolded proteins in the central nervous system [64, 71].

Because it is not found in nonneuronal sources, UCH-L1 is a specific biomarker of brain lesions [64]. After traumatic brain injury and subarachnoid hemorrhage, this protein is released to CSF [64]. In Papa et al.'s study, which includes 96 patients with traumatic brain injury and 199 controls, UCH-L1 was detectable in serum within one hour after the injury and was associated with GCS scoring, CT lesions, and the need for neurosurgical intervention [22].

4.7. Microtubule-Associated Protein 2 (MAP2). Microtubule-associated protein 2 (MAP2) is thought to be a dendrite-specific protein and, according to some authors, it is a good biomarker for dendritic injury [71]. In Mondello et al., MAP2 concentrations correlated with the Glasgow Outcome Scale Extended (GOSE) and the Levels of Cognitive Functioning Scale (LCFS), measured at six months after injury [21].

4.8. Myelin Basic Protein (MBP). Myelin basic protein (MBP) represents 30% of the protein content of myelin. The protein consists of four isoforms with molecular weights ranging from 14 to 21.5 kDa. Changes in MBP concentrations were observed after cortex contusion in an animal model. However, there is no evidence for the use of MBP as a biomarker after traumatic brain injury or in intracranial hypertension in humans [71].

4.9. α-II Spectrin Breakdown Products (SBDP) 150, 145, and 120. The α-II spectrin protein forms part of the axolemmal cytoskeleton, stabilizes the structure of myelinated axons, and is a major substrate in calpain-1 and calpain-2 and caspase-3, which are involved in cellular necrosis and apoptosis [71]. The calpain-specific 150- and 145-kDa SBDPs are used as biomarkers of necrotic neuronal death, and the caspase-3-specific 120-kDa SBDP is used as a biomarker of apoptosis [71]. In study of 40 adult patients with traumatic brain injury, mean CSF concentrations of SBDP-145 and SBDP-120 were higher in patients with brain injury who died than in those who survived. SBDP-145 levels >6 ng/mL and SBDP-120 levels >17.55 ng/mL strongly predicted death. The authors concluded that SBDP-145 seems more accurate in predicting outcomes in patients suffering from traumatic brain injury [17].

4.10. Micro-RNA (miRNA). Micro-RNA (miRNA) particles are small molecules involved with regulation of gene expression [70]. MiRNA plays an important role in orthopedic diseases, such as osteoarthritis and rheumatoid arthritis [76]. Changes in microRNA concentrations were observed in patients with bone tumors [77]. The comparison of patients with severe brain injury and healthy volunteers revealed that decreases in the levels of miR-16 and miR-92a and increased levels of miR-765 were strong markers of severe traumatic brain injury at 25 to 48 hours after injury [71].

5. Biomarkers of Brain Damage in Orthopedic Patients

Increased levels of biomarkers were observed after orthopedic procedures and bone fractures.

Kinoshita et al. [9] examined 14 patients, half of which underwent total knee arthroplasty (TKA) with bone cement. The other half underwent intramedullary nail stabilization of the tibia. All procedures were performed with tourniquet and ischemia. In the TKA group, in blood samples withdrawn 15 minutes after tourniquet release, there was a statistically significant elevation of S100B serum level in comparison to the group in which tibial fracture was stabilized with an intramedullary nail. The authors suggested that the increase was caused by the transient injury of brain tissues caused by the bone cement [9].

Tomaszewski et al. examined changes in S100B protein levels in patients who underwent total hip arthroplasty, with or without bone cement. In both groups of patients, the mean preoperative concentration of S100B protein was comparable to that in the healthy subjects and reached the maximum just after the operation. In the cemented group, the level was significantly higher than in the noncement group, and normalization was slower. Elevated serum S100B protein levels may be due to the release of S100B protein from bone

marrow, as well as the transfer of cellular materials from the site of the surgery through the bloodstream into the brain. Because all patients with intraoperative mean blood pressure dropping below 50 mmHg were excluded from the study, hypotension was eliminated as a possible cause of the elevation of S100B concentration [18].

In their study of 83 patients older than 65 years undergoing elective total hip arthroplasty, Ji et al. analyzed the perioperative concentration of the Tau protein, the phosphorylated Tau protein (pTau), 42 amino acids in the form of amyloid β1 (Aβ1-42), Tau/Aβ1-42, pTau/Aβ1-42, brain-derived neurotropic factor (BDNF), IL-6, IL-1β, C-reactive protein (CRP), and malondialdehyde (MDA). They found that patients who developed POCD had significantly higher levels of IL-1β, Tau/Aβ1-42 ratio, and pTau/Aβ1-42 ratio and the lower level of Aβ1-42 in the cerebrospinal fluid, compared to the non-POCD group. There was no difference in CFS levels of tau protein, pTau, BDNF, and IL-6 between both groups. The authors concluded that such biomarkers might predispose the development of POCD in aged patients after hip replacement surgery under spinal anesthesia [23]. Similarly, Xie et al.'s study involving 136 patients who had total knee or hip replacement surgery found that preoperative CSF Aβ40/Tau and Aβ42/Tau ratios were associated with the postoperative scores of neurocognitive tests. Therefore, the Aβ/Tau ratio may identify patients with a higher risk of POCD development [24].

However, increased serum concentration of the S100B protein was observed after injuries, which did not include brain damage. The highest levels of the S100B protein were noted in patients with long bone fractures [8]. Studies conducted on patients with isolated bone fractures without brain injury revealed that patients with hip, radius, or tibia fractures had significantly higher concentrations of the S100B protein, but those with phalange, hand, or foot fractures did not [78]. Animal studies showed increased S100B serum levels after bilateral femur fractures in rats; these results indicated that bone marrow could be a potential source of the S100B protein [10]. Increased serum levels of the S100B protein were found in patients with acute spinal fracture, but without head injury [79]. Observations of 233 patients after trauma found that the highest concentrations of S100B (1.68 μg/L on admission and 0.31 μg/L after 6 hours) were noted in patients suffering from multitrauma with head injury. There were no differences in the S100B levels in patients with or without isolated head injury (0.47 and 0.14 μg/L and 0.49 and 0.15 μg/L, resp.) [80].

van Munster et al. analyzed the serum concentrations of S100B protein and NSE in 120 patients with hip fracture and a mean age of 83.9 years. Sixty-two patients experienced delirium. The authors observed a difference between the levels of S100B, but not NSE, in the first samples taken during delirium and the samples from nondelirious patients [15]. The simultaneous comparison of cortisol, IL-6, IL-8, and S100B protein revealed that the highest levels of cortisol and IL-8 were observed before delirium but the highest levels of IL-6 and S100B were observed during delirium. In multivariable analysis, cortisol, logIL-6, and logS100B were associated with delirium, but when adjusted for preexisting cognitive impairment, only logS100B remained associated [81]. With the exception of the previously cited work of van Munster et al., NSE concentration and delirium in orthopedic patients have received scant attention in the literature published in English.

Anckarsäter analyzed the perioperative levels of five CSF biomarkers: the Tau protein, pTau protein, Aβ42, neurofilament light (NFL), and GFAP in 35 patients undergoing knee arthroplasty under regional blockade. CSF Tau and GFAP concentrations increased, whereas pTau, Aβ42, and NFL were unchanged. CSF Tau and pTau significantly correlated with the CSF/serum albumin ratio as an indicator of blood-brain barrier permeability. The CSF Tau protein concentration also correlated with the administered doses of bupivacaine [25]. Witlox et al.'s study of 66 older adults with hip fracture found no differences in preoperative CSF Aβ1-42, Tau protein, and pTau in patients who did and did not develop delirium during hospitalization [19]. Summary of clinical studies on biomarkers of brain damage and their relation to orthopedic surgery and/or postoperative cognitive disorders was shown in Table 1.

6. Possible Explanation of Increased Concentration of Biomarkers of Brain Damage in Orthopedic Patients

The relationship between stress response, neuroinflammation, and biomarkers was previously mentioned. The question of surgical technique is also important. During some orthopedic procedures, bone cement is used to fix the elements of the implants to the bone base. However, it has been shown that the use of cement can lead to hemodynamic instability, a decrease in cardiac output, heart contractility, systemic vascular resistance, and blood pressure, that is, the so-called bone cement implantation syndrome [82]. Hemodynamic changes affect cerebral perfusion, as in the relation between S100B concentration and degree of shock [66]. Although the presence of bone cement inside the medullar cavity itself did not produce hypotension, hemodynamic instability was often observed when the prosthesis stem into the bone is hammered into the bone [83] and when the pressure inside the marrow cavity increases. The higher the pressure, the better the penetration of the cement into the bone and the greater the strength of osteosynthesis. However, because of the increased pressure, the translocation of the cellular material at the site of the surgery into the systemic circulation was facilitated, causing this material to reach the lungs via the bloodstream. The diameter of the lung capillaries is about 8 μm. In 1956, Niden and Aviado showed the possibility of transferring glass spheres up to 420 μm in diameter through the pulmonary vessels [84]. The second method used to circumvent the pulmonary filter was via the foramen ovale, which in one-third of the population is closed only functionally. Thus, embolic material could be transferred into the brain. In ultrasound examination the presence of cellular material from the site of the surgery in the circulatory system is shown by as a "snow flurry." In Hayakawa et al. [85], the "snow flurry" was observed from the beginning of the reaming of the femoral canal until the end of the surgery, and

Table 1: Summary of clinical studies on biomarkers of brain damage and their relation to orthopedic surgery and/or postoperative cognitive disorders.

Author(s)	Study design	Results	Conclusions	Reference
Anderson et al., 2001	Analysis of serum S100B concentrations for a normal population ($n = 459$) and multitrauma patients without head injury ($n = 17$).	The mean serum S100B concentration for a normal healthy population was 0.032 μg/L. Among trauma patients, serum S100B levels were highest after bone fractures and thoracic contusions. Burns and minor bruises also produced increased S100B levels.	Trauma, even in the absence of head trauma, results in high serum concentrations of S100B. S100B may have a negative predictive value to exclude brain tissue damage after trauma.	[8]
Kinoshita et al., 2003	Patients ($n = 14$) undergoing TKA with bone cement use ($n = 7$) or reamed intramedullary nailing for tibial fracture ($n = 7$).	The serum level of S100B was increased after a pneumatic tourniquet deflation in the TKA group compared with the tibial fracture group.	In patients undergoing TKA, bone cement may transiently induce astroglial injury, although it does not alter neurological outcomes.	[9]
Pelinka et al., 2003	Bilateral femur fracture in 10 anesthetized rats.	S100B concentration was increased after bilateral femur fracture and reached a peak 30–120 minutes after fracture.	S100B is increased after bilateral femur fracture without hemorrhagic shock in rats.	[10]
Stolz et al., 2004	Patients ($n = 37$) undergoing aortic valve replacement.	New DWI lesions (14 patients, 3 with focal deficits) correlated with age, preexisting T2 lesion volume, and postoperative S100B concentrations after surgery. In a forward stepwise canonical discrimination model, only T2 lesion volume was a relevant variable.	The volume of preexisting T2 lesions is related to the development of perioperative DWI lesions.	[11]
Ramlawi et al., 2006	Patients ($n = 40$) undergoing cardiac surgery under CPB.	The incidence of NCD was 40%. Both NSE and tau protein were elevated in the presence of NCD compared with those without NCD. S100B increase was not different between the NCD and control patients. Cardiotomy suction increased S100B levels; NSE and tau were not influenced.	NSE and tau are better associated with NCD and less influenced by cardiotomy suction compared with S100B.	[12]
Stålnacke et al., 2006	Female soccer players ($n = 44$) before and after a competition.	Concentration of both S100B and NSE was increased after the game, with correlation between S100 concentration and both the number of head injuries and other trauma events.	S100B and NSE were increased by game activities. The increases in S100B concentration were related to the number of head injuries and other trauma events.	[13]
Taurino et al., 2008	Patients ($n = 15$) undergoing carotid endarteriectomy.	MMP-9 levels were higher in patients with carotid stenosis versus controls, significantly in those with cerebral lesions at neuroimaging.	MMP-9 assay could be useful in the evaluation of carotid lesions to help identify those at highest risk of a neurologic event.	[14]

Table 1: Continued.

Author(s)	Study design	Results	Conclusions	Reference
van Munster et al., 2009	Patients ($n = 120$) aged 65 years or more with hip fracture.	The incidence of delirium was 51.7%. Delirious state, pre- or postoperative status, and type of fracture were associated with S100B levels. The highest S100B levels were found "during" delirium. No difference in S100B or NSE levels was seen regardless of subtype of delirium.	Delirium was associated with increased level of S100B.	[15]
Gaudet et al., 2010	Patients ($n = 73$) undergoing carotid endarteriectomy.	Approximately 19% of eligible patients developed NCD. Compared to patients without NCD, this group had both higher total and activity MMP-9 levels at baseline.		[16]
Mondello et al., 2010	Adult patients ($n = 40$) with severe TBI who underwent ventriculostomy.	Mean CSF levels of SBDPs were higher in TBI patients than in controls. SBDP145 provided accurate diagnoses at all time-points examined, while SBDP120 release was more accurate 24 h after injury. Within 24 h after injury, SBDP145 CSF levels correlated with GCS scores, while SBDP120 levels correlated with age. SBDP levels were higher in patients who died than in those who survived. SBDP145 levels (>6 ng/mL) and SBDP120 levels (>17.55 ng/mL) strongly predicted death.	CSF SBDP levels can predict injury severity and mortality after severe TBI and can be useful complements to clinical assessment.	[17]
Tomaszewski et al., 2010	Patients ($n = 60$) undergoing THA with ($n = 30$) or without ($n = 30$) bone cement use.	Following surgery, the S100B levels were increased in both groups. However, S100B concentration in the cement group was higher and its normalization was slower, in comparison to the noncement group. No clear changes in neuropsychological tests between both groups were observed.	There was a relationship between bone cement implantation and elevated S100B postoperatively; however, neuropsychological test results did not reflect this.	[18]
Witlox et al., 2011	Participants ($n = 77$) aged 75 and older admitted for surgical repair of acute hip fracture.	Postoperative delirium occurred in 39.5%. Preoperative CSF Aβ1-42, tau, and P-Tau levels were not different between participants who did and did not develop delirium.	CSF markers for plaque and tangle formation are not strongly associated with delirium risk in older adults with hip fracture.	[19]

Table 1: Continued.

Author(s)	Study design	Results	Conclusions	Reference
Jones et al., 2012	Participants ($n = 68$) over 60 years old following major surgery.	Baseline NSE and the change in NSE levels between baseline and 24 h were correlated with the change in CAMCOG score between baseline and 52 weeks.	NSE may be a useful predictor of individuals at risk of more severe long-term cognitive decline.	[20]
Mondello et al., 2012	Patients ($n = 16$) with severe TBI (GCS $\leq$ 8) 6 months after injury and in 16 controls.	Severe TBI patients had higher serum MAP-2 concentrations than controls with no history of TBI at 6 months after injury. MAP-2 levels correlated with the GOSE and LCFS at month 6. Lower serum levels of MAP-2 were observed in VS patients compared to non-VS patients.	Severe TBI results in a chronic release of MAP-2 in patients with higher levels of consciousness, suggesting that remodeling of synaptic junctions and neuroplasticity processes occur several months after injury. The data indicate MAP-2 as a potential marker for emergence to higher levels of cognitive function.	[21]
Papa et al., 2012	Adult patients ($n = 96$) with blunt head trauma.	Mean UCH-L1 levels in patients with positive CT scans were higher in comparison to those with negative CT.	UCH-L1 is detectable in serum within an hour of injury and is associated with measures of injury severity including the GCS score, CT lesions, and NSI.	[22]
Ji et al., 2013	Patients ($n = 83$) older than 65 years undergoing elective THA.	POCD occurred in 24.6% at 7 days after surgery. Patients with POCD had significantly higher IL-1β, Tau/Aβ1-42, P-Tau/Aβ1-42, and a lower level of Aβ1-42 in CSF when compared with the non-POCD group. There were no differences in preoperative CSF levels of Tau, IL-6, and P-Tau as well as plasma levels of IL-1β, IL-6, BDNF, and CRP between POCD and non-POCD groups.	The POCD patients were associated with higher postoperative plasma levels of MDA and higher IL-1β and lower Aβ1-42 levels in preoperative CSF that might predispose the development of POCD in aged patients following THA with spinal anesthesia.	[23]
Xie et al., 2013	Patients ($n = 136$) undergoing THA/TKA.	Preoperative CSF Aβ-42/tau ratio was associated with postoperative Hopkins Verbal Learning Test Retention and the Benton Judgment of Line Orientation. Aβ-40/tau ratio was associated with Brief Visuospatial Memory Test Total Recall.	Preoperative CSF Aβ/tau ratio is associated with postoperative changes. The presence of biomarkers, specifically the Aβ/tau ratio, may identify patients at higher risk for cognitive changes after surgery.	[24]

Table 1: Continued.

Author(s)	Study design	Results	Conclusions	Reference
Anckarsäter et al., 2014	Patients ($n = 35$) undergoing TKA under spinal anesthesia.	CSF T-Tau concentrations increased during and after surgery and were correlated with the administered doses of bupivacaine. P-Tau, Aβ-42, and NFL remained unchanged, while the mean GFAP level increased with a large standard deviation. CSF T-Tau and P-Tau correlated with the CSF/serum albumin ratios.	Bupivacaine may be involved in impaired cortical axonal integrity during nonneurological surgery.	[25]
Gempp et al., 2014	Divers ($n = 59$) with neurological DCS and 37 asymptomatic divers.	NSE, but not S100B protein, was higher in the DCS group than in controls.	NSE was found to be useful for the diagnosis of neurological DCS. Reliability of S100B was not demonstrated.	[26]

BNDF: brain-derived neurotrophic factor; CAMCOG score: Cambridge Assessment for Mental Disorder in the Elderly; CPB: cardiopulmonary bypass; CRP: C reactive protein; CSF: cerebrospinal fluid; CT: computer tomography; DCS: decompression sickness; DWI: diffusion-weighted imaging; GCS: Glasgow Coma Scale; GFAP: glial fibrillary acidic protein; GOSE: Glasgow Outcome Scale; LCFS: Level of Cognitive Function Scale; NCD: neurocognitive decline; NFL: neurofilament light; NSE: neuron-specific enolase; NSI: neurosurgical intervention; POCD: postoperative cognitive dysfunction; SBDPs: αII-spectrin breakdown products; TBI: traumatic brain injury; THA: total hip arthroplasty; TKA: total knee arthroplasty; UCH: ubiquitin C-terminal hydrolase; VS: vegetative state.

it intensified while the cemented prosthesis stem was being inserted into the bone. This was not noted during procedures that did not use bone cement. A histological examination of the elements forming the "snow flurry" revealed the presence of amorphous eosinophilic particles with fibrin attached to their surface. The same effect was noted in patients who had undergone cemented hip arthroplasty during the whole procedure, either before or after the use of bone cement. Fat particles or bone marrow was not detected in any sample; the authors thought that they had examined "bone dust" particles with attached fibrin fibers [85]. The work was limited to a relatively small group of only seven patients. In Kim et al., the histological examination of samples from the right atrium revealed the presence of fat particles in 34% and 44% of procedures and the presence of bone marrow cells in 13% and 11% of procedures, with and without bone cement, respectively [86]. The contribution of bone cement to the etiology of thromboembolic events was suggested [56]. Clark et al. showed a transient, but statistically significant, decrease of cardiac output by 33% and of stroke volume by 44% during procedures that used bone cement. Before the use of bone cement, there were no changes between the two (i.e., with and without cement) groups. Because embolic material was released either before or after the use of bone cement, the decrease in cardiac output and stroke volume might have been followed by the embolic material originating from bone marrow or vasodilatation caused by a monomer [87]. An animal studies with dog showed that an intravenous injection of the acrylic acid monomer did not affect the partial pressures of oxygen and carbon dioxide in the arterial blood. Mild and transient hypotension was observed, while monomer concentration in the pulmonary artery was much higher than that noted in usual clinical situations [88].

It should be noted that discussing the role of bone cement only in increased concentrations of biomarkers and the etiology of POCD is an oversimplification. The role of advanced age in the patients, their comorbidities, disturbances in blood flow (because of such problems such as atrial fibrillation and immobilization), and the consequences of long bone fractures can lead to the increased incidence of thromboembolic events, as described above.

Another issue concerns the effect of previously prescribed medications, the duration of hospitalization, the role of administered pharmacotherapy, and the impact of the anesthetic procedure on the development of postoperative cognitive decline.

7. Biomarkers of Brain Damage, Delirium, POCD, and Anesthetic Procedures

Previous research has considered the influence of different types of anesthesia (general versus regional) on elderly patients. Previously published clinical studies did not show the prevalence of any anesthesia in POCD prevention [6]. Evered et al. compared the incidence of POCD in 644 patients who underwent coronary angiography under sedation, total hip replacement surgery under general anesthesia, and coronary artery bypass graft surgery (CABG) under general anesthesia to 34 subjects in control group. The authors observed a higher incidence of POCD in elderly patients at day 7 after CABG than after the orthopedic procedure. However, the POCD at three months after the operation was independent of the type of surgery and anesthesia used [89]. However, a systematic review of Zywiel et al. on the influence of anesthesia and pain management on cognitive dysfunction after joint arthroplasty suggested that general anesthesia might be associated with increased risk of postoperative cognitive decline in the early postoperative period, compared to regional anesthesia, although the effect was not seen beyond seven days [90]. Some predisposing and precipitating factors associated with delirium and/or POCD, such as age, preexisting cognitive impairment, severe illness, anemia, immobilization, decreased oral intake, dehydration, sleep deprivation, and urinary catheter use, were common in all patients, regardless of the type of anesthesia. Regional anesthesia can be induced with a lower number of drugs, compared to general anesthesia. Moreover, the pain control is better and the incidence of thromboembolic complications is lower. However, the contraindications to neuroaxial blockade include disturbances in coagulation and circulatory failure. Thus, a number of orthopedic procedures on the lower limbs are performed under general anesthesia.

Neurotransmitters take part in the regulation of conscience, memory, and learning through the central cholinergic system [36]. Hence, the interactions between anesthetic drugs and this system may be important in the pathogenesis and development of POCD. There are two main classes of cholinergic receptors: nicotinic and muscarinic. Nicotinic acetylcholine receptors (nAChRs) are ligand-gated cation channels, and muscarinic acetylcholine receptors (mAChRs) are ligand-gated K+ channels, which are divided into five subtypes (M1–M5). The agonists of central mAChRs and nAChRs may improve, while the antagonists could impair performance in cognition, learning, and memory [36].

Volatile anesthetics and ketamine are potent inhibitors of nAChRs. Desflurane selectively binds the M1 subtype. Sevoflurane depresses the M1 and M2 subtypes, whereas isoflurane interferes only with the M3 subtype. All barbiturates are competitive antagonists of mAChRs. Propofol acts on mAChRs and nAChRs, but in concentrations higher than those used clinically do. Fentanyl and morphine inhibit signals mediated by both types of receptors, and remifentanil does not change the release of acetylcholine from cholinergic nerves. Furthermore, neuromuscular blocking agents or neostigmine administered during general anesthesia can influence cholinergic transmission [36].

Another question concerns the possible neurotoxicity of general anesthetics. The findings of both cell-culture and animal studies suggest that anesthetics may cause neuroapoptosis, caspase activation, neurodegeneration, β-amyloid protein accumulation, and oligomerization, leading to deficits in cognition. It has been shown that desflurane has a less harmful neurotoxic profile compared to other volatile anesthetics [46]. This finding was supported by Zhang et al. [91], who observed that the administration of isoflurane, but not desflurane, was associated with an increase in human CSF amyloid-β 40 concentrations at 24 hours after anesthesia,

compared to the values observed in patients under spinal anesthesia. Desflurane, but not isoflurane, was associated with the decrease in amyloid-β 42 levels at two hours after anesthesia. In this study, both isoflurane and desflurane did not significantly affect the concentration of the tau protein in human CSF [91].

Hudetz et al. [92, 93] found that a single administration of the intravenous anesthetic ketamine at 0.5 mg/kg during the induction of anesthesia reduced the incidence of POCD to one week after cardiac surgery. The authors concluded that the anti-inflammatory properties of ketamine produced this result.

The results of two studies [94, 95] analyzing the influence of the multimodal anesthetic technique on the incidence of POCD were conflicting. However, methodological inconsistencies obscured the clear interpretation of the results [90].

7.1. Postoperative Pain Management Strategy and Postoperative Cognitive Decline. Effective postoperative pain management in the postoperative period minimizes the use of opioids, which can decrease the incidence of postoperative cognitive decline [90]. Zywiel et al. [90] cited 12 studies that analyzed the influence of different postoperative pain management strategies on the risk of POCD. Langford et al. [96], in their study of 525 patients who underwent major noncardiac surgery, found decreased incidence of POCD on the second day after surgery (1.8% versus 5%), with the intravenous administration of parecoxib, compared to the placebo. Marino et al. [97] investigated the efficacy of continuous lumbar or femoral block, and YaDeau et al. [98] described the efficacy of single-shot femoral nerve block after TKA. These regional techniques decreased the incidence of POCD in orthopedic patients. Interestingly, the intra-articular administration of bupivacaine did not change the incidence of POCD after TKA, compared to the placebo [90].

The postoperative use of opioids is associated with a higher risk of development of POCD, regardless of par-enteral drug administration (intravenous, intramuscular, or epidural). The use of morphine, compared to fentanyl, was associated with the increased risk of POCD, when opioids were administered either intravenously [99, 100] or epidurally [101]. It also was found that the intravenous administration of opioids was associated with the higher incidence of POCD, compared to oral drug administration [90].

8. Presurgery Neuroanatomical Biomarkers for Postoperative Cognitive Decline

Previous studies have focused on the evaluation of brain damage markers in the postoperative period and their correlation with postoperative cognitive decline. However, of greater importance is the identification of the predictive factors of postoperative cognitive disorders amongst patients scheduled for surgery. It is known that certain cerebral regions, such as the entorhinal cortex (ERC) and the hippocampus, may change with Alzheimer disease. Leukoaraiosis and lacunae volume may indicate vulnerability for postoperative executive dysfunction [102]. Price et al. [102] analyzed the hypothesis that presurgical neuroanatomical markers, such as MRI-based hippocampus/ERC and leukoaraiosis/lacunae volume, may predict cognitive changes in the postoperative period. Their findings suggested that the value of presurgery ERC/hippocampal volumes as neuroanatomical predictors for cognitive decline was limited. However, perioperative leukoaraiosis and lacunae volume, as neuroimaging evidence of microvascular disease, helped explain postoperative executive function decline.

The results are preliminary as yet; nevertheless, these observations are interesting and should be a stimulus for further research.

9. Optimization of Surgical and Anesthetic Procedures in the Prevention of POCD

A fast-track set-up reduces the duration of hospitalization. Krenk et al. showed that when the length of stay of patients who underwent hip and knee arthroplasty was reduced from 7 to 10 days, with a median of 3 days, no cases of postoperative delirium were observed in the analyzed population [103]. In a series of 225 patients over 60 years, no cases of postoperative delirium were observed, and the incidence of POCD was reduced by more than 50% at one week, postoperatively [104]. The most recent data confirmed the above observations [105].

It is important to achieve the proper level of anesthesia during surgery. As mentioned previously, surgery-induced stress response has unwanted cardiovascular, metabolic, and immunological effects. On the other hand, overly deep levels of anesthesia may decrease cardiac function and organ perfusion. Therefore, the question of the potential neurotoxicity of general anesthetics remains unanswered. Farag et al. analyzed patients under general anesthesia; those with lower values on the Bispectral Index (BIS) had fewer disturbances in cognitive functions, especially in information processing, between the fourth and sixth weeks after surgery [106]. However, this observation seems isolated. Steinmetz et al. analyzed 70 patients with cerebral state index monitoring (CSI) and found no significant association between deep (CSI < 40) and light (CSI > 60) anesthesia [107]. Chan et al. found that BIS-guided anesthesia reduced anesthetic exposure and decreased the risk of POCD at three months after surgery. The authors concluded that when the depth of anesthesia is maintained at BIS values from 40 to 60, for every 1,000 patients undergoing major surgery, 23 were prevented from POCD and 83 were prevented from delirium [108]. BIS-guided anesthesia also improved the outcomes of surgical procedures [109].

During noncardiac surgery, significant cerebral desaturation occurred in up to 30% of patients [109]. Papadopoulos et al. described the association of cognitive dysfunction in elderly patients with hip fractures and low values of cerebral oxygenation [110]. Thus, the monitoring of cerebral oxygen saturation may be promising in the reduction of subtle neurologic deficits [111], particularly in patients who undergo total hip arthroplasty [112]. However, in a systematic review of cardiac surgery patients, Zheng et al. suggested that data are insufficient to conclude that interventions to improve cerebral regional saturation prevent stroke or POCD [113].

10. Summary

Although cognitive dysfunction in hospitalized patients is important both clinically and socially, it is difficult to analyze methodologically. Disturbances at the cellular level can manifest as mood disorders and lead to deterioration in patients' functioning and social assessment. It is very difficult to define either the normal state or the pathology of cognitive functions.

Because of the increase in age at hospitalization as well as in the number of orthopedic procedures, the issue of postoperative cognitive decline is gaining importance. A previous review on POCD and brain damage markers following large joint arthroplasty was published in 2011 [114]. Since then, knowledge on the biomarkers of brain damage and their correlation with cognitive impairment is becoming much more detailed. Studies on the utility of the different substances as potential biomarkers are being performed. The results of studies on cerebral oxygen saturation measured by near-red spectroscopy and its correlation with postoperative cognitive decline carry great promise. Despite the need for further tests, it is now known that patients at risk of postoperative cognitive disorders should be identified before surgery. From this perspective, the results of studies on neuroanatomical biomarkers will likely have future clinical applications.

The identification of patients with preexisting risk factors for POCD, shortening the period of time preceding the surgery, the appropriate technique used in the procedure, and adequate intraoperative monitoring as well as physical and intellectual exercises, nutrition, and medication play important roles in decreasing the incidence of neurocognitive deficits in the elderly.

Conflict of Interests

The author declares that there is no conflict of interests regarding the publication of this paper.

References

[1] L. S. Rasmussen, "Defining postoperative cognitive dysfunction," *European Journal of Anaesthesiology*, vol. 15, no. 6, pp. 761–764, 1998.

[2] T. G. Monk and C. C. Price, "Postoperative cognitive disorders," *Current Opinion in Critical Care*, vol. 17, no. 4, pp. 376–381, 2011.

[3] L. Krenk, L. S. Rasmussen, and H. Kehlet, "New insights into the pathophysiology of postoperative cognitive dysfunction," *Acta Anaesthesiologica Scandinavica*, vol. 54, no. 8, pp. 951–956, 2010.

[4] A. Morandi, P. P. Pandharipande, J. C. Jackson, G. Bellelli, M. Trabucchi, and E. W. Ely, "Understanding terminology of delirium and long-term cognitive impairment in critically ill patients," *Best Practice and Research: Clinical Anaesthesiology*, vol. 26, no. 3, pp. 267–276, 2012.

[5] S. Deiner and J. H. Silverstein, "Postoperative delirium and cognitive dysfunction," *British Journal of Anaesthesia*, vol. 103, no. 1, pp. i41–i46, 2009.

[6] C. L. Wu, W. Hsu, J. M. Richman, and S. N. Raja, "Postoperative cognitive function as an outcome of regional anesthesia and analgesia," *Regional Anesthesia and Pain Medicine*, vol. 29, no. 3, pp. 257–268, 2004.

[7] C. C. Price, C. W. Garvan, and T. G. Monk, "Type and severity of cognitive decline in older adults after noncardiac surgery," *Anesthesiology*, vol. 108, no. 1, pp. 8–17, 2008.

[8] R. E. Anderson, L.-O. Hansson, O. Nilsson, R. Dijlai-Merzoug, and G. Settergren, "High serum S100b levels for trauma patients without head injuries," *Neurosurgery*, vol. 48, no. 6, pp. 1255–1260, 2001.

[9] H. Kinoshita, H. Iranami, K. Fujii et al., "The use of bone cement induces an increase in serum astroglial S-100B protein in patients undergoing total knee arthroplasty," *Anesthesia & Analgesia*, vol. 97, no. 6, pp. 1657–1660, 2003.

[10] L. E. Pelinka, L. Szalay, M. Jafarmadar, R. Schmidhammer, H. Redl, and S. Bahrami, "Circulating S100B is increased after bilateral femur fracture without brain injury in the rat," *British Journal of Anaesthesia*, vol. 91, no. 4, pp. 595–597, 2003.

[11] E. Stolz, T. Gerriets, A. Kluge, W.-P. Klövekorn, M. Kaps, and G. Bachmann, "Diffusion-weighted magnetic resonance imaging and neurobiochemical markers after aortic valve replacement: implications for future neuroprotective trials?" *Stroke*, vol. 35, no. 4, pp. 888–892, 2004.

[12] B. Ramlawi, J. L. Rudolph, S. Mieno et al., "Serologic markers of brain injury and cognitive function after cardiopulmonary bypass," *Annals of Surgery*, vol. 244, no. 4, pp. 593–600, 2006.

[13] B.-M. Stålnacke, A. Ohlsson, Y. Tegner, and P. Sojka, "Serum concentrations of two biochemical markers of brain tissue damage S-100B and neurone specific enolase are increased in elite female soccer players after a competitive game," *British Journal of Sports Medicine*, vol. 40, no. 4, pp. 313–316, 2006.

[14] M. Taurino, S. Raffa, M. Mastroddi et al., "Metalloproteinase expression in carotid plaque and its correlation with plasma levels before and after carotid endarterectomy," *Vascular and Endovascular Surgery*, vol. 41, no. 6, pp. 516–521, 2008.

[15] B. C. van Munster, C. M. Korse, S. E. de Rooij, J. M. Bonfrer, A. H. Zwinderman, and J. C. Korevaar, "Markers of cerebral damage during delirium in elderly patients with hip fracture," *BMC Neurology*, vol. 9, article 21, 2009.

[16] J. G. Gaudet, G. T. Yocum, S. S. Lee et al., "MMP-9 levels in elderly patients with cognitive dysfunction after carotid surgery," *Journal of Clinical Neuroscience*, vol. 17, no. 4, pp. 436–440, 2010.

[17] S. Mondello, S. A. Robicsek, A. Gabrielli et al., "αiI-spectrin breakdown products (SBDPs): diagnosis and outcome in severe traumatic brain injury patients," *Journal of Neurotrauma*, vol. 27, no. 7, pp. 1203–1213, 2010.

[18] D. Tomaszewski, Z. Rybicki, and M. Mozański, "The influence of bone cement implantation in primary hip arthroplasty on S100B protein serum concentration and patients' cognitive functions as markers of brain damage," *European Journal of Trauma and Emergency Surgery*, vol. 36, no. 1, pp. 31–43, 2010.

[19] J. Witlox, K. J. Kalisvaart, J. F. M. De Jonghe et al., "Cerebrospinal fluid β-amyloid and tau are not associated with risk of delirium: a prospective cohort study in older adults with hip fracture," *Journal of the American Geriatrics Society*, vol. 59, no. 7, pp. 1260–1267, 2011.

[20] E. L. Jones, N. Gauge, O. B. Nilsen et al., "Analysis of neuron-specific enolase and S100B as biomarkers of cognitive decline following surgery in older people," *Dementia and Geriatric Cognitive Disorders*, vol. 34, no. 5-6, pp. 307–311, 2012.

[21] S. Mondello, A. Gabrielli, S. Catani et al., "Increased levels of serum MAP-2 at 6-months correlate with improved outcome in

survivors of severe traumatic brain injury," *Brain Injury*, vol. 26, no. 13-14, pp. 1629–1635, 2012.

[22] L. Papa, L. M. Lewis, S. Silvestri et al., "Serum levels of ubiquitin C-terminal hydrolase distinguish mild traumatic brain injury from trauma controls and are elevated in mild and moderate traumatic brain injury patients with intracranial lesions and neurosurgical intervention," *Journal of Trauma and Acute Care Surgery*, vol. 72, no. 5, pp. 1335–1344, 2012.

[23] M.-H. Ji, H.-M. Yuan, G.-F. Zhang et al., "Changes in plasma and cerebrospinal fluid biomarkers in aged patients with early postoperative cognitive dysfunction following total hip-replacement surgery," *Journal of Anesthesia*, vol. 27, no. 2, pp. 236–242, 2013.

[24] Z. Xie, S. McAuliffe, C. A. Swain et al., "Cerebrospinal fluid aβ to tau ratio and postoperative cognitive change," *Annals of Surgery*, vol. 258, no. 2, pp. 364–369, 2013.

[25] R. Anckarsäter, H. Anckarsäter, S. Bromander, K. Blennow, C. Wass, and H. Zetterberg, "Non-neurological surgery and cerebrospinal fluid biomarkers for neuronal and astroglial integrity," *Journal of Neural Transmission*, vol. 121, no. 6, pp. 649–653, 2014.

[26] E. Gempp, P. Louge, S. de Maistre, L. Emile, and J.-E. Blatteau, "Neuron-specific enolase and S100B protein levels in recreational scuba divers with neurological decompression sickness," *Diving and Hyperbaric Medicine*, vol. 44, no. 1, pp. 26–29, 2014.

[27] G. Blaise, R. Taha, and Y. Qi, "Postoperative cognitive dysfunction (POCD)," *Anesthesiology Rounds*, vol. 6, no. 4, 2007.

[28] B. T. Veering, "Management of anaesthesia in elderly patients," *Current Opinion in Anaesthesiology*, vol. 12, no. 3, pp. 333–336, 1999.

[29] J. Canet, J. Raeder, L. S. Rasmussen et al., "Cognitive dysfunction after minor surgery in the elderly," *Acta Anaesthesiologica Scandinavica*, vol. 47, no. 10, pp. 1204–1210, 2003.

[30] D. P. Fines and A. M. Severn, "Anaesthesia and cognitive disturbance in the elderly," *Continuing Education in Anaesthesia, Critical Care and Pain*, vol. 6, no. 1, pp. 37–40, 2006.

[31] T. C. Kyziridis, "Post-operative delirium after hip fracture treatment: a review of the current literature," *GMS Psycho-Social Medicine*, vol. 3, pp. 1–12, 2006.

[32] A. Singh and J. F. Antognini, "Perioperative pharmacology in elderly patients," *Current Opinion in Anaesthesiology*, vol. 23, no. 4, pp. 449–454, 2010.

[33] J. T. Moller, P. Cluitmans, L. S. Rasmussen et al., "Long-term postoperative cognitive dysfunction in the elderly: ISPOCD1 study," *The Lancet*, vol. 351, no. 9106, pp. 857–861, 1998.

[34] M. Coburn, A. Fahlenkamp, N. Zoremba, and G. Schaelte, "Postoperative cognitive dysfunction: incidence and prophylaxis," *Anaesthesist*, vol. 59, no. 2, pp. 177–185, 2010.

[35] T. N. Harwood, "Optimizing outcome in the very elderly surgical patient," *Current Opinion in Anaesthesiology*, vol. 13, no. 3, pp. 327–332, 2000.

[36] V. Fodale, L. B. Santamaria, D. Schifilliti, and P. K. Mandal, "Anaesthetics and postoperative cognitive dysfunction: a pathological mechanism mimicking Alzheimer's disease," *Anaesthesia*, vol. 65, no. 4, pp. 388–395, 2010.

[37] J. P. Desborough, "The stress response to trauma and surgery," *British Journal of Anaesthesia*, vol. 85, no. 1, pp. 109–117, 2000.

[38] A. W. Lemstra, K. J. Kalisvaart, R. Vreeswijk, W. A. van Gool, and P. Eikelenboom, "Pre-operative inflammatory markers and the risk of postoperative delirium in elderly patients," *International Journal of Geriatric Psychiatry*, vol. 23, no. 9, pp. 943–948, 2008.

[39] R. Ologunde and D. Ma, "Do inhalational anesthetics cause cognitive dysfunction?" *Acta Anaesthesiologica Taiwanica*, vol. 49, no. 4, pp. 149–153, 2011.

[40] A. Kalb, C. von Haefen, M. Sifringer et al., "Acetylcholinesterase inhibitors reduce neuroinflammation and -degeneration in the cortex and hippocampus of a surgery stress rat model," *PLoS ONE*, vol. 8, no. 5, Article ID e62679, 2013.

[41] L. Peng, L. Xu, and W. Ouyang, "Role of peripheral inflammatory markers in Postoperative Cognitive Dysfunction (POCD): a meta-analysis," *PLoS ONE*, vol. 8, no. 11, Article ID e79624, 2013.

[42] J. L. Rudolph, B. Ramlawi, G. A. Kuchel et al., "Chemokines are associated with delirium after cardiac surgery," *The Journals of Gerontology Series A: Biological Sciences and Medical Sciences*, vol. 63, no. 2, pp. 184–189, 2008.

[43] X. Wu, Y. Lu, Y. Dong et al., "The inhalation anesthetic isoflurane increases levels of proinflammatory TNF-α, IL-6, and IL-1β," *Neurobiology of Aging*, vol. 33, no. 7, pp. 1364–1378, 2012.

[44] T. Schilling, A. Kozian, M. Senturk et al., "Effects of volatile and intravenous anesthesia on the alveolar and systemic inflammatory response in thoracic surgical patients," *Anesthesiology*, vol. 115, no. 1, pp. 65–74, 2011.

[45] A. E. Hudson and H. C. Hemmings, "Are anaesthetics toxic to the brain?" *British Journal of Anaesthesia*, vol. 107, no. 1, pp. 30–37, 2011.

[46] P. Vlisides and Z. Xie, "Neurotoxicity of general anesthetics: an update," *Current Pharmaceutical Design*, vol. 18, no. 38, pp. 6232–6240, 2012.

[47] Y. Dong, G. Zhang, B. Zhang et al., "The common inhalational anesthetic sevoflurane induces apoptosis and increases β-amyloid protein levels," *Archives of Neurology*, vol. 66, no. 5, pp. 620–631, 2009.

[48] R. A. Whittington, L. Virág, F. Marcouiller et al., "Propofol directly increases tau phosphorylation," *PLoS ONE*, vol. 6, no. 1, Article ID e16648, 2011.

[49] H. Abildstrom, M. Christiansen, V. D. Siersma, and L. S. Rasmussen, "Apolipoprotein E genotype and cognitive dysfunction after noncardiac surgery," *Anesthesiology*, vol. 101, no. 4, pp. 855–861, 2004.

[50] J. E. Scott, J. L. Mathias, and A. C. Kneebone, "Postoperative cognitive dysfunction after total joint arthroplasty in the elderly: a meta-analysis," *Journal of Arthroplasty*, vol. 29, no. 2, pp. 261.e1–267.e1, 2014.

[51] H. Deo, G. West, C. Butcher, and P. Lewis, "The prevalence of cognitive dysfunction after conventional and computer-assisted total knee replacement," *Knee*, vol. 18, no. 2, pp. 117–120, 2011.

[52] D. M. Colonna, D. Kilgus, W. Brown, V. Challa, D. A. Stump, and D. M. Moody, "Acute brain fat embolization occurring after total hip arthroplasty in the absence of a patent foramen ovale," *Anesthesiology*, vol. 96, no. 4, pp. 1027–1029, 2002.

[53] G. Riding, K. Dally, S. Hutchinson, S. Rao, M. Lovell, and C. McCollum, "Paradoxical cerebral embolisation. An explanation for fat embolism syndrome," *Journal of Bone and Joint Surgery—Series B*, vol. 86, no. 1, pp. 95–98, 2004.

[54] K. Jenkins, F. Chung, R. Wennberg, E. E. Etchells, and R. Davey, "Fat embolism syndrome and elective knee arthroplasty," *Canadian Journal of Anesthesia*, vol. 49, no. 1, pp. 19–24, 2002.

[55] K. M. Fallon, J. G. Fuller, and P. Morley-Forster, "Fat embolization and fatal cardiac arrest during hip arthroplasty with methylmethacrylate," *Canadian Journal of Anesthesia*, vol. 48, no. 7, pp. 626–629, 2001.

[56] R. Scroop, J. Eskridge, and G. W. Britz, "Paradoxical cerebral arterial embolization of cement during intraoperative vertebroplasty: case report," *American Journal of Neuroradiology*, vol. 23, no. 5, pp. 868–870, 2002.

[57] M. R. Sukernik, B. Mets, and E. Bennett-Guerrero, "Patent foramen ovale and its significance in the perioperative period," *Anesthesia and Analgesia*, vol. 93, no. 5, pp. 1137–1146, 2001.

[58] T. Ingebrigtsen and B. Romner, "Biochemical serum markers for brain damage: a short review with emphasis on clinical utility in mild head injury," *Restorative Neurology and Neuroscience*, vol. 21, no. 3-4, pp. 171–176, 2003.

[59] I. Marenholz, C. W. Heizmann, and G. Fritz, "S100 proteins in mouse and man: from evolution to function and pathology (including an update of the nomenclature)," *Biochemical and Biophysical Research Communications*, vol. 322, no. 4, pp. 1111–1122, 2004.

[60] C. W. Heizmann, "S100B protein in clinical diagnostics: assay specificity," *Clinical Chemistry*, vol. 50, no. 1, pp. 249–251, 2004.

[61] M. Shaaban Ali, M. Harmer, and R. Vaughan, "Serum S100 protein as a marker of cerebral damage during cardiac surgery," *British Journal of Anaesthesia*, vol. 85, no. 2, pp. 287–298, 2000.

[62] A. Raabe, O. Kopetsch, A. Woszczyk et al., "Serum S-100B protein as a molecular marker in severe traumatic brain injury," *Restorative Neurology and Neuroscience*, vol. 21, no. 3-4, pp. 159–169, 2003.

[63] R. L. Eckert, A.-M. Broome, M. Ruse, N. Robinson, D. Ryan, and K. Lee, "S100 proteins in the epidermis," *Journal of Investigative Dermatology*, vol. 123, no. 1, pp. 23–33, 2004.

[64] J. P. Cata, B. Abdelmalak, and E. Farag, "Neurological biomarkers in the perioperative period," *British Journal of Anaesthesia*, vol. 107, no. 6, pp. 844–858, 2011.

[65] A. Kleindienst and M. R. Bullock, "A critical analysis of the role of the neurotrophic protein S100B in acute brain injury," *Journal of Neurotrauma*, vol. 23, no. 8, pp. 1185–1200, 2006.

[66] L. E. Pelinka, "Serum markers of severe traumatic brain injury: are they useful?" *Indian Journal of Critical Care Medicine*, vol. 8, no. 3, pp. 190–193, 2005.

[67] B.-M. Stålnacke, Y. Tegner, and P. Sojka, "Playing ice hockey and basketball increases serum levels of S-100B in elite players: a pilot study," *Clinical Journal of Sport Medicine*, vol. 13, no. 5, pp. 292–302, 2003.

[68] R. Donato, F. Riuzzi, and G. Sorci, "Causes of elevated serum levels of S100B protein in athletes," *European Journal of Applied Physiology*, vol. 113, no. 3, pp. 819–820, 2013.

[69] I. Salama, P. S. Malone, F. Mihaimeed, and J. L. Jones, "A review of the S100 proteins in cancer," *European Journal of Surgical Oncology*, vol. 34, no. 4, pp. 357–364, 2008.

[70] O. Piazza, E. Russo, S. Cotena, G. Esposito, and R. Tufano, "Elevated S100B levels do not correlate with the severity of encephalopathy during sepsis," *British Journal of Anaesthesia*, vol. 99, no. 4, pp. 518–521, 2007.

[71] S. Yokobori, K. Hosein, S. Burks, I. Sharma, S. Gajavelli, and R. Bullock, "Biomarkers for the clinical differential diagnosis in traumatic brain injury—a systematic review," *CNS Neuroscience & Therapeutics*, vol. 19, no. 8, pp. 556–565, 2013.

[72] L. E. Pelinka, A. Kroepfl, M. Leixnering, W. Buchinger, A. Raabe, and H. Redl, "GFAP versus S100B in serum after traumatic brain injury: relationship to brain damage and outcome," *Journal of Neurotrauma*, vol. 21, no. 11, pp. 1553–1561, 2004.

[73] L. E. Pelinka, A. Kroepfl, R. Schmidhammer et al., "Glial fibrillary acidic protein in serum after traumatic brain injury and multiple trauma," *Journal of Trauma: Injury Infection & Critical Care*, vol. 57, no. 5, pp. 1006–1012, 2004.

[74] L. Schiff, N. Hadker, S. Weiser, and C. Rausch, "A literature review of the feasibility of glial fibrillary acidic protein as a biomarker for stroke and traumatic brain injury," *Molecular Diagnosis and Therapy*, vol. 16, no. 2, pp. 79–92, 2012.

[75] Y. Sun, Q. Qin, Y.-J. Shang et al., "The accuracy of glial fibrillary acidic protein in acute stroke differential diagnosis: a meta-analysis," *Scandinavian Journal of Clinical and Laboratory Investigation*, vol. 73, no. 8, pp. 601–606, 2013.

[76] T. Nakasa, Y. Nagata, K. Yamasaki, and M. Ochi, "A mini-review: microRNA in arthritis," *Physiological Genomics*, vol. 43, no. 10, pp. 566–570, 2011.

[77] M. Nugent, "MicroRNA function and dysregulation in bone tumors: the evidence to date," *Cancer Management and Research*, vol. 6, no. 1, pp. 15–25, 2014.

[78] J. Undén, J. Bellner, M. Eneroth, C. Alling, T. Ingebrigtsen, and B. Romner, "Raised serum S100B levels after acute bone fractures without cerebral injury," *The Journal of Trauma Injury Infection and Critical Care*, vol. 58, no. 1, pp. 59–61, 2005.

[79] S. J. Lee, C. W. Kim, K. J. Lee et al., "Elevated serum S100B levels in acute spinal fracture without head injury," *Emergency Medicine Journal*, vol. 27, no. 3, pp. 209–212, 2010.

[80] S. Ohrt-Nissen, L. Friis-Hansen, B. Dahl, J. Stensballe, B. Romner, and L. S. Rasmussen, "How does extracerebral trauma affect the clinical value of S100B measurements?" *Emergency Medicine Journal*, vol. 28, no. 11, pp. 941–944, 2011.

[81] B. C. van Munster, P. H. Bisschop, A. H. Zwinderman et al., "Cortisol, interleukins and S100B in delirium in the elderly," *Brain and Cognition*, vol. 74, no. 1, pp. 18–23, 2010.

[82] A. J. Donaldson, H. E. Thomson, N. J. Harper, and N. W. Kenny, "Bone cement implantation syndrome," *British Journal of Anaesthesia*, vol. 102, no. 1, pp. 12–22, 2009.

[83] N. E. Sharrock, J. D. Beckman, E. C. Inda, and J. J. Savarese, "Anesthesia for orthopedic surgery," in *Miller's Anesthesia*, p. 2417, Elsevier Churchill Livingstone, London, UK, 2005.

[84] A. H. Niden and D. M. Aviado, "Effects of pulmonary embolism on the pulmonary circulation with special reference to arteriovenous shunts in the lung," *Circulation Research*, vol. 4, no. 1, pp. 67–73, 1956.

[85] M. Hayakawa, Y. Fujioka, Y. Morimoto, A. Okamura, and O. Kemmotsu, "Pathological evaluation of venous emboli during total hip arthroplasty," *Anaesthesia*, vol. 56, no. 6, pp. 571–575, 2001.

[86] Y.-H. Kim, S.-W. Oh, and J.-S. Kim, "Prevalence of fat embolism following bilateral simultaneous and unilateral total hip arthroplasty performed with or without cement: a prospective, randomized clinical study," *Journal of Bone and Joint Surgery—Series A*, vol. 84, no. 8, pp. 1372–1379, 2002.

[87] D. I. Clark, A. B. Ahmed, B. R. Baxendale, and C. G. Moran, "Cardiac output during hemiarthroplasty of the hip," *Journal of Bone and Joint Surgery—Series B*, vol. 83, no. 3, pp. 414–418, 2001.

[88] M. Concepcion, "Anesthesia for orthopedic surgery," in *Principles and Practice of Anesthesiology*, pp. 2113–2137, Mosby, 1998.

[89] L. Evered, D. A. Scott, B. Silbert, and P. Maruff, "Postoperative cognitive dysfunction is independent of type of surgery and anesthetic," *Anesthesia and Analgesia*, vol. 112, no. 5, pp. 1179–1185, 2011.

[90] M. G. Zywiel, A. Prabhu, A. V. Perruccio, and R. Gandhi, "The influence of anesthesia and pain management on cognitive dysfunction after joint arthroplasty: a systematic review," *Clinical*

Orthopaedics and Related Research, vol. 472, no. 5, pp. 1453–1466, 2014.

[91] B. Zhang, M. Tian, H. Zheng et al., "Effects of anesthetic isoflurane and desflurane on human cerebrospinal fluid Aβ and τ level," *Anesthesiology*, vol. 119, no. 1, pp. 52–60, 2013.

[92] J. A. Hudetz, K. M. Patterson, Z. Iqbal et al., "Ketamine attenuates delirium after cardiac surgery with cardiopulmonary bypass," *Journal of Cardiothoracic and Vascular Anesthesia*, vol. 23, no. 5, pp. 651–657, 2009.

[93] J. A. Hudetz, Z. Iqbal, S. D. Gandhi et al., "Ketamine attenuates post-operative cognitive dysfunction after cardiac surgery," *Acta Anaesthesiologica Scandinavica*, vol. 53, no. 7, pp. 864–872, 2009.

[94] J. R. Hebl, S. L. Kopp, M. H. Ali et al., "A comprehensive anesthesia protocol that emphasizes peripheral nerve blockade for total knee and total hip arthroplasty," *Journal of Bone and Joint Surgery A*, vol. 87, no. 12, pp. 63–70, 2005.

[95] C. L. Peters, B. Shirley, and J. Erickson, "The effect of a new multimodal perioperative anesthetic regimen on postoperative pain, side effects, rehabilitation, and length of hospital stay after total joint arthroplasty," *The Journal of Arthroplasty*, vol. 21, no. 6, supplement 2, pp. 132–138, 2006.

[96] R. M. Langford, G. P. Joshi, T. J. Gan et al., "Reduction in opioid-related adverse events and improvement in function with parecoxib followed by valdecoxib treatment after non-cardiac surgery: a randomized, double-blind, placebo-controlled, parallel-group trial," *Clinical Drug Investigation*, vol. 29, no. 9, pp. 577–590, 2009.

[97] J. Marino, J. Russo, M. Kenny, R. Herenstein, E. Livote, and J. E. Chelly, "Continuous lumbar plexus block for postoperative pain control after total hip arthroplasty a randomized controlled trial," *Journal of Bone and Joint Surgery A*, vol. 91, no. 1, pp. 29–37, 2009.

[98] J. T. YaDeau, J. B. Cahill, M. W. Zawadsky et al., "The effects of femoral nerve blockade in conjunction with epidural analgesia after total knee arthroplasty," *Anesthesia and Analgesia*, vol. 101, no. 3, pp. 891–895, 2005.

[99] I. A. Herrick, S. Ganapathy, W. Komar et al., "Postoperative cognitive impairment in the elderly: choice of patient-controlled analgesia opioid," *Anaesthesia*, vol. 51, no. 4, pp. 356–360, 1996.

[100] C. T. Hartrick, M. H. Bourne, K. Gargiulo, C. V. Damaraju, S. Vallow, and D. J. Hewitt, "Fentanyl iontophoretic transdermal system for acute-pain management after orthopedic surgery: a comparative study with morphine intravenous patient-controlled analgesia," *Regional Anesthesia and Pain Medicine*, vol. 31, no. 6, pp. 546–554, 2006.

[101] O. A. Ilahi, J. P. Davidson, and H. S. Tullos, "Continuous epidural analgesia using fentanyl and bupivacaine after total knee arthroplasty," *Clinical Orthopaedics and Related Research*, no. 299, pp. 44–52, 1994.

[102] C. C. Price, J. J. Tanner, I. Schmalfuss et al., "A pilot study evaluating presurgery neuroanatomical biomarkers for postoperative cognitive decline after total knee arthroplasty in older adults," *Anesthesiology*, vol. 120, no. 3, pp. 601–613, 2014.

[103] L. Krenk, L. S. Rasmussen, T. B. Hansen, S. Bogø, K. Søballe, and H. Kehlet, "Delirium after fast-track hip and knee arthroplasty," *British Journal of Anaesthesia*, vol. 108, no. 4, pp. 607–611, 2012.

[104] L. Krenk, L. S. Rasmussen, and H. Kehlet, "Delirium in the fast-track surgery setting," *Best Practice and Research: Clinical Anaesthesiology*, vol. 26, no. 3, pp. 345–353, 2012.

[105] L. Krenk, H. Kehlet, T. Bæk Hansen, S. Solgaard, K. Soballe, and L. S. Rasmussen, "Cognitive dysfunction after fast-track hip and knee replacement," *Anesthesia & Analgesia*, vol. 118, no. 5, pp. 1034–1040, 2014.

[106] E. Farag, G. J. Chelune, A. Schubert, and E. J. Mascha, "Is depth of anesthesia, as assessed by the Bispectral Index, related to postoperative cognitive dysfunction and recovery?" *Anesthesia and Analgesia*, vol. 103, no. 3, pp. 633–640, 2006.

[107] J. Steinmetz, K. S. Funder, B. T. Dahl, and L. S. Rasmussen, "Depth of anaesthesia and post-operative cognitive dysfunction," *Acta Anaesthesiologica Scandinavica*, vol. 54, no. 2, pp. 162–168, 2010.

[108] M. T. V. Chan, B. C. P. Cheng, T. M. C. Lee, and T. Gin, "BIS-guided anesthesia decreases postoperative delirium and cognitive decline," *Journal of Neurosurgical Anesthesiology*, vol. 25, no. 1, pp. 33–42, 2013.

[109] C. Ballard, E. Jones, N. Gauge et al., "Optimised anaesthesia to reduce post operative cognitive decline (POCD) in older patients undergoing elective surgery, a randomised controlled trial," *PLoS ONE*, vol. 7, no. 6, Article ID e37410, 2012.

[110] G. Papadopoulos, M. Karanikolas, A. Liarmakopoulou, G. Papathanakos, M. Korre, and A. Beris, "Cerebral oximetry and cognitive dysfunction in elderly patients undergoing surgery for hip fractures: A prospective observational study," *The Open Orthopaedics Journal*, vol. 6, pp. 400–405, 2012.

[111] E. de Tournay-Jett, G. Dupuis, L. Bherer, A. Deschamps, R. Cartier, and A. Denault, "The relationship between cerebral oxygen saturation changes and postoperative cognitive dysfunction in elderly patients after coronary artery bypass graft surgery," *Journal of Cardiothoracic and Vascular Anesthesia*, vol. 25, no. 1, pp. 95–104, 2011.

[112] R. Lin, F. Zhang, Q. Xue, and B. Yu, "Accuracy of regional cerebral oxygen saturation in predicting postoperative cognitive dysfunction after total hip arthroplasty: regional cerebral oxygen saturation predicts POCD," *Journal of Arthroplasty*, vol. 28, no. 3, pp. 494–497, 2013.

[113] F. Zheng, R. Sheinberg, M.-S. Yee, M. Ono, Y. Zheng, and C. W. Hogue, "Cerebral near-infrared spectroscopy monitoring and neurologic outcomes in adult cardiac surgery patients: a systematic review," *Anesthesia & Analgesia*, vol. 116, no. 3, pp. 663–676, 2013.

[114] D. Tomaszewski, "Postoperative cognitive dysfunction (POCD) and markers of brain damage after big joints arthroplasty," in *Recent Advances in Arthroplasty*, S. K. Fokter, Ed., pp. 3–14, InTech, Rijeka, Croatia, 2011.

Hindawi Publishing Corporation
BioMed Research International
Volume 2015, Article ID 402642, 6 pages
http://dx.doi.org/10.1155/2015/402642

Clinical Study

Circulating S100B and Adiponectin in Children Who Underwent Open Heart Surgery and Cardiopulmonary Bypass

Alessandro Varrica,[1] Angela Satriano,[1] Alessandro Frigiola,[1] Alessandro Giamberti,[1] Guido Tettamanti,[1] Luigi Anastasia,[1] Erika Conforti,[1] Antonio D. W. Gavilanes,[2] Luc J. Zimmermann,[2] Hans J. S. Vles,[2] Giovanni Li Volti,[3] and Diego Gazzolo[4]

[1]*Department of Pediatric Cardiac Surgery IRCCS San Donato Milanese Hospital, Via Morandi 30, 20097 San Donato Milanese, Italy*
[2]*Department of Pediatrics, Neonatology and Child Neurology, Maastricht University, P. Debyelaan 25, 5800 Maastricht, Netherlands*
[3]*Department of Drug Sciences, Section of Biochemistry, University of Catania, Viale A. Doria 6, 95125 Catania, Italy*
[4]*Department of Maternal Fetal and Neonatal Medicine, C. Arrigo Children's Hospital, Spalto Marengo 46, 15100 Alessandria, Italy*

Correspondence should be addressed to Alessandro Varrica; a.varrica@virgilio.it

Received 26 June 2014; Accepted 26 October 2014

Academic Editor: Giovanni Scapagnini

Background. S100B protein, previously proposed as a consolidated marker of brain damage in congenital heart disease (CHD) newborns who underwent cardiac surgery and cardiopulmonary bypass (CPB), has been progressively abandoned due to S100B CNS extra-source such as adipose tissue. The present study investigated CHD newborns, if adipose tissue contributes significantly to S100B serum levels. *Methods*. We conducted a prospective study in 26 CHD infants, without preexisting neurological disorders, who underwent cardiac surgery and CPB in whom blood samples for S100B and adiponectin (ADN) measurement were drawn at five perioperative time-points. *Results*. S100B showed a significant increase from hospital admission up to 24 h after procedure reaching its maximum peak ($P < 0.01$) during CPB and at the end of the surgical procedure. Moreover, ADN showed a flat pattern and no significant differences ($P > 0.05$) have been found all along perioperative monitoring. ADN/S100B ratio pattern was identical to S100B alone with the higher peak at the end of CPB and remained higher up to 24 h from surgery. *Conclusions*. The present study provides evidence that, in CHD infants, S100B protein is not affected by an extra-source adipose tissue release as suggested by no changes in circulating ADN concentrations.

1. Introduction

Advances in cardiothoracic surgical and anesthetic techniques, including cardiopulmonary bypass (CPB), have substantially decreased mortality, expanding the horizon to address functional neurologic and cardiac outcomes in long-term survivors [1]. Acute neurocardiac morbidities in congenital heart disease (CHD) infants are well described and interest in the functional status of survivors now stretches beyond the newborn period to childhood, adolescence, and adulthood [2]. Newborn heart surgery represents a period of planned and deliberate hypoxia-ischemia (HI) injury, which is the price to pay in the treatment or palliation of CHD. To date, the possibility of detecting infants at risk for mortality and morbidity is limited since clinical, laboratory, and standard monitoring procedures may be silent or unreliable [3]. Thus, a practical and sensitive marker able to offer physicians a useful tool for clinical is therefore eagerly awaited.

In the last decade a brain constituent, namely, S100B protein, has been proposed as a well-established marker of brain damage and death [4–10], since elevated S100B concentrations in different biological fluids have been found in adults, infants, and fetuses at risk for brain damage [4–15]. S100B is an acidic calcium-modulated protein of low molecular weight, first identified by Moore as a protein

fraction detectable in the central nervous system (CNS) in glial and Schwann cells and in specific neuronal subpopulations [16]. With regard to CHD infants who underwent cardiac surgery and CPB, S100B has been shown to be increased in the perioperative period [17, 18], to correlate with different CPB phases [19] and with increased cerebrovascular resistance and brain damage [20]. However, protein's assessment in CHD infants for CPB monitoring has been progressively abandoned on the basis of S100B extra CNS site of concentrations including adipose tissue [21]. The issue is still controversial and matter of debate. From one side, a contamination originating by mediastinal tissues on S100B releasing into systemic circulation has been suggested [22–25]. From the other side, it has been shown that extracranial sources of S100B do not affect serum levels and protein's diagnostic value in neurological diseases in intact subjects [26]. In this setting, data in nonintact patients such as without traumatic brain or bodily injury from accident or surgery are still lacking.

Therefore, the objective of this current study was to determine, in CHD newborns, if adipose tissue sources contribute significantly to serum levels of S100B by means of the longitudinal measurement of adiponectin (ADN), the most abundant adipose-derived protein in humans [27] and S100B at different perioperative time-points.

2. Materials and Methods

2.1. Patients. From March 2010 to September 2011, we conducted an observational study in which 26 infants (15 males and 11 females) from 0 to 9 months of age (mean 30.4 months), without preexisting neurological disorders or other comorbidities, admitted to our referral centers for the correction of congenital heart defects (Table 1). Exclusion criteria included need for inotropic support or mechanical ventilation prior to surgery, recent cardiac arrest, and weight of less than 2 kg.

Informed consent from parents was obtained before patient inclusion in the study, which was approved by the local human-investigation committee.

Blood samples were drawn at five predetermined time-points in the preoperative period as follows: before the surgical procedure (time 0, $T0$); during the surgical procedure before CPB (time 1, $T1$); at the end of CPB (time 2, $T2$); at the end of the surgical procedure (time 3, $T3$); 24 h after the surgical procedure (time 4, $T4$). At these time-points ADN levels and ADN/S100B ratio were measured. Clinical parameters (peripheral temperature, nasopharyngeal temperature, pump flow rate, mean blood pressure, and arterial pH) were recorded at all sample times for the purpose of monitoring the general pattern of the surgical procedure.

2.1.1. Anesthetic Technique. After premedication with midazolam 0.5 mg/Kg bw (rectal/intramuscular), induction was achieved with oxygen and 3% sevofluorane administered via mask (single breath induction), followed by intravenous sufentanil 1 (g/Kg bw) and vecuronium (0.15 mg/Kg bw). Maintenance was achieved with 3% sevofluorane (except during CPB) and with additional doses of sufentanil (0.5 g/Kg bw) and vecuronium (0.1 mg/Kg bw) every 30–40 min. During CPB, in the absence of sevofluorane, additional midazolam at 0.2 mg/Kg bw dosage was given. Sufentanil infusion at 0.25 g/Kg bw was continued in the intensive care unit for sedation.

Table 1: General characteristics and perioperative data in the infants admitted into the study. Data are given as mean ± SD.

Parameters	
Age (months)	41.6 ± 30.4
Sex (male/female)	15/11
Weight (Kg)	11.5 ± 4.7
Type of surgery	
Great artery transposition (no)	4
Ventricular septal defect (no)	5
Total anomalous pulmonary vein connection (no)	4
Tetralogy of fallot (no)	2
Double outlet right ventricle (no)	3
Complete A-V canal defect (no)	2
Atrial septal defect (no)	6
CPB duration (min) (no)	89.9 ± 43.4
Cross clamp duration (min)	45.1 ± 32.2
Temperature in CPB (°C) median	31.8 ± 3.5
MUF (no)	20

AV: atrioventricular; CPB: cardiopulmonary bypass; and MUF: modified ultrafiltration.

2.1.2. Cardiopulmonary Bypass Management. CPB was established after systemic heparinization (3 mg/Kg bw) by standard single stage aortic and bicaval cannulation and was maintained via nonpulsatile pump flow with a membrane oxygenator (Dideco Laboratories, Modena, Italy). Flow velocity was kept at 120–150 mL/Kg bw and mean arterial blood pressure at 45 mmHg; hypothermia was attained by core and surface cooling. Mean CPB duration time was 90 ± 43 min; mean rewarming time was 15 ± 8 min (mean ± SD), calculated from the final temperature during hypothermic circulatory arrest to 36.5°C. The minimum temperature reached was 27.2°C. The pump priming solution was composed of electrolyte solutions (Normosol-R 250 to 650 mL, Abbott Hospital Products, Abbott Park, IL, USA or Plasma-Lyte A, Travenol Laboratories, Inc., Deerfield, IL, USA), albumin (25%), heparin 1000 to 5000 units in the total solution, sodium bicarbonate (25–30 mEq/L), and packed red blood cells or fresh frozen plasma. A standard circuit prime total volume was used, according to body-weight varying from 400 mL (bw < 4.5 Kg) to 600 mL (bw > 4.5 Kg and bw < 7.5 kg) and to 700 mL (bw > 7.7 kg). Packed red blood cells (200 to 500 mL) were transfused as necessary to maintain a hematocrit level above 30% during CPB [26]. Protamine (1 mg for each mg of heparin) was administered at the end of CPB.

The α-stat regimen was used, and the $PaCO_2$ was maintained between 35 and 40 mmHg, without mathematical

correction for the effects of the temperature, by varying the membrane oxygenator gas flow.

2.1.3. Adiponectin Measurement. Serum ADN concentrations were determined by an enzyme-linked immunosorbent assay (Human Adiponectin ELISA, EZHADP-61 K; Linco Research). Sensitivity limit for this assay is 0.78 ng/mL for Human Adiponectin (20 μL sample size). The appropriate range of the assay is 1.56 to 200 ng/mL Human Adiponectin (20 μL sample size). The results were evaluated according to ng/mL.

2.1.4. S100B Measurement. Samples for S100B measurements at the seven monitoring time-points were drawn from a catheter inserted in the jugular vein. Heparin-treated blood samples were immediately centrifuged at 900 g for 10 min and the supernatants were stored at −70°C before measurement. The S100B protein concentration was measured in all samples using a commercially available two-site immunoradiometric assay kit (Sangtec 100; AD Sangtec Medical, Bromma, Sweden) specific to the β-subunit of the protein, which is known to be present mostly (80–96%) in the human brain [28]. Each measurement was performed in duplicate and the mean values are reported. The limit of sensitivity of the assay was 0.02 μg/L. The precision (CV) was <10%.

2.1.5. Neurological Follow-Up. Neurological development was assessed by physical examination, preoperatively and on the 7th postoperative day, based on Amiel-Tison's criteria [29]. In particular, resistance against passive movements, visual pursuit, reaching and grasping, and responses to visual and acoustic stimuli were tested by the same examiner, who did not know of the subjects' presurgical condition.

2.2. Statistical Analysis. ADN and S100B plasma concentrations are expressed as median and 5–95% coefficient intervals (CI). Comparisons at the different monitoring time-points were analyzed by Kruskal-Wallis one-way ANOVA. Linear regression analysis was used for correlation between ADN and S100B and various parameters (CPB, cooling, and rewarming duration; body core temperature; arterial blood pH, arterial oxygen and carbon dioxide partial pressures, and base excess; and mean arterial blood pressure and heart rate). Statistical significance was set at $P < 0.05$.

3. Results

In Table 1 patients' characteristics are reported. Clinical, laboratory, and standard monitoring parameters recorded at the predetermined time-points remained within the reference limits and therefore were not different ($P > 0.05$; for all) in all infants. Intraoperative parameters such as CPB, cross-clamping, cooling, and rewarming durations were within reference ranges and no perioperative complications have been shown. No complications in the postoperative period have been reported and no overt neurological disease was detected at discharge from hospital.

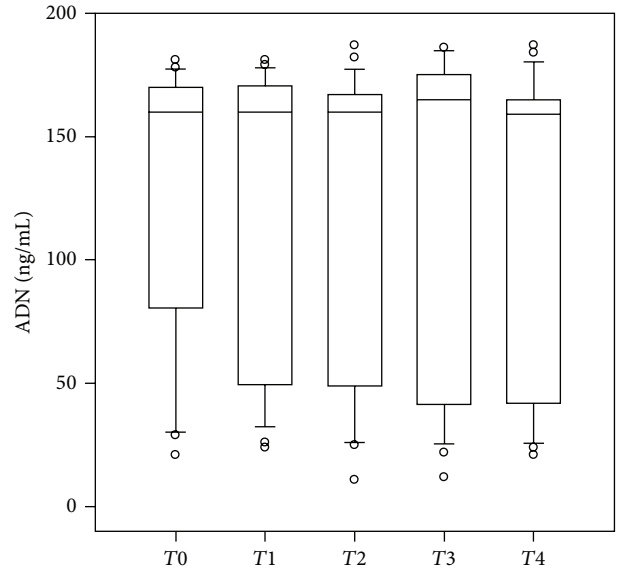

Figure 1: Adiponectin (ADN) (ng/mL) blood concentrations expressed as median and coefficient intervals ($CI_{5-95\%}$) at different monitoring time-points (before the surgical procedure ($T0$); during the surgical procedure after sternotomy before CPB ($T1$); at the end CPB ($T2$); at the end of the surgical procedure ($T3$); and at 24 h after the surgical procedure (time 4, $T4$)).

ADN was measurable in all samples collected. ADN pattern at different monitoring time-points showed a flat trend and therefore no significant differences ($P > 0.05$, for all) have been found all along perioperative monitoring up to 24 h from surgery ($T0$–$T4$) (Figure 1).

S100B was measurable in all samples collected. S100B pattern at different monitoring time-points was characterized by a protein's significant increase ($P < 0.01$, for all), reaching its highest peak at the end of CPB and remaining stable up to 24 h from surgery (Figure 2(a)).

Linear regression analysis showed no significant correlations ($P > 0.05$, for all) between ADN and S100B at all monitoring time-points ($T0$–$T4$) and between ADN and CPB ($r = 0.08$; $P = 0.73$) and cross clamp ($r = 0.05$; $P = 0.82$) durations. Conversely, S100B significantly correlated with CPB ($r = 0.53$; $P = 0.003$) and at cross clamp ($r = 0.65$; $P < 0.01$) durations.

ADN/S100B ratio pattern was characterized by a significant increase ($P < 0.01$) from $T0$ to $T3$ reaching its dip at $T2$ and returning at $T4$ at preoperative levels. No significant correlations ($P > 0.05$, for all) between ADN/S100B ratio and CPB ($r = 0.12$; $P = 0.56$) and cross clamp ($R = 0.19$; $P = 0.35$) duration have been found (Figure 2(b)).

4. Discussion

Despite recent advances in cardiac surgery and CPB management, the possibility of detecting infants at risk for neonatal mortality and morbidity is still faraway due to limitations in the standard monitoring procedures currently performed [1, 2]. In this setting, brain biomarkers previously suggested

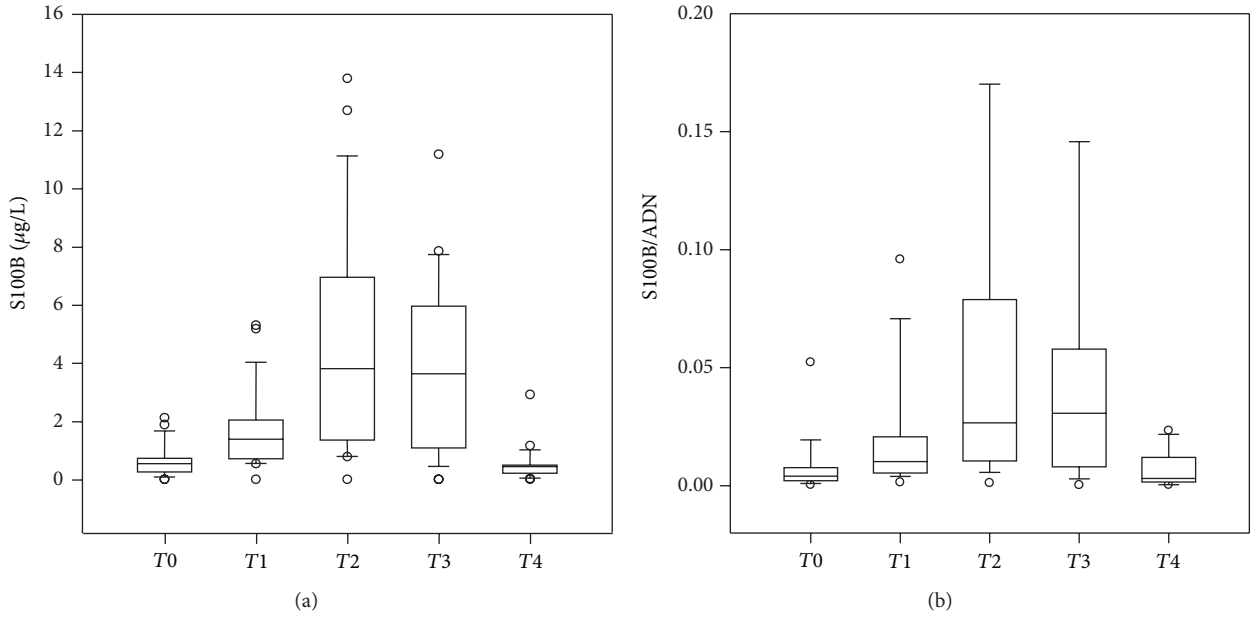

Figure 2: (a) S100B (μg/L) blood concentrations expressed as median and coefficient intervals ($CI_{5-95\%}$) at different monitoring time-points (before the surgical procedure ($T0$); during the surgical procedure after sternotomy before CPB ($T1$); at the end CPB ($T2$); at the end of the surgical procedure ($T3$) and at 24 h after the surgical procedure (time 4, $T4$)). $^{*}P < 0.01$ versus $T0$. (b) S100B (μg/L) and adiponectin (ADN) (ng/mL) blood concentrations expressed as median and coefficient intervals ($CI_{5-95\%}$) at different monitoring time-points (before the surgical procedure ($T0$); during the surgical procedure after sternotomy before CPB ($T1$); at the end CPB ($T2$); at the end of the surgical procedure ($T3$); and at 24 h after the surgical procedure (time 4, $T4$)). $^{*}P < 0.01$ versus $T0$.

as promising tools disappointed expectations and, to date, a trustable biomarker of brain damage in the perioperative period is still eagerly awaited. This holds for S100B protein, first reported as a useful tool and later on abandoned for brain monitoring of CHD adults and children [18–21]. The explanations are still controversial and debated although the main resides in a contamination by protein' extrasources such as adipose tissue [22–25].

The present study provides evidence that, in CHD infants, S100B protein is not affected by an extrasource adipose tissue release as suggested by no changes in circulating ADN concentrations. Furthermore, the ADN/S100B ratio pattern was superimposable to S100B alone all along the perioperative period.

The finding of ADN trend in the perioperative period is not surprising and fits, in part, previous observations in pediatric patients where decreased ADN levels have been reported [27]. The discrepancies are several and reside in the number, timing, and the length of the monitoring time-points and in the different CPB management (mild versus moderate hypothermia). In this setting, hypothermia is known to activate an exaggerated release of proinflammatory cytokines and of endogenous cortisol that may be responsible of decreased ADN transcription and blood levels [27, 30, 31]. Anyway, further investigations comparing ADN pattern under different CPB management such as mild versus moderate/deep hypothermia are so justified.

The finding of increased S100B levels and flat ADN/S100B ratio enforces the debating issue on the protein' *pros and cons* as brain stress/damage marker in CHD patients. From one hand, the absence of any interference in circulating S100B in the perioperative period is in agreement with previous observations, both in adults and children, reporting no compromise on the diagnostic value of S100B in neurological diseases *in intact subjects* (without traumatic brain or bodily injury from accident or surgery) [26]. These findings are also consistent with the usefulness of the protein in brain monitoring of CHD infants [18–20]. On the other hand, the discrepancy with previous observations warrants further consideration in terms of contamination following invasive procedures during CPB. This refers to CPB standard procedures, known to increase mediastinum release of the protein, as pericardial suction blood re-/autotransfusion, zero-balanced ultra-filtration, and pericardial blood processing with cell-saving devices [22–25, 32–34]. The high S100B levels at the site of reinfusion is *per se* of limited relevance because of the known mediastinum site of concentration of the protein. In fact, once S100B was measured in systemic circulation, after reinfusion procedures, its concentration did not appear to be affected by mediastinum source [35]. The main explanations reside in lowest S100B extrasources' concentrations when compared with the total amount of the protein in the CNS [36]. Although, there are no observations in pediatric and postnatal periods in whom protein distribution in CNS and other tissues can differ or not from adults [37], in the latter (estimated for a 70 Kg man) the absolute amount of S100B in the tissue (calculated in micrograms) showed the highest protein's concentration in brain (538.000 μg: 90.9%) followed by muscles (42.000 μg: 7.1%), adipose tissue (10.500 μg: 1.77%), heart (1.000 μg: 0.2%),

and liver (200 μg: 0.03%) [36]. Taken together, the possibility that adipose tissue could constitute a significant source of contamination affecting S100B diagnostic value seems to be fairly remote.

Among different S100B sites of contamination cardiac tissue extrasource deserves further consideration [36]. In particular (i) in rat model of myocardial infarction it has been shown that S100B may play a dual role in cardiomyocytes survival or death (i.e., necrosis and apoptosis) through a RAGE-dependent mechanism, and (ii) S100B, once released from damaged myocytes, with consequent leakage of the protein into the systemic circulation, is approximately 1000-fold less than the amount of protein required to induce apoptosis [38]. Indeed, local high S100B concentration was detected only at the site of myocardial infarction and, finally, (iii) in humans, cardiac tissue contamination on S100B has been justified by a correlation between troponin I and S100B [23] although a hypoxia mediated effect could be reasonably the main explanation of the increase in circulating biomarkers' levels [3, 4]. Altogether, bearing in mind the extremely low protein' concentrations in cardiac tissue the present findings suggest that the possibility of a cardiac tissue extrasource contamination on circulating S100B levels argue against this hypothesis. Conversely, it is reasonable to suppose that the upregulation of S100B protein is a consequence of hypoxia itself, instead of dead cells belonging to the necrosis/apoptosis area. To this regard, it has been demonstrated both in humans and in sheep model that acute hypoxemia is able to induce a significant increase in S100B release within 15 minute form insult in absence of any CNS damage [39]. This is of great relative interest to this contest because, as shown in our series, it is possible to argue that H-I insult occurring during CPB phase may trigger protein's release due to "multiorgan" stress of whom CNS constitutes the majority of the total protein's amount [3, 4, 36]. In this regard, further studies aimed at investigating potential confounding factors such as S100A1 and RAGE and the S100A1B dimer interactions in the cascade of events leading to cell death and apoptosis are still needed.

In conclusion, our results showing, in nonintact patients, that S100B protein is not affected by an extrasource adipose tissue release during the perioperative period open up further studies, in wider populations, aimed at confirming protein's role of early marker of hypoxia and CNS stress/damage in CHD children.

List of Abbreviations

CPB: Cardiopulmonary bypass
CHD: Congenital heart diseases
CNS: Central nervous system
ADN: Adiponectin
SD: Standard deviation
CI: Coefficient intervals.

Conflict of Interests

The authors declare that there is no conflict of interests regarding the publication of this paper.

Acknowledgments

This study is part of the I.O. Ph.D. International Program, under the auspices of the Italian Society of Neonatology and of the Neonatal Clinical Biochemistry Research Group, and was partially supported by grants to Diego Gazzolo from I Colori della Vita Foundation, Italy.

References

[1] A. Kansy, Z. Tobota, P. Maruszewski, and B. Maruszewski, "Analysis of 14,843 neonatal congenital heart surgical procedures in the European association for cardiothoracic surgery congenital database," *Annals of Thoracic Surgery*, vol. 89, no. 4, pp. 1255–1259, 2010.

[2] D. C. Bellinger, R. A. Jonas, L. A. Rappaport et al., "Developmental and neurologic status of children after heart surgery with hypothermic circulatory arrest or low-flow cardiopulmonary bypass," *The England Journal of Medicine*, vol. 332, no. 9, pp. 549–555, 1995.

[3] R. Donato, B. R. Cannon, G. Sorci et al., "Functions of S100 proteins," *Current Molecular Medicine*, vol. 13, no. 1, pp. 24–57, 2013.

[4] F. Michetti, V. Corvino, M. C. Geloso et al., "The S100B protein in biological fluids: more than a lifelong biomarker of brain distress," *Journal of Neurochemistry*, vol. 120, no. 5, pp. 644–659, 2012.

[5] B. W. Schäfer and C. W. Heizmann, "The S100 family of EF-hand calcium-binding proteins: functions and pathology," *Trends in Biochemical Sciences*, vol. 21, no. 4, pp. 134–140, 1996.

[6] G. Fanò, S. Biocca, S. Fulle, M. A. Mariggio, S. Belia, and P. Calissano, "The S-100: a protein family in search of a function," *Progress in Neurobiology*, vol. 46, no. 1, pp. 71–82, 1995.

[7] C. W. Heizmann, "Ca2+-binding S100 proteins in the central nervous system," *Neurochemical Research*, vol. 24, no. 9, pp. 1097–1100, 1999.

[8] P. Florio, F. Michetti, M. Bruschettini et al., "Amniotic fluid S100B protein in mid-gestation and intrauterine fetal death," *The Lancet*, vol. 364, no. 9430, pp. 270–272, 2004.

[9] D. Gazzolo, A. Frigiola, M. Bashir et al., "Diagnostic accuracy of S100B urinary testing at birth in full-term asphyxiated newborns to predict neonatal death," *PLoS ONE*, vol. 4, no. 2, Article ID e4298, 2009.

[10] D. Gazzolo, P. Florio, S. Ciotti et al., "S100B protein in urine of preterm newborns with ominous outcome," *Pediatric Research*, vol. 58, no. 6, pp. 1170–1174, 2005.

[11] D. Gazzolo, E. Marinoni, R. di Iorio, M. Lituania, P. L. Bruschettini, and F. Michetti, "Circulating S100β protein is increased in intrauterine growth-retarded fetuses," *Pediatric Research*, vol. 51, no. 2, pp. 215–219, 2002.

[12] D. Gazzolo, D. Grutzfeld, F. Michetti et al., "Increased S100B in cerebrospinal fluid of infants with bacterial meningitis: relationship to brain damage and routine cerebrospinal fluid findings," *Clinical Chemistry*, vol. 50, no. 5, pp. 941–944, 2004.

[13] D. Gazzolo, P. Vinesi, M. Bartocci et al., "Elevated S100 blood level as an early indicator of intraventricular hemorrhage in preterm infants: Correlation with cerebral Doppler velocimetry," *Journal of the Neurological Sciences*, vol. 170, no. 1, pp. 32–35, 1999.

[14] D. Gazzolo, P. Florio, S. Ciotti et al., "S100B protein in urine of preterm newborns with ominous outcome," *Pediatric Research*, vol. 58, no. 6, pp. 1170–1174, 2005.

[15] P. Florio, E. Marinoni, R. di Iorio et al., "Urinary S100B protein concentrations are increased in intrauterine growth-retarded newborns," *Pediatrics*, vol. 118, no. 3, pp. e747–e754, 2006.

[16] B. W. Moore, "A soluble protein characteristic of the nervous system," *Biochemical and Biophysical Research Communications*, vol. 19, no. 6, pp. 739–744, 1965.

[17] S. Westaby, P. Johnsson, A. J. Parry et al., "Serum S100 protein: a potential marker for cerebral events during cardiopulmonary bypass," *Annals of Thoracic Surgery*, vol. 61, no. 1, pp. 88–92, 1996.

[18] P. M. Bokesch, E. Appachi, M. Cavaglia, E. Mossad, and R. B. B. Mee, "A glial-derived protein, S100B, in neonates and infants with congenital heart disease: evidence for preexisting neurologic injury," *Anesthesia and Analgesia*, vol. 95, no. 4, pp. 889–892, 2002.

[19] D. Gazzolo, P. Vinesi, M. C. Geloso et al., "S100 blood concentrations in children subjected to cardiopulmonary by-pass," *Clinical Chemistry*, vol. 44, no. 5, pp. 1058–1060, 1998.

[20] D. Gazzolo, P. Masetti, M. Kornacka, R. Abella, P. Bruschettini, and F. Michetti, "Phentolamine administration increases blood S100B protein levels in pediatric open-heart surgery patients," *Acta Paediatrica*, vol. 92, no. 12, pp. 1427–1432, 2003.

[21] J. Vaage and R. Anderson, "Biochemical markers of neurologic injury in cardiac surgery: the rise and fall of S100β," *Journal of Thoracic and Cardiovascular Surgery*, vol. 122, no. 5, pp. 853–855, 2001.

[22] J. Babin-Ebell, P. Roth, J. Reese, M. Bechtel, and A. Mortasawi, "Serum S100B levels in patients after cardiac surgery: possible sources of contamination," *Thoracic and Cardiovascular Surgeon*, vol. 55, no. 3, pp. 168–172, 2007.

[23] S. A. Snyder-Ramos, T. Gruhlke, H. Bauer et al., "Cerebral and extracerebral release of protein S100B in cardiac surgical patients," *Anaesthesia*, vol. 59, no. 4, pp. 344–349, 2004.

[24] H. Jönsson, P. Johnsson, M. Bäckström, C. Alling, C. Dautovic-Bergh, and S. Blomquist, "Controversial significance of early S100B levels after cardiac surgery," *BMC Neurology*, vol. 4, article 24, 2004.

[25] S. Svenmarker and K. G. Engström, "The inflammatory response to recycled pericardial suction blood and the influence of cell-saving," *Scandinavian Cardiovascular Journal*, vol. 37, no. 3, pp. 158–164, 2003.

[26] N. Pham, V. Fazio, L. Cucullo et al., "Extracranial sources of S100B do not affect serum levels," *PLoS ONE*, vol. 5, no. 9, Article ID e12691, 2010.

[27] A. Thaler, H. Kanety, T. Avni et al., "Postoperative adiponectin levels in pediatric patients undergoing open heart surgery," *BioMed Research International*, vol. 2013, Article ID 408680, 7 pages, 2013.

[28] R. Jensen, D. R. Marshak, C. Anderson, T. J. Lukas, and D. M. Watterson, "Characterization of human brain S100 protein fraction: amino acid sequence of S100β," *Journal of Neurochemistry*, vol. 45, no. 3, pp. 700–705, 1985.

[29] C. Amiel-Tison, "Neurological evaluation of the maturity of newborn infants," *Archives of Disease in Childhood*, vol. 43, no. 227, pp. 89–93, 1968.

[30] H. T. F. de Mendonça-Filho, K. C. Pereira, M. Fontes et al., "Circulating inflammatory mediators and organ dysfunction after cardiovascular surgery with cardiopulmonary bypass: a prospective observational study," *Critical Care*, vol. 10, no. 2, article R46, 2006.

[31] H. Tilg and A. R. Moschen, "Inflammatory mechanisms in the regulation of insulin resistance," *Molecular Medicine*, vol. 14, no. 3-4, pp. 222–231, 2008.

[32] M. Carrier, A. Denault, J. Lavoie, and L. P. Perrault, "Randomized controlled trial of pericardial blood processing with a cell-saving device on neurologic markers in elderly patients undergoing coronary artery bypass graft surgery," *Annals of Thoracic Surgery*, vol. 82, no. 1, pp. 51–55, 2006.

[33] M. de Baar, J. C. Diephuis, K. G. M. Moons, J. Holtkamp, R. Hijman, and C. J. Kalkman, "The effect of zero-balanced ultrafiltration during cardiopulmonary bypass on S100b release and cognitive function," *Perfusion*, vol. 18, no. 1, pp. 9–14, 2003.

[34] M. Carrier, A. Denault, J. Lavoie, and L. P. Perrault, "Randomized controlled trial of pericardial blood processing with a cell-saving device on neurologic markers in elderly patients undergoing coronary artery bypass graft surgery," *The Annals of Thoracic Surgery*, vol. 82, no. 1, pp. 51–55, 2006.

[35] H. Jönsson, "S100B and cardiac surgery: possibilities and limitations," *Restorative Neurology and Neuroscience*, vol. 21, no. 3-4, pp. 151–157, 2003.

[36] H. Haimoto, S. Hosoda, and K. Kato, "Differential distribution of immunoreactive S100-α and S100-β proteins in normal nonnervous human tissues," *Laboratory Investigation*, vol. 57, no. 5, pp. 489–498, 1987.

[37] E. Cacciari, S. Milani, A. Balsamo et al., "Italian cross-sectional growth charts for height, weight and BMI (2 to 20 yr)," *Journal of Endocrinological Investigation*, vol. 29, no. 7, pp. 581–593, 2006.

[38] J. N. Tsoporis, S. Izhar, H. Leong-Poi, J.-F. Desjardins, H. J. Huttunen, and T. G. Parker, "S100B interaction with the receptor for advanced glycation end products (RAGE): a novel receptor-mediated mechanism for myocyte apoptosis postinfarction," *Circulation Research*, vol. 106, no. 1, pp. 93–101, 2010.

[39] D. A. Giussani, A. S. Thakor, R. Frulio, and D. Gazzolo, "Acute hypoxia increases S100β protein in association with blood flow redistribution away from peripheral circulations in fetal sheep," *Pediatric Research*, vol. 58, no. 2, pp. 179–184, 2005.

Hindawi Publishing Corporation
BioMed Research International
Volume 2015, Article ID 769763, 10 pages
http://dx.doi.org/10.1155/2015/769763

Review Article

Regeneration, Plasticity, and Induced Molecular Programs in Adult Zebrafish Brain

Mehmet Ilyas Cosacak,[1,2] Christos Papadimitriou,[1,2] and Caghan Kizil[1,2]

[1] *German Centre for Neurodegenerative Diseases (DZNE), The Helmholtz Association, Arnoldstraße 18, 01307 Dresden, Germany*
[2] *DFG-Center for Regenerative Therapies Dresden (CRTD), Cluster of Excellence at the TU Dresden, Fetscherstraße 105, 01307 Dresden, Germany*

Correspondence should be addressed to Caghan Kizil; caghan.kizil@dzne.de

Received 25 June 2014; Revised 25 September 2014; Accepted 25 September 2014

Academic Editor: Giovanni Li Volti

Regenerative capacity of the brain is a variable trait within animals. Aquatic vertebrates such as zebrafish have widespread ability to renew their brains upon damage, while mammals have—if not none—very limited overall regenerative competence. Underlying cause of such a disparity is not fully evident; however, one of the reasons could be activation of peculiar molecular programs, which might have specific roles after injury or damage, by the organisms that regenerate. If this hypothesis is correct, then there must be genes and pathways that (a) are expressed only after injury or damage in tissues, (b) are biologically and functionally relevant to restoration of neural tissue, and (c) are not detected in regenerating organisms. Presence of such programs might circumvent the initial detrimental effects of the damage and subsequently set up the stage for tissue redevelopment to take place by modulating the plasticity of the neural stem/progenitor cells. Additionally, if transferable, those "molecular mechanisms of regeneration" could open up new avenues for regenerative therapies of humans in clinical settings. This review focuses on the recent studies addressing injury/damage-induced molecular programs in zebrafish brain, underscoring the possibility of the presence of genes that could be used as biomarkers of neural plasticity and regeneration.

1. Introduction

The brain is an intricate and complex network of hard-wired neurons and glia that sustain a tremendously complex architectural integrity and central physiological function throughout the life of vertebrates. In contrast to what Ramon y Cajal proposed in 1928 [1], we now know that the nervous system is not fixed and immutable, but is quite plastic in its nature so as to respond to physiological and external stimuli. The terms of adult neurogenesis and plasticity, therefore, denote the overall ability of the brain—in general the nervous system—to remodel its cellular composition and synaptic wiring on demand.

2. Plasticity in Mammalian Brains Is Limited

The adult vertebrate brains display a large variety of neural plasticities, which includes the dynamic recruitment of the synapses, and neurogenesis upon the proliferative activity of the neural stem cells (NSCs). Neurogenesis in adult mammalian brain is a result of localized niches of stem cells [2–7]. In adult mammals, although several regions of the brains were suggested to be neurogenic [8–11], canonical zones are believed to exist in the telencephalon [12, 13] in two distinct neurogenic areas: the subventricular zone (SVZ) of the lateral ventricle and the subgranular zone of the dentate gyrus in the hippocampus (SGZ) [2, 3, 14–17]. In rodents, the SVZ niche consists of heterogeneous neural stem cells that give rise to different cell types [7, 18]. The SVZ contains relatively quiescent astrocyte-like neural stem cells and these astrocytes get activated upon damage or injury yielding in quite poor regeneration due to scarce newborn neurons, inability to form lost neuronal cell types, and low survival [19–27]. Another type of astrocytic cells is the parenchymal astroglia, which is one of the major cell types reacting to any injury by increasing their proliferation

rate [24, 28–30]. Despite their neurogenic potential *in vitro*, these astroglia do not form neurons *in vivo* [28, 31–33]. Upon injury, parenchymal astrocytes remain within their lineage and amplify themselves as a scar is formed [28, 34–36]. Such a gliotic scar hampers axonal regeneration by generating an impermeable physical barrier [37–39], which exacerbates the insufficient cellular reconstitution and neural recuperation.

Several stimuli including traumatic injuries, chronic loss of neurons, environmental changes, cognitive input, and disease states can induce plasticity response in the brain [40–46]. The disruption of such a plasticity response and mutilation of adult neurogenesis not only are causes of improper regenerative ability, but also lead to cognitive impairment and psychiatric disorders [47, 48]. For instance, hippocampal atrophy and reduced adult neurogenesis due to impaired activity of the NSCs were found to correlate with the cognitive dysfunction and memory performance [49]. Additionally the fact that some antipsychotic drugs elevate the proliferation of the NSCs [50] suggests a strong functional relevance of adult neurogenesis to schizophrenia—the exact cause of which is unknown but the onset and progression of the disease correlate with wrongly structured or absent neural circuits involved in production of neurotransmitters such as dopamine or the ones associated with cognitive functions. One hallmark of the pathophysiology of the psychiatric disorders is reduced size of the hippocampus—a prominent region of the brain involved in formation of memory, spatial navigation, and consolidation of thought. Since hippocampus is a region that generates neurons throughout the lifespan of humans utilizing neural stem cells, such observations suggest that the reduced plasticity of neural stem cells (NSCs) and hampered adult neurogenesis might be a major cause of psychiatric disorders.

Severe neuronal damage in case of medial cerebral arterial occlusion (MCAO) or ischemic injury was also shown to induce plasticity in mammalian brains [19, 27, 51–53]. MCAO results in infarcts and neuronal death in large regions of the brain including the striatum and cortex. Upon such an insult, the progeny of the NSCs at the SVZ diverts their normal migratory routes to these nonneurogenic regions and generates neurons that populate the infarct areas [19, 27]. Although the number of neurons is meager, the subtypes of the neurons are not exactly matching the lost ones and the survival of newborn neurons is poor. Additionally, mammalian brains were also suggested to bear plasticity upon neurodegenerative conditions [41, 43, 45, 54], although this ability is not fully translated into functional recovery. Several studies have shown that neural stem cell is affected during chronic neurodegeneration; for instance, postmortem analyses of Huntington's patients showed thicker SVZ and increased proliferation of ventricular cells [41], chemically induced epileptic seizures transiently increase the production of neuroblasts in the hippocampus and the SVZ [45], and, in an experimental model of murine prion disease and postmortem analyses of Creutzfeldt-Jacob patients, hippocampal neurogenesis was found to increase [42], while in Parkinson's patients cell proliferation is dramatically hampered [43]. These findings constitute an overall indication that mammalian brains might have a widespread but unfavorable plasticity response, which endows us an incentive for aiming at regenerative therapies by manipulating the stem cell behavior *in vivo*.

3. Zebrafish Has an Extensive Plasticity in Its Adult Brain

In nature, in contrast to mammals, several vertebrates display a striking ability of widespread adult neurogenesis and brain plasticity [5, 55–58]. One of these organisms is zebrafish, which possess an extensive adult neurogenesis response of its NSCs and can regenerate its brain upon traumatic lesions [59–62]. This is in stark contrast to mammalian brains, which poorly regenerate, despite prevalent adult neurogenesis in two neurogenic niches of the forebrain. Various zones of stem cell activity were described in adult zebrafish brain [63–67]. These zones generate neurons that are integrated into the circuitry as BrdU labeling experiments resulted in various lineages of newborn neurons in parenchymal regions after several weeks of BrdU pulse [63, 64]. The majority of the stem/progenitor cells are of radial glial cells (RGCs) [5, 56, 68]. RGCs express markers such as GFAP, glutamine synthetase, vimentin, S100B, aromatase-B, BLBP, or *her4.1* [60, 63, 64, 69–72]. With such properties, adult zebrafish brain is quite more plastic than their mammalian counterparts. Additionally, in contrast to mammals, the adult fish brain regenerates even after severe traumatic lesions without overt scar formation [60, 61]. Injury to the dorsal telencephalon elevates the levels of the proliferation of ventricularly located neurogenic progenitors: RGCs [59, 60, 62]. Thus, mammals and zebrafish have a substantial difference in their abilities to recuperate neuronal damage in their central nervous system. Additionally, the genes and pathways involved in the initiation and maintenance of such an extensive regenerative response in zebrafish brain are largely unknown, rendering zebrafish as an excellent model to investigate those molecular programs.

4. Induced Molecular Programs Enable Plasticity Response during Zebrafish Brain Regeneration

The process of regeneration definitely involves turning on "redevelopment." For instance, if a neuron will be generated, genes that govern the specification and differentiation of that particular subtype of neuron during development—such as Delta-Notch signaling or pathways leading to subtype specification, axonogenesis, or synaptogenesis—become active again. However, in case of neuronal loss, be it acute or chronic, nonphysiological events that are normally not seen during development take place. These include stress response, inflammation, wound healing mechanisms, and other phenomena related to the breach of the homeostatic balance. In most cases, these phenomena were shown to be detrimental for the regenerative ability in mammals [73–80], and they have to be overcome for regeneration to succeed. On the other hand, zebrafish can regenerate even though experiencing such nonphysiological circumstances. Therefore, a plausible

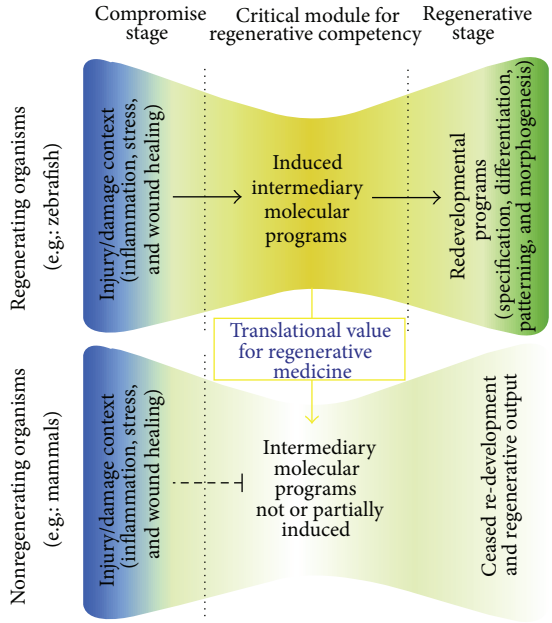

Figure 1: Induced intermediary molecular programs enable regeneration. In regenerating and nonregenerating organisms, injury or damage leads to similar initial events such as inflammation, stress, and wound healing response. There is increasing evidence that regenerating organisms such as zebrafish induce the expression of genes that are functionally essential for regenerative response including the modulation of stem cell plasticity, cell proliferation, differentiation, and survival. These genes and pathways constitute the "induced intermediary molecular programs," which set up the stage for reopening the developmental programs of specification, differentiation, patterning, and morphogenesis. One of the reasons why regeneration is not efficient in mammals could be the lack of activation of these intermediary genes. Therefore, the intermediary molecular programs bear a significant value for translational aspects of regenerative medicine and can be used as biomarkers of plasticity and regenerative ability.

hypothesis is that the organisms that can regenerate might be using some "intermediary" molecular programs that link the initial events to the redevelopment of tissues (Figure 1). These intermediate programs could be specifically induced after neuronal loss and might be crucial to regenerative success as they might set the stage to alleviate the negative consequences of homeostatic compromise and to turn on the programs of redevelopment. A scientific challenge based on this hypothesis is to identify such putative intermediary genes and pathways in regenerating organisms. Thus, zebrafish serves as a promising animal model to this purpose.

Several studies have so far shown that, during regeneration of the adult zebrafish tissues, genes that are not expressed during the development of the corresponding tissues can be induced [81–91]. Specifically in adult zebrafish brain, acute inflammation has been shown to contribute to activation of neural progenitor cells with radial glial identity [77, 86]. Leukotriene C4 (LTC4) was shown to emanate from immune cells that populate the brain tissue after lesion and activate an intracellular signal transduction in radial glial cells, where the cysteinyl leukotriene receptor 1 (*cystlr1*) is present [86]. Injection of LTC4 using cerebroventricular microinjection (CVMI) [70, 92] is sufficient to increase the proliferation of radial glial cells and subsequent regenerative neurogenesis by activating regeneration-specific molecular program involving the zinc finger transcription factor *gata3*. This gene is interesting as it is not expressed during development and homeostatic adult telencephalons of the zebrafish brain, but is induced in the RGCs shortly after lesion [84]. Knockdown experiments using CVMI and Gata3 antisense morpholinos showed that Gata3 does not partake in regulation of constitutive neurogenesis, but is specifically required for the injury-induced cell proliferation response of the ventricular neurogenic progenitor cells and subsequent reactive neurogenesis: two hallmarks of the regenerative response gata3 are injury induced in other regenerating organs of zebrafish and are functionally required for the proliferation of progenitor cells [84]. Such a dynamic expression and biological relevance of gata3 suggests that this gene might be part of a molecular program zebrafish might be using universally for regenerating its tissues. Additionally, *gata3* has not been documented to be activated in mammalian brains upon injury or insult so far, suggesting that such genes like *gata3* might underlie the disparity between the regenerative capacities of zebrafish and mammalian brains. Therefore, such molecular programs or novel epistatic interactions could be used as biomarkers of brain injury and regenerative response.

Another study identified the 7-pass transmembrane domain chemokine receptor *Cxcr5* as a gene required for regenerative neurogenesis but not for increased proliferation of the radial glial cells [83]. Cxcr5 is expressed at low levels in the RGCs in homeostatic unlesioned adult zebrafish telencephalon and is predominantly absent in neurons. After a lesion, *cxcr5* expression increases dramatically in periventricular neurons [83]. Blocking this chemokine signaling by overexpressing a dominant negative version of the Cxcr5 receptor that lacks the transmembrane domains 5, 6, and 7, which renders the receptor incapable of eliciting an intracellular signaling cascade, does not result in any change in RGC proliferation in unlesioned or lesioned brains. However, the same genetic knockdown results in reduced number of newborn neurons only after lesion [83]. Similarly, morpholino-mediated knockdown of *cxcr5* gene in adult zebrafish brain leads to similar reduction of regenerative neurogenesis [83]. Conversely, when the full-length Cxcr5 is overexpressed, production of new neurons increased significantly only after lesion despite no change in RGC proliferation. These findings suggest that Cxcr5-mediated chemokine signaling might be specifically required for generation of neurons after acute neuronal loss and might also serve as a biomarker for regenerative neurogenesis.

Alternatively, some molecular programs could be turned off or overridden during regeneration of adult zebrafish brain [93]. For instance, estradiol was shown to hamper proliferation of progenitor cells in the adult zebrafish brain under homeostatic conditions, while this regulation does not take place during regeneration [93]. Since radial glial cells specifically express the aromatase that synthesizes estrogen [72], certain physiological conditions might downregulate signaling pathways that are prevalent during homeostatic state.

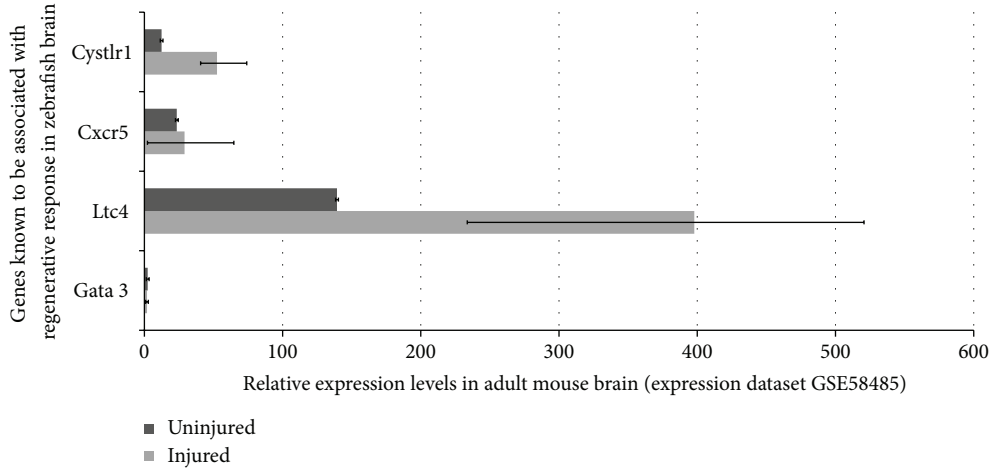

Figure 2: Relative expression levels of regeneration-associated genes of adult zebrafish brain in mouse brain before and after lesion based on publicly available gene expression datasets.

Collectively, an important but still partial list of molecular programs that allow the special regenerative response in the zebrafish brain was identified as described above. Interestingly, some of those programs are induced only during regenerative stage and are essential for production of newborn neurons. These findings suggest that regenerating organisms such as zebrafish could use special molecular programs to enable regenerative neurogenesis, and these programs might be responsible for different regenerative capacities of zebrafish and mammalian brains.

5. Missing Regeneration Programs in Mammals?

Experimental data suggests that the crucial need for induced intermediary programs in zebrafish makes regeneration possible [56, 77, 83, 84, 86]. A very valid and intriguing question is therefore whether those regeneration programs would be activated in mammalian brains after neuronal loss. Several gene expression datasets on central nervous system injuries are publicly available on repositories such as Array Express (http://www.ebi.ac.uk/arrayexpress/) and Gene Expression Omnibus (GEO) (http://www.ncbi.nlm.nih.gov/geo/). To find out whether the regeneration programs of zebrafish are activated in mammalian models of injury, we investigated the expression levels of those genes in one representative dataset (Figure 2). In this dataset, gene expression profiles of injured and uninjured mouse brains are compared. The expression values of the genes presented in the pathway analysis map are based on the Query Data Set GSE58484 (Gene Expression Omnibus accession number) [94]. The injured group reflects the gene expression from wild type B6 mice at 3 days after a traumatic brain injury at the ipsilateral neocortex (Datasets: GSM1412408, GSM1412409, and GSM1412410). The control samples show the gene expression values at the neocortex of uninjured wild type B6 mice (Datasets: GSM1412411, GSM1412412, and GSM1412413). When we checked the expression levels of three genes experimentally known to be required for regeneration in zebrafish, *gata3*, *cxcr5*, *cystlr1*, we found that *cystlr1* is expressed in high levels after injury, while *cxcr5* and *gata3* are unchanged (Figure 2). Interestingly, *gata3* expression is very low before and after injury, almost at nonexistent levels. *Cxcr5* is also expressed at low levels and statistically is not different than that of nondetectable levels. These findings suggest that it is quite possible that the inability to activate regeneration programs and genes, two of which are *cxcr5* and *gata3*, might be one of the underlying reasons why mammalian brains could not turn on regeneration mechanisms. This hypothesis also points to the importance of further experiments to elucidate more genes participating in regeneration response of adult zebrafish central nervous system.

Hypothetically, the regeneration genes if turned on in mammalian brains could modulate further pathways and genes. This modulation might run through two ways: (1) regeneration genes can regulate downstream genes and pathways that are already known to be associated with them; (2) regeneration genes could regulate completely novel genes and pathways. The latter scenario is impossible to predict without experimental studies, which will aim to identify downstream gene regulation of regeneration factors after misexpression studies such as knockdown, knockout, or overexpression. However, the former scenario can be predicted using already existing interaction maps. In order to find out this interaction map and pathway analysis for *gata3* and *cxcr5*, we used publicly available online in silico tools, such as GeneMANIA, a prediction tool for functional interaction maps and pathways based on a large data of functional interaction data (http://genemania.org/). When we included *gata3* and *cxcr5* into query and also added three proneural genes Neurogenin1 (Ngn1), achaete-scute complex homolog 1 (Ascl1), and Notch1 to narrow down the interaction map to neurogenic pathways, we found two particular maps for human and mouse (Figure 3). These maps revealed several potential map partners, which are hypothetically the genes that could be regulated if *gata3* and *cxcr5* would have been expressed in mammalian brains after injury regarding the first scenario above. When we analyzed the expression

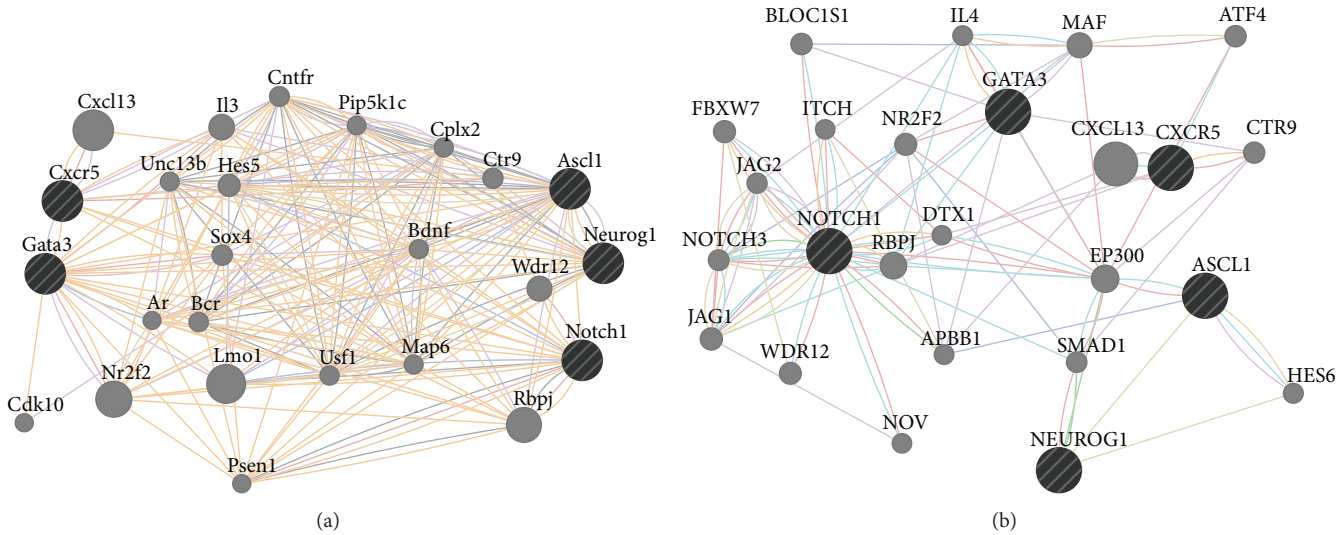

FIGURE 3: GeneMANIA interaction maps. Predicted interaction maps of *Gata3* and *Cxcr5* in mouse (a) and humans (b). See text for more details. Connections: red: physical interaction; violet: coexpression; orange: predicted; cyan: common pathway; blue: colocalization.

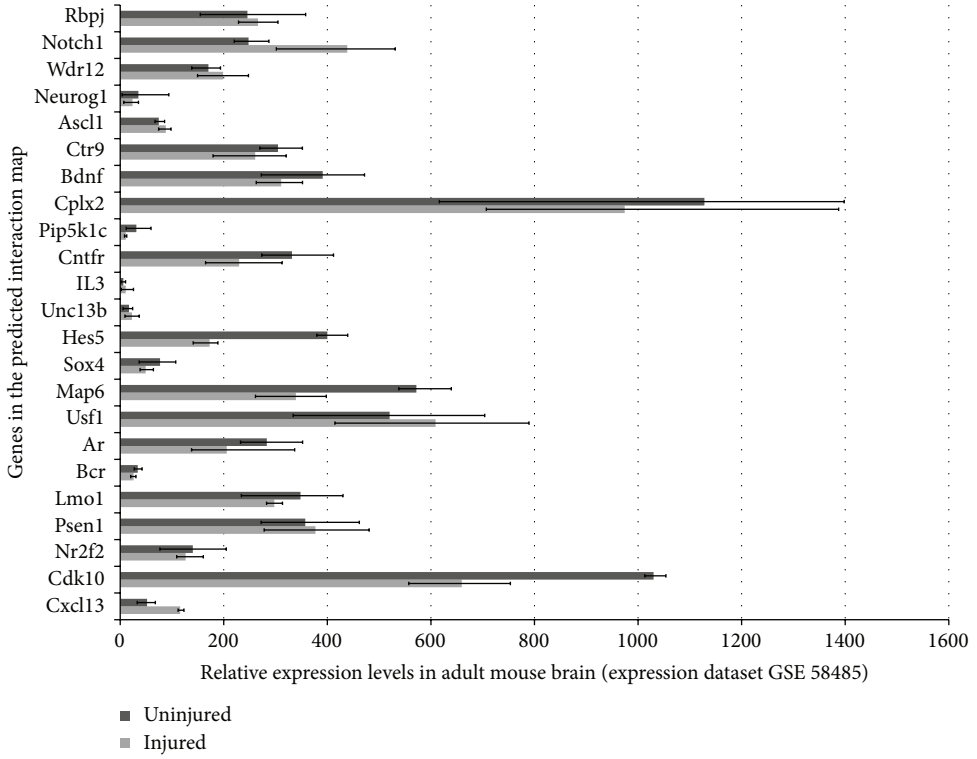

FIGURE 4: Relative expression levels of GeneMANIA-predicted map partners of Gata3 and Cxcr5 in experimental mouse brain injury gene expression datasets. See text for details.

levels of those potential map partners in the original mouse brain injury dataset, we found that several of these genes—for instance, *Bcr*, *Unc13b*, *IL3*, and *Pip5k1c*—were either expressed at very low levels or unexpressed (Figure 4). These genes are taking part in regulating diverse events including cell cycle, neurotransmitter release, long-term potentiation of synapses, second messenger pathways, cytokine signaling, cell fate determination, and cell migration [95–102]. Thus, activation of regeneration factors in mammals could have the potential to modulate all these molecular events, which might be misregulated in the absence of such factors, two of which could be *gata3* and *cxcr5*. As new molecular players will be identified experimentally, the interaction and regulation map could be widened. Potential candidates could also be analyzed for their expression and function in mammalian central nervous system to see whether they could convey

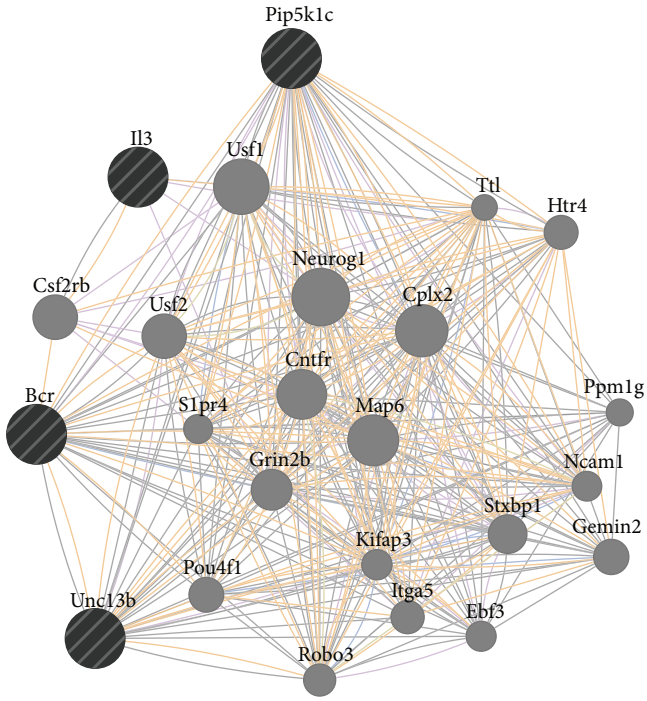

Figure 5: GeneMANIA iteratively predicted interaction map. The interaction map of genes that might be regulated by regeneration factors based on experimental injury models of mouse brain. *Il3*, *Pip5k1c*, *Bcr*, and *Unc13b* generate a map that contains genes that could be regulated by these genes if they would be expressed or regulated by regeneration factors in mouse brain. The map partners include various genes related to neurogenesis, such as *Neurog1*, *Robo3*, and *Pou4f1*.

the regenerative ability in mammalian nervous tissue. For instance, when predicted interaction maps and pathway analysis are made for *Bcr*, *Unc13b*, *IL3*, and *Pip5k1c* in mouse, several genes are included in the map (Figure 5), which could serve as a starting point for functional epistatic analyses of regenerative ability.

6. Neurodegeneration as a Means of Addressing Stem Cell Plasticity in Zebrafish

Specific regions of the zebrafish brain are strikingly conserved with mammalian brains [103, 104], and this allows zebrafish to be used as an excellent model for neurodegeneration. Several transgenic or mutant zebrafish lines were generated to model neurodegeneration in fish [105–108]. Various techniques ranging from morpholino knockdown of specific disease-related genes [109, 110] to the use of neuronal promoters for driving mutant versions of different neurodegeneration-associated proteins [111–116], or generating mutants for loss of/function studies [117–122] were used. These models provide important information of the pathophysiology of the disease progression and underlying molecular programs. Like the genes induced after traumatic injury in zebrafish brains, neurodegeneration models are also likely to give us insights on biomarkers that could be pragmatically utilized in regenerative medicine. These biomarkers can also be used to find out the "druggable" candidates that could be harnessed in clinical settings for regenerative therapies.

7. Conclusion

Zebrafish serves as a yet developing but quite promising organism for modeling human diseases [123]. The premise of zebrafish is its ease in getting at the mechanisms underlying the *in vivo* regenerative aptitude. Understanding such mechanisms would thus be instrumental in addressing questions on the presence of special molecular mechanisms and on whether we can activate those programs in mammalian brains to achieve functional recovery utilizing the endogenous stem cells. Here, we wish to underscore the need to further test the hypothesis that induced molecular programs utilized by adult zebrafish brain might give insight into how we can coax mammalian neural stem cells to proliferate and enhance the adult neurogenesis response in compromised adult brains. With simple *in silico* tools, such genes and pathways can also help researchers to hypothesize the molecular basis of regenerative ability also in mammalian brains.

Conflict of Interests

The authors declare that there is no conflict of interests regarding the publication of this paper.

Authors' Contribution

Mehmet Ilyas Cosacak and Christos Papadimitriou contributed equally.

Acknowledgments

Caghan Kizil is funded by German Centre for Neurodegenerative Diseases (DZNE), Dresden, the Helmholtz Association (HGF) through Young Investigator Program (VH-NG-1021), Center for Regenerative Therapies Dresden (CRTD), and TU Dresden (FZ-111, Fund no. 043_261518).

References

[1] S. Ramon y Cajal, *Cajal's Degeneration and Regeneration of the Nervous System (History of Neuroscience)*, vol. 1st, Oxford University Press, New York, NY, USA, 1991.

[2] J. Altman, "Autoradiographic and histological studies of postnatal neurogenesis. IV. Cell proliferation and migration in the anterior forebrain, with special reference to persisting neurogenesis in the olfactory bulb.," *Journal of Comparative Neurology*, vol. 137, no. 4, pp. 433–457, 1969.

[3] J. Altman and G. D. Das, "Post-natal origin of microneurones in the rat brain," *Nature*, vol. 207, no. 5000, pp. 953–956, 1965.

[4] A. Alvarez-Buylla, B. Seri, and F. Doetsch, "Identification of neural stem cells in the adult vertebrate brain," *Brain Research Bulletin*, vol. 57, no. 6, pp. 751–758, 2002.

[5] J. Kaslin, J. Ganz, and M. Brand, "Proliferation, neurogenesis and regeneration in the non-mammalian vertebrate brain," *Philosophical Transactions of the Royal Society B: Biological Sciences*, vol. 363, no. 1489, pp. 101–122, 2008.

[6] J. Morrens, W. van den Broeck, and G. Kempermann, "Glial cells in adult neurogenesis," *Glia*, vol. 60, no. 2, pp. 159–174, 2012.

[7] F. Doetsch, J. M. García-Verdugo, and A. Alvarez-Buylla, "Cellular composition and three-dimensional organization of the subventricular germinal zone in the adult mammalian brain," *Journal of Neuroscience*, vol. 17, no. 13, pp. 5046–5061, 1997.

[8] L. Bonfanti and P. Peretto, "Adult neurogenesis in mammals—a theme with many variations," *European Journal of Neuroscience*, vol. 34, no. 6, pp. 930–950, 2011.

[9] A. Ernst, K. Alkass, S. Bernard et al., "Neurogenesis in the striatum of the adult human brain," *Cell*, vol. 156, no. 5, pp. 1072–1083, 2014.

[10] K. L. Spalding, O. Bergmann, K. Alkass et al., "XDynamics of hippocampal neurogenesis in adult humans," *Cell*, vol. 153, no. 6, pp. X1219–1227, 2013.

[11] D. V. Hansen, J. H. Lui, P. R. L. Parker, and A. R. Kriegstein, "Neurogenic radial glia in the outer subventricular zone of human neocortex," *Nature*, vol. 464, no. 7288, pp. 554–561, 2010.

[12] F. Doetsch and C. Scharff, "Challenges for brain repair: Insights from adult neurogenesis in birds and mammals," *Brain, Behavior and Evolution*, vol. 58, no. 5, pp. 306–322, 2001.

[13] S. A. Goldman and F. Nottebohm, "Neuronal production, migration, and differentiation in a vocal control nucleus of the adult female canary brain," *Proceedings of the National Academy of Sciences of the United States of America*, vol. 80, no. 8, pp. 2390–2394, 1983.

[14] A. Carleton, L. T. Petreanu, R. Lansford, A. Alvarez-Buylla, and P.-M. Lledo, "Becoming a new neuron in the adult olfactory bulb," *Nature Neuroscience*, vol. 6, no. 5, pp. 507–518, 2003.

[15] G. Kempermann, D. Gast, G. Kronenberg, M. Yamaguchi, and F. H. Gage, "Early determination and long-term persistence of adult-generated new neurons in the hippocampus of mice," *Development*, vol. 130, no. 2, pp. 391–399, 2003.

[16] C. Lois and A. Alvarez-Buylla, "Long-distance neuronal migration in the adult mammalian brain," *Science*, vol. 264, no. 5162, pp. 1145–1148, 1994.

[17] M. B. Luskin, "Restricted proliferation and migration of postnatally generated neurons derived from the forebrain subventricular zone," *Neuron*, vol. 11, no. 1, pp. 173–189, 1993.

[18] F. T. Merkle, Z. Mirzadeh, and A. Alvarez-Buylla, "Mosaic organization of neural stem cells in the adult brain," *Science*, vol. 317, no. 5836, pp. 381–384, 2007.

[19] A. Arvidsson, T. Collin, D. Kirik, Z. Kokaia, and O. Lindvall, "Neuronal replacement from endogenous precursors in the adult brain after stroke," *Nature Medicine*, vol. 8, no. 9, pp. 963–970, 2002.

[20] M. S. Brill, J. Ninkovic, E. Winpenny et al., "Adult generation of glutamatergic olfactory bulb interneurons," *Nature Neuroscience*, vol. 12, no. 5, pp. 1524–1533, 2010.

[21] T. Collin, A. Arvidsson, Z. Kokaia, and O. Lindvall, "Quantitative analysis of the generation of different striatal neuronal subtypes in the adult brain following excitotoxic injury," *Experimental Neurology*, vol. 195, no. 1, pp. 71–80, 2005.

[22] S. H. Im, J. H. Yu, E. S. Park et al., "Induction of striatal neurogenesis enhances functional recovery in an adult animal model of neonatal hypoxic-ischemic brain injury," *Neuroscience*, vol. 169, no. 1, pp. 259–268, 2010.

[23] Y. Kim and F. G. Szele, "Activation of subventricular zone stem cells after neuronal injury," *Cell and Tissue Research*, vol. 331, no. 1, pp. 337–345, 2008.

[24] S. Robel, B. Berninger, and M. Götz, "The stem cell potential of glia: lessons from reactive gliosis," *Nature Reviews Neuroscience*, vol. 12, no. 2, pp. 88–104, 2011.

[25] N. L. Sundholm-Peters, H. K. C. Yang, G. E. Goings, A. S. Walker, and F. G. Szele, "Subventricular zone neuroblasts emigrate toward cortical lesions," *Journal of Neuropathology and Experimental Neurology*, vol. 64, no. 12, pp. 1089–1100, 2005.

[26] P. Thored, U. Heldmann, W. Gomes-Leal et al., "Long-term accumulation of microglia with proneurogenic phenotype concomitant with persistent neurogenesis in adult subventricular zone after stroke," *Glia*, vol. 57, no. 8, pp. 835–849, 2009.

[27] T. Yamashita, M. Ninomiya, P. H. Acosta et al., "Subventricular zone-derived neuroblasts migrate and differentiate into mature neurons in the post-stroke adult striatum," *Journal of Neuroscience*, vol. 26, no. 24, pp. 6627–6636, 2006.

[28] A. Buffo, I. Rite, P. Tripathi et al., "Origin and progeny of reactive gliosis: a source of multipotent cells in the injured brain," *Proceedings of the National Academy of Sciences of the United States of America*, vol. 105, no. 9, pp. 3581–3586, 2008.

[29] P. J. Borner, M. Thallmair, and F. H. Gage, "Defining the NG2-expressing cell of the adult CNS," *Journal of Neurocytology*, vol. 31, no. 6-7, pp. 469–480, 2002.

[30] M. Pekny and M. Nilsson, "Astrocyte activation and reactive gliosis," *Glia*, vol. 50, no. 4, pp. 427–434, 2005.

[31] M. R. Costa, M. Götz, and B. Berninger, "What determines neurogenic competence in glia?" *Brain Research Reviews*, vol. 63, no. 1-2, pp. 47–59, 2010.

[32] C. Heinrich, R. Blum, S. Gascón et al., "Directing astroglia from the cerebral cortex into subtype specific functional neurons," *PLoS Biology*, vol. 8, no. 5, Article ID e1000373, 2010.

[33] M. Karow, R. Sánchez, C. Schichor et al., "Reprogramming of pericyte-derived cells of the adult human brain into induced neuronal cells," *Cell Stem Cell*, vol. 11, no. 4, pp. 471–476, 2012.

[34] A. Buffo, M. R. Vosko, D. Ertürk et al., "Expression pattern of the transcription factor Olig2 in response to brain injuries: implications for neuronal repair," *Proceedings of the National Academy of Sciences of the United States of America*, vol. 102, no. 50, pp. 18183–18188, 2005.

[35] K. A. Burns, B. Murphy, S. C. Danzer, and C.-Y. Kuan, "Developmental and post-injury cortical gliogenesis: a genetic fate-mapping study with nestin-CreER mice," *GLIA*, vol. 57, no. 10, pp. 1115–1129, 2009.

[36] C. B. Johansson, S. Momma, D. L. Clarke, M. Risling, U. Lendahl, and J. Frisén, "Identification of a neural stem cell in the adult mammalian central nervous system," *Cell*, vol. 96, no. 1, pp. 25–34, 1999.

[37] J. W. Fawcett and R. A. Asher, "The glial scar and central nervous system repair," *Brain Research Bulletin*, vol. 49, no. 6, pp. 377–391, 1999.

[38] A. Rolls, R. Shechter, and M. Schwartz, "The bright side of the glial scar in CNS repair," *Nature Reviews Neuroscience*, vol. 10, no. 3, pp. 235–241, 2009.

[39] M. V. Sofroniew, "Molecular dissection of reactive astrogliosis and glial scar formation," *Trends in Neurosciences*, vol. 32, no. 12, pp. 638–647, 2009.

[40] G. Kempermann, H. van Praag, and F. H. Gage, "Activity-dependent regulation of neuronal plasticity and self repair," *Progress in Brain Research*, vol. 127, pp. 35–48, 2000.

[41] M. A. Curtis, E. B. Penney, A. G. Pearson et al., "Increased cell proliferation and neurogenesis in the adult human Huntington's disease brain," *Proceedings of the National Academy of Sciences of the United States of America*, vol. 100, no. 15, pp. 9023–9027, 2003.

[42] D. Gomez-Nicola, S. Suzzi, M. Vargas-Caballero et al., "Temporal dynamics of hippocampal neurogenesis in chronic neurodegeneration," *Brain*, vol. 137, no. 8, pp. 2312–2328, 2014.

[43] G. U. Höglinger, P. Rizk, M. P. Muriel et al., "Dopamine depletion impairs precursor cell proliferation in Parkinson disease," *Nature Neuroscience*, vol. 7, no. 7, pp. 726–735, 2004.

[44] M. Nahmani and G. G. Turrigiano, "Adult cortical plasticity following injury: recapitulation of critical period mechanisms?" *Neuroscience*, 2014.

[45] J. M. Parent, V. V. Valentin, and D. H. Lowenstein, "Prolonged seizures increase proliferating neuroblasts in the adult rat subventricullar zone-olfactory bulb pathway," *Journal of Neuroscience*, vol. 22, no. 8, pp. 3174–3188, 2002.

[46] G. Kempermann, D. Gast, and F. H. Gage, "Neuroplasticity in old age: sustained fivefold induction of hippocampal neurogenesis by long-term environmental enrichment," *Annals of Neurology*, vol. 52, no. 2, pp. 135–143, 2002.

[47] A. J. Eisch, H. A. Cameron, J. M. Encinas, L. A. Meltzer, G.-L. Ming, and L. S. Overstreet-Wadiche, "Adult neurogenesis, mental health, and mental illness: hope or hype?" *Journal of Neuroscience*, vol. 28, no. 46, pp. 11785–11791, 2008.

[48] G. Kempermann, J. Krebs, and K. Fabel, "The contribution of failing adult hippocampal neurogenesis to psychiatric disorders," *Current Opinion in Psychiatry*, vol. 21, no. 3, pp. 290–295, 2008.

[49] E. Antonova, T. Sharma, R. Morris, and V. Kumari, "The relationship between brain structure and neurocognition in schizophrenia: a selective review," *Schizophrenia Research*, vol. 70, no. 2-3, pp. 117–145, 2004.

[50] C. A. Jones, D. J. Watson, and K. C. Fone, "Animal models of schizophrenia," *British Journal of Pharmacology*, vol. 164, no. 4, pp. 1162–1194, 2011.

[51] K. Jin, X. Wang, L. Xie et al., "Evidence for stroke-induced neurogenesis in the human brain," *Proceedings of the National Academy of Sciences of the United States of America*, vol. 103, no. 35, pp. 13198–13202, 2006.

[52] T. H. McNeill, S. A. Brown, E. Hogg, H.-W. Cheng, and C. K. Meshul, "Synapse replacement in the striatum of the adult rat following unilateral cortex ablation," *Journal of Comparative Neurology*, vol. 467, no. 1, pp. 32–43, 2003.

[53] H. Nakatomi, T. Kuriu, S. Okabe et al., "Regeneration of hippocampal pyramidal neurons after ischemic brain injury by recruitment of endogenous neural progenitors," *Cell*, vol. 110, no. 4, pp. 429–441, 2002.

[54] N. J. Haughey, D. Liu, A. Nath, A. C. Borchard, and M. P. Mattson, "Disruption of neurogenesis in the subventricular zone of adult mice, and in human cortical neuronal precursor cells in culture, by amyloid β-peptide: implications for the pathogenesis of Alzheimer's disease," *NeuroMolecular Medicine*, vol. 1, no. 2, pp. 125–135, 2002.

[55] H. Grandel and M. Brand, "Comparative aspects of adult neural stem cell activity in vertebrates," *Development Genes and Evolution*, vol. 223, no. 1-2, pp. 131–147, 2013.

[56] C. Kizil, J. Kaslin, V. Kroehne, and M. Brand, "Adult neurogenesis and brain regeneration in zebrafish," *Developmental Neurobiology*, vol. 72, no. 3, pp. 429–461, 2012.

[57] E. M. Tanaka and P. Ferretti, "Considering the evolution of regeneration in the central nervous system," *Nature Reviews Neuroscience*, vol. 10, no. 10, pp. 713–723, 2009.

[58] G. K. H. Zupanc, "Adult neurogenesis and neuronal regeneration in the brain of teleost fish," *Journal of Physiology Paris*, vol. 102, no. 4–6, pp. 357–373, 2008.

[59] N. Kishimoto, K. Shimizu, and K. Sawamoto, "Neuronal regeneration in a zebrafish model of adult brain injury," *Disease Models and Mechanisms*, vol. 5, no. 2, pp. 200–209, 2012.

[60] V. Kroehne, D. Freudenreich, S. Hans, J. Kaslin, and M. Brand, "Regeneration of the adult zebrafish brain from neurogenic radial glia-type progenitors," *Development*, vol. 138, no. 22, pp. 4831–4841, 2011.

[61] E. V. Baumgart, J. S. Barbosa, L. Bally-cuif, M. Götz, and J. Ninkovic, "Stab wound injury of the zebrafish telencephalon: a model for comparative analysis of reactive gliosis," *Glia*, vol. 60, no. 3, pp. 343–357, 2012.

[62] M. März, R. Schmidt, S. Rastegar, and U. Strahle, "Regenerative response following stab injury in the adult zebrafish telencephalon," *Developmental Dynamics*, vol. 240, no. 9, pp. 2221–2231, 2011.

[63] H. Grandel, J. Kaslin, J. Ganz, I. Wenzel, and M. Brand, "Neural stem cells and neurogenesis in the adult zebrafish brain: origin, proliferation dynamics, migration and cell fate," *Developmental Biology*, vol. 295, no. 1, pp. 263–277, 2006.

[64] B. Adolf, P. Chapouton, C. S. Lam et al., "Conserved and acquired features of adult neurogenesis in the zebrafish telencephalon," *Developmental Biology*, vol. 295, no. 1, pp. 278–293, 2006.

[65] Y. Ito, H. Tanaka, H. Okamoto, and T. Ohshima, "Characterization of neural stem cells and their progeny in the adult zebrafish optic tectum," *Developmental Biology*, vol. 342, no. 1, pp. 26–38, 2010.

[66] J. Kaslin, J. Ganz, M. Geffarth, H. Grandel, S. Hans, and M. Brand, "Stem cells in the adult zebrafish cerebellum: initiation and maintenance of a novel stem cell niche," *Journal of Neuroscience*, vol. 29, no. 19, pp. 6142–6153, 2009.

[67] P. Chapouton, K. J. Webb, C. Stigloher et al., "Expression of hairy/enhancer of split genes in neural progenitors and neurogenesis domains of the adult zebrafish brain," *Journal of Comparative Neurology*, vol. 519, no. 9, pp. 1748–1769, 2011.

[68] P. Chapouton, R. Jagasia, and L. Bally-Cuif, "Adult neurogenesis in non-mammalian vertebrates," *BioEssays*, vol. 29, no. 8, pp. 745–757, 2007.

[69] J. Ganz, J. Kaslin, S. Hochmann, D. Freudenreich, and M. Brand, "Heterogeneity and Fgf dependence of adult neural progenitors in the zebrafish telencephalon," *Glia*, vol. 58, no. 11, pp. 1345–1363, 2010.

[70] C. Kizil and M. Brand, "Cerebroventricular microinjection (CVMI) into adult zebrafish brain is an efficient misexpression method for forebrain ventricular cells," *PLoS ONE*, vol. 6, no. 11, Article ID e27395, 2011.

[71] S. L. Chen, M. März, and U. Strähle, "gfap and nestin reporter lines reveal characteristics of neural progenitors in the adult zebrafish brain," *Developmental Dynamics*, vol. 238, no. 2, pp. 475–486, 2009.

[72] E. Pellegrini, K. Mouriec, I. Anglade et al., "Identification of aromatase-positive radial glial cells as progenitor cells in the ventricular layer of the forebrain in zebrafish," *Journal of Comparative Neurology*, vol. 501, no. 1, pp. 150–167, 2007.

[73] J. E. Burda and M. V. Sofroniew, "Reactive gliosis and the multicellular response to CNS damage and disease," *Neuron*, vol. 81, no. 2, pp. 229–248, 2014.

[74] C. T. Ekdahl, J.-H. Claasen, S. Bonde, Z. Kokaia, and O. Lindvall, "Inflammation is detrimental for neurogenesis in adult brain," *Proceedings of the National Academy of Sciences of the United States of America*, vol. 100, no. 23, pp. 13632–13637, 2003.

[75] C. T. Ekdahl, Z. Kokaia, and O. Lindvall, "Brain inflammation and adult neurogenesis: the dual role of microglia," *Neuroscience*, vol. 158, no. 3, pp. 1021–1029, 2009.

[76] G. Juhasz, G. Hullam, N. Eszlari et al., "Brain galanin system genes interact with life stresses in depression-related phenotypes," *Proceedings of the National Academy of Sciences of the United States of America*, vol. 111, no. 16, pp. E1666–E1673, 2014.

[77] N. Kyritsis, C. Kizil, and M. Brand, "Neuroinflammation and central nervous system regeneration in vertebrates," *Trends in Cell Biology*, vol. 24, no. 2, pp. 128–135, 2014.

[78] B. Moreno-López, C. Romero-Grimaldi, J. A. Noval, M. Murillo-Carretero, E. R. Matarredona, and C. Estrada, "Nitric oxide is a physiological inhibitor of neurogenesis in the adult mouse subventricular zone and olfactory bulb," *Journal of Neuroscience*, vol. 24, no. 1, pp. 85–95, 2004.

[79] R. Shechter and M. Schwartz, "CNS sterile injury: just another wound healing?" *Trends in Molecular Medicine*, vol. 19, no. 3, pp. 135–143, 2013.

[80] M. L. Monje, H. Toda, and T. D. Palmer, "Inflammatory blockade restores adult hippocampal neurogenesis," *Science*, vol. 302, no. 5651, pp. 1760–1765, 2003.

[81] T. Becker, R. R. Bernhardt, E. Reinhard, M. F. Wullimann, E. Tongiorgi, and M. Schachner, "Readiness of zebrafish brain neurons to regenerate a spinal axon correlates with different expression of specific cell recognition molecules," *Journal of Neuroscience*, vol. 18, no. 15, pp. 5789–5803, 1998.

[82] P. Bormann, L. W. A. Roth, D. Andel, M. Ackermann, and E. Reinhard, "zfNLRR, a novel leucine-rich repeat protein is preferentially expressed during regeneration in zebrafish," *Molecular and Cellular Neurosciences*, vol. 13, no. 3, pp. 167–179, 1999.

[83] C. Kizil, S. Dudczig, N. Kyritsis et al., "The chemokine receptor cxcr5 regulates the regenerative neurogenesis response in the adult zebrafish brain," *Neural Development*, vol. 7, no. 1, article 27, 2012.

[84] C. Kizil, N. Kyritsis, S. Dudczig et al., "Regenerative neurogenesis from neural progenitor cells requires injury-induced expression of Gata3," *Developmental Cell*, vol. 23, no. 6, pp. 1230–1237, 2012.

[85] C. Kizil, G. W. Otto, R. Geisler, C. Nüsslein-Volhard, and C. L. Antos, "*Simplet* controls cell proliferation and gene transcription during zebrafish caudal fin regeneration," *Developmental Biology*, vol. 325, no. 2, pp. 329–340, 2009.

[86] N. Kyritsis, C. Kizil, S. Zocher et al., "Acute inflammation initiates the regenerative response in the adult zebrafish brain," *Science*, vol. 338, no. 6112, pp. 1353–1356, 2012.

[87] B. B. Millimaki, E. M. Sweet, and B. B. Riley, "Sox2 is required for maintenance and regeneration, but not initial development, of hair cells in the zebrafish inner ear," *Developmental Biology*, vol. 338, no. 2, pp. 262–269, 2010.

[88] A. Raya, C. M. Koth, D. Büscher et al., "Activation of Notch signaling pathway precedes heart regeneration in zebrafish," *Proceedings of the National Academy of Sciences of the United States of America*, vol. 100, supplement 1, pp. 11889–11895, 2003.

[89] S. Stewart, Z.-Y. Tsun, and J. C. I. Belmonte, "A histone demethylase is necessary for regeneration in zebrafish," *Proceedings of the National Academy of Sciences of the United States of America*, vol. 106, no. 47, pp. 19889–19894, 2009.

[90] Y. Fang, V. Gupta, R. Karra, J. E. Holdway, K. Kikuchi, and K. D. Poss, "Translational profiling of cardiomyocytes identifies an early Jak1/Stat3 injury response required for zebrafish heart regeneration," *Proceedings of the National Academy of Sciences of the United States of America*, vol. 110, no. 33, pp. 13416–13421, 2013.

[91] C. Kizil, B. Kuchler, J. J. Yan et al., "Simplet/Fam53b is required for Wnt signal transduction by regulating beta-catenin nuclear localization," *Development*, vol. 141, pp. 3529–3539, 2014.

[92] C. Kizil, A. Iltzsche, J. Kaslin, and M. Brand, "Micromanipulation of gene expression in the adult zebrafish brain using cerebroventricular microinjection of morpholino oligonucleotides," *Journal of Visualized Experiments: JoVE*, no. 75, Article ID e50415, 2013.

[93] N. Diotel, C. Vaillant, C. Gabbero et al., "Effects of estradiol in adult neurogenesis and brain repair in zebrafish," *Hormones and Behavior*, vol. 63, no. 2, pp. 193–207, 2013.

[94] C. Israelsson, A. Kylberg, H. Bengtsson, L. Hillered, and T. Ebendal, "Interacting chemokine signals regulate dendritic cells in acute brain injury," *PLoS ONE*, vol. 9, no. 8, Article ID e104754, 2014.

[95] G. Bazzoni, N. Carlesso, J. D. Griffin, and M. E. Hemler, "Bcr/Abl expression stimulates integrin function in hematopoietic cell lines," *The Journal of Clinical Investigation*, vol. 98, no. 2, pp. 521–528, 1996.

[96] H. J. Junge, J.-S. Rhee, O. Jahn et al., "Calmodulin and Munc13 form a Ca^{2+} sensor/effector complex that controls short-term synaptic plasticity," *Cell*, vol. 118, no. 3, pp. 389–401, 2004.

[97] V. Kaartinen, I. Gonzalez-Gomez, J. W. Voncken et al., "Abnormal function of astroglia lacking Abr and Bcr RacGAPs," *Development*, vol. 128, no. 21, pp. 4217–4227, 2001.

[98] L. Sheu, E. A. Pasyk, J. Ji et al., "Regulation of insulin exocytosis by Munc13-1," *The Journal of Biological Chemistry*, vol. 278, no. 30, pp. 27556–27563, 2003.

[99] Y. Yang and N. Calakos, "Munc13-1 is required for presynaptic long-term potentiation," *Journal of Neuroscience*, vol. 31, no. 33, pp. 12053–12057, 2011.

[100] U. Stelzl, U. Worm, M. Lalowski et al., "A human protein-protein interaction network: a resource for annotating the proteome," *Cell*, vol. 122, no. 6, pp. 957–968, 2005.

[101] Y. Sun, A. C. Hedman, X. Tan, N. J. Schill, and R. A. Anderson, "Endosomal type Iγ PIP 5-kinase controls EGF receptor lysosomal sorting," *Developmental Cell*, vol. 25, no. 2, pp. 144–155, 2013.

[102] B. D. Wright, L. Loo, S. E. Street et al., "The lipid kinase PIP5K1C regulates pain signaling and sensitization," *Neuron*, vol. 82, no. 4, pp. 836–847, 2014.

[103] J. Ganz, J. Kaslin, D. Freudenreich, A. Machate, M. Geffarth, and M. Brand, "Subdivisions of the adult zebrafish subpallium by molecular marker analysis," *Journal of Comparative Neurology*, vol. 520, no. 3, pp. 633–655, 2012.

[104] T. Mueller and M. F. Wullimann, "An evolutionary interpretation of teleostean forebrain anatomy," *Brain, Behavior and Evolution*, vol. 74, no. 1, pp. 30–42, 2009.

[105] M. A. G. Sosa, R. de Gasperi, and G. A. Elder, "Modeling human neurodegenerative diseases in transgenic systems," *Human Genetics*, vol. 131, no. 4, pp. 535–563, 2012.

[106] E. Málaga-Trillo, E. Salta, A. Figueras, C. Panagiotidis, and T. Sklaviadis, "Fish models in prion biology: underwater issues," *Biochimica et Biophysica Acta*, vol. 1812, no. 3, pp. 402–414, 2011.

[107] Y. Xi, S. Noble, and M. Ekker, "Modeling neurodegeneration in zebrafish," *Current Neurology and Neuroscience Reports*, vol. 11, no. 3, pp. 274–282, 2011.

[108] W. Xia, "Exploring Alzheimer's disease in zebrafish," *Journal of Alzheimer's Disease*, vol. 20, no. 4, pp. 981–990, 2010.

[109] M. Newman, B. Tucker, S. Nornes, A. Ward, and M. Lardelli, "Altering presenilin gene activity in zebrafish embryos causes changes in expression of genes with potential involvement in Alzheimer's disease pathogenesis," *Journal of Alzheimer's Disease*, vol. 16, no. 1, pp. 133–147, 2009.

[110] V. Sallinen, J. Kolehmainen, M. Priyadarshini, G. Toleikyte, Y.-C. Chen, and P. Panula, "Dopaminergic cell damage and vulnerability to MPTP in Pink1 knockdown zebrafish," *Neurobiology of Disease*, vol. 40, no. 1, pp. 93–101, 2010.

[111] Q. Bai, J. A. Garver, N. A. Hukriede, and E. A. Burton, "Generation of a transgenic zebrafish model of Tauopathy using a novel promoter element derived from the zebrafish eno2 gene," *Nucleic Acids Research*, vol. 35, no. 19, pp. 6501–6516, 2007.

[112] K. C. O'Donnell, A. Lulla, M. C. Stahl, N. D. Wheat, J. M. Bronstein, and A. Sagasti, "Axon degeneration and PGC-1α-mediated protection in a zebrafish model of α-synuclein toxicity," *Disease Models and Mechanisms*, vol. 7, no. 5, pp. 571–582, 2014.

[113] D. Paquet, R. Bhat, A. Sydow et al., "A zebrafish model of tauopathy allows in vivo imaging of neuronal cell death and drug evaluation," *Journal of Clinical Investigation*, vol. 119, no. 5, pp. 1382–1395, 2009.

[114] D. Paquet, B. Schmid, and C. Haass, "Transgenic zebrafish as a novel animal model to study tauopathies and other neurodegenerative disorders in vivo," *Neurodegenerative Diseases*, vol. 7, no. 1–3, pp. 99–102, 2010.

[115] H. G. Tomasiewicz, D. B. Flaherty, J. P. Soria, and J. G. Wood, "Transgenic zebrafish model of neurodegeneration," *Journal of Neuroscience Research*, vol. 70, no. 6, pp. 734–745, 2002.

[116] A. Williams, S. Sarkar, P. Cuddon et al., "Novel targets for Huntington's disease in an mTOR-independent autophagy pathway," *Nature Chemical Biology*, vol. 4, no. 5, pp. 295–305, 2008.

[117] O. Anichtchik, H. Diekmann, A. Fleming, A. Roach, P. Goldsmith, and D. C. Rubinsztein, "Loss of PINK1 function affects development and results in neurodegeneration in zebrafish," *Journal of Neuroscience*, vol. 28, no. 33, pp. 8199–8207, 2008.

[118] S. Bretaud, C. Allen, P. W. Ingham, and O. Bandmann, "p53-dependent neuronal cell death in a DJ-1-deficient zebrafish model of Parkinson's disease," *Journal of Neurochemistry*, vol. 100, no. 6, pp. 1626–1635, 2007.

[119] I. Guella, A. Pistocchi, R. Asselta et al., "Mutational screening and zebrafish functional analysis of GIGYF2 as a Parkinson-disease gene," *Neurobiology of Aging*, vol. 32, no. 11, pp. 1994–2005, 2011.

[120] U. Leimer, K. Lun, H. Romig et al., "Zebrafish (Danio rerio) presenilin promotes aberrant amyloid β-peptide production and requires a critical aspartate residue for its function in amyloidogenesis," *Biochemistry*, vol. 38, no. 41, pp. 13602–13609, 1999.

[121] B. Schmid and C. Haass, "Genomic editing opens new avenues for zebrafish as a model for neurodegeneration," *Journal of Neurochemistry*, vol. 127, no. 4, pp. 461–470, 2013.

[122] D. Sheng, D. Qu, K. H. H. Kwok et al., "Deletion of the WD40 domain of LRRK2 in zebrafish causes parkinsonism-like loss of neurons and locomotive defect," *PLoS Genetics*, vol. 6, no. 4, 2010.

[123] G. J. Lieschke and P. D. Currie, "Animal models of human disease: zebrafish swim into view," *Nature Reviews Genetics*, vol. 8, no. 5, pp. 353–367, 2007.

Hindawi Publishing Corporation
BioMed Research International
Volume 2015, Article ID 610605, 13 pages
http://dx.doi.org/10.1155/2015/610605

Research Article

Posterior Cingulate Lactate as a Metabolic Biomarker in Amnestic Mild Cognitive Impairment

Kurt E. Weaver,[1,2] Todd L. Richards,[1,2] Rebecca G. Logsdon,[3] Ellen L. McGough,[4] Satoshi Minoshima,[1] Elizabeth H. Aylward,[5] Natalia M. Kleinhans,[1,2] Thomas J. Grabowski,[1,2,6] Susan M. McCurry,[3] and Linda Teri[3]

[1] *Department of Radiology, University of Washington, P.O. Box 357115, Seattle, WA 98195, USA*
[2] *Integrated Brain Imaging Center, University of Washington, Seattle, WA 98195, USA*
[3] *Department of Psychosocial and Community Health, University of Washington, Seattle, WA 98195, USA*
[4] *Department of Rehabilitation Medicine, University of Washington, Seattle, WA 98195, USA*
[5] *Center for Integrative Brain Research, Seattle Children's Research Institute, Seattle, WA 98101, USA*
[6] *Department of Neurology, University of Washington, Seattle, WA 98195, USA*

Correspondence should be addressed to Kurt E. Weaver; weaverk@uw.edu

Received 25 June 2014; Accepted 19 October 2014

Academic Editor: Giovanni Li Volti

Mitochondrial dysfunction represents a central factor within the pathogenesis of the Alzheimer's disease (AD) spectrum. We hypothesized that in vivo measurements of lactate (lac), a by-product of glycolysis, would correlate with functional impairment and measures of brain health in a cohort of 15 amnestic mild cognitive impairment (aMCI) individuals. Lac was quantified from the precuneus/posterior cingulate (PPC) using 2-dimensional J-resolved magnetic resonance spectroscopy (MRS). Additionally, standard behavioral and imaging markers of aMCI disease progression were acquired. PPC lac was negatively correlated with performance on the Wechsler logical memory tests and on the minimental state examination even after accounting for gray matter, cerebral spinal fluid volume, and age. No such relationships were observed between lac and performance on nonmemory tests. Significant negative relationships were also noted between PPC lac and hippocampal volume and PPC functional connectivity. Together, these results reveal that aMCI individuals with a greater disease progression have increased concentrations of PPC lac. Because lac is upregulated as a compensatory response to mitochondrial impairment, we propose that J-resolved MRS of lac is a noninvasive, surrogate biomarker of impaired metabolic function and would provide a useful means of tracking mitochondrial function during therapeutic trials targeting brain metabolism.

1. Introduction

Effectively all contemporary theories of Alzheimer's disease (AD) pathogenesis integrate impaired brain metabolism into the concert of factors precipitating neurodegeneration and clinical disability. One of the earliest observable metabolic impairments consistently linked with cognitive dysfunction across the AD spectrum is reduced brain glucose metabolism [1]. Studies of [18F] fluorodeoxyglucose uptake using positron emission tomography (FDG-PET) reveal that glucose hypometabolism in amnestic mild cognitive impairment (aMCI), a cohort of individuals at increased risk for transitioning to AD, is associated with poorer memory capacity [2] and reductions in hippocampal volume [3]. At a systems level, FDG-PET hypometabolism in aMCI tends to develop more within regions of the default mode network (DMN) [4]. The precuneus/posterior cingulate (PPC), one of the main integrative hubs of the DMN, is particularly sensitive to reductions in glucose consumption. The PPC is highly interconnected with the hippocampus and the interaction between the two structures plays a critical role in orchestrating episodic memory recall [5, 6]. Combined, these and many other findings have led to the use of FDG-PET as a biomarker for tracking AD-related metabolic impairments

and a prediction that FDG-PET will help increase the clinical efficacy of therapeutics targeting brain metabolism abnormalities [7].

However, numerous other well documented metabolic impairments have been noted constituting additional and likely overlapping pathological processes (reviewed in [8, 9]). The general interpretation from an extensive animal and human literature is that prodromal stages of AD, including aMCI, are marked with reduced vascular integrity, compromised mitochondrial function and elevated oxidative stress [1, 10, 11]. As a result, mitochondrial bioenergetics has become a source of therapeutic targets in predemented stages of the spectrum [12, 13].

In analogous clinical scenarios presenting with disrupted mitochondrial function (e.g., mitochondrial disorders such as Leigh syndrome or MELAS [14, 15]), lactate (lac), the byproduct of anaerobic glycolysis, is elevated in part as compensation for aerobic metabolic impairment [16–18]. Thus, 1H magnetic resonance spectroscopic (MRS) quantification of lac is often used as a diagnostic marker for inborn errors of metabolism [15, 19] as well as other clinical scenarios affecting basal metabolic function (e.g., hypoxia/ischemia [20]). Taken together, we hypothesize that concentrations of brain lac would serve as a biomarker of metabolic impairment across the aMCI spectrum, potentially as a reflection of mitochondrial dysfunction.

As far as we are aware, only two previous MRS reports have attempted to quantify brain lac in AD. Stoppe et al. [21] reported no differences between patients and controls in lac concentrations extracted from a voxel in the parietal lobe. More critically, Ernst et al. [22] failed altogether to detect a lac signal in AD from either prefrontal or lateral temporal cortex. The lack of signal change or detection within these studies may stem from a variety of concerns such as choice of location (i.e., spectra may have been acquired from cortex showing relative immunity to AD pathology) or perhaps and a more likely scenario as a result of spectral overlap and contamination [23]. Both previous studies relied on a standard "short-TE" spectroscopic approach. This technique which acquires frequency induction decays (FIDs) at a single echo time (typically between 30–35 ms) provides reliable quantification of the classic MRS metabolites including N-acetylaspartate [NAA] but yields limited quantification capacity for metabolites with overlapping resonance frequencies [24]. Within the MR proton spectrum the lac signature exists as a doublet peak located at 1.35 ppm. This peak however is buried within a robust lipid and macromolecule resonance at overlapping frequencies. Therefore using traditional single shot short-TE spectroscopic imaging, a significant rise in concentration (e.g., as seen during mitochondrial disease) is usually necessary to expose the lac doublet [25].

The purpose of this study is to first reexamine whether brain lac could be quantified in vivo using noninvasive imaging in a group aMCI subjects. We focused specifically on the PPC because of the consistent reductions reported across the FDG-PET literature in aMCI (c.f. [26]). To circumvent the known spectral contamination concerns of lac, we capitalized on the J-coupling behavior of the lac molecule. We quantified PPC lac using 2-dimensional J-resolved magnetic resonance spectroscopy (J-rMRS) [27]. 2D J-rMRS enables the separation of J-coupling information from chemical shift by encoding J-coupling in the t2 dimension of a 2D spectrum using an array of echo times [28]. The addition of this second frequency dimension allows for separation of lac from lipids and macromolecules, molecules that lack J-coupling properties. Second, we contrasted PPC lac with behavioral and imaging characteristics that are commonly used as markers of disease progression across the AD spectrum. Specifically, PET studies consistently observe that PPC metabolic impairments in aMCI and AD are significantly associated with memory dysfunction, hippocampal volumetry, and other imaging markers of disease pathology (see [1] for review). By correlating PPC lac with known markers of disease progression, we aim to establish the validity of PPC lac as a valid metabolic biomarker in aMCI.

2. Material and Methods

2.1. Subjects and Cognitive Screening. Fifteen community-dwelling aMCI individuals (mean age 85.5 yrs. old, 5 males) were included (see Table 1 for demographics). Study recruitment and screening consisted of a semistructured interview, neuropsychological screening tests, and an expert consensus panel to review screening data. Participants were classified as having amnestic MCI based on the Petersen criteria [29] and was determined from a combination of cognitive test scores, screening interview data, and consensus case review to identify persons with memory problems that would be consistent with a clinical subtype of single domain amnestic MCI, including (1) memory complaint, (2) impaired memory for age and education, (3) preserved general cognitive function, (4) essentially preserved activities of daily living, and (5) not already diagnosed with dementia. Specific measures included self-reported memory loss, evidence of objective memory impairment, no functional impairment, and ability to live independently. All subjects had Clinical Dementia Rating scores of 0.5, consistent with aMCI and at least a high school education. Subjects were free of any other psychiatric or neurological disease. Cognitive tests included (1) the minimental state exam (MMSE) for global cognition, (2) the logical memory I and II subscales of the Wechsler memory scale-revised for immediate and delayed recall, and (3) the Alzheimer's disease assessment scale. Executive functioning was assessed with the Stroop Interference Task and Trails A & B tests. Two subjects were unable to complete the Stroop task due to color blindness. The study was approved by the University of Washington Institutional Review Board and all participants provided informed consent.

Amnestic MCI is generally assumed to be a transition period between normal aging and Alzheimer dementia. Although the diagnostic criteria have been debated, aMCI is commonly defined as a specific impairment in memory that is greater than one would expect for age with a relative normal sparing of other cognitive abilities including attention, judgment, reasoning, and perception. Our sample of aMCI participants included MMSE scores ranging from 21–30, including three individuals with scores of less than 25,

Table 1: Subject demographics, clinical assessment, and lactate MRS outcomes.

Subject	Gender	Age	Handedness*	MMSE	ADAS-Cog$	Lactate (mM)	PPC MRS voxel Proportion tissue types		
							GM	WM	CSF
MCI1	M	89	Left	23	11.67	0.795	0.34	0.37	0.29
MCI2	F	94	Right	28	9	0.713	0.37	0.33	0.3
MCI3	M	86	Right	21	12.67	0.709	0.31	0.41	0.28
MCI4	F	82	Right	30	11.67	0.587	0.35	0.37	0.27
MCI5	F	87	Right	22	10.33	0.725	0.3	0.46	0.24
MCI6	F	86	Right	26	9.33	0.490	0.35	0.4	0.25
MCI7	F	83	Right	25	8.67	0.871	0.33	0.4	0.28
MCI8	M	79	Right	26	10.33	0.686	0.4	0.41	0.19
MCI9	F	80	Right	29	10.33	0.222	0.36	0.48	0.16
MCI10	F	87	Right	29	8.33	0.163	0.34	0.4	0.25
MCI11	F	82	Right	25	9.33	0.527	0.36	0.39	0.21
MCI12	F	85	Right	28	9	0.483	0.39	0.4	0.21
MCI13	F	82	Right	27	8.67	0.359	0.33	0.46	0.21
MCI14	M	88	Right	27	8.67	0.987	0.35	0.38	0.27
MCI15	M	93	Right	29	9.67	0.491	0.34	0.38	0.26

*Based on self-report.
MMSE: minimental state examination.
$Total (combined) score.
GM: grey matter; WM: white matter; CSF: cerebral spinal fluid.

scores that are typically considered outside of the aMCI range (Table 1). However, all subjects had CDR scores of 0.5 and a mean ADAS-cog total score of 9.84 ± 1.3 SD, which falls in range with previous published studies of aMCI individuals (c.f. [30]: 11.3 ± 4.4 SD) and is lower than individuals meeting probable AD diagnostic criteria (18.0 ± 6.0). Thus, while most of the participants meet the Petersen criteria for aMCI [31] a few individuals may have been at or near the early transition period of AD at the time of scanning.

2.2. MRI Acquisition. Scanning procedures were conducted on a Philips 3.0 T Achieva scanner using an 8-channel SENSE head coil. The scanning protocol included a Magnetization prepared rapid gradient echo (MPRAGE) high-resolution T1 sequence (repetition time (TR)/echo time (TE)/flip angle: 6.5 milliseconds (ms)/3 ms/8°; matrix size of 256 × 256 and with 170 sagittally collected slices and a slice thickness of 1 mm), which was reconstructed in real-time to guide MRS voxel placement and offline hippocampal volumetric calculation.

2.3. 1H J-Resolved Magnetic Resonance Spectroscopy

2.3.1. Spectral Estimation of Lactate. For each subject, a 2-dimensional J-rMRS acquisition sequence (Figure 1) was acquired from a 4 × 4 × 4 cm voxel that was placed within the PPC, bilaterally. Because lac typically exists in low concentrations in normal physiological conditions, a large voxel size was selected to improve signal to noise. The parameters used for the 2D J-rMRS sequence were PRESS single voxel pulse sequence, TE-steps = 24 (32–492 ms, 20 ms increments, only the 2nd echo intervals were incremented surrounding the 2nd 180 leaving the 1st echo intervals fixed surrounding the 1st 180 in the PRESS pulse sequence), TR = 2 s, spectral bandwidth = 2000 Hz, complex time points = 2048, NEX = 12, and total scan duration = 9.6 min. A spectrum was also acquired with and without water suppression (TE 32 ms) for processing with LCmodel.

2.4. Resting State fMRI. An 8-minute resting state, echo planar fMRI sequence (TR/TE/FA: 2000/21/90°, 68 axially oriented slices; matrix size 64 × 64) was acquired to quantify functional connectivity across subjects. Five "dummy" volumes were acquired but excluded from analyses in order to stabilize T1 equilibrium effects. Physiological activity was collected using a custom-made LabView monitoring system with pulse oximetry and a respiratory belt.

3. Analysis

3.1. MRS Preprocessing. Short echo metabolites fits and quantification were accomplished using LCmodel. Metabolite uncertainties were expressed as % standard deviations (SD). Percent SD, FWHM (full width at half maximum, an estimate of peak width), and S/N (signal-to-noise ratio) were used as determinants of spectrum quality. Free-induction decays (FIDs) were input into the software package and were zero-filled to double the points and filtered with a finite discrete convolution to account for field inhomogeneities and eddy currents. During preprocessing the residual water signal was subtracted by using a decomposition-fitting algorithm. FIDs were then zero- and first-order phase corrected and smoothed using a 1.1 Hz exponential dampening filter. A nonlinear, least squares analysis estimated the metabolite concentrations and their uncertainties.

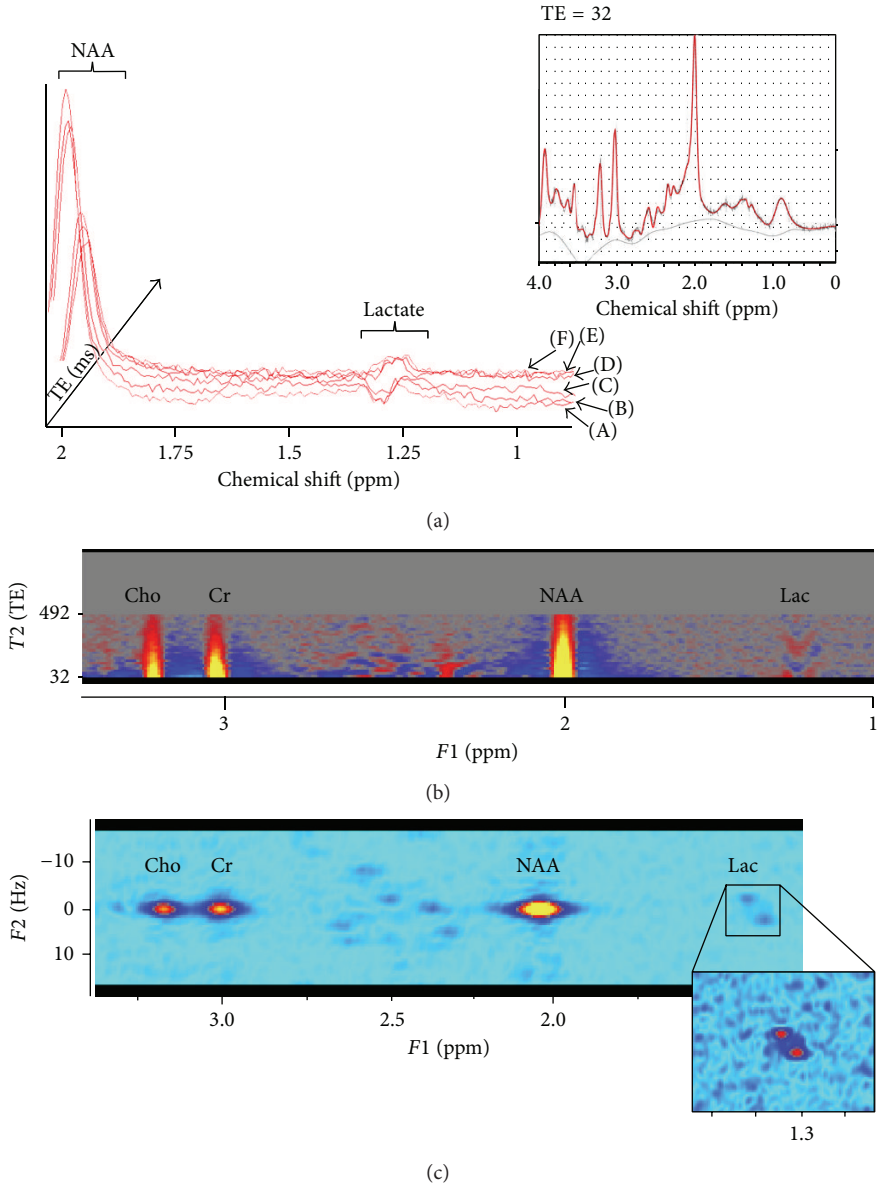

Figure 1: *1H J-resolved MRS lac imaging and analyses*. (a) 3D-plot of averaged, phased proton spectra (filtered for viewing from 2 to 0.8 ppm) for 6 selected echo times (A: 72 ms, B: 92 ms, C: 112 ms, D: 232 ms, E: 252 ms, and F: 272 ms) reveals the inversion of the lac doublet located at 1.3 ppm. The full 1H spectrum at echo time of 32 ms (inset) was used to fit the classic 1H short echo NAA metabolite for absolute quantification using LCmodel. (b) Fourier transformation of the standard acquisition dimension (i.e., chemical shift) converts each FID to a frequency spectrum (F1). The NAA signal for each echo time for each individual was used for quality control purposes and for phase stabilization. No tilt correction was applied in order to inspect possible corruption by T2 noise. (c) A second Fourier transform was applied to the data along the incremented echo time (spectral dimension or F2), converting the oscillating phases of each of the coupled metabolite peaks to their respective frequency components. This contour plot of the 2D spectra, along with projections on the F1 and F2 axes over the chemical shift frequency range was used to localize, isolate, and quantify lactate at the chemical shift frequency of 1.33 ppm at J-resolved frequency of 7.5 Hz.

3.2. MRS Analysis. The raw 2D MRS spectra (2048 complex points along the t1 dimension and 24 points along the t2 dimension) were processed offline. One of the spectra (at TE 32 ms, see Figure 1(a) inset) was isolated and used to calculate absolute concentrations of NAA under the t1 dimension. NAA spectral fits were accomplished with LCmodel using standard procedures. Absolute concentrations of NAA were obtained by scaling the in vivo spectrum to the unsuppressed endogenous water peak and are reported in units that approximate millimolar (mM) concentrations.

Partial volume corrections were made by calculating the fraction of cerebral spinal fluid (CSF) for each voxel. CSF, gray matter (GM) and white matter (WM) volume measurements of the PPC voxel were obtained through intensity estimates using the FANTASM MIPAV algorithm (http://mipav.cit.nih.gov/pubwiki/index.php/Main_Page).

Metabolite values were then normalized to correct CSF partial volume effects to = 100% brain tissue using: $C = C_o * (1/(1 - \mathrm{FCSF}))$ where C = concentration, C_o = metabolite concentration from LCmodel output, and FCSF = estimated fraction CSF in order.

The 2D MRS analyses were achieved through in-house software and included a filtered (Sine-bell) Fourier transformation (FT) of the standard chemical shift dimension (t1), which was used to convert each FID to a frequency spectrum (f1). A second FT was then applied to the data along the incremented echo time or spectral dimension (t2), converting the oscillating phases of each of the coupled metabolite peaks to their respective frequency components (f2). After the 2D FT, spectra were converted to power estimates by adding the real squared to the imaginary squared output from the 2D FT. No phasing was necessary for the final FT output due to phasings/frequency shift corrections after the 1st FT to correct for phase imperfections/instabilities of the scanner. The 2D spectra were then plotted as contour plots (Figures 1(b) and 1(c)), revealing the J-coupled frequency of lac at 1.3 ppm as an off midline frequency. The volume under the 2D spectrum (i.e., area under the curve) was determined for lac using manual peak picking on contours and calculated as a ratio to NAA. To estimate absolute concentration, lac values were then multiplied by the LCmodel output of CSF adjusted NAA concentrations.

3.3. Hippocampal Volumes. MPRAGE scans were reconstructed into a 1 × 1 × 1 mm 3D volume. Hippocampal volumes were determined on the MPRAGE through a combination of semiautomatic segmentation and extraction using FMRIB's Integrated Registration and Segmentation Tool (FIRST) in FMRIB's Software Library (FSL) version 4.1.5. Following FIRST extraction of hippocampal masks, an expert, blind rater (EHA) inspected and made manual adjustments when necessary so each mask conformed to established rules and boundaries [32].

3.4. Intracranial Volumes (ICV). The ICV for each individual was calculated using a stereologic Cavalieri technique [33] implemented through MEASURE software. Volumes were calculated from a 3D grid of points overlaying the intracranial cavity. This grid was manually identified for each subject by a single rater (KEW). The selected area included all points falling within the cerebrum, cerebellum, sulcal and ventricular CSF, and brainstem superior to the foramen magnum. Volumes were then estimated using the Gundersen formula [34].

3.5. Resting State fMRI (rsfMRI). At the individual level, preprocessing steps to minimize nonneural sources of noise included skull stripping, motion correction with FSL MCFLIRT using a six-parameter rigid body correction and a trilinear interpolation algorithm, with alignment occurring to the middle volume, physiological correction using RETROICOR (implemented through AFNI image processing software [35]), spatial smoothing using 8 mm full width half maximum (FWHM) Gaussian kernel and a low pass temporal filter of 0.1 Hz., grand-mean intensity normalization and linear drift removal. Note that a hardware malfunction prevented the acquisition of physiological activity in one subject. To control physiological noise for this subject within the fMRI data, we calculated and regressed mean resting state white matter and CSF signal prior to spatial smoothing and temporal filtering.

Posterior cingulate seed point functional connectivity analysis was conducted using FSL FEAT toolbox (http://www.fmrib.ox.ac.uk/fsl/feat), importing the coordinates from a previous FDG-PET study of glucose metabolism of preclinical AD as the seed point location [26]. Individual posterior cingulate functional connectivity maps were generated across the whole brain. For each individual, the MNI template brain was initially registered into native fMRI space and the mean time course from a rectangular seed point (4 × 1 × 1 cm) was extracted. The 6 covariates (the 6 motion parameters) were added into a multiple regression analysis as nuisance variables of no-interest. The seed point time course was then entered into whole-brain, voxelwise general linear model analysis using a fixed-effects model and normalizing at the individual level by converting estimates into Z-scores.

3.6. Statistical Analyses. Statistical relationships between metabolite concentrations and clinical cognitive variables were investigated using parametric partial correlations correcting for numerous known confounds including age and CSF and WM volumes within the MRS voxel. Statistical significance across regressions was determined at a standard alpha level ($P < 0.05$). We also computed significant relationships across rsfMRI PPC functional connectivity and PPC lac concentrations at the group level. Individual seed point rsfMRI time series were orthogonalized and analyses were carried out using a mixed-effects model (FLAME) incorporating PPC MRS lac concentrations as a covariate of interest. Corrections for multiple comparisons were carried out at the cluster level using Gaussian random field theory (minimum voxel Z-score, 2.3; cluster significance, $P < 0.05$, corrected).

4. Results

From our 2D spectral editing techniques, we observed the characteristic lac doublet signature extracted from the PPC in all 15 aMCI participants (for representative see Figures 1(a)–1(c)). Lac quantification was accomplished using a combination of 2D spectral transforms and LCmodel metabolite estimation. Across subjects these values ranged from 0.16 millimolar (mM) to 0.98 mM (mean 0.587 mM, see Table 1) which are in line with previous efforts to quantify lac under normoxic conditions, localized to superior frontoparietal cortex estimated around 0.5 mM [36], and are in good agreement with quantification estimates from more contemporary findings [37].

4.1. PPC Lactate Is Specifically Associated with Memory Capacity in aMCI. Across subjects, lac concentration was

Table 2: Regions of peak Z-scores of voxels showing a significant negative correlation between PPC lac concentration and posterior cingulate functional connectivity.

Region	Z-score	Hemisphere	MNI coordinates (mm)			BA
			x	y	z	
Posterior cingulate	7.63	R	16	−40	34	31
Lateral occipital cortex/angular gyrus	7.23	L	−38	−68	16	39
Lateral occipital cortex/angular gyrus	6.93	R	40	−60	12	39
Anterior parahippocampal gyrus	6.92	L	−16	0	−26	34
Hippocampus/parahippocampal gyrus	6.77	L	−26	−38	2	36
Thalamus	6.35	R	12	−22	14	N/A
Inferior temporal gyrus/temporal pole	6.08	L	−36	0	−52	20
Superior temporal sulcus	5.47	R	46	4	−26	22
Hippocampus	5.25	L	−22	−22	−20	N/A
Anterior parahippocampal gyrus	5.12	R	22	2	−26	34
Posterior orbital gyrus/subgenual/putamen	4.94	R	20	4	−14	25
Insular cortex	3.36	R	42	−6	−6	13

BA: Brodmann area.

significantly negatively correlated with memory performance on the WMS-R immediate and delayed recall subscales and the MMSE (Figure 2(b)). Negative correlations remained significant after accounting for gray matter (GM) and cerebrospinal fluid (CSF) volumes from the PPC voxel, as well as age (i.e., partial correlations adjusting for GM, CSF, and age; lac and 1, delayed recall: $r = -0.622$, $P = 0.031$, 2, immediate recall: $r = -0.608$, $P = 0.036$ on the WMS, and 3, MMSE: $r = -0.600$, $P = 0.039$). However, no significant associations were observed between lac levels and neuropsychological tasks not specifically tapping memory-related processes (i.e., $P > 0.05$ for Stroop task; Trails A&B; ADAS-Cog total score; Figure 2(c)).

4.2. PPC Lactate Is Associated with aMCI Brain Pathology. Given the highly specific nature of the lac-memory associations, we sought to determine if lac concentrations across participants were associated with additional indices of disease progression. We first determined left and right hippocampal volumes from the high-resolution T1 MPRAGE. After adjusting for intracranial volumes (ICV), both the left and right hippocampal volumes were negatively correlated with PPC lac levels (Figure 3(a)). Partial correlations adjusting for PPC CSF, GM, and age were not significant ($P > 0.05$). However after removing CSF from the regression model, the correlations were significant ($r = 0.589$, $P = 0.032$ for the left hippocampus, and $r = 0.432$, $P = 0.044$, for the right hippocampus), suggesting an interaction between PPC CSF concentration, lac concentrations, and hippocampal volume.

Resting state fMRI scans were acquired to examine the association between PPC lac and posterior cingulate functional connectivity. After correcting for physiological activity (i.e., cardiac cycle and respiration), whole-brain, voxelwise resting state time courses were extracted from a seed point placed at the site of maximum decrease of FDG-PET consumption across probable preclinical AD patients in a previous study [26], a location which overlapped with the placement of the MRS voxel (Figure 3(b)) in all subjects. Lac concentrations were then entered into a group-level analysis as a covariate of interest using a mixed-effects model and correcting for multiple comparisons at the cluster level using a Gaussian random field theory (minimum voxel Z-score, 2.3; cluster significance, $P = 0.05$, corrected). Significant negative correlations between PPC functional connectivity and lac concentrations across the group were observed throughout the temporal lobe (Figure 3(b) and Table 2). In particular, the left hippocampus (Figure 3(b), left side) as well as the parahippocampal gyrus bilaterally had a substantial number of voxels showing significant negative correlations between the degree of posterior cingulate functional connectivity and PPC lac concentrations.

5. Discussion

We observed that J-rMRS quantification of lactate, the by-product of the anaerobic metabolic process of glycolysis, within a cortical node of the system for memory retrieval is significantly associated with common cognitive and imaging markers of disease progression (e.g., delayed memory function, hippocampal volume, and functional connectivity) in a cohort of aMCI individuals. Previous MRS efforts have failed to detect differences or a lac resonance altogether [21, 22]. This discrepancy is likely due to fact that these studies did not account for the background of overlapping lipid and macromolecule contamination that occurs at the same chemical shift frequency exhibited by lac. J-rMRS is a more sensitive means for isolating lac than traditional short-TE MRS methods because it utilizes the J-coupling properties of lac, physical properties lacking in macromolecules and lipids.

Collectively, we propose J-rMRS as a complementary and/or alternative metabolic biomarker to track the metabolic status in aMCI and possibly AD. MRS is completely noninvasive. Quantification of metabolically active biomolecules with MRS requires minimal time commitment while providing in vivo access to disease-sensitive tissue of interest. Consequently MRS is appropriate and routinely

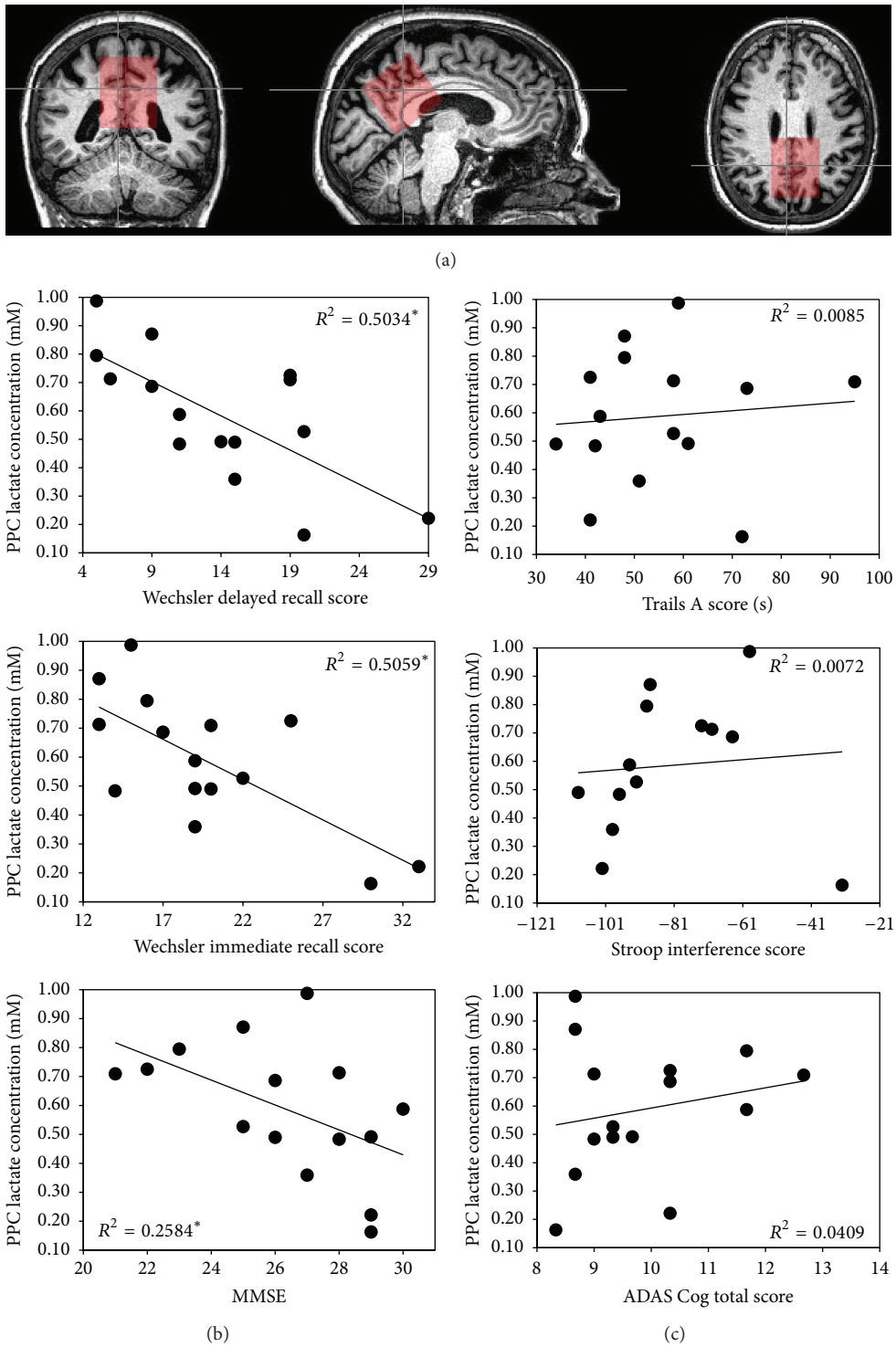

Figure 2: *Posterior cingulate and precuneus (PPC) MRS voxel and lac specific associations.* (a) During scanning, a 4 × 4 × 4 cm voxel (shown in red) was placed bilaterally, centered on medial parietal lobe, covering the posterior cingulate, the precuneus, in most individuals the retrosplenial cortex and in a few individuals the isthmus. A large voxel size is required to provide high lac signal to noise. To ensure consistent placement across subjects, the voxel was centered along the midline, placed just anterior to the parietoccipital fissure and angled in-line with cerebellar tentorium. The voxel was toggled left-to-right to avoid as much ventricular CSF as possible. PPC lac concentrations (y-axes) were correlated with performance on various neuropsychological tests including (b) memory based tasks and (c) non-memory specific tasks. *Correlations were significant at $P < 0.05$ (partial correlations) after correcting for age, GM, and CSF. No correlations on non-memory tasks were statistically significant.

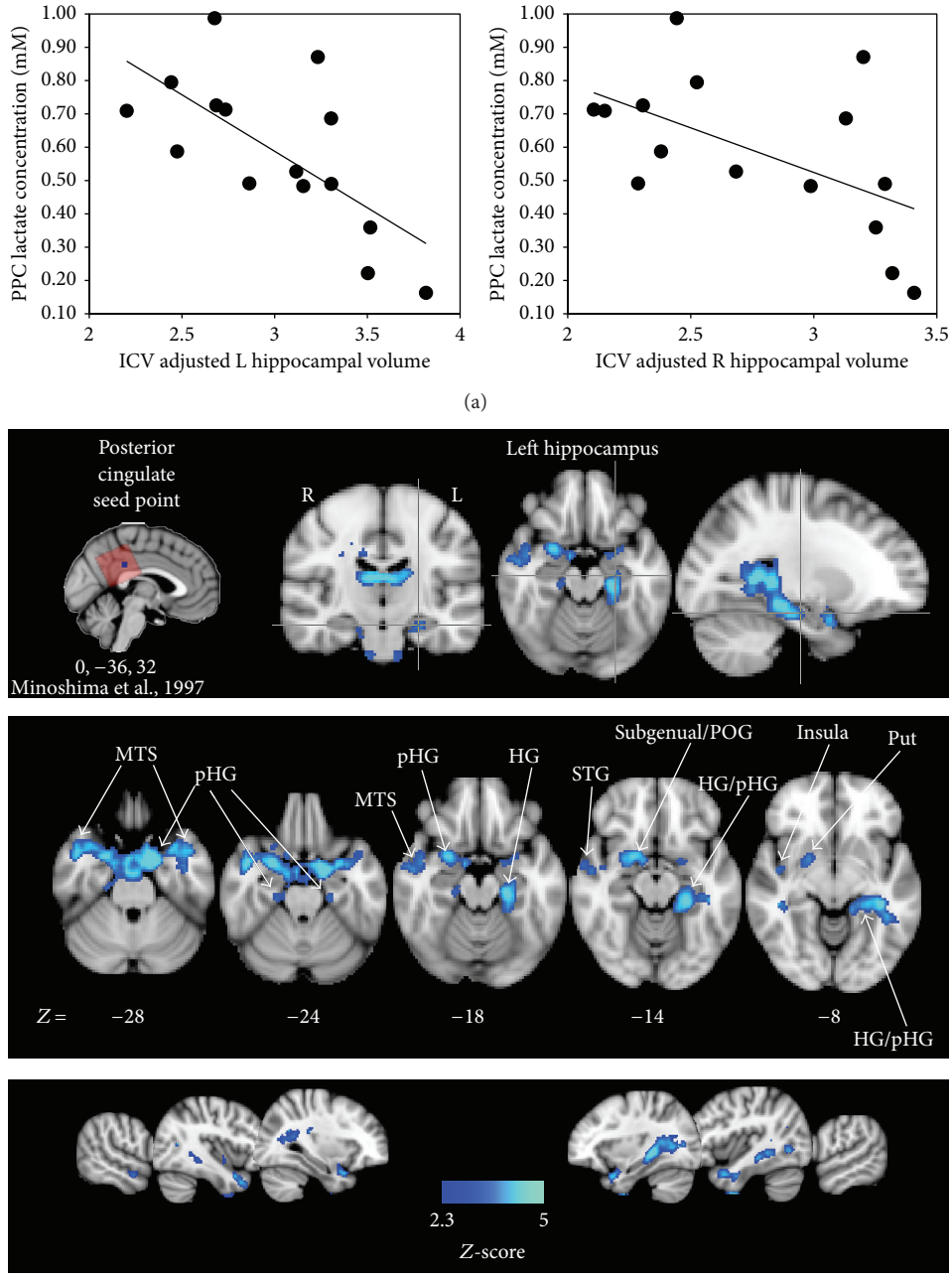

Figure 3: *PPC lac correlations and brain pathology in aMCI.* (a) PPC lac negatively correlates with ICV adjusted L (left) and R (right) hippocampal volumes. (b) Regions of posterior cingulate resting state fMRI functional connectivity that negatively correlate with PPC lac concentrations across aMCI. The PPC seed point (upper left inset) was selected with reference to the site of maximum FDG-PET impairment in a group of preclinical probable AD patients [26] and was contained within MRS voxel locations in all subjects (red transparent box). Z-statistics were calculated utilizing a Gaussian random field theory, thresholded using clusters determined by $Z > 2.3$ and a (corrected) cluster significance threshold of $P = 0.05$. Blue voxels showing significant negative correlations between the strength of functional connectivity and PPC lac concentrations, displayed on the MNI152 template brain and in radiological convention, were generally located within the temporal lobe including medial temporal loci (e.g., left hippocampus in upper left green crosshairs) and various subcortical structures (see Table 2). Coordinates (X, Y, and Z) are in millimeters in MNI space. MTG: middle temporal gyrus. pHG: parahippocampal gyrus. STS: superior temporal sulcus. HG: hippocampal gyrus. STG: superior temporal gyrus. POG: posterior orbital gyrus. Put: putamen.

used in clinical diagnostics for metabolic disorders [19, 38]. Relative to FDG PET, J-rMRS would likely provide a preferable means of tracking metabolic decline when repeated measurements over short time periods are necessary, for example in clinical trials targeting metabolic function and examining therapeutic response [12, 39].

5.1. PPC Lac Concentrations as a Function of Disease Severity. PPC lac levels were only significantly associated with cognitive tests of memory (including the WMS-R delayed and immediate recall, Figure 2(b)). Critical for prediction of AD conversion is the observation that aMCI individuals presenting with the most impacted delayed recall are at greatest risk for developing AD [40]. The observed negative association between lac and memory function indicates that higher levels of PPC lac are related to poorer memory retention, with nearly 50% of the variance in WMS-R subscales performance attributed to PPC lac concentrations (Figure 2(b)). Our explicit statistical adjustments for age, CSF concentrations of lac [27], and GM volume within the PPC voxel (c.f. [41]) give further justification in interpreting the finding as a disease-specific effect. This point is further supported by the significant negative relationship between PPC lac concentration and MMSE scores, a traditional clinical assessment tool. Although follow-up studies will be needed to determine whether individuals with higher PPC lac concentrations are more likely to convert to AD, these observations do suggest elevated levels of PPC lac are linked to aMCI behavioral impairment and by extension are likely related to disease-specific brain pathology.

We tested this assumption by examining the association of PPC lac with two common markers aMCI/AD brain pathology: hippocampal volume and posterior cingulate functional connectivity (Figure 3). The negative correlations between PPC lac levels and hippocampal volume (Figure 3(a)) parallel PPC FDG-PET observations and support the notion that hippocampal atrophy is associated with PPC metabolic function in AD [3]. It is worth commenting on the observation that PPC CSF concentrations accounted for a portion of variance in hippocampal volumes (but not the PPC lac, memory associations). This suggests the possibility of measureable lac concentrations within CSF, a notion that has yet to be explored in aMCI (as far as we are aware), and possibly contributing to the overall PPC lac concentrations across participants. However PPC lac was still significantly correlated with memory ability across the sample even after controlling CSF concentration within the PPC voxel. This would indicate that the concentration of PPC lac, above and beyond CSF levels, is significantly associated with aMCI behavioral impairment, a cognitive process that is in part a function of hippocampal-PPC interactions [5, 6].

In an attempt to reconcile spatial differences between the location of the PPC MRS voxel and the FDG-PET discrepancies in aMCI/AD, we imported the coordinates corresponding to the greatest reduction in FDG-PET utilization from a previous PET study of probable prodromal AD [26] as a seed point location for the resting state time point analysis. Individuals with higher concentrations of PPC lac had greater reductions of functional connectivity between the PPC and numerous cortical and subcortical regions, including the left hippocampus, parahippocampal gyrus, and middle temporal gyrus (Figure 3(b) and Table 2), a spatial topography that parallels resting state functional connectivity maps extracted from the posterior cingulate in neurologically normal individuals [42]. Previous imaging efforts have shown that the strength of connectivity between the hippocampus and the PPC predicts memory capacity in cognitively intact older adults [5] and that this connectivity is degraded in aMCI [43] and AD [44]. Here our functional connectivity observations support the hypothesis that PPC lac concentration is in part attributed to reduced hippocampal input [41].

The negative relationships between PPC lac and memory function, hippocampal volume, and posterior cingulate functional connectivity indicates that individuals presenting with a greater progression of disease state have increased concentrations of PPC lac. Such characteristics have been shown to predict (with varying degrees of success) which aMCI individuals are most likely to convert to AD [40, 44–46]. Thus, it is feasible that PPC lac concentration may also be a marker of conversion. Because PPC lac-behavioral associations were independent of age, this line of reasoning would posit a critical concentration threshold of PPC lac that would distinguish normal aging from aMCI from AD.

5.2. Mechanisms of Lac Production and AD Pathology. Brain lac is produced from the conversion of glucose through glycolysis occurring to a large degree within the cytosol of astrocytes [16]. The byproduct of glycolysis is pyruvate. Classic models of brain metabolism suggest that under normoxic conditions pyruvate enters mitochondria and the oxidative TCA cycle and electron transport chain yielding high levels of ATP. However, in situations when metabolic demands exceed oxygen supply, pyruvate is alternatively catalyzed into lac via the enzymatic activity of lactate dehydrogenase. This combined process, which is referred to as anaerobic glycolysis, yields significantly lower but more rapid amounts of ATP relative to respiration and oxidative phosphorylation [47]. Sustained periods of low oxygen concentrations result in continued production of lac and eventual lactic acidosis. While some studies have shown that concentrations of brain lac can rise as a result of continuous neural stimulation [48], elevated brain lac is generally considered to reflect pathology induced from hypoxia or ischemia [49] or other metabolic crises [50]. However, in certain clinical situations (e.g., congenital mitochondrial disorders) in which mitochondrial function is compromised and cannot sustain ATP levels needed to fuel cellular processes [15], energy requirements are met (at least initially) through a compensatory upregulation of anaerobic glycolysis [17] which leads to elevated lac concentrations [16].

Based upon quantitative reports of metabolic pathology, similar physiological pressures are at play in aMCI all of which could lead to elevated lac in aMCI individuals further along across the disease progression. The conventional interpretation would predict that progressive mitochondrial dysfunction and/or heightened hypoperfusion-induced hypoxia routinely noted throughout the AD spectrum [10, 51] would

lead to increases in anaerobic glycolysis, a mitochondrial-independent process as compensation for declining cerebrovascular function/mitochondrial ATP output and accumulating lac concentrations [52].

However, this hypothesis would need to be reconciled with the known reductions of glucose metabolism in the PPC [1, 26, 41] since the supportive fuel for anaerobic glycolysis is glucose. That is, the downregulation of PPC glucose consumption commonly noted in aMCI/AD pathology would in fact, contrary to our observations, predict decreased levels of lac in individuals with more severe pathology. One leading notion underlying FDG-PET impairments in aMCI and AD, particularly within the PPC, is a slow but gradual reduction of energy requirements stemming from damage to the cellular constituents (e.g., synapses) with high metabolic demand [53]. Abnormal mitochondrial function in AD results in an overproduction of reactive oxygen species, increased oxidative stress, and damage [13]. As a consequence, neuronal cell types with higher concentrations of mitochondria, (particularly within axons and synaptic terminals) relative to glial cells are subject to greater levels of AD-induced metabolic impairment, increased oxidative stress, and a greater likelihood of cell damage and death. Therefore, it is conceivable that while neurons and synapses, the tissue substrates likely responsible for driving FDG-PET reductions [54], suffer a greater burden of AD-induced tissue damage, glial cells including astrocytes remain relatively spared (i.e., degraded from AD pathogenesis). Decreasing synaptic function and neuron numbers would reduce net glucose requirements, while a simultaneous response to astrocytic mitochondrial dysfunction would elevate anaerobic glycolysis ultimately driving up lac concentrations. In support of such a metabolic scenario, an in vitro study observed that cultured astrocytes stimulated with a toxic form of the ABeta peptide produced significantly more lac relative to astrocytes that were bathed in a control peptide [55]. Possible additional (and by no means mutually exclusive) mechanisms include the astrocytic response seen during severe hypoxia or ischemia where delivery of brain glucose (and oxygen) is toxically reduced. In MCI and AD, chronic reductions in PPC glucose may result in utilization of astrocytically stored glycogen, a molecule that can be consumed as an alternative energy source to power anaerobic glycolysis and thus raise lac concentrations [56]. Additionally, Bubber and colleagues observed a negative correlation between pyruvate dehydrogenase complex activity in AD postmortem brain tissue and CDR scores taken just prior to autopsy [57]. The pyruvate dehydrogenase complex, a complex consisting of three enzymes housed within the mitochondrial matrix, is responsible in part for converting pyruvate into acetyl-CoA, an enzyme used in the TCA cycle and electron transport chain (i.e., cellular respiration). If this complex is degraded, pyruvate is alternatively catalyzed into lac via lactate dehydrogenase, a core characteristic of pyruvate dehydrogenase complex deficiency (PDCD) syndrome [58].

5.3. Applications of J-rMRS Lac as a Metabolic Biomarker in aMCI. Numerous pharmacological and biobehavioral efforts are underway that aim to mollify and normalize metabolic instabilities in at-risk populations [12, 13, 51]. FDG-PET is expected to play a significant role in these studies as a means of tracking cerebral metabolic function. An ideal biomarker of disease progression isolates the physiological process being targeted by a therapeutic. This is a critical factor for assessing therapeutic response as it maximizes the ability to "see" preservations and/or improvements at the physiological level while minimizing the need to rely on functional/behavioral outcomes [39]. Mitochondrial physiology is currently one of the main avenues of investigation for the pharmacological restoration of metabolism in AD [13, 51]. Indeed some therapeutic success has been noted both in vitro and cognitive restoration when applying a mitochondrial-targeted antioxidant to a transgenic mouse model of AD [12]. Most metabolic biomarker efforts to date have either pursued PET imaging or measurements of various peripheral or central metabolically active molecules from the blood or CSF, respectively. However, to anticipate similar success within human clinical trials, a biomarker capable of specifically tracking (a) mitochondrial function or (b) a physiological process that reflects mitochondrial function from the tissue of interest is required. An imaging-based biomarker that is specifically sensitive to mitochondrial dysfunction within specific disease-sensitive cortical regions has not yet been published [59]. At a systems level, FDG-PET reductions in aMCI are assumed to reflect a global loss of tissue substrate in the brain, resulting from both a downstream effect stemming from hippocampal neuronal death leading to subsequent axonal withdrawal and synapse loss (diaschisis) as well as local neuronal and gray matter (GM) atrophy [1, 41]. Altogether, we propose that tracking lac concentrations from AD-sensitive brain regions such as the PPC will provide greater physiology specificity for monitoring the effects of mitochondrial uncoupling and cerebrovascular hypoperfusion across the disease spectrum.

5.4. Caveats and Limitations. We show that PPC lac is significantly associated with common aMCI markers of disease progression. Despite the overwhelmingly strong correlations, we cannot specifically conclude that PPC lac is elevated in aMCI until statistical comparisons can be made against age-matched controls presenting with normal memory and cognitive function. Rather we argue that PPC lac provides a means of noninvasively tracking the metabolic status of individuals presenting with significant memory complications. Moreover, we cannot rule out the possibility of elevated lac (as a function of disease pathology) as a more global phenomenon due to the fact that lac concentrations were not quantified from a control region. Given that FDG-PET abnormalities (although generally not uniform across aMCI) have been observed within other association cortices [1], it would not be surprising if lac concentrations are elevated in aMCI in additional cortex, for example, across the DMN and including the medial temporal lobe [4]. Tracking changes in lac over time within subjects will be specifically critical for validating the hypothesis of PPC lac as a biomarker of metabolic dysfunction.

5.5. Conclusions. Here we provide preliminary evidence that PPC lac quantified with J-rMRS is negatively associated with markers of disease progression in aMCI, a commonly assumed prodrome of AD. Based on lac imaging of mitochondrial and metabolic disorders, we propose that the well-established alterations in normal metabolic physiology that are linked to disease progression (i.e., mitochondrial impairment and/or cerebrovascular complications leading to hypoxia) likely give rise to exacerbated anaerobic glycolysis and detectable brain lac in aMCI. Accordingly, these relationships suggest that our lac concentrations likely reflect the metabolic status of the PPC, brain tissue that is exceptionally vulnerable to AD pathology. Future studies will need to combine FDG-PET and J-rMRS to determine if PPC lac is associated with the typical glucose consumption deficits. As a result of the completely noninvasive nature of MR imaging, J-rMRS provides a viable and likely preferable means of tracking metabolic function and dysfunction across multiple time points throughout the AD continuum. A link between PPC FDG-PET levels and lac concentrations may suggest the possibility that J-rMRS can augment or potentially supplant the metabolic monitoring capacities of PET. Moreover, future studies will need to link specific markers of mitochondrial dysfunction and/or cerebrovascular impairment with fluctuations in lac concentration across aMCI individuals. If quantitative studies of mitochondrial and cerebrovascular function are indeed tied lac concentrations, our results suggest an in vivo means of interrogating a metabolic process that is the current focus of a number of therapeutic trials [12, 51]. A biomarker providing a greater specificity for the therapeutically targeted pathophysiological process, together with cognitive restoration, will be critical factors establishing direct disease-modifying effects [39].

Conflict of Interests

The authors declare that there is no conflict of interests regarding the publication of this paper.

Acknowledgments

This work was supported by Grant NIH RO1AG14777 from the National Institute on Aging and a T32-NR-007106 from the National Institute of Nursing Research.

References

[1] L. Mosconi, A. Pupi, and M. J. de Leon, "Brain glucose hypometabolism and oxidative stress in preclinical Alzheimer's disease," *Annals of the New York Academy of Sciences*, vol. 1147, pp. 180–195, 2008.

[2] G. Chételat, B. Desgranges, V. de la Sayette et al., "Dissociating atrophy and hypometabolism impact on episodic memory in mild cognitive impairment," *Brain*, vol. 126, no. 9, pp. 1955–1967, 2003.

[3] S. Yamaguchi, K. Meguro, M. Itoh et al., "Decreased cortical glucose metabolism correlates with hippocampal atrophy in Alzheimer's disease as shown by MRI and PET," *Journal of Neurology, Neurosurgery and Psychiatry*, vol. 62, no. 6, pp. 596–600, 1997.

[4] L. L. Beason-Held, "Dementia and the default mode," *Current Alzheimer Research*, vol. 8, no. 4, pp. 361–365, 2011.

[5] L. Wang, P. LaViolette, K. O'Keefe et al., "Intrinsic connectivity between the hippocampus and posteromedial cortex predicts memory performance in cognitively intact older individuals," *NeuroImage*, vol. 51, no. 2, pp. 910–917, 2010.

[6] C. Sestieri, M. Corbetta, G. L. Romani, and G. L. Shulman, "Episodic memory retrieval, parietal cortex, and the default mode network: functional and topographic analyses," *Journal of Neuroscience*, vol. 31, no. 12, pp. 4407–4420, 2011.

[7] E. M. Reiman, "Fluorodeoxyglucose positron emission tomography: emerging roles in the evaluation of putative Alzheimer's disease-modifying treatments," *Neurobiology of Aging*, vol. 32, supplement 1, pp. S44–S47, 2011.

[8] V. T. Marchesi, "Alzheimer's dementia begins as a disease of small blood vessels, damaged by oxidative-induced inflammation and dysregulated amyloid metabolism: implications for early detection and therapy," *The FASEB Journal*, vol. 25, no. 1, pp. 5–13, 2011.

[9] A.-L. Lin and D. L. Rothman, "What have novel imaging techniques revealed about metabolism in the aging brain?" *Future Neurology*, vol. 9, no. 3, pp. 341–354, 2014.

[10] C. Iadecola, "Neurovascular regulation in the normal brain and in Alzheimer's disease," *Nature Reviews Neuroscience*, vol. 5, no. 5, pp. 347–360, 2004.

[11] W. Dai, O. L. Lopez, O. T. Carmichael, J. T. Becker, L. H. Kuller, and H. M. Gach, "Mild cognitive impairment and Alzheimer disease: patterns of altered cerebral blood flow at MR imaging," *Radiology*, vol. 250, no. 3, pp. 856–866, 2009.

[12] M. J. Mcmanus, M. P. Murphy, and J. L. Franklin, "The mitochondria-targeted antioxidant mitoq prevents loss of spatial memory retention and early neuropathology in a transgenic mouse model of Alzheimer's disease," *Journal of Neuroscience*, vol. 31, no. 44, pp. 15703–15715, 2011.

[13] P. H. Reddy, R. Tripathi, Q. Troung et al., "Abnormal mitochondrial dynamics and synaptic degeneration as early events in Alzheimer's disease: implications to mitochondria-targeted antioxidant therapeutics," *Biochimica et Biophysica Acta*, vol. 1822, no. 5, pp. 639–649, 2012.

[14] P. E. Sijens, G. P. A. Smit, L. A. Rödiger et al., "MR spectroscopy of the brain in Leigh syndrome," *Brain and Development*, vol. 30, no. 9, pp. 579–583, 2008.

[15] R. P. Saneto, S. D. Friedman, and D. W. Shaw, "Neuroimaging of mitochondrial disease," *Mitochondrion*, vol. 8, no. 5-6, pp. 396–413, 2008.

[16] A. Schurr, "Lactate: the ultimate cerebral oxidative energy substrate?" *Journal of Cerebral Blood Flow & Metabolism*, vol. 26, no. 1, pp. 142–152, 2006.

[17] A. Almeida, J. Almeida, J. P. Bolaños, and S. Moncada, "Different responses of astrocytes and neurons to nitric oxide: the role of glycolytically generated ATP in astrocyte protection," *Proceedings of the National Academy of Sciences of the United States of America*, vol. 98, no. 26, pp. 15294–15299, 2001.

[18] C. Berthet, H. Lei, J. Thevenet, R. Gruetter, P. J. Magistretti, and L. Hirt, "Neuroprotective role of lactate after cerebral ischemia," *Journal of Cerebral Blood Flow and Metabolism*, vol. 29, no. 11, pp. 1780–1789, 2009.

[19] D. D. M. Lin, T. O. Crawford, and P. B. Barker, "Proton MR spectroscopy in the diagnostic evaluation of suspected

mitochondrial disease," *American Journal of Neuroradiology*, vol. 24, no. 1, pp. 33–41, 2003.

[20] E. B. Cady, "Magnetic resonance spectroscopy in neonatal hypoxic-ishaemic insults," *Child's Nervous System*, vol. 17, no. 3, pp. 145–149, 2001.

[21] G. Stoppe, H. Bruhn, P. J. W. Pouwels, W. Hänicke, and J. Frahm, "Alzheimer disease: absolute quantification of cerebral metabolites in vivo using localized proton magnetic resonance spectroscopy," *Alzheimer Disease and Associated Disorders*, vol. 14, no. 2, pp. 112–119, 2000.

[22] T. Ernst, L. Chang, R. Melchor, and C. M. Mehringer, "Frontotemporal dementia and early Alzheimer disease: differentiation with frontal lobe H-1 MR spectroscopy," *Radiology*, vol. 203, no. 3, pp. 829–836, 1997.

[23] V. Govindaraju, K. Young, and A. A. Maudsley, "Proton NMR chemical shifts and coupling constants for brain metabolites," *NMR in Biomedicine*, vol. 13, pp. 129–153, 2000.

[24] S. R. Dager, N. M. Corrigan, T. L. Richards, and S. Posse, "Research applications of magnetic resonance spectroscopy to investigate psychiatric disorders," *Topics in Magnetic Resonance Imaging*, vol. 19, no. 2, pp. 81–96, 2008.

[25] D. P. Soares and M. Law, "Magnetic resonance spectroscopy of the brain: review of metabolites and clinical applications," *Clinical Radiology*, vol. 64, no. 1, pp. 12–21, 2009.

[26] S. Minoshima, B. Giordani, S. Berent, K. A. Frey, N. L. Foster, and D. E. Kuhl, "Metabolic reduction in the posterior cingulate cortex in very early Alzheimer's disease," *Annals of Neurology*, vol. 42, no. 1, pp. 85–94, 1997.

[27] Y. Li, A. P. Chen, J. C. Crane, S. M. Chang, D. B. Vigneron, and S. J. Nelson, "Three-dimensional J-resolved H-1 magnetic resonance spectroscopic imaging of volunteers and patients with brain tumors at 3T," *Magnetic Resonance in Medicine*, vol. 58, no. 5, pp. 886–892, 2007.

[28] M. A. Thomas, L. N. Ryner, M. P. Mehta, P. A. Turski, and J. A. Sorenson, "Localized 2D J-resolved 1H MR spectroscopy of human brain tumors in vivo," *Journal of Magnetic Resonance Imaging*, vol. 6, no. 3, pp. 453–459, 1996.

[29] R. C. Petersen, G. E. Smith, S. C. Waring, R. J. Ivnik, E. G. Tangalos, and E. Kokmen, "Mild cognitive impairment: clinical characterization and outcome," *Archives of Neurology*, vol. 56, pp. 303–308, 1999.

[30] M. Grundman, R. C. Petersen, S. H. Ferris et al., "Mild cognitive impairment can be distinguished from Alzheimer disease and normal aging for clinical trials," *Archives of Neurology*, vol. 61, no. 1, pp. 59–66, 2004.

[31] R. C. Petersen, R. Doody, A. Kurz, and etal, "Current concepts in mild cognitive impairment," *Archives of Neurology*, vol. 58, pp. 1985–1992, 2001.

[32] N. A. Honeycutt, P. D. Smith, E. Aylward et al., "Mesial temporal lobe measurements on magnetic resonance imaging scans," *Psychiatry Research*, vol. 83, no. 2, pp. 85–94, 1998.

[33] P. E. Barta, L. Dhingra, R. Royall, and E. Schwartz, "Improving sterological estimates for the volume of structures identified in three-dimensional arrays of spatial data," *Journal of Neuroscience Methods*, vol. 75, no. 2, pp. 111–118, 1997.

[34] H. J. G. Gundersen, P. Bagger, T. F. Bendtsen et al., "The new stereological tools: disector, fractionator, nucleator and point sampled intercepts and their use in pathological research and diagnosis," *APMIS*, vol. 96, no. 7–12, pp. 857–881, 1988.

[35] G. H. Glover, T. Q. Li, and D. Ress, "Image-based method for retrospective correction of physiological motion effects in fMRI: RETROICOR," *Magnetic Resonance in Medicine*, vol. 44, pp. 162–167, 2000.

[36] C. C. Hanstock, D. L. Rothman, J. W. Prichard, T. Jue, and R. G. Shulman, "Spatially localized 1H NMR spectra of metabolites in the human brain," *Proceedings of the National Academy of Sciences of the United States of America*, vol. 85, no. 6, pp. 1821–1825, 1988.

[37] R. A. E. Edden, A. D. Harris, K. Murphy et al., "Edited MRS is sensitive to changes in lactate concentration during inspiratory hypoxia," *Journal of Magnetic Resonance Imaging*, vol. 32, no. 2, pp. 320–325, 2010.

[38] N. M. Corrigan, T. L. Richards, S. D. Friedman, H. Petropoulos, and S. R. Dager, "Improving 1H MRSI measurement of cerebral lactate for clinical applications," *Psychiatry Research-Neuroimaging*, vol. 182, no. 1, pp. 40–47, 2010.

[39] K. Blennow, "Biomarkers in Alzheimer's disease drug development," *Nature Medicine*, vol. 16, no. 11, pp. 1218–1222, 2010.

[40] P. Chen, G. Ratcliff, S. H. Belle, J. A. Cauley, S. T. DeKosky, and M. Ganguli, "Cognitive tests that best discriminate between presymptomatic AD and those who remain nondemented," *Neurology*, vol. 55, no. 12, pp. 1847–1853, 2000.

[41] N. Villain, B. Desgranges, F. Viader et al., "Relationships between hippocampal atrophy, white matter disruption, and gray matter hypometabolism in Alzheimer's disease," *The Journal of Neuroscience*, vol. 28, no. 24, pp. 6174–6181, 2008.

[42] D. S. Margulies, J. L. Vincent, C. Kelly et al., "Precuneus shares intrinsic functional architecture in humans and monkeys," *Proceedings of the National Academy of Sciences of the United States of America*, vol. 106, no. 47, pp. 20069–20074, 2009.

[43] C. Sorg, V. Riedl, M. Mühlau et al., "Selective changes of resting-state networks in individuals at risk for Alzheimer's disease," *Proceedings of the National Academy of Sciences of the United States of America*, vol. 104, no. 47, pp. 18760–18768, 2007.

[44] Y. Zhou, J. H. Dougherty Jr., K. F. Hubner, B. Bai, R. L. Cannon, and R. K. Hutson, "Abnormal connectivity in the posterior cingulate and hippocampus in early Alzheimer's disease and mild cognitive impairment," *Alzheimer's and Dementia*, vol. 4, no. 4, pp. 265–270, 2008.

[45] G. Chételat, B. Desgranges, V. De la Sayette, F. Viader, F. Eustache, and J.-C. Baron, "Mild cognitive impairment: can FDG-PET predict who is to rapidly convert to Alzheimer's disease?" *Neurology*, vol. 60, no. 8, pp. 1374–1377, 2003.

[46] A. Drzezga, N. Lautenschlager, H. Siebner et al., "Cerebral metabolic changes accompanying conversion of mild cognitive impairment into alzheimer's disease: a PET follow-up study," *European Journal of Nuclear Medicine and Molecular Imaging*, vol. 30, no. 8, pp. 1104–1113, 2003.

[47] C. P. Chi and E. L. Roberts Jr., "Energy substrates for neurons during neural activity: a critical review of the astrocyte-neuron lactate shuttle hypothesis," *Journal of Cerebral Blood Flow and Metabolism*, vol. 23, no. 11, pp. 1263–1281, 2003.

[48] J. Prichard, D. Rothman, E. Novotny et al., "Lactate rise detected by 1H NMR in human visual cortex during physiologic stimulation," *Proceedings of the National Academy of Sciences of the United States of America*, vol. 88, no. 13, pp. 5829–5831, 1991.

[49] L. Shalak and J. M. Perlman, "Hypoxic-ischemic brain injury in the term infant-current concepts," *Early Human Development*, vol. 80, no. 2, pp. 125–141, 2004.

[50] P. E. Sijens, P. C. Levendag, C. J. Vecht, P. van Dijk, and M. Oudkerk, "1H MR spectroscopy detection of lipids and lactate in metastatic brain tumors," *NMR in Biomedicine*, vol. 9, pp. 65–71, 1996.

[51] G. Aliev, H. H. Palacios, B. Walrafen, A. E. Lipsitt, M. E. Obrenovich, and L. Morales, "Brain mitochondria as a primary target in the development of treatment strategies for Alzheimer disease," *International Journal of Biochemistry and Cell Biology*, vol. 41, no. 10, pp. 1989–2004, 2009.

[52] G. A. Dienel and N. F. Cruz, "Imaging brain activation: simple pictures of complex biology," *Annals of the New York Academy of Sciences*, vol. 1147, pp. 139–170, 2008.

[53] D. J. Selkoe, "Alzheimer's disease is a synaptic failure," *Science*, vol. 298, no. 5594, pp. 789–791, 2002.

[54] M. Kadekaro, A. M. Crane, and L. Sokoloff, "Differential effects of electrical stimulation of sciatic nerve on metabolic activity in spinal cord and dorsal root ganglion in the rat," *Proceedings of the National Academy of Sciences of the United States of America*, vol. 82, no. 17, pp. 6010–6013, 1985.

[55] I. Allaman, M. Gavillet, M. Bélanger et al., "Amyloid-beta aggregates cause alterations of astrocytic metabolic phenotype: impact on neuronal viability," *Journal of Neuroscience*, vol. 30, no. 9, pp. 3326–3338, 2010.

[56] D. J. Rossi, J. D. Brady, and C. Mohr, "Astrocyte metabolism and signaling during brain ischemia," *Nature Neuroscience*, vol. 10, no. 11, pp. 1377–1386, 2007.

[57] P. Bubber, V. Haroutunian, G. Fisch, J. P. Blass, and G. E. Gibson, "Mitochondrial abnormalities in Alzheimer brain: mechanistic implications," *Annals of Neurology*, vol. 57, no. 5, pp. 695–703, 2005.

[58] M. I. Shevell, P. M. Matthews, C. R. Scriver et al., "Cerebral dysgenesis and lactic acidemia: an MRI/MRS phenotype associated with pyruvate dehydrogenase deficiency," *Pediatric Neurology*, vol. 11, no. 3, pp. 224–229, 1994.

[59] J. P. Blass, "A new approach to treating Alzheimer's disease," *Annals of the New York Academy of Sciences*, vol. 1147, pp. 122–128, 2008.

Hindawi Publishing Corporation
BioMed Research International
Volume 2015, Article ID 736104, 12 pages
http://dx.doi.org/10.1155/2015/736104

Review Article

Role and Importance of IGF-1 in Traumatic Brain Injuries

Annunziato Mangiola,[1] Vera Vigo,[1] Carmelo Anile,[1] Pasquale De Bonis,[2] Giammaria Marziali,[1] and Giorgio Lofrese[1]

[1] *Institute of Neurosurgery, Catholic University School of Medicine, Largo Agostino Gemelli 8, 00168 Rome, Italy*
[2] *Sant'Anna Hospital, Via Aldo Moro 8, 44100 Ferrara, Italy*

Correspondence should be addressed to Giorgio Lofrese; giorgio.lofrese@gmail.com

Received 27 June 2014; Accepted 24 December 2014

Academic Editor: Leon Spicer

It is increasingly affirmed that most of the long-term consequences of TBI are due to molecular and cellular changes occurring during the acute phase of the injury and which may, afterwards, persist or progress. Understanding how to prevent secondary damage and improve outcome in trauma patients, has been always a target of scientific interest. Plans of studies focused their attention on the posttraumatic neuroendocrine dysfunction in order to achieve a correlation between hormone blood level and TBI outcomes. The somatotropic axis (GH and IGF-1) seems to be the most affected, with different alterations between the acute and late phases. IGF-1 plays an important role in brain growth and development, and it is related to repair responses to damage for both the central and peripheral nervous system. The IGF-1 blood levels result prone to decrease during both the early and late phases after TBI. Despite this, experimental studies on animals have shown that the CNS responds to the injury upregulating the expression of IGF-1; thus it appears to be related to the secondary mechanisms of response to posttraumatic damage. We review the mechanisms involving IGF-1 in TBI, analyzing how its expression and metabolism may affect prognosis and outcome in head trauma patients.

1. Introduction

Biomarkers are indicators of a specific biological or disease state that can be measured in both the affected tissue and peripheral body fluids. These markers are represented by altered enzymatic activity, changes in protein expression or posttranslational modification, altered gene expression, protein or lipid metabolites, or a combination of these parameters [1]. Over the years an increasing importance has been placed on the analysis of disease-specific biomarkers, thus revolutionizing the diagnostic, prognostic, and therapeutic approach of various human pathologies [2], including cancer, heart failure, infections, genetic disorders, and traumatic injuries [1]. On these grounds, in the last years a growing interest has developed in biochemical markers of brain damage related to traumatic and vascular events [3].

Traumatic brain injury (TBI) is a nondegenerative, noncongenital insult to the brain from an external mechanical force, causing temporary or permanent neurological dysfunction. It is a common cause of death and disability in industrialized countries for both adults and children, with sequels ranging from physical disabilities to long-term behavioural, cognitive, psychological, and social defects [4]. Under the TBI the injury has to be distinguished primarily, caused by the mechanical damage to the nervous and vascular structures, and secondly, due to the evolution of a cascade of secondary events that compromise the function, structure damage and further promote cell death [5].

The neurological insult and outcome of TBI patients are both currently diagnosed and estimated through clinical examinations of the level of consciousness such as Glasgow Coma Scale; various imaging techniques, including CT, MRI, and positron emission tomography; and assessment of other vital parameters (e.g., intracranial pressure and electroencephalogram) [6]. These diagnostic tools have proved to be frustratingly limited, especially in the intensive care unit setting; thus the search for surrogate markers, detectable in serum and/or CSF, could provide further information about the extent of neuronal damage, which is crucial in estimating prognosis and outcome [6].

Different studies have proven that most of the long-term consequences of TBI are due to molecular and cellular changes occurring during the acute phase of the injury and which may, afterwards, persist or progress [7, 8]. Because of these reasons, the search for predictive serological markers of outcome in TBI began over 20 years ago [9], and the list of putative biomarkers for traumatic brain injury continues to grow as do the conflicting results of their utility in various injury paradigms [10]. A variety of proteins, small molecules, and lipid products have been proposed as potential biomarkers of brain damage from TBI [1].

To date, the majority of TBI researches have been focused on protein profiling such as S100B, GFAP, NSE, MBP, FABPS, a-II spectrin, phosphorylated neurofilament H, and ubiquitin C-terminal hydrolase, which can be all identified in serum or/and cerebral spinal fluid (CSF) helping to evaluate injury severity and correlate with morbidity and mortality [1].

Another important modification observed after TBI is the increased serum and/or CSF concentrations of acute phase proteins (e.g., C-reactive protein, amyloid A, proinflammatory cytokines (e.g., IL-1, TNF-a, and IL-6), anti-inflammatory cytokines (IL-10, transforming growth factor beta, or TGF-b), and chemokines (e.g., ICAM-1, macrophage inflammatory protein- (MIP-) 1, and MIP-2)). The CSF and/or serum level modifications of these markers have been related with injury and sometimes with outcome through time-specific changes in response to TBI [1].

Among the potential biomarkers involved in primary and secondary injuries should be counted also metabolites of neurotransmitters, second messengers, ions and glycolytic intermediates, such as cAMP, whose concentration in CSF was found to correlate with the grade of coma, or N-acetylaspartate (NAA) that seems to predict eventual neuropsychological deficits [1].

During the last two decades many evidences have suggested a hormonal crucial role in influencing the damage after TBI, being hormones usually involved in the stress response occurring in critical illness [11]. Therefore several studies focused their attention on posttraumatic endocrine dysfunction, attempting to correlate it with TBI outcome. In this contest, blood modifications of growth hormone (GH) and IGF-1 concentration appear to be the most affected, with various authors increasingly assigning a greater value to IGF-1. This molecule seems to play important roles in both the pathogenesis and the secondary response to brain damage. Thus we tried to understand, through the literature, if there are grounds to identify the IGF-1 as a crucial marker in serum and CSF of those patients suffering from traumatic brain injuries.

2. IGF-1 in the CNS

The IGF-related peptides may affect brain function by either local tissue expression or by peripheral circulating peptides crossing the BBB via transcytosis [12]. IGF-1 is part of a well-structured family peptide. The IGF signaling system is composed of three ligands (IGF-1, IGF-2, and insulin), three cell membrane receptors (IGF-1R, IGF-2R, and the insulin receptor IR), and several associated proteins, namely, IRS and SHC. IGF-1 circulates in the plasma as complexes formed with IGFBPs that probably serve several biological functions. The vast majority of IGF-1 (99%) is bound to IGFBP3 or IGFBP5 and is coupled with a glycoprotein called the acid labile subunit. The final binding of IGF-1 to its own receptor IGF-1R triggers a conformational change that causes tyrosine autophosphorylation and transphosphorylation, enhancing its tyrosine kinase activity [13]. These events bring about recruitment of IRS, CRK, and SHC, leading to the activation of three main pathways: the MAPK/Ras-Raf-Erk pathway, the phosphatidylinositol-3-kinase/AKT/mTOR (PI3K/AKT) pathway, and the Janus kinase/signal transducer and activator of transcription (JAK/STAT) pathway [14]. There are two sources of production of IGF-1, yielding different functions to this molecule: the liver generates IGF-1, which acts as a prolongation of the GH under tonic pituitary stimulation of hepatic synthesis; IGF-1 is also produced locally by many types of peripheral cells under basal conditions and in response to inflammatory stimuli. In this sense, although it is mainly produced by the liver (70%), IGF-1 can be secreted by every tissue. More specifically IGF-1 and the IGF-1R are expressed in close proximity to each other in various brain regions, suggesting a paracrine or autocrine functional loop in physiological and pathophysiological mechanisms [15]. Receptors for IGF-1 are virtually present on all cell types but they are mainly located on those cells of mesenchymal origin, such as fibroblasts, chondrocytes, and osteoblasts [16]. In human's brain, IGF-1 receptors are found predominantly in the hippocampus and parahippocampal areas, but also amygdala, cerebellum, and cortex express them [17]. BBB uptake of circulating IGFs involves the IGF-1R and the low-density lipoprotein receptor-related protein 1 (LRP1), through which IGFs can reach the CSF as well as the aforementioned anatomical targets [12]. Although there is evidence that IGF-1 is transported across the BBB via transcytosis [18], a significant amount of IGF-1 is undoubtedly produced in the brain, confirmed by the fact that IGF-1 mRNA has been found predominantly in the adult rats brain stem and cerebellum [19].

IGF-1 stimulates the proliferation and differentiation of oligodendrocytes supporting myelination of the CNS, being involved in the differentiation of neurons to specific cell types. It can increase levels of neurotransmitters, neurotransmitter receptors, and proteins of the cytoskeleton; it can inhibit apoptosis in neurons [19]; it stimulates dendrite growth, angiogenesis, and amyloid clearance [12, 20].

Moreover disruption of the IGF-1 gene, leading to loss of function, induces neuronal loss in the hippocampus and striatum [21]. As demonstrated in aged rats, there is a permanent neurogenesis in the dentate gyrus of the hippocampus of mammals decreasing with age up to a 60% reduction in the differentiation of new cells to neurons. This trend depends on environmental factors, hormones, and growth factors such as IGF-1 and this evidence is confirmed by the fact that reduction could be reversed by intracerebroventricular administration of IGF-1 [22]. Thus, it can be assumed that the age-dependent decline in the expression of both IGF-1 and IGF-1 receptor could be a possible contributing factor to the development of cognitive deficits seen in the elderly.

These cognitive impairments were reversible by prolonged systemic administration of IGF-1 and suggested

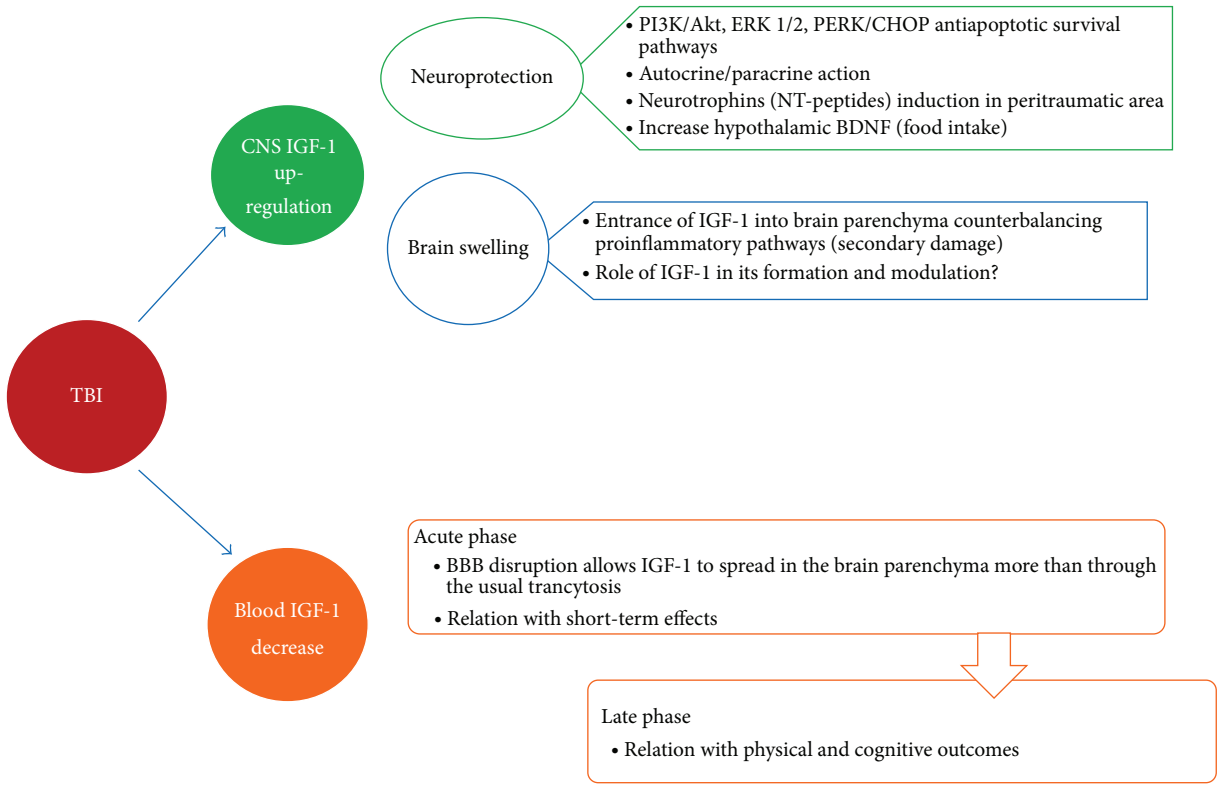

Figure 1: Effects of TBI on IGF-1 expression and metabolism with consequent biological and clinical manifestations.

that the neurotrophic actions of IGF-1 affect glutamatergic synapses within the hippocampal circuitries, thereby affecting learning and memory [12].

3. IGF-1 in the CNS Pathologies

IGF-1 plays an important role in brain growth and development [23], and it is involved in repair responses to damage for both the central and peripheral nervous system [24–26]. IGF neurotrophic activity, together with its binding proteins and signalling receptors, is suggested to be fundamental in the recovery of neural tissue from injury [27]. This evidence is supported by the CNS response to injury through the upregulation of the IGF-1 expression.

In this sense different studies concerning the CNS have revealed an impressive IGF-1 induction after different brain insults such as ischemia [28, 29] and cortical injuries [30–32] as well as injuries of the spinal cord [33]. The major role of IGF-1 in hypoxic/ischemic damage, through its modulation of the cellular response stimulating the repair mechanisms, is increasingly being recognized. Serum IGF-1 levels have been proved to be depressed following acute stroke in the human being [29, 34], while in rodent models brain IGF-1 levels resulted in increase in the perilesional stroke area [28], thus likely revealing a neuroprotective role. It seems also that poststroke serum IGF-1 levels are correlated with outcome from ischemic brain injury, with its higher levels reducing lethality [34]. In the wake of this evidence many studies have shown the beneficial effect of IGF-1 administration after stroke, reducing neuronal loss and infarct volume, while increasing glial proliferation [35, 36].

A significant body of data has identified IGF-1 both as a major regulator of amyloid β-peptide (Aβ) physiology and as an important factor in the pathogenesis of Alzheimer's disease (AD) [12]. A recent study demonstrates that lower IGF-1 serum levels are associated with an increased risk of developing AD dementia, while higher serum results are related to greater total brain volumes and may protect against subclinical and clinical neurodegeneration [37].

Moreover, IGF-1 appears to be linked with repair processes after brain damage, controlling the regeneration of injured peripheral nerves [38] seeming to be relevant in ameliorating clinical outcomes in animal models of amyotrophic lateral sclerosis [38]. Some data also suggest that aberrations in IGF expression or function are involved in brain tumorigenesis such as gliomas, neuroectodermal tumours, and neuroblastomas [39].

4. Role of IGF-1 in TBI: Experimental Studies

Apart from its aforementioned role in hypoxic/ischemic stroke, neoplastic and other degenerative diseases, the activity of IGF-1 in the CNS seems to be pivotal even in traumatic brain injuries (Figure 1) with a number of recent findings supporting a role for IGF-1 in wound healing in the brain. IGF-1 is a potent mitogen and can induce differentiation of neural cells in vitro, including neurons, astrocytes, oligodendrocytes, and endothelial cells. It may also influence similar

functions in vivo, exerting its mitogenic and trophic effects on a variety of cell types, after brain injury [40], thus leading some authors to study its changes in brain tissue reproducing TBI on animal models [29].

A significantly increased IGF-1 expression after TBI has been widely observed. Li et al. [30] determined the responsiveness of the IGF-1 gene in adolescent mice brain tissue, after penetrating injury; the hormone value was higher on 3 days after injury and remained elevated during the week after, compared to the control group. Sandberg Nordqvista et al. [31] noted an increase of IGF-1 mRNA, with a peak at 24 h after the impact, in their rats contusion model. Madathil et al. [23] also showed a very early (6 h) concomitant increase of IGF-1 in the central area of impact site with a decrease in the injury periphery, where instead IGF-1 hyperexpression was delayed. Walter et al. [32] showed that IGF-1, after penetrating CNS injury in rats, acts in an autocrine/paracrine way to regulate cellular responses, with its limited availability being modulated by the differential presence of stimulatory and inhibitory IGF binding proteins. Several evidences suggest that IGF-1 may play a role in the regulation of reactive astrogliosis, which is one of the most prominent manifestations of the repair response in the mature CNS [41, 42], typically occurring in a delayed fashion within and around areas of neuronal damage, with glial scar formation progressing over several days [43]. IGF-1 has also been proved to stimulate in vitro the astrocyte migration in response to axonal injury [44].

The activities performed by IGF-1 in response to injury begin by binding to its receptor (IGF-1R), which is expressed by neurons, stem cells, and most glial cells [15, 45]. Little is known about IGF-1R expression in response to TBI and Sandberg Nordqvista et al. [31] observed no change in IGF-1R mRNA from 1 to 7 days, following weight drop injury in rats. Instead Walter et al. [32] showed an increased expression of IGF-R protein in the early stage (1–7 days) of penetrant cerebral wounds model. Rubovitch et al. [46] proved that IGF-1R was phosphorylated after mild-TBI, with a time dependent activation at maximum 24 hours. The link between IGF-1 and its receptor leads to the activation of antiapoptotic pathways, whose major are represented by PI3-kinase/Akt and MAP-kinase [47]. As a matter of fact, Madathil et al. [23] showed that, in mouse contusive brain, injury-induced IGF-1 increase may provoke cellular changes through the Akt pathway, as it increases as phosphorylated Akt and/or total Akt, promoting cell survival. Rubovitch et al. [46] confirmed the activation of the Akt pathway and also showed the activation of ERK1/2 following mild-TBI. IGF-1 may even exert its neuroprotective activity after mild-TBI in mice through the PERK/CHOP pathway, which activates the survival/antiapoptotic arm of the endoplasmic reticulum (ER) stress machinery [48].

An interesting role seems to be played by the IGF binding proteins in mediating the activity of IGF-1 after neuronal injury. Usually they are expressed in a variety of tissues and bind IGF-1 and IGF-2, modulating the biological effects with both inhibitory and stimulatory effects [49]. Ni et al. [50] showed that the overexpression of IGFBP-1 impairs brain development and reduces glial cell proliferation in response to injury, in transgenic mice. Sandberg Nordqvista [31] noticed a significant upregulation of IGFBP-2 mRNA in cortical areas close to the injury site and observed a spatial correlation between posttraumatic swelling and increase in IGFBP-2 and -4 mRNA levels. Therefore they hypothesized the involvement of IGF-1 and its binding proteins in the oedema formation and modulation. Walter et al. [32] verified in the acute phase of injury (1–7 days) increased levels of IGFBP-1, -2, -3, -6 localized in injury responsive astrocytes, neurons, and cells of the monocyte lineage, probably facilitating the effects of IGF-1. On the other hand they found a later increase (7–14 days) of IGFBP-4 and -5 localized in the astrocytes and neurons, probably having a role in downregulating the chronic effects of IGF-1. Sandberg Nordqvist et al. [51] also proved that the upregulation of the IGF-1 and IGFBP-2 and -4 is glutamate dependent. Indeed the induction of IGF-1 expression was completely blocked by noncompetitive N-methyl-D-aspartate (NMDA) antagonist (MK-801 or CNQX) in the brain of rats.

The main clinical signs and symptoms reported in patients with mild-TBI include memory disorders and affective lability [52–54]. Many experimental studies suggest that circulating IGF-1 levels are related to cognitive deficits in the aging and amnesic models [55]. The severity of the trauma-induced apoptotic neurodegeneration in the brains of 3–30-day-old rats had been demonstrated to be age dependent and highest in 7-day-old animals. Thus, apoptotic neurodegeneration has been suggested to contribute in an age-dependent fashion to neuropathological outcome of head trauma [56]. Recent results have shown that IGF-1 may even regulate neurogenesis in the adult rat hippocampus [56]. The cognitive dysfunction after TBI may therefore result from hippocampal damage; indeed Schober et al. [57] reported for the first time that hippocampal IGF-1B mRNA increased after developmental TBI in the brain of the rats. Ozdemir et al. [55] proved that the decrease of circulating IGF-1 levels after TBI was associated with cognition and hippocampal damage in 7-day-old rat pups subjected to contusion injury. IGF-1 could also be involved with posttraumatic anxiety disorder. Baykara et al. [58] investigated the effects of progesterone on traumatic brain injury-induced anxiety in 7-day-old rat pups subjected to contusion injury; they found that progesterone treatment decreased TBI-induced anxiety and serum corticosterone levels, while increasing serum IGF-1 levels. In the study of Madathil et al. [43] moderate or severe contusion brain injuries were induced in mice with conditional (postnatal) overexpression of IGF-1, revealing that the astrocyte-derived IGF-1 exerts autocrine effects on astrocytes, reduces regional hippocampal neurodegeneration, and improves posttraumatic cognitive and motor function.

Considering the role of IGF-1 in repair processes, neurogenesis, and posttraumatic anxiety disorders, some authors have conducted experimental studies on the administration of IGF-1.

Assuming the neuroprotective effect of IGF-1 administration in models of cerebral ischemia and spinal cord injury [59], the disruption of blood-brain barrier that starts as early as minutes after brain damage and persists until 7 days after injury, depending on trauma severity [60, 61], may allow

systemic IGF-1 to permeate the brain parenchyma improving behavioral outcome in TBI [62]. Based on these evidences, strategies to either increase the endogenous upregulation or supplement it with exogenous IGF-1 may improve neuronal survival after TBI. Kazanis et al. [63], using a model of penetrating brain injury, analysed the beneficial effects of postinjury administration of IGF-1 both at the cellular level and on the animals physical condition. IGF-1 administration resulted in a significant decrease, in the peritraumatic area, of the number of Hsp70 and TUNEL positive cells, which are both typical markers of cell injury. Additionally, they noted an improvement of the total "motor activity" of injured rats, an increased food intake, and an attenuated postinjury body weight loss. In another study Kazanis et al. [40] showed that administering IGF-1 immediately after the trauma reversed the injury-induced decrease in brain-derived neurotrophic factor (BDNF) and neurotrophin-3 (NT-3) in the peritraumatic area, at 4 and 12 h and one week after injury, and it completely voided the effects of injury in the adjacent region. These results demonstrated that IGF-1 administration following TBI could mediate repair and protective processes, also changing neurotrophins levels. Schober et al. [57] found that cognitive outcome improved after administration of erythropoietin (EPO) or insulin-like growth factor-1 (IGF-1), using a controlled cortical impact model of 17-day-old rats. Rubovitch et al. [46] assessed that IGF-1 administration prevented spatial memory deficits following mild-TBI. They also interestingly noticed that blocking the IGF-1R signalling in mild-TBI mice did not increase the spatial memory deficit. The data imply the possibility that the nature of the intrinsic mild-TBI-induced activation of the IGF-1R pathway is different from the one activated by the exogenous administration of IGF-1.

5. Role of GH and IGF-1 in TBI: Clinical Studies

One of the most important consequences of the TBI is the posttraumatic neuroendocrine dysfunction (NED) that refers to a variety of conditions caused by imbalances in the body's hormone production directly related to the pituitary, hypothalamus, and their axes [64]. A recent literature review suggests that the incidence of NED in mild-TBI is 16.8%, while the incidence with moderate TBI has been reported at 10.9% [65]. NED symptoms include fatigue, insomnia, impaired cognition, memory loss, concentrating difficulty, and emotional and mood disturbances, all depending on the severity of the specific hormonal deficiency [66, 67].

The NED pathophysiology following TBI is not completely understood and several mechanisms of injury have been suggested to be involved [68]: compression of the pituitary gland and/or the hypothalamic nuclei due to oedema, skull base fracture, haemorrhage, increased ICP, hypoxic insult, or direct mechanical injury to the hypothalamus, pituitary stalk, or the pituitary gland [69–71]. Nevertheless the factors predisposing to the development of posttraumatic hypopituitarism are still under debate. Some authors postulated that endocrine derangements are related to the severity of the head trauma, as represented by GCS on admission in the ICU, and to high intracranial pressure [72–74]. They demonstrated an association with the extent of brain CT findings [75]; others instead did not find any correlation between the head trauma and the endocrine dysfunction [76, 77]. Overall it seems that the severity of TBI, assessed by initial GCS, is not generally associated with the presence of hypopituitarism, because the initial GCS is not enough discriminative to assess reliably the severity of injury. However a more severe clinical status seems to predict a higher risk of secondary hypogonadism [78]. Therefore routine screening for hormone disturbances in unselected patients after TBI is unlikely to be cost-effective. Screening should be advised in all patients with symptoms and signs of hypopituitarism and a history of TBI and based on earlier reports, probably also in patients with more severe forms of TBI necessitating neurosurgical intervention or admission to an ICU [79]. In both moderate and severe TBI the most affected axis of posttraumatic endocrine dysfunction is the somatotropic one with both cerebrospinal fluid and serum levels of IGF-1 demonstrated to be decreased in adult patients with major head injury [55]. IGF-1 plasma concentrations in patients with TBI are typically below the normal physiologic range of 150–400 ng/mL [80]. In literature GHD prevalence varied from 2 to 66%, with up to 39% of cases suffering from severe deficiency [81]. Several factors could explain this percentage variability, including different time interval between TBI and the assessment of pituitary function (from 24 h to 35 years), type and severity of the brain injury, different methods to evaluate pituitary function reserve such as tests and hormonal assays, criteria for the diagnosis, and selection criteria not excluding those patients in whom, besides a history of TBI, alternative causes of pituitary dysfunction have not been ruled out [82, 83]. To avoid this bias, patients should be followed up at least 1 year after the trauma, as suggested in the consensus guidelines for the evaluation and diagnosis of patients with possible GHD [83]. The absence of a gold standard test for GHD will always raise questions regarding the true occurrence of a GH deficiency after TBI [84]. Therefore analyses of GH especially under multiple pharmacological treatment, as in TBI patients, should be interpreted with caution [85]. Consensus guidelines to overcome confounding factors in TBI patients state that the GH/IGF-1 deficiency should be evaluated through a first line measurement of the basal anterior pituitary hormones, by dynamic endocrine testing such as the glucagon stimulation test, followed by the second line growth hormone releasing tests (GHRH), arginine test and GHRH + GHRP-6 and/or insulin tolerance test [86, 87]. Moreover, the results of GH stimulation tests are confounded by BMI, with higher BMI being associated with decreased GH responses. Although BMI-adjusted reference values have been reported, none of the studies on TBI-associated GHD reports adjusted their cut-off values for BMI [83].

It seems fairly accepted that in the long-term phase of TBI (3 months onwards) GH and IGF-1 blood levels appear frequently reduced with different prevalences. In this sense Kelly et al. [70] found 18% GH defect among patients with TBI, and Lieberman et al. [76] reported 15%, whereas Agha et al.

[88] and Aimaretti et al. [89], respectively, indicated 18% and 37% of GH reduction and Abadi et al. [90] showed IGF-1 deficiency in 24% patients three months after injury. These controversial data are certainly due to the lack of standardization of the patients cohorts, the inclusion of different types of severity of the trauma (mild, moderate, and severe), and the different methods used in the hormonal dosage.

A contradictory literature characterizes even the discussion about GH and IGF-1 levels following TBI in the acute phase of injury. Plasma IGF-1 concentrations do not seem to be a reliable reflection of GH secretion or action in the setting of acute illness [88]. In fact some authors reported an increase of GH levels in the acute phase and others show a relation with high ICP [72, 91]. Other studies instead show GH levels remaining relatively normal or slightly elevated throughout the acute setting in mild, moderate, and severe TBI [92, 93].

On the other hand some evidences suggest that IGF-1 decrease in the acute phase of injury with reduced serum IGF-1 and IGFBP-3 levels reported in the first 48–60 h following TBI [94]. In a recent study [85] a transient decrease in serum IGF-1 has been recognized with low levels on day 1 and then restored towards normal on day 4 after severe TBI. Interestingly blood IGF-1 levels do not appear to be related to GH value in the acute phase of injury. In fact low IGF-1 with elevated GH levels have been shown in the acute posttraumatic phase, as well as a normalization of GH with an increase of IGF-1 in the following weeks after the acute event [95]. According to these data Agha et al. and Dimopoulou et al. showed no statistical differences in plasma IGF-1 concentrations between the GH-sufficient and GH-deficient groups, after severe TBI [75, 88].

The detection of a peripheral resistance to GH action, manifested by elevated plasma GH concentrations, with low plasma IGF-1 concentrations, underlines the influence on plasma IGF-1 levels even by factors other than GH secretion and action [88, 96]. Although GH and nutrition represent the major factors regulating IGF-1 expression in the liver, as well as in a number of other organs [97], in some tissues IGF-1 expression appears to be modulated by specific trophic factors. In this sense there are evidences supporting injuries as factors able to influence the brain expression of IGF-1 [39] as much as GH [98] and nutrition [99] do. The role of the trauma-induced elevation in IGF-1 is unclear, but it is feasible that IGF-1 upregulation in surviving neurons may act to limit the progression of cell death, induce progenitor cell differentiation, or promote neurite outgrowth [23].

6. GH and IGF-1 Deficiency

Several pieces of data clearly demonstrated that GH deficiency is the most common pituitary deficit with a 20% incidence of severe GHD one year after TBI. In patients with mild and moderate traumatic brain injury, pituitary function may improve over time in a considerable number of patients but, although rarely, may also worsen over a 3-year period. Patients with severe TBI, instead, usually suffer from persistent GHD up to 3 years after trauma [100]. Normal pituitary function in the short term, although rarely, becomes impaired later on. Thus, brain-injured patients must always undergo neuroendocrine follow-up over time to monitor pituitary function and eventually provide appropriate hormonal replacement [67].

It is widely accepted that the somatotropic axis plays both a central role in the development and growth of CNS and a protective role in dementia, traumatic and ischemic injuries of the brain [101]. The major studies used the GHRH-arginine test as the primary test to evaluate the GH-IGF-1 axis, adopting a peak GH of 9.0 mcg/L as a cut-off value, whereas recent clinical practice guidelines recommend a limit value of 4.1 mcg/L [102]. According to a multicenter study, which used a sensitive immunochemiluminescent two-site assay, this cut-point provides the best compromise in terms of specificity and sensitivity for the diagnosis of adult GH deficiency through the GHRH-arginine test, thus minimizing the misclassification of multiple pituitary hormone deficiencies and control subjects [103].

GH and IGF-1 deficiencies are associated with multiple physical, metabolic, and neuropsychological manifestations including diminished lean body mass, disrupted lipoprotein and carbohydrate metabolism, reduced bone mineral density, and impaired cardiac function, as well as decline in cognitive functioning, fatigue, and diminished quality of life [104].

In the early stages of life, growth retardation after TBI is the hallmark of potential damage to the hypothalamic-pituitary function of the GH/IGF-1 axis. Because of the similarity of some TBI sequelae to those of untreated hypopituitarism, it is frequently postulated that hormone deficits may contribute to the chronic disability of TBI survivors. In this context, a recent study has shown that GH-insufficient TBI patients have higher levels of fatigue than GH-sufficient TBI patients up to 6–9 months after the trauma [105]. Thus, providing appropriate diagnosis of this deficiency is crucial, as the subsequent management using growth hormone (GH) replacement therapy has been ascertained to be effective [106].

It has also been noticed that the combination of IGF-1 and GH therapy improves metabolic and nutritional parameters after TBI. IGF-1 induced changes of BDNF in the anterolateral hypothalamic area could be related to the effects of IGF-1 in controlling food intake, which have been implicated in the protective actions of IGF-1 following injury, since BDNF levels have been shown to change in conditions of altered food intake [40]. More specifically the ameliorative effect of IGF-1 could be primarily attributed to its effect in increasing food intake, the parameter shown to have the strongest improvement since inadequate nutrition is known to be a major clinical problem following brain trauma. The latter typically causes a hypermetabolic stress to the organism and IGF-1 is shown to act as a potent anabolic agent in such cases [64].

A postinjury rapid increase in plasma IGF-1 concentrations to more than 350 ng/mL seems transiently to improve both nitrogen retention and trend in 6-month outcomes [107]. Indeed Hatton et al. [108], comparing combination IGF-1/GH therapy and a placebo treatment on 97 patients with moderate to severe TBI, noticed a positive nitrogen balance during the first 24 hours in the treated group with

a positive trend throughout all the treatment period. The combination of IGF-1 and GH after moderate to severe acute TBI produced sustained improvement in metabolic and nutritional end-points, such as the hyperglycemia, insulin resistance, and compromise of the immune system and continous loss of protein.

7. Discussion

Worldwide TBI is one of the major causes of death and disability. This is why understanding how to prevent secondary damage and improve outcomes in patients suffering from head injury has always been a target of scientific interest. An increasing number of experimental results suggest that most of the long-term consequences of TBI are due to molecular and cellular changes that occur during the acute phase of the injury and which persist, or even progress, subsequently [40]. Thus nowadays, the success of therapeutic interventions following TBI is strongly dependent even on the complex molecular signalling cascades targeting [9].

Many authors focused their attention on the posttraumatic neuroendocrine dysfunction in order to achieve a correlation between hormones blood level and TBI outcomes.

In the contemporary literature the hormonal processes belonging to the somatotropic axis result to be the most affected by TBI, with different alterations between the acute and late phases. Levels of IGF-1 transcript begin to increase between 1 and 3 days after lesion and remain elevated throughout the second week following injury. These results further support a role that locally produced IGF-1 is the expression of the brain's response to injury [30]. Specific studies could not, however, determine whether the increased concentration of IGF-1 resulted from local synthesis within the damaged region or from damaged blood vessels since serum has the highest levels of IGF-1 in the body [64]. Nevertheless the specific IGF-1 upregulation at the site of the lesion has led to the suggestion that IGF-1 may be involved in the process of tissue healing, playing a role in the neuroprotective and/or neurorepairing response of brain tissue to trauma [40].

In the long-term evaluation the serum levels of GH and IGF-1 seem to decrease, determining multiple physical, metabolic, and neuropsychological manifestations. Their early recognition and prompt replacement therapy are likely to be crucial in the management of GHD patients recovering from TBI [84]: authors adopting a combination therapy of GH and IGF-1 showed improved outcomes, taking in account both physical and cognitive aspects.

Therefore an important question is whether circulating IGF-1 levels are predictive of cognitive dysfunction resulting from hippocampal damage following traumatic injury especially in developing brain. In animal models, it was shown that decreased serum IGF-1 levels resulted in cognitive deficits and IGF-1 deficiency led to impaired learning and memory in adulthood. Various experimental studies found that low-serum IGF-1 levels were related to cognitive dysfunction following traumatic injury. Further studies need to be carried out on human subjects or experimental models in order to evaluate the time course or damage-dependent IGF-1 levels in TBI. Therapy strategies that increase circulating IGF-1 may be highly promising, in this sense, for preventing the unfavorable outcomes of traumatic damage particularly in young children [55].

It is still controversial whether an alteration of blood IGF-1 is due to its subordination to GH or not. Moreover some studies have recently demonstrated that the evaluation of neuroendocrine processes in the acute phase of the injury also involves a peripheral resistance to GH actions, thus highlighting other factors likely influencing IGF-1 levels.

Although a recent study shows no correlations between IGF-1 levels and 3 months' outcome [85], experimental studies in animals have revealed a role of IGF-1 in the context of the secondary mechanisms of response to posttraumatic damage. In fact many authors verified that while the systemic level of IGF-1 decreases, the CNS responds to the injury upregulating the expression of IGF-1. A subset of molecules in the IGF cascade thus responds to traumatic injury with transient but striking increase in mRNA synthesis. It is possible that the selective change in IGF binding protein mRNAs seen following injury serves to relocate growth factors to cells in need of posttraumatic repair [23, 30, 31]. Therefore IGF-1 behaves as a neuroprotective peptide, activating many signalling pathways that promote cells survival, acting in an autocrine/paracrine way to regulate cellular responses, regulating the reactive astrogliosis while stimulating proliferation and differentiation of oligodendrocytes that support myelination of the CNS. Astroglial cells provide physical and metabolic support for neurons and their processes often end on blood vessels. They are highly enriched in IGF-1 receptors and IGF-1 has stimulatory effects on astrocyte multiplication and glucose uptake [51]. Astrocytosis may also be beneficial after injury by forming a physical and biochemical barrier to separate a contused area from healthy tissue, limiting the spread of inflammatory molecules and cells. Indeed, removal of reactive astrocytes after TBI has been shown to worsen tissue loss and behavioral performance [43].

Numerous experimental studies have shown that IGF-1 provides long-term protection to mature oligodendrocytes, mainly by inhibiting oligodendroglial apoptosis but also through its mitogenic properties upon the oligodendroglial precursors. Irrespective of the mechanisms, IGF-1 induced maintenance of neurotrophins within the peritraumatic area could be involved in the previously reported effect of IGF-1 in preserving tissue homeostasis [40].

An interesting role seems to be played by IGF-1 in the development of posttraumatic oedema, which represents a critical and therapeutically insidious problem in TBI patients, especially in moderate and severe injuries. It is possible that localized breakdown of the blood-brain barrier could increase local brain levels of selective growth factors and thus contribute to the wound healing process. Glial cells have been reported to internalize plasma proteins and retain them over a long term, suggesting that extravasated plasma proteins may serve physiological functions in wound healing [109].

In the eventuality that IGF binding proteins are involved in the pathogenesis of oedema formation, modulation of the molecular components in this response may be an accessible route towards the development of novel therapeutic agents aimed at minimizing brain damage [31]. Although it is not

well ascertained if these proteins belong to the proinflammatory pathway of oedema or rather if they play a protective anti-inflammatory role, certainly this is a root to figure out if by rating the expression of IGF and its binding proteins the time of posttraumatic oedema formation and all its sequelae could be monitored. Since central administration of IGF-1 can rescue neurons in the cortex, striatum, hippocampus, dentate gyrus, and thalamus following hypoxic injury, local production following injury is believed to be meaningful in the wound healing process [109]. Knowledge of the stepwise events controlling wound healing following brain injury should contribute to the tailored treatment of affected patients.

Administration of peptides or drugs which induce or repress peptide expression may optimize healing and minimize excessive scar tissue formation. As gene therapy techniques become increasingly sophisticated and efficient, expression plasmid, viral vector, or oligonucleotide administration may become commonplace strategies. Treatments may be most effective if tailored to specific forms of injury or to specific regions of the brain. Nevertheless, effective treatment of brain injuries with drugs, peptides, or genes will require a thorough understanding of the complex cellular changes and intercellular interactions which occur following the insult [108].

8. Conclusions

Strategies to either increase the endogenous upregulation of IGF-1 after TBI or supplement it with exogenous IGF-1 may improve neuronal survival after TBI [23]. In this context, the use of antidiabetic agents (e.g., metformin) and GLP-1 mimetic agents (e.g., liraglutide) has been suggested. These drugs cross the BBB, elicit neuroprotective activities, and, importantly, are safe and well-tolerated medicines. Along with more recent data linking brain insulin/IGF-1 function to the etiology of a number of neurodegenerative diseases will, undoubtedly, translate into more clinically oriented avenues of research in the near future. Depending on each personal genetic background, antidiabetic drugs and other molecules potentially interacting with the IGF-1 system may probably play a role in the next future when facing TBI and other nervous system pathologies. It is expected that future studies will take advantage of postgenomic technologies in order to generate molecular and/or biochemical signatures aimed at identifying patients who may benefit from these therapies [12].

We believe that new prospective studies should investigate the changes of IGF-1 in blood and assess their possible correlation with the cascade of events secondary to trauma.

The identification of IGF-1 as a biomarker of posttraumatic injury could help in the future to understand whether and how to plan the hormone replacement therapy to prevent secondary damage of trauma and to improve the patients outcome.

It is too early to figure out IGF-1 as a strategic agent in a therapeutic context. Moreover in terms of drugs and other therapies, research suggests that a single highly effective pharmacological agent for TBI is still unlikely to be discovered but that improved knowledge of the pathophysiology, together with the continuing advances in the field of gene therapy, will provide the mechanistic clues to direct a mosaic of therapeutic interventions.

Abbreviations

CNS: Central nervous system
TBI: Traumatic brain injury
CT: Computed tomography
MRI: Magnetic resonance imaging
CSF: Cerebrospinal fluid
GH: Growth hormone
IGF: Insulin-like growth factor
IGFBP: Insulin-like growth factor binding protein
BBB: Blood-brain barrier
AD: Alzheimer's disease
NED: Neuroendocrine dysfunction
GHD: GH deficiency
BDNF: Brain-derived neurotrophic factor.

Conflict of Interests

The authors declare that there is no conflict of interests regarding the publication of this paper.

References

[1] P. K. Dash, J. Zhao, G. Hergenroeder, and A. N. Moore, "Biomarkers for the diagnosis, prognosis, and evaluation of treatment efficacy for traumatic brain injury," *Neurotherapeutics*, vol. 7, no. 1, pp. 100–114, 2010.

[2] M. V. DeFazio, R. A. Rammo, J. R. Robles, H. M. Bramlett, W. D. Dietrich, and M. R. Bullock, "The potential utility of blood-derived biochemical markers as indicators of early clinical trends following severe traumatic brain injury," *World Neurosurgery*, vol. 81, no. 1, pp. 151–158, 2014.

[3] S. Giacoppo, P. Bramanti, M. Barresi et al., "Predictive biomarkers of recovery in traumatic brain injury," *Neurocritical Care*, vol. 16, no. 3, pp. 470–477, 2012.

[4] E. Richmond and A. D. Rogol, "Traumatic brain injury: endocrine consequences in children and adults," *Endocrine*, vol. 45, no. 1, pp. 3–8, 2014.

[5] P. M. Kochanek, R. S. B. Clark, R. A. Ruppel et al., "Biochemical, cellular, and molecular mechanisms in the evolution of secondary damage after severe traumatic brain injury in infants and children: lessons learned from the bedside," *Pediatric Critical Care Medicine*, vol. 1, no. 1, pp. 4–19, 2000.

[6] B. J. Zink, J. Szmydynger-Chodobska, and A. Chodobski, "Emerging concepts in the pathophysiology of traumatic brain injury," *Psychiatric Clinics of North America*, vol. 33, no. 4, pp. 741–756, 2010.

[7] H. M. Bramlett, W. Dalton Dietrich, E. J. Green, and R. Busto, "Chronic histopathological consequences of fluid-percussion brain injury in rats: effects of post-traumatic hypothermia," *Acta Neuropathologica*, vol. 93, no. 2, pp. 190–199, 1997.

[8] C. E. Dixon, P. M. Kochanek, H. Q. Yan et al., "One-year study of spatial memory performance, brain morphology, and cholinergic markers after moderate controlled cortical impact in rats," *Journal of Neurotrauma*, vol. 16, no. 2, pp. 109–122, 1999.

[9] C. T. Forde, S. K. Karri, A. M. H. Young, and C. S. Ogilvy, "Predictive markers in traumatic brain injury: opportunities for a serum biosignature," *British Journal of Neurosurgery*, vol. 28, no. 1, pp. 8–15, 2014.

[10] F. G. Strathmann, S. Schulte, K. Goerl, and D. J. Petron, "Blood-based biomarkers for traumatic brain injury: evaluation of research approaches, available methods and potential utility from the clinician and clinical laboratory perspectives," *Clinical Biochemistry*, vol. 47, no. 10-11, pp. 876–888, 2014.

[11] A. K. Wagner, E. H. McCullough, C. Niyonkuru et al., "Acute serum hormone levels: characterization and prognosis after severe traumatic brain injury," *Journal of Neurotrauma*, vol. 28, no. 6, pp. 871–888, 2011.

[12] H. Werner and D. LeRoith, "Insulin and insulin-like growth factor receptors in the brain: physiological and pathological aspects," *European Neuropsychopharmacology*, vol. 24, no. 12, pp. 1947–1953, 2014.

[13] S. Favelyukis, J. H. Till, S. R. Hubbard, and W. T. Miller, "Structure and autoregulation of the insulin-like growth factor 1 receptor kinase," *Nature Structural Biology*, vol. 8, no. 12, pp. 1058–1063, 2001.

[14] F. I. Arnaldez and L. J. Helman, "Targeting the insulin growth factor receptor 1," *Hematology/Oncology Clinics of North America*, vol. 26, no. 3, pp. 527–542, 2012.

[15] C. Bondy, H. Werner, C. T. Roberts Jr., and D. LeRoith, "Cellular pattern of type-I insulin-like growth factor receptor gene expression during maturation of the rat brain: comparison with insulin-like growth factors I and II," *Neuroscience*, vol. 46, no. 4, pp. 909–923, 1992.

[16] P. E. Vos, H. P. F. Koppeschaar, W. R. de Vries, and J. H. J. Wokke, "Insulin-like growth factor-I: clinical studies," *Drugs of Today*, vol. 34, no. 1, pp. 79–90, 1998.

[17] A. Adem, S. S. Jossan, R. d'Argy et al., "Insulin-like growth factor 1 (IGF-1) receptors in the human brain: quantitative autoradiographic localization," *Brain Research*, vol. 503, no. 2, pp. 299–303, 1989.

[18] M. Coculescu, "Blood-brain barrier for human growth hormone and insulin-like growth factor-I," *Journal of Pediatric Endocrinology and Metabolism*, vol. 12, no. 2, pp. 113–124, 1999.

[19] B. Anlar, K. A. Sullivan, and E. L. Feldman, "Insulin-like growth factor-I and central nervous system development," *Hormone and Metabolic Research*, vol. 31, no. 2-3, pp. 120–125, 1999.

[20] M. M. Niblock, J. K. Brunso-Bechtold, and D. R. Riddle, "Insulin-like growth factor I stimulates dendritic growth in primary somatosensory cortex," *The Journal of Neuroscience*, vol. 20, no. 11, pp. 4165–4176, 2000.

[21] K. D. Beck, L. Powell-Braxton, H.-R. Widmer, J. Valverde, and F. Hefti, "Igf1 gene disruption results in reduced brain size, CNS hypomyelination, and loss of hippocampal granule and striatal parvalbumin-containing neurons," *Neuron*, vol. 14, no. 4, pp. 717–730, 1995.

[22] R. J. Lichtenwalner, M. E. Forbes, S. A. Bennett, C. D. Lynch, W. E. Sonntag, and D. R. Riddle, "Intracerebroventricular infusion of insulin-like growth factor-I ameliorates the age-related decline in hippocampal neurogenesis," *Neuroscience*, vol. 107, no. 4, pp. 603–613, 2001.

[23] S. K. Madathil, H. N. Evans, and K. E. Saatman, "Temporal and regional changes in IGF-1/IGF-1R signaling in the mouse brain after traumatic brain injury," *Journal of Neurotrauma*, vol. 27, no. 1, pp. 95–107, 2010.

[24] D. Edwall, M. Schalling, E. Jennische, and G. Norstedt, "Induction of insulin-like growth factor I messenger ribonucleic acid during regeneration of rat skeletal muscle," *Endocrinology*, vol. 124, no. 2, pp. 820–825, 1989.

[25] H.-A. Hansson, E. Jennische, and A. Skottner, "Regenerating endothelial cells express insulin-like growth factor-I immunoreactivity after arterial injury," *Cell and Tissue Research*, vol. 250, no. 3, pp. 499–505, 1987.

[26] A. D. Stiles, I. R. S. Sosenko, A. J. D'Ercole, and B. T. Smith, "Relation of kidney tissue somatomedin-C/insulin-like growth factor I to postnephrectomy renal growth in the rat," *Endocrinology*, vol. 117, no. 6, pp. 2397–2401, 1985.

[27] A. Logan, J. J. Oliver, and M. Berry, "Growth factors in CNS repair and regeneration," *Progress in Growth Factor Research*, vol. 5, no. 4, pp. 379–405, 1994.

[28] E. J. Beilharz, V. C. Russo, G. Butler et al., "Co-ordinated and cellular specific induction of the components of the IGF/IGFBP axis in the rat brain following hypoxic-ischemic injury," *Molecular Brain Research*, vol. 59, no. 2, pp. 119–134, 1998.

[29] S. Schwab, M. Spranger, S. Krempien, W. Hacke, and M. Bettendorf, "Plasma insulin-like growth factor I and IGF binding protein 3 levels in patients with acute cerebral ischemic injury," *Stroke*, vol. 28, no. 9, pp. 1744–1748, 1997.

[30] X. S. Li, M. Williams, and W. P. Bartlett, "Induction of IGF-1 mRNA expression following traumatic injury to the postnatal brain," *Molecular Brain Research*, vol. 57, no. 1, pp. 92–96, 1998.

[31] A. C. Sandberg Nordqvista, H. von Holst, S. Holmin, V. R. Sara, B.-M. Bellander, and M. Schalling, "Increase of insulin-like growth factor (IGF)-1, IGF binding protein-2 and -4 mRNAs following cerebral contusion," *Molecular Brain Research*, vol. 38, no. 2, pp. 285–293, 1996.

[32] H. J. Walter, M. Berry, D. J. Hill, and A. Logan, "Spatial and temporal changes in the insulin-like growth factor (IGF) axis indicate autocrine/paracrine actions of IGF-I within wounds of the rat brain," *Endocrinology*, vol. 138, no. 7, pp. 3024–3034, 1997.

[33] D. L. Yao, N. R. West, C. A. Bondy et al., "Cryogenic spinal cord injury induces astrocytic gene expression of insulin-like growth factor I and insulin-like growth factor binding protein 2 during myelin regeneration," *Journal of Neuroscience Research*, vol. 40, no. 5, pp. 647–659, 1995.

[34] L. Denti, V. Annoni, E. Cattadori et al., "Insulin-like growth factor 1 as a predictor of ischemic stroke outcome in the elderly," *American Journal of Medicine*, vol. 117, no. 5, pp. 312–317, 2004.

[35] J. Guan, L. Bennet, P. D. Gluckman, and A. J. Gunn, "Insulin-like growth factor-1 and post-ischemic brain injury," *Progress in Neurobiology*, vol. 70, no. 6, pp. 443–462, 2003.

[36] W. R. Schäbitz, T. T. Hoffmann, S. Heiland et al., "Delayed neuroprotective effect of insulin-like growth factor-I after experimental transient focal cerebral ischemia monitored with MRI," *Stroke*, vol. 32, no. 5, pp. 1226–1233, 2001.

[37] A. J. Westwood, A. Beiser, C. DeCarli et al., "Insulin-like growth factor-1 and risk of Alzheimer dementia and brain atrophy," *Neurology*, vol. 82, no. 18, pp. 1613–1619, 2014.

[38] S. Doré, K. Satyabrata, and R. Quirion, "Rediscovering an old friend, IFG-I: potential use in the treatment of neurodegenerative diseases," *Trends in Neurosciences*, vol. 20, no. 8, pp. 326–331, 1997.

[39] A. J. D'Ercole, P. Ye, A. S. Calikoglu, and G. Gutierrez-Ospina, "The role of the insulin-like growth factors in the central nervous system," *Molecular Neurobiology*, vol. 13, no. 3, pp. 227–255, 1996.

[40] I. Kazanis, M. Giannakopoulou, H. Philippidis, and F. Stylianopoulou, "Alterations in IGF-I, BDNF and NT-3 levels

following experimental brain trauma and the effect of IGF-I administration," *Experimental Neurology*, vol. 186, no. 2, pp. 221–234, 2004.

[41] I. Dusart and M. E. Schwab, "Secondary cell death and the inflammatory reaction after dorsal hemisection of the rat spinal cord," *European Journal of Neuroscience*, vol. 6, no. 5, pp. 712–724, 1994.

[42] N. Latov, G. Nilaver, E. A. Zimmerman et al., "Fibrillary astrocytes proliferate in response to brain injury: a study combining immunoperoxidase technique for glial fibrillary acidic protein and radioautography of tritiated thymidine," *Developmental Biology*, vol. 72, no. 2, pp. 381–384, 1979.

[43] S. K. Madathil, S. W. Carlson, J. M. Brelsfoard, P. Ye, A. J. D'Ercole, and K. E. Saatman, "Astrocyte-specific overexpression of insulin-like growth factor-1 protects hippocampal neurons and reduces behavioral deficits following traumatic brain injury in mice," *PLoS ONE*, vol. 8, no. 6, Article ID e67204, 2013.

[44] A. Faber-Elman, A. Solomon, J. A. Abraham, M. Marikovsky, and M. Schwartz, "Involvement of wound-associated factors in rat brain astrocyte migratory response to axonal injury: in vitro simulation," *The Journal of Clinical Investigation*, vol. 97, no. 1, pp. 162–171, 1996.

[45] G. A. Werther, M. Abate, A. Hogg et al., "Localization of insulin-like growth factor-I mRNA in rat brain by in situ hybridization—relationship to IGF-I receptors," *Molecular Endocrinology*, vol. 4, no. 5, pp. 773–778, 1990.

[46] V. Rubovitch, S. Edut, R. Sarfstein, H. Werner, and C. G. Pick, "The intricate involvement of the Insulin-like growth factor receptor signaling in mild traumatic brain injury in mice," *Neurobiology of Disease*, vol. 38, no. 2, pp. 299–303, 2010.

[47] W.-H. Zheng, S. Kar, S. Doré, and R. Quirion, "Insulin-like growth factor-1 (IGF-1): a neuroprotective trophic factor acting via the Akt kinase pathway," *Journal of Neural Transmission. Supplementum*, no. 60, pp. 261–272, 2000.

[48] V. Rubovitch, A. Shachar, H. Werner, and C. G. Pick, "Does IGF-1 administration after a mild traumatic brain injury in mice activate the adaptive arm of ER stress?" *Neurochemistry International*, vol. 58, no. 4, pp. 443–446, 2011.

[49] S. Shimasaki and N. Ling, "Identification and molecular characterization of insulin-like growth factor binding proteins (IGFBP-1, -2, -3, -4, -5 and -6)," *Progress in Growth Factor Research*, vol. 3, no. 4, pp. 243–266, 1991.

[50] W. Ni, K. Rajkumar, J. I. Nagy, and L. J. Murphy, "Impaired brain development and reduced astrocyte response to injury in transgenic mice expressing IGF binding protein-1," *Brain Research*, vol. 769, no. 1, pp. 97–107, 1997.

[51] A.-C. Sandberg Nordqvist, S. Holmin, M. Nilsson, T. Mathiesen, and M. Schalling, "MK-801 inhibits the cortical increase in IGF-1, IGFBP-2 and IGFBP-4 expression following trauma," *NeuroReport*, vol. 8, no. 2, pp. 455–460, 1997.

[52] A. Finset, A. W. Anke, E. Hofft, K. S. Roaldsen, J. Pillgram-Larsen, and J. K. Stanghelle, "Cognitive performance in multiple trauma patients 3 years after injury," *Psychosomatic Medicine*, vol. 61, no. 4, pp. 576–583, 1999.

[53] R. J. Hamm, B. G. Lyeth, L. W. Jenkins, D. M. O'Dell, and B. R. Pike, "Selective cognitive impairment following traumatic brain injury in rats," *Behavioural Brain Research*, vol. 59, no. 1-2, pp. 169–173, 1993.

[54] S. Margulies, "The postconcussion syndrome after mild head trauma Part II: is migraine underdiagnosed?" *Journal of Clinical Neuroscience*, vol. 7, no. 6, pp. 495–499, 2000.

[55] D. Ozdemir, B. Baykara, I. Aksu et al., "Relationship between circulating IGF-1 levels and traumatic brain injury-induced hippocampal damage and cognitive dysfunction in immature rats," *Neuroscience Letters*, vol. 507, no. 1, pp. 84–89, 2012.

[56] M. A. I. Åberg, N. D. Åberg, H. Hedbäcker, J. Oscarsson, and P. S. Eriksson, "Peripheral infusion of IGF-I selectively induces neurogenesis in the adult rat hippocampus," *Journal of Neuroscience*, vol. 20, no. 8, pp. 2896–2903, 2000.

[57] M. E. Schober, B. Block, J. C. Beachy, K. D. Statler, C. C. Giza, and R. H. Lane, "Early and sustained increase in the expression of hippocampal IGF-1, but Not EPO, in a developmental rodent model of traumatic brain injury," *Journal of Neurotrauma*, vol. 27, no. 11, pp. 2011–2020, 2010.

[58] B. Baykara, I. Aksu, E. Buyuk et al., "Progesterone treatment decreases traumatic brain injury induced anxiety and is correlated with increased serum IGF-1 levels; Prefrontal cortex, amygdala, hippocampus neuron density; And reduced serum corticosterone levels in immature rats," *Biotechnic and Histochemistry*, vol. 88, no. 5, pp. 250–257, 2013.

[59] N. D. Aberg, K. G. Brywe, and J. Isgaard, "Aspects of growth hormone and insulin-like growth factor-I related to neuroprotection, regeneration, and functional plasticity in the adult brain," *TheScientificWorldJournal*, vol. 6, pp. 53–80, 2006.

[60] S. L. Smith, P. K. Andrus, J.-R. Zhang, and E. D. Hall, "Direct measurement of hydroxyl radicals, lipid peroxidation, and blood- brain barrier disruption following unilateral cortical impact head injury in the rat," *Journal of Neurotrauma*, vol. 11, no. 4, pp. 393–404, 1994.

[61] K. E. Saatman, K. J. Feeko, R. L. Pape, and R. Raghupathi, "Differential behavioral and histopathological responses to graded cortical impact injury in mice," *Journal of Neurotrauma*, vol. 23, no. 8, pp. 1241–1253, 2006.

[62] K. E. Saatman, P. C. Contreras, D. H. Smith et al., "Insulin-like growth factor-1 (IGF-1) improves both neurological motor and cognitive outcome following experimental brain injury," *Experimental Neurology*, vol. 147, no. 2, pp. 418–427, 1997.

[63] I. Kazanis, E. Bozas, H. Philippidis, and F. Stylianopoulou, "Neuroprotective effects of insulin-like growth factor-I (IGF-I) following a penetrating brain injury in rats," *Brain Research*, vol. 991, no. 1-2, pp. 34–45, 2003.

[64] T. A. West and S. Sharp, "Neuroendocrine dysfunction following mild TBI: when to screen for it," *Journal of Family Practice*, vol. 63, no. 1, pp. 11–16, 2014.

[65] F. Tanriverdi, K. Unluhizarci, and F. Kelestimur, "Pituitary function in subjects with mild traumatic brain injury: a review of literature and proposal of a screening strategy," *Pituitary*, vol. 13, no. 2, pp. 146–153, 2010.

[66] F. Tanriverdi, K. Unluhizarci, I. Kocyigit et al., "Brief communication: pituitary volume and function in competing and retired male boxers," *Annals of Internal Medicine*, vol. 148, no. 11, pp. 827–831, 2008.

[67] G. Aimaretti, M. R. Ambrosio, C. Di Somma et al., "Residual pituitary function after brain injury-induced hypopituitarism: a prospective 12-month study," *Journal of Clinical Endocrinology and Metabolism*, vol. 90, no. 11, pp. 6085–6092, 2005.

[68] J. R. Dusick, C. Wang, P. Cohan, R. Swerdloff, and D. F. Kelly, "Pathophysiology of hypopituitarism in the setting of brain injury," *Pituitary*, vol. 15, no. 1, pp. 2–9, 2012.

[69] S. Benvenga, A. Campennì, R. M. Ruggeri, and F. Trimarchi, "Hypopituitarism secondary to head trauma," *The Journal of Clinical Endocrinology and Metabolism*, vol. 85, no. 4, pp. 1353–1361, 2000.

[70] D. F. Kelly, I. T. Gaw Gonzalo, P. Cohan, N. Berman, R. Swerdloff, and C. Wang, "Hypopituitarism following traumatic brain injury and aneurysmal subarachnoid hemorrhage: a preliminary report," *Journal of Neurosurgery*, vol. 93, no. 5, pp. 743–752, 2000.

[71] X.-Q. Yuan and C. E. Wade, "Neuroendocrine abnormalities in patients with traumatic brain injury," *Frontiers in Neuroendocrinology*, vol. 12, no. 3, pp. 209–230, 1991.

[72] R. Chiolero, Y. Schutz, N. de Tribolet, J.-P. Felber, J. Freeman, and E. Jequier, "Plasma pituitary hormone levels in severe trauma with or without head injury," *Journal of Trauma*, vol. 28, no. 9, pp. 1368–1374, 1988.

[73] H. Matsuura, S. Nakazawa, and I. Wakabayashi, "Thyrotropin-releasing hormone provocative release of prolactin and thyrotropin in acute head injury," *Neurosurgery*, vol. 16, no. 6, pp. 791–795, 1985.

[74] P. D. Woolf, L. A. Lee, R. W. Hamill, and J. V. McDonald, "Thyroid test abnormalities in traumatic brain injury: correlation with neurologic impairment and sympathetic nervous system activation," *American Journal of Medicine*, vol. 84, no. 2, pp. 201–208, 1988.

[75] I. Dimopoulou, S. Tsagarakis, M. Theodorakopoulou et al., "Endocrine abnormalities in critical care patients with moderate-to-severe head trauma: incidence, pattern and predisposing factors," *Intensive Care Medicine*, vol. 30, no. 6, pp. 1051–1057, 2004.

[76] S. A. Lieberman, A. L. Oberoi, C. R. Gilkison, B. E. Masel, and R. J. Urban, "Prevalence of neuroendocrine dysfunction in patients recovering from traumatic brain injury," *Journal of Clinical Endocrinology and Metabolism*, vol. 86, no. 6, pp. 2752–2756, 2001.

[77] M. Bondanelli, M. R. Ambrosio, A. Margutti et al., "Evidence for integrity of the growth hormone/insulin-like growth factor-1 axis in patients with severe head trauma during rehabilitation," *Metabolism*, vol. 51, no. 10, pp. 1363–1369, 2002.

[78] H. J. Schneider, M. Schneider, B. Saller et al., "Prevalence of anterior pituitary insufficiency 3 and 12 months after traumatic brain injury," *European Journal of Endocrinology*, vol. 154, no. 2, pp. 259–265, 2006.

[79] A. W. van der Eerden, M. T. B. Twickler, F. C. G. J. Sweep et al., "Should anterior pituitary function be tested during follow-up of all patients presenting at the emergency department because of traumatic brain injury?" *European Journal of Endocrinology*, vol. 162, no. 1, pp. 19–28, 2010.

[80] K. T. Rockich, J. C. Hatton, R. J. Kryscio, B. A. Young, and R. A. Blouin, "Effect of recombinant human growth hormone and insulin-like growth factor-1 administration on IGF-1 and IGF-binding protein-3 levels in brain injury," *Pharmacotherapy*, vol. 19, no. 12, pp. 1432–1436, 1999.

[81] E. Fernandez-Rodriguez, I. Bernabeu, A. I. Castro, F. Kelestimur, and F. F. Casanueva, "Hypopituitarism following traumatic brain injury: determining factors for diagnosis," *Frontiers in Endocrinology*, vol. 2, article 25, 2011.

[82] V. Gasco, F. Prodam, L. Pagano et al., "Hypopituitarism following brain injury: when does it occur and how best to test?" *Pituitary*, vol. 15, no. 1, pp. 20–24, 2012.

[83] N. E. Kokshoorn, M. J. E. Wassenaar, N. R. Biermasz et al., "Hypopituitarism following traumatic brain injury: prevalence is affected by the use of different dynamic tests and different normal values," *European Journal of Endocrinology*, vol. 162, no. 1, pp. 11–18, 2010.

[84] A. Munoz and R. Urban, "Neuroendocrine consequences of traumatic brain injury," *Current Opinion in Endocrinology, Diabetes and Obesity*, vol. 20, no. 4, pp. 354–358, 2013.

[85] Z. Olivecrona, P. Dahlqvist, and L.-O. D. Koskinen, "Acute neuro-endocrine profile and prediction of outcome after severe brain injury," *Scandinavian Journal of Trauma, Resuscitation and Emergency Medicine*, vol. 21, article 33, 2013.

[86] A. Agha, B. Rogers, M. Sherlock et al., "Anterior pituitary dysfunction in survivors of traumatic brain injury," *The Journal of Clinical Endocrinology & Metabolism*, vol. 89, no. 10, pp. 4929–4936, 2004.

[87] T. Bushnik, J. Englander, and L. Katznelson, "Fatigue after TBI: association with neuroendocrine abnormalities," *Brain Injury*, vol. 21, no. 6, pp. 559–566, 2007.

[88] A. Agha, B. Rogers, D. Mylotte et al., "Neuroendocrine dysfunction in the acute phase of traumatic brain injury," *Clinical Endocrinology*, vol. 60, no. 5, pp. 584–591, 2004.

[89] G. Aimaretti, M. R. Ambrosio, C. Di Somma et al., "Traumatic brain injury and subarachnoid haemorrhage are conditions at high risk for hypopituitarism: screening study at 3 months after the brain injury," *Clinical Endocrinology*, vol. 61, no. 3, pp. 320–326, 2004.

[90] M. R. H. Abadi, M. Ghodsi, M. Merazin, and H. Roozbeh, "Pituitary function impairment after moderate traumatic brain injury," *Acta Medica Iranica*, vol. 49, no. 7, pp. 438–441, 2011.

[91] J. M. Hackl, M. Gottardis, C. Wieser et al., "Endocrine abnormalities in severe traumatic brain injury—a cue to prognosis in severe craniocerebral trauma?" *Intensive Care Medicine*, vol. 17, no. 1, pp. 25–29, 1991.

[92] J. Wagner, J. R. Dusick, D. L. McArthur et al., "Acute gonadotroph and somatotroph hormonal suppression after traumatic brain injury," *Journal of Neurotrauma*, vol. 27, no. 6, pp. 1007–1019, 2010.

[93] F. Della Corte, A. Mancini, D. Valle et al., "Provocative hypothalamopituitary axis tests in severe head injury: correlations with severity and prognosis," *Critical Care Medicine*, vol. 26, no. 8, pp. 1419–1426, 1998.

[94] M. Jeevanandam, N. J. Holaday, and S. R. Petersen, "Plasma levels of insulin-like growth factor binding protein-3 in acute trauma patients," *Metabolism: Clinical and Experimental*, vol. 44, no. 9, pp. 1205–1208, 1995.

[95] R. Wildburger, N. Zarkovic, G. Leb, S. Borovic, K. Zarkovic, and F. Tatzber, "Post-traumatic changes in insulin-like growth factor type 1 and growth hormone in patients with bone fractures and traumatic brain injury," *Wiener Klinische Wochenschrift*, vol. 113, no. 3-4, pp. 119–126, 2001.

[96] G. L. Smith, "Somatomedin carrier proteins," *Molecular and Cellular Endocrinology*, vol. 34, no. 2, pp. 83–89, 1984.

[97] D. R. Clemmons and L. E. Underwood, "Nutritional regulation of IGF-I and IGF binding proteins," *Annual Review of Nutrition*, vol. 11, pp. 393–412, 1991.

[98] M. A. Hynes, J. J. van Wijk, P. J. Brooks, A. J. D'Ercole, M. Jansen, and P. K. Lund, "Growth hormone dependence of somatomedin-C/insulin-like growth factor-I and insulin-like growth factor-II messenger ribonucleic acids," *Molecular Endocrinology*, vol. 1, no. 3, pp. 233–242, 1987.

[99] W. L. Lowe Jr., M. Adamo, H. Werner, C. T. Roberts Jr., and D. LeRoith, "Regulation by fasting of rat insulin-like growth factor I and its receptor. Effects on gene expression and binding," *The Journal of Clinical Investigation*, vol. 84, no. 2, pp. 619–626, 1989.

[100] F. Tanriverdi, H. Ulutabanca, K. Unluhizarci, A. Selcuklu, F. F. Casanueva, and F. Kelestimur, "Three years prospective investigation of anterior pituitary function after traumatic brain injury: a pilot study," *Clinical Endocrinology*, vol. 68, no. 4, pp. 573–579, 2008.

[101] H. J. Schneider, U. Pagotto, and G. K. Stalla, "Central effects of the somatotropic system," *European Journal of Endocrinology*, vol. 149, no. 5, pp. 377–392, 2003.

[102] M. E. Molitch, D. R. Clemmons, S. Malozowski, G. R. Merriam, and M. L. Vance, "Evaluation and treatment of adult growth hormone deficiency: An endocrine society clinical practice guideline," *Journal of Clinical Endocrinology and Metabolism*, vol. 96, no. 6, pp. 1587–1609, 2011.

[103] B. M. Biller, M. H. Samuels, A. Zagar et al., "Sensitivity and specificity of six tests for the diagnosis of adult GH deficiency," *The Journal of Clinical Endocrinology and Metabolism*, vol. 87, no. 5, pp. 2067–2079, 2002.

[104] F. Prodam, M. Caputo, S. Belcastro et al., "Quality of life, mood disturbances and psychological parameters in adult patients with GH deficiency," *Panminerva Medica*, vol. 54, no. 4, pp. 323–331, 2012.

[105] D. F. Kelly, D. L. McArthur, H. Levin et al., "Neurobehavioral and quality of life changes associated with growth hormone insufficiency after complicated mild, moderate, or severe traumatic brain injury," *Journal of Neurotrauma*, vol. 23, no. 6, pp. 928–942, 2006.

[106] P. Reimunde, A. Quintana, B. Castañón et al., "Effects of growth hormone (GH) replacement and cognitive rehabilitation in patients with cognitive disorders after traumatic brain injury," *Brain Injury*, vol. 25, no. 1, pp. 65–73, 2010.

[107] J. Hatton, R. P. Rapp, K. A. Kudsk et al., "Intravenous insulin-like growth factor-I (IGF-I) in moderate-to-severe head injury: a phase II safety and efficacy trial," *Journal of Neurosurgery*, vol. 86, no. 5, pp. 779–786, 1997.

[108] J. Hatton, R. Kryscio, M. Ryan, O. Linda, and B. Young, "Systemic metabolic effects of combined insulin-like growth factor-I and growth hormone therapy in patients who have sustained acute traumatic brain injury," *Journal of Neurosurgery*, vol. 105, no. 6, pp. 843–852, 2006.

[109] J. L. Cook, V. Marcheselli, J. Alam, P. L. Deininger, and N. G. Bazan, "Temporal changes in gene expression following cryogenic rat brain injury," *Molecular Brain Research*, vol. 55, no. 1, pp. 9–19, 1998.

Hindawi Publishing Corporation
BioMed Research International
Volume 2015, Article ID 276029, 8 pages
http://dx.doi.org/10.1155/2015/276029

Research Article

Intra-Amniotic LPS Induced Region-Specific Changes in Presynaptic Bouton Densities in the Ovine Fetal Brain

Eveline Strackx,[1,2] Reint K. Jellema,[1,2] Rebecca Rieke,[1,2] Ruth Gussenhoven,[1,2] Johan S. H. Vles,[1] Boris W. Kramer,[1,2] and Antonio W. D. Gavilanes[1,2,3]

[1] *School for Mental Health and Neuroscience, Faculty of Health, Medicine and Life Sciences, Maastricht University and European Graduate, School of Neuroscience (EURON), Universiteitssingel 50, Room 1.152, 6229 MD Maastricht, Netherlands*
[2] *Department of Pediatrics-Neonatology, Maastricht University Medical Center (MUMC), Postbus 5800, 6202 AZ Maastricht, Netherlands*
[3] *Institute of Biomedicine, Faculty of Medicine, Catholic University of Guayaquil, Avenue Carlos Julio Arosemena, Km. 1 1/2 Via Daule, Guayaquil, Ecuador*

Correspondence should be addressed to Antonio W. D. Gavilanes; danilo.gavilanes@mumc.nl

Received 30 June 2014; Accepted 14 December 2014

Academic Editor: Diego Gazzolo

Rationale. Chorioamnionitis has been associated with increased risk for fetal brain damage. Although, it is now accepted that synaptic dysfunction might be responsible for functional deficits, synaptic densities/numbers after a fetal inflammatory challenge have not been studied in different regions yet. Therefore, we tested in this study the hypothesis that LPS-induced chorioamnionitis caused profound changes in synaptic densities in different regions of the fetal sheep brain. *Material and Methods*. Chorioamnionitis was induced by a 10 mg intra-amniotic LPS injection at two different exposure intervals. The fetal brain was studied at 125 days of gestation (term = 150 days) either 2 (LPS2D group) or 14 days (LPS14D group) after LPS or saline injection (control group). Synaptophysin immunohistochemistry was used to quantify the presynaptic density in layers 2-3 and 5-6 of the motor cortex, somatosensory cortex, entorhinal cortex, and piriforme cortex, in the nucleus caudatus and putamen and in CA1/2, CA3, and dentate gyrus of the hippocampus. *Results*. There was a significant reduction in presynaptic bouton densities in layers 2-3 and 5-6 of the motor cortex and in layers 2-3 of the entorhinal and the somatosensory cortex, in the nucleus caudate and putamen and the CA1/2 and CA3 of the hippocampus in the LPS2D compared to control animals. Only in the motor cortex and putamen, the presynaptic density was significantly decreased in the LPS14 D compared to the control group. No changes were found in the dentate gyrus of the hippocampus and the piriforme cortex. *Conclusion*. We demonstrated that LPS-induced chorioamnionitis caused a decreased density in presynaptic boutons in different areas in the fetal brain. These synaptic changes seemed to be region-specific, with some regions being more affected than others, and seemed to be transient in some regions.

1. Introduction

Chorioamnionitis or inflammation/infection of the fetal membranes has been associated with numerous adverse outcomes, like preterm labor and delivery, premature rupture of the membranes, perinatal mortality, and permanent neurological morbidity [1–4]. Several clinical and experimental studies have demonstrated that an intrauterine infection is most closely related to an increased risk for white matter disease and subsequent cerebral palsy [5–7]. Therefore, cerebral palsy has long been the principal neurological outcome of clinical interest.

However, it is increasingly recognized now that neonates exposed to chorioamnionitis are at risk for a whole spectrum of neurobehavioral and cognitive defects [8, 9]. They do not always develop white matter disease but might suffer from grey matter injury, like neuronal programmed cell death, axonal, or dendritic abnormalities, neuronal disorganization, and so forth. [10–13]. In addition, synaptic ultrastructure and density have been shown to be affected after different adverse

developmental conditions, like intrauterine growth retardation, malnutrition, and hypoxia [14–22]. Although, it is now accepted that synaptic dysfunction might be responsible for functional deficits, synaptic densities/numbers after a clinical representative fetal inflammatory challenge have not been studied so far.

We therefore aimed to investigate the effect of intra-amniotic inflammation on synaptic density in different brain structures. To study this, pregnant sheep were injected intra-amniotically with lipopolysaccharide (LPS) [11, 23, 24]. In this model, we previously demonstrated that intra-amniotic LPS resulted in an interval-dependent activation of microglia, active astrogliosis, and apoptotic cell death in the brain [11]. In addition, we showed a decrease in synapses expression in the hippocampus [25]. For the current study, we used again synaptophysin immunohistochemistry as an established marker for the quantification of the synaptic density in different regions of the cerebral cortex, the striatum, and the hippocampus. [26–29]. We hypothesized that intra-amniotic inflammation causes a profound loss in synaptic density in different regions of the brain. Synaptic density was assessed after 2 and 14 days of intra-amniotic LPS exposure to test synaptic plasticity following intra-amniotic inflammation.

2. Materials and Methods

2.1. Animals and Surgical Procedures. All experimental procedures were approved by the Animal Ethics Board of the University of Maastricht on animal welfare according to Dutch governmental regulations. All efforts were taken to minimize the pain and stress levels experienced by the animals and to minimize the number of animals necessary to produce reliable scientific data. Time-mated pregnant Texel ewes bearing both singletons and twins were housed outdoors. Food and water were provided ad libitum. They were randomly assigned to one of the three experimental groups, receiving either LPS or saline. The first group received LPS at day 123 of gestation ($n = 5$), the second group received LPS at day 111 of gestation ($n = 6$), and the third group received a control saline injection at either day 111 or 123 of gestation ($n = 7$) (Figure 1). LPS (10 mg solved in 2 mL sterile and filtered saline) purchased from Sigma (Escherichia coli 055:B5; Sigma Chemical, St. Louis, MO) or saline was injected intra-amniotically under ultrasound guidance [30]. At day 125 of gestation (full-term = 150 days) pregnant ewes were anesthetized and all fetuses were delivered by Caesarean section. Fetuses were killed by a lethal injection of pentobarbital and decapitated. The brain was removed and halved along the midline with one halve being immersion fixed for immunohistochemical analysis. The presence of histological chorioamnionitis was demonstrated by the influx of inflammatory cells into the fetal membranes [31].

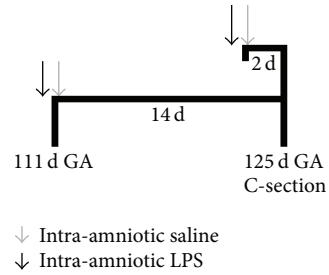

Figure 1: Overview of the experimental setup. Chorioamnionitis was induced by intra-amniotic injections of LPS 2 days (GA = 123 d, $n = 5$) and 14 days (GA = 111 d, $n = 6$) before delivery at GA 125 d (normal GA = 150 d). For the control group ($n = 7$), saline injections were given 2 days or 2 weeks before delivery as well. Endotoxin injections are indicated as black arrows, and saline injections are indicated as grey arrows. GA: gestational age.

2.2. Tissue Preparation and Synaptophysin Immunohistochemistry. Brains were embedded in paraffin and cut in 7 μm-thick section using a microtome. Synaptophysin immunostaining was used to analyze presynaptic bouton densities. Synaptophysin is an integral membrane protein located in the synaptic vesicles and an established marker to detect nerve terminals [32]. All sections were processed simultaneously to guarantee identical conditions. First, sections were deparaffinized. All washing and dilutions steps of the antibodies were done by TBS (0.01 M) with 0.2% Triton-X-100 (TBS-T) at room temperature. In order to minimize the background staining, all sections were preincubated with 5% normal goat serum (Sigma, Netherlands) for 30 minutes. Furthermore, normal goat serum (5%) was added to all solutions containing antibodies. An antisynaptophysin antibody (monoclonal mouse; Boehringer-Mannheim, Germany) was used as a primary antibody overnight at a dilution of 1 : 750 at room temperature, followed by immersion with a donkey anti-mouse biotinylated secondary antibody (1 : 100; Jackson laboratories,) for 2 h. Brain sections were further processed using the avidin biotin complex technique with 3,3-diaminobenzidine (DAB) to obtain a color reaction (Vector laboratories, USA). After the labeling procedures, sections were dehydrated in ascending ethanol concentrations, cleared with xylene, and cover-slipped with DePex.

2.3. Quantitative Analysis of Synaptophysin Staining. Presynaptic bouton densities were analyzed in different cortical, striatal, and hippocampal areas: (1) motor cortex, (2) somatosensory cortex, (3) entorhinal cortex, (4) piriforme cortex, (5) nucleus caudatus, (6) putamen, (7) CA1-2, (8) CA3, and (9) dentate gyrus. All cortical areas were divided in two: layers 2-3 and layers 5-6. Layers 2 and 3 were taken together because these layers are mainly responsible for corticocortical afferent and efferent connections, while layers 5 and 6 were taken together, because they are the principal source of subcortical efferent connections [33]. Layer 4 was excluded, since, in some areas, like the entorhinal cortex, this layer lacks cell bodies [34].

Identification of the different areas occurred according to the sheep brain atlas of the Michigan State University by anatomical landmarks [35]. For every section ($n = \pm 10$/animal), measurements were performed for each region of interest in two adjacent areas of 5823 μm^2. Data of all measurements per subregion of interest per animal were pooled. Data were expressed as numbers of synaptic boutons per square micrometer ($1/\mu m^2$).

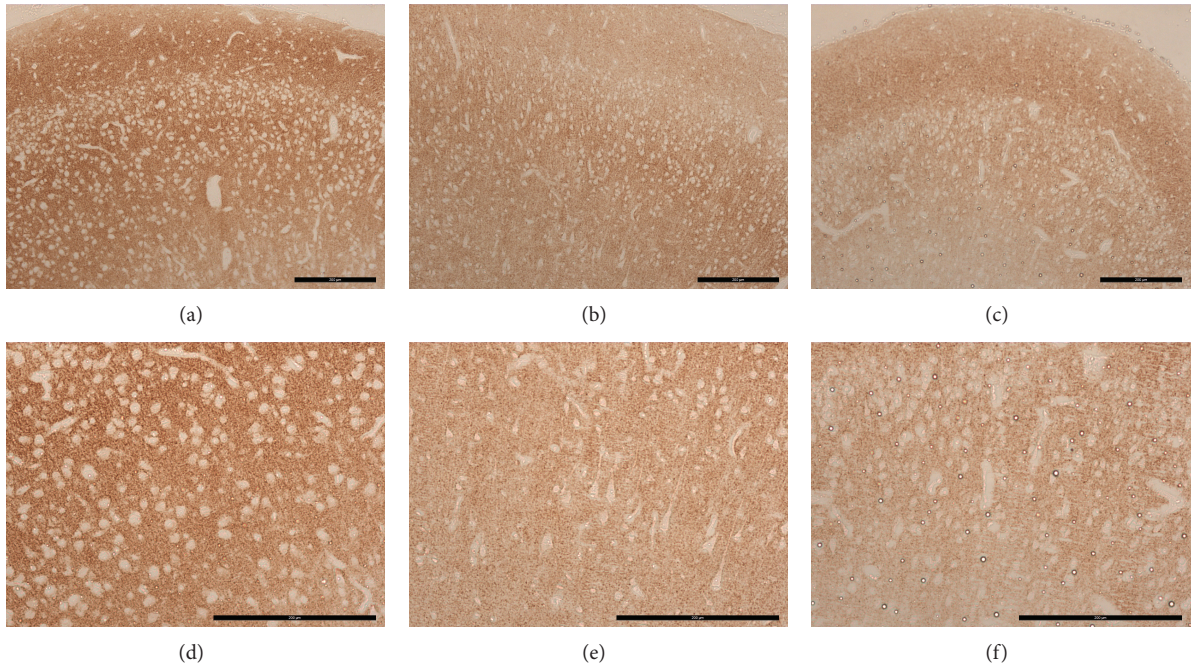

Figure 2: Photographs of synaptophysin immunoreactivity in the motor cortex. (a)–(c) Representative images of synaptophysin immunoreactive presynaptic boutons in the motor cortex (scale bar = 200 μm) of a control (a), a LPS2D animal (b), and a LPS14D animal (c). (d)–(f) Representative images of synaptophysin immunoreactive presynaptic boutons in the motor cortex layers 5-6 (scale bar = 200 μm) of a control (d), a LPS2D animal (e), and a LPS14D animal (f). Intra-amniotic LPS exposure significantly decreased synaptophysin staining in the motor cortex layers 5-6 compared to control animals (see also Figure 3(a)).

The immunoreactive punctae were estimated by calculating the density of the synaptophysin-immunoreactive presynaptic boutons, like previously described by van de Berg et al. [36]. Analysis was done using an Olympus AX-70 microscope. For each subregion, photos were taken from two randomly chosen areas at magnification ×100, using an Olympus F-view cooled CCD camera (Olympus, Tokyo).

The synaptic punctae were detected, using the image analyzing system Cell^P (Soft Imaging System, Münster, Germany). All measurements were performed at a single focal plane. Background levels were equalized and a shading correction was carried out by the software to correct for irregularities in illumination. Using a trial and error method, the threshold values, providing the most accurate measurement compared to direct visual counting, were selected. Once the ideal threshold value was found, it was saved in the computer program and kept the same for all measurements. All blood vessels and cell bodies and tissue out of focus were excluded.

2.4. Statistical Analysis. All data are represented as mean + standard error of means (+ SEM). For each parameter normality was tested using a Kolmogorov-Smirnov test. All data were normally distributed. Differences in bouton density were tested using a one-way analysis of variance (ANOVA). All significant effects were analyzed in more detail using post hoc Bonferroni tests. The accepted level of statistical significance was $P < 0.05$ for all analyses. All calculations were done using the Statistical Package for the Social Sciences (SPSS 15.0 software, Chicago, IL, USA).

3. Results

Figure 2 depicts representative images of synaptophysin immunoreactivity in the motor cortex of control and LPS exposed animals. Figure 3 shows the results of the quantitative analysis of presynaptic immunoreactivity in the different cortical areas analyzed. The synaptophysin immunoreactivity was restricted to small punctae, representing presynaptic boutons. There were no apparent differences in the morphological appearance of the punctae between groups.

In the motor cortex (Figure 3(a)), the mean presynaptic bouton density significantly decreased in the LPS 2D ($P < 0.01$) and the LPS 14D ($P < 0.05$) group compared to controls in both layers 2-3 and layers 5-6. In the entorhinal cortex (Figure 3(b)) as well as the somatosensory cortex (Figure 3(c)), significantly lower mean presynaptic bouton densities were seen in the LPS 2D group compared to controls in layers 2-3 only ($P < 0.05$). In both cortical areas a trend towards a decreased synaptic density in the LPS14D group was observed as well ($0.05 < P < 0.1$). No significant differences were found in the piriforme cortex (Figure 3(d)).

Figure 4 shows the results for striatum, which was subdivided into the caudate nucleus and the putamen. In both the caudate nucleus and the putamen, there was a significant decrease in the density of presynaptic boutons in the LPS 2D group compared to controls ($P < 0.05$). In the putamen, the mean presynaptic bouton density was significantly lower in the LPS14D group compared to the control group ($P < 0.05$).

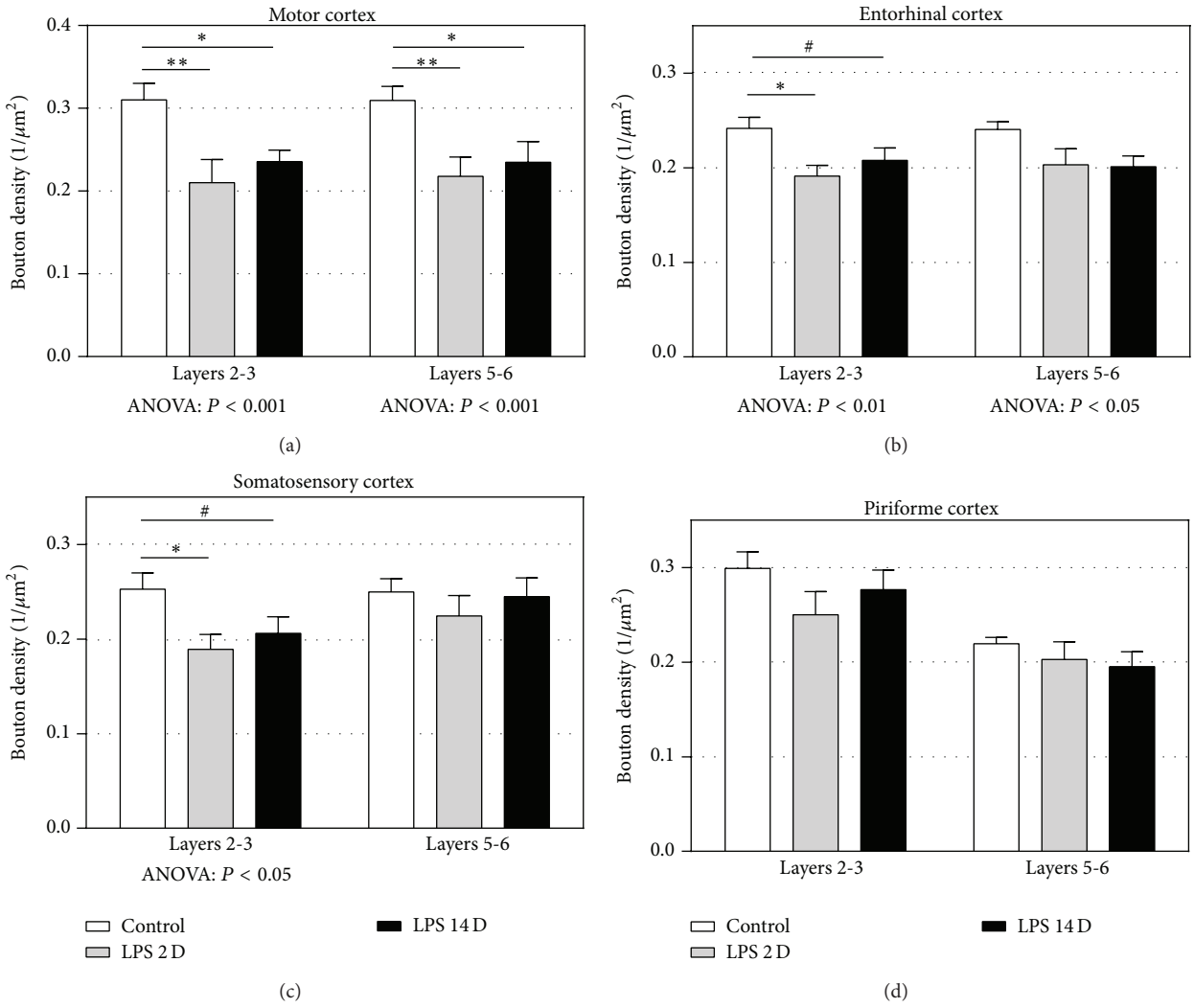

Figure 3: The results of the quantitative analysis of the presynaptic bouton density ($1/\mu m^2$) in layers 2-3 and layers 5-6 of different cortical areas. (a) The mean density of presynaptic boutons in the motor cortex. LPS2D and LPS14D animals showed a significant decrease compared to control animals in both layers. (b) The mean density of presynaptic boutons in the entorhinal cortex. LPS2D animals had a significantly lower density in layers 2-3 compared to controls and LPS14D animals showing a trend. (c) The mean density of presynaptic boutons in the somatosensory cortex. LPS2D animals had a lower density in layers 2-3 compared to controls and LPS14D animals showing a trend. (d) The mean density of presynaptic boutons in the piriforme cortex. All data are expressed as mean + SEM. ($^{*}P < 0.05$; $^{**}P < 0.01$ and $^{\#}0.05 < P < 0.1$).

Figure 5 depicts the results of the presynaptic bouton densities for the different subregions of the hippocampus. In the CA1/2 region, the mean density of presynaptic boutons was significantly less in the LPS 2D group compared to the control group ($P < 0.01$). In the CA3 area, LPS 2D animals had significantly lower bouton densities compared to control animals ($P < 0.05$). In addition, there was a significant difference between the LPS2D and the LPS14D groups, showing that after 14 days the densities were back to control levels ($P < 0.01$). In the dentate gyrus, no significant differences were found between the groups.

4. Discussion

The purpose of this study was to assess the effect of intra-amniotic inflammation on synaptic densities in different areas of the sheep brain. Our findings show that LPS-induced intra-amniotic inflammation significantly reduced presynaptic density 2 days after LPS exposure compared to controls in all layers of the motor cortex, in layers 2-3 of the entorhinal and somatosensory cortex, in the CA1/2 and CA3 regions of the hippocampus and the caudate nucleus and putamen. After 14 days of intra-amniotic LPS exposure synaptic density was not significantly lower compared to controls in most regions analysed. This might indicate that the preterm brain is capable of restoring neuronal connectivity after an inflammatory challenge.

Synaptic densities were calculated using an immunohistochemical staining for synaptophysin. This glycosylated protein, located primarily in type I and type II small synaptic vesicles, is an established marker for presynaptic nerve endings. It is important to mention that synaptophysin is

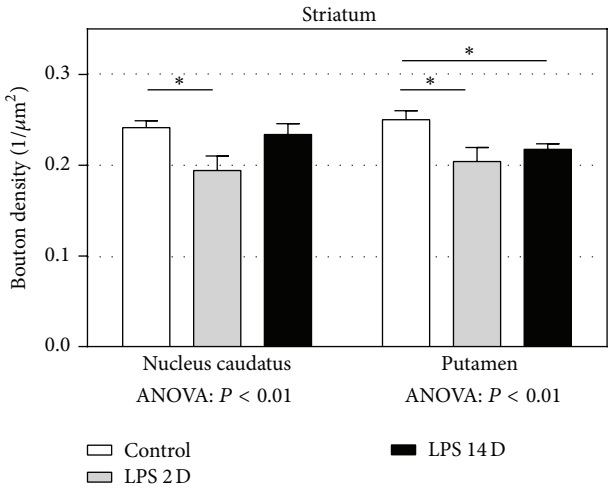

Figure 4: The results of the quantitative analysis of the presynaptic bouton density ($1/\mu m^2$) in the striatum. The mean density of presynaptic boutons in nucleus caudatus and putamen was significantly lower in the LPS2D group compared to controls. In the putamen, there was also a significant decrease in the LPS14D group compared to the control group. All data are expressed as mean + SEM. ($^*P < 0.05$).

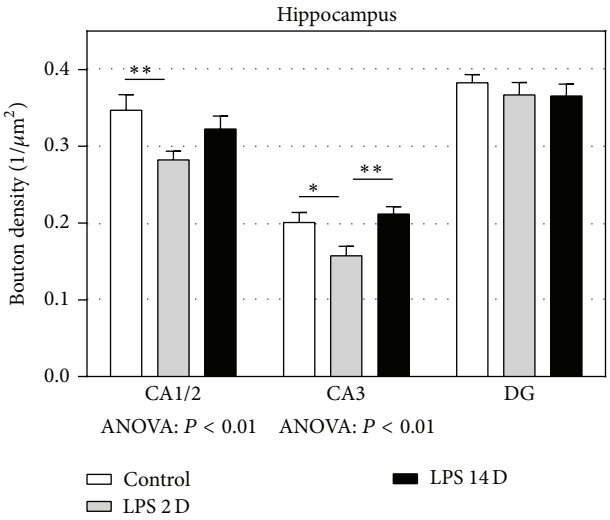

Figure 5: The results of the quantitative analysis of the presynaptic bouton density ($1/\mu m^2$) in the hippocampus. The mean density of presynaptic boutons in CA1/2 area was significantly lower in the LPS2D group compared to controls. In the CA3 area, there was a significant decrease in the LPS2D group compared to both the control and the LPS14D group. No significant differences were found in the DG. All data are expressed as mean + SEM. ($^*P < 0.05$; $^{**}P < 0.01$) CA: cornu ammonis; DG: dentate gyrus.

present in at least 95% of all neocortical synapses and that its expression profile parallels the time course of synaptogenesis [26–29].

4.1. LPS-Induced Chorioamnionitis Caused a Significant Loss in Presynaptic Densities in Different Regions of the Brain. In this study, chorioamnionitis significantly reduced the presynaptic 2 days after LPS exposure compared to controls in all layers of the motor cortex, in layers 2-3 of the entorhinal and somatosensory cortex, and in the CA1/2 and CA3 regions of the hippocampus and the caudate nucleus and putamen. Recently, Soumiya et al. showed that a maternal injection with poly I:C in mice also caused a significant decrease in synaptophysin-positive puncta surrounding cortical neuronal cell bodies [37]. Furthermore no other reports are available on synaptic densities and numbers after a clinical relevant fetal inflammatory challenge. Nevertheless, similar results were found after different adverse developmental conditions, like malnutrition, hypoxia, hypothyroidism, intrauterine growth retardation, and antenatal glucocorticoids [14–21]. For example, Colberg and colleagues found the loss of synaptic densities in layer 3 of the cortex and CA1 of the hippocampus and the caudate nucleus [17, 19] after antenatal betamethasone treatment in sheep. Likewise, lower synaptic densities were found in the visual cortex in growth-retarded fetuses and the hippocampus and cerebellum in neonatal rats after different hypoxic-ischemic insults [18, 20, 21].

The mechanism by which synapses are lost is not known yet. However, in this chorioamnionitis model, the loss of synapses may be regulated by the microglia in the brain. Microglia have shown to make direct contacts with neuronal synapses and after transient cerebral ischemia the duration of these contacts are prolonged and followed by the disappearance of the presynaptic bouton [38]. Therefore activated microglia may be involved in synapse stripping [39]. In addition, synapse loss can be caused by secretion of cytokines as part of the immune response of activated microglia during critical periods of brain and synapse development. In particular, IL1β and TNFα have been shown to be neurotoxic [40–42]. For example, both TNFα and IL1β may potentiate glutamate-mediated excitotoxicity and neurodegeneration by increasing NMDA receptor functioning [43–46]. We previously demonstrated in these same animals an activation of microglia in different regions of the brain, like hippocampus, which is consistent with prior work in similar and other animal models [11, 25, 47, 48]. Although we did not directly prove that the microglia are mechanistically involved, these current results point to an activation of this inflammatory cascade in the fetal brain at the moment the synapse loss is present [25]. Whether this inflammatory pathway only is sufficient to induce these synaptic changes or whether this pathway only represents a secondary mechanism awaits further research.

In addition, this reduced presynaptic density after LPS-induced chorioamnionitis in this current study can be the result of several processes. First, different neuronal changes can cause the loss of synapses. For example, degeneration of dendritic structures, loss of dendritic spines, or retraction of axonal processes might cause synapse loss without losing the actual neuron itself [49]. Burd et al. already showed that intrauterine infusion of LPS can cause a significant reduction in the number of dendrites in mice cortical neurons [13]. Furthermore, Kondo and colleagues reported long-term changes in dendritic spines after an intraperitoneal LPS injection in adult mice [50]. Second, lower synaptic densities can be caused by the actual loss of neurons in that specific area as well as by the loss of neurons in regions

that have extensive projections to that area. In a previous study, we already demonstrated neuron loss in these animals in the frontal cortex and the hippocampus [11]. Moreover, a prenatal exposure to LPS in rats leads to the loss of striatal dopaminergic neurons [51]. Furthermore, we have to keep in mind that lower synaptophysin-reactivity can also be the result of conformational changes of the protein, alterations in the synthesis, or degradation or a decrease in the amount of presynaptic vesicles instead of only the loss of actual presynaptic terminals [17].

4.2. The Reduced Presynaptic Densities Seem to be Region-Specific and Transient in Some Regions. After 14 days of intra-amniotic LPS exposure synaptic density was not significantly lower compared to controls in most regions analysed. This indicates that, after a first injurious hit, the density of presynaptic boutons is restored probably due to the plasticity of the preterm brain. In some region, like the motor cortex and the putamen, however, there is still a significant reduction in presynaptic density in the LPS14D group compared to control animals. Most likely, this region-specific recovery may be due to the maturity of the cerebral area. Cortical neurogenesis occurs later than, for example, hippocampal or striatal neurogenesis [52]. Furthermore, Rees et al. found that the formation of new neuronal processes is retarded if the neurons are particularly vulnerable at the time of the insult but will recover, after a certain delay, if the axonal and dendritic outgrowth is already established and the development is well advanced at that time [53]. The same may hold true for the differences seen in the cortical layers. Cortical layers 2-3 seem to be more affected than cortical layers 5-6. These layers may be more affected, because, at least in humans, synaptogenesis occurs later in the lower layers [54]. In addition, Soumiya et al. also showed that the synaptic development of the upper-layer neurons of the somatosensory cortex seems to be more affected than the deeper-layer neurons in offspring after a maternal viral challenge [37]. In addition, our study shows that the piriforme cortex and the dentate gyrus of the hippocampus seem to be less vulnerable for synaptic alterations at this time point.

4.3. Implications and General Conclusion. Recent studies demonstrate that an intrauterine infection associated with preterm birth is related to motor disabilities, as well as learning, social, and other behavioural problems [4, 55–58]. However, not all of these neonates show explicit evidence of structural brain damage, like WMD or periventricular leukomalacia, during ultrasounds or MRI imaging [59, 60]. Therefore, neuronal and grey matter damage may have a significant contribution to these bad outcomes. This presumes that more subtle neuronal injury might be present, like minor neuronal cell loss or synaptic disturbances, which is not always visible during radiological imaging. In this study, we reported the loss of presynaptic terminals in different cortical areas, as well as the hippocampus and striatum. The loss of these presynaptic nerve terminals would suggest functional disturbances in the neuronal network and synaptic transmission. Therefore our results could suggest that this LPS-induced fetal synaptic damage may contribute to the altered neurobehavioural state often described in children exposed to antenatal inflammation by modulating neuronal connectivity.

In conclusion, the present study demonstrated that 2-day intra-amniotic LPS exposure resulted in decreased density in presynaptic boutons in the motor, entorhinal, and somatosensory cortex, in the CA1-2 and CA3 areas of the hippocampus and the nucleus caudate and putamen. These synaptic changes seemed to be region-specific, with some regions being more affected than others, After 14 days of intra-amniotic LPS exposure synaptic density was not significantly lower compared to controls in most regions analysed. This might indicate that the preterm brain is capable of restoring neuronal connectivity after an inflammatory challenge.

Even though these synaptic changes appeared to be transient in some regions, the effects of chorioamnionitis of fetal brain development cannot be disregarded and further research is needed, since these observations could contribute to our understanding of the pathogenesis of the neurobehavioral problems caused by a fetal inflammatory challenge.

Conflict of Interests

The authors declare that there is no conflict of interests regarding the publication of this paper.

References

[1] R. L. Goldenberg, J. C. Hauth, and W. W. Andrews, "Intrauterine infection and preterm delivery," *The New England Journal of Medicine*, vol. 342, no. 20, pp. 1500–1507, 2000.

[2] K. B. Nelson, J. M. Dambrosia, J. K. Grether, and T. M. Phillips, "Neonatal cytokines and coagulation factors in children with cerebral palsy," *Annals of Neurology*, vol. 44, no. 4, pp. 665–675, 1998.

[3] R. Romero, R. Gomez, F. Ghezzi, M. Mazor, S. S. Edwin, and S. M. Berry, "A fetal systemic inflammatory response is followed by the spontaneous onset of preterm parturition," *The American Journal of Obstetrics and Gynecology*, vol. 179, no. 1, pp. 186–193, 1998.

[4] O. Dammann, K. C. K. Kuban, and A. Leviton, "Perinatal infection, fetal inflammatory response, white matter damage, and cognitive limitations in children born preterm," *Mental Retardation and Developmental Disabilities Research Reviews*, vol. 8, no. 1, pp. 46–50, 2002.

[5] D. J. Murphy, S. Sellers, I. Z. MacKenzie, P. L. Yudkin, and A. M. Johnson, "Case-control study of antenatal and intrapartum risk factors for cerebral palsy in very preterm singleton babies," *The Lancet*, vol. 346, no. 8988, pp. 1449–1454, 1995.

[6] U. Verma, N. Tejani, S. Klein et al., "Obstetric antecedents of intraventricular hemorrhage and periventricular leukomalacia in the low-birth-weight neonate," *The American Journal of Obstetrics and Gynecology*, vol. 176, no. 2, pp. 275–281, 1997.

[7] J. M. Perlman, "White matter injury in the preterm infant: an important determination of abnormal neurodevelopment outcome," *Early Human Development*, vol. 53, no. 2, pp. 99–120, 1998.

[8] L. B. Versland, K. Sommerfelt, and I. Elgen, "Maternal signs of chorioamnionitis: persistent cognitive impairment in low-birthweight children," *Acta Paediatrica*, vol. 95, no. 2, pp. 231–235, 2006.

[9] N. Nasef, A. Shabaan, P. Schurr et al., "Effect of clinical and histological chorioamnionitis on the outcome of preterm infants," *The American Journal of Perinatology*, vol. 30, no. 1, pp. 59–68, 2013.

[10] M. Huleihel, H. Golan, and M. Hallak, "Intrauterine infection/inflammation during pregnancy and offspring brain damages: possible mechanisms involved," *Reproductive Biology and Endocrinology*, vol. 2, article 17, 2004.

[11] A. W. D. Gavilanes, E. Strackx, B. W. Kramer et al., "Chorioamnionitis induced by intraamniotic lipopolysaccharide resulted in an interval-dependent increase in central nervous system injury in the fetal sheep," *The American Journal of Obstetrics and Gynecology*, vol. 200, no. 4, pp. 437.e1–437.e8, 2009.

[12] H. Hagberg and C. Mallard, "Effect of inflammation on central nervous system development and vulnerability," *Current Opinion in Neurology*, vol. 18, no. 2, pp. 117–123, 2005.

[13] I. Burd, A. I. Bentz, J. Chai et al., "Inflammation-induced preterm birth alters neuronal morphology in the mouse fetal brain," *Journal of Neuroscience Research*, vol. 88, no. 9, pp. 1872–1881, 2010.

[14] D. G. Jones and S. E. Dyson, "Synaptic junctions in undernourished rat brain—an ultrastructural investigation," *Experimental Neurology*, vol. 51, no. 3, pp. 529–535, 1976.

[15] B. G. Cragg, "The development of cortical synapses during starvation in the rat," *Brain*, vol. 95, no. 1, pp. 143–150, 1972.

[16] B. G. Cragg, "Synapses and membranous bodies in experimental hypothyroidism," *Brain Research*, vol. 18, no. 2, pp. 297–307, 1970.

[17] I. Antonow-Schlorke, B. Kühn, T. Müller et al., "Antenatal betamethasone treatment reduces synaptophysin immunoreactivity in presynaptic terminals in the fetal sheep brain," *Neuroscience Letters*, vol. 297, no. 3, pp. 147–150, 2001.

[18] M. Bisignano and S. Rees, "The effects of intrauterine growth retardation on synaptogenesis and mitochondrial formation in the cerebral and cerebellar cortices of fetal sheep," *International Journal of Developmental Neuroscience*, vol. 6, no. 5, pp. 453–460, 1988.

[19] C. Colberg, I. Antonow-Schlorke, T. Müller, H. Schubert, O. W. Witte, and M. Schwab, "Recovery of glucocorticoid-related loss of synaptic density in the fetal sheep brain at 0.75 of gestation," *Neuroscience Letters*, vol. 364, no. 2, pp. 130–134, 2004.

[20] C. H. Horner, H. A. Davies, and M. G. Stewart, "Hippocampal synaptic density and glutamate immunoreactivity following transient cerebral ischaemia in the chick," *European Journal of Neuroscience*, vol. 10, no. 12, pp. 3913–3917, 1998.

[21] S. S. Stepanov, E. D. Sergeyeva, V. V. Semchenko, and V. A. Akulinin, "An ultrastructural study into the effect of global transient cerebral ischaemia on the synaptic population of the cerebellar cortex in rats," *Resuscitation*, vol. 39, no. 1-2, pp. 99–106, 1998.

[22] E. Kuypers, D. Ophelders, R. K. Jellema, S. Kunzmann, A. W. Gavilanes, and B. W. Kramer, "White matter injury following fetal inflammatory response syndrome induced by chorioamnionitis and fetal sepsis: lessons from experimental ovine models," *Early Human Development*, vol. 88, no. 12, pp. 931–936, 2012.

[23] A. W. Gavilanes, M. Gantert, E. Strackx et al., "Increased EEG delta frequency corresponds to chorioamnionitis-related brain injury," *Frontiers in Bioscience (Scholar Edition)*, vol. 2, pp. 432–438, 2010.

[24] V. Bieghs, E. Vlassaks, A. Custers et al., "Chorioamnionitis induced hepatic inflammation and disturbed lipid metabolism in fetal sheep," *Pediatric Research*, vol. 68, no. 6, pp. 466–472, 2010.

[25] E. Kuypers, R. K. Jellema, D. R. M. G. Ophelders et al., "Effects of intra-amniotic lipopolysaccharide and maternal betamethasone on brain inflammation in fetal sheep," *PLoS ONE*, vol. 8, no. 12, Article ID e81644, 2013.

[26] M. L. Grunnet, "A lectin and synaptophysin study of developing brain," *Pediatric Neurology*, vol. 13, no. 2, pp. 157–160, 1995.

[27] N. Leclerc, P. W. Beesley, I. Brown et al., "Synaptophysin expression during synaptogenesis in the rat cerebellar cortex," *Journal of Comparative Neurology*, vol. 280, no. 2, pp. 197–212, 1989.

[28] E. Masliah, R. D. Terry, M. Alford, and R. DeTeresa, "Quantitative immunohistochemistry of synaptophysin in human neocortex: an alternative method to estimate density of presynaptic terminals in paraffin sections," *Journal of Histochemistry and Cytochemistry*, vol. 38, no. 6, pp. 837–844, 1990.

[29] F. Navone, R. Jahn, G. di Gioia, H. Stukenbrok, P. Greengard, and P. de Camilli, "Protein p38: an integral membrane protein specific for small vesicles of neurons and neuroendocrine cells," *Journal of Cell Biology*, vol. 103, no. 6, part 1, pp. 2511–2527, 1986.

[30] A. H. Jobe, J. P. Newnham, K. E. Willet et al., "Effects of antenatal endotoxin and glucocorticoids on the lungs of preterm lambs," *The American Journal of Obstetrics and Gynecology*, vol. 182, no. 2, pp. 401–408, 2000.

[31] M. Gantert, R. K. Jellema, H. Heineman et al., "Lipopolysaccharide-induced chorioamnionitis is confined to one amniotic compartment in twin pregnant sheep," *Neonatology*, vol. 102, pp. 81–88, 2012.

[32] G. Thiel, "Synapsin I, synapsin II, and synaptophysin: marker proteins of synaptic vesicles," *Brain Pathology*, vol. 3, no. 1, pp. 87–95, 1993.

[33] E. R. Kandel, J. H. Schwartz, and T. M. Jessell, "The cerebral cortex is concerned with cognitive functioning," in *Principles of Neural Science*, J. Butler and H. Lebowitz, Eds., pp. 324–329, McGraw-Hill, New York, NY, USA, 4th edition, 2000.

[34] H. Braak and E. Braak, "On areas of transition between entorhinal allocortex and temporal isocortex in the human brain. Normal morphology and lamina-specific pathology in Alzheimer's disease," *Acta Neuropathologica*, vol. 68, no. 4, pp. 325–332, 1985.

[35] J. I. Johnson, K. D. Sudheimer, K. K. Davis, and B. M. Winn, "Brain atlas of the sheep on the internet for courses in neurobiology," *The American Zoologist*, vol. 40, no. 6, p. 1080, 2000.

[36] W. D. J. van de Berg, A. Blokland, A. C. Cuello et al., "Perinatal asphyxia results in changes in presynaptic bouton number in striatum and cerebral cortex—a stereological and behavioral analysis," *Journal of Chemical Neuroanatomy*, vol. 20, no. 1, pp. 71–82, 2000.

[37] H. Soumiya, H. Fukumitsu, and S. Furukawa, "Prenatal immune challenge compromises development of upper-layer but not deeper-layer neurons of the mouse cerebral cortex," *Journal of Neuroscience Research*, vol. 89, no. 9, pp. 1342–1350, 2011.

[38] H. Wake, A. J. Moorhouse, S. Jinno, S. Kohsaka, and J. Nabekura, "Resting microglia directly monitor the functional state of synapses in vivo and determine the fate of ischemic terminals," *Journal of Neuroscience*, vol. 29, no. 13, pp. 3974–3980, 2009.

[39] B. D. Trapp, J. R. Wujek, G. A. Criste et al., "Evidence for synaptic stripping by cortical microglia," *Glia*, vol. 55, no. 4, pp. 360–368, 2007.

[40] Y. Yamasaki, N. Matsuura, H. Shozuhara et al., "Interleukin-1 as a pathogenetic mediator of ischemic brain damage in rats," *Stroke*, vol. 26, no. 4, pp. 676–681, 1995.

[41] S. M. Allan, L. C. Parker, B. Collins, R. Davies, G. N. Luheshi, and N. J. Rothwell, "Cortical cell death induced by IL-1 is mediated via actions in the hypothalamus of the rat," *Proceedings of the National Academy of Sciences of the United States of America*, vol. 97, no. 10, pp. 5580–5585, 2000.

[42] F. C. Barone, B. Arvin, R. F. White et al., "Tumor necrosis factor-alpha. A mediator of focal ischemic brain injury," *Stroke*, vol. 28, no. 6, pp. 1233–1244, 1997.

[43] B. Viviani, S. Bartesaghi, F. Gardoni et al., "Interleukin-1β enhances NMDA receptor-mediated intracellular calcium increase through activation of the Src family of kinases," *The Journal of Neuroscience*, vol. 23, no. 25, pp. 8692–8700, 2003.

[44] B. Viviani, F. Gardoni, S. Bartesaghi et al., "Interleukin-1 beta released by gp120 drives neural death through tyrosine phosphorylation and trafficking of NMDA receptors," *The Journal of Biological Chemistry*, vol. 281, no. 40, pp. 30212–30222, 2006.

[45] X. C. Ma, P. E. Gottschall, L. T. Chen, M. Wiranowska, and C. P. Phelps, "Role and mechanisms of interleukin-1 in the modulation of neurotoxicity," *NeuroImmunoModulation*, vol. 10, no. 4, pp. 199–207, 2002.

[46] C. C. Chao and S. Hu, "Tumor necrosis factor-alpha potentiates glutamate neurotoxicity in human fetal brain cell cultures," *Developmental Neuroscience*, vol. 16, no. 3-4, pp. 172–179, 1994.

[47] M. J. Bell and J. M. Hallenbeck, "Effects of intrauterine inflammation on developing rat brain," *Journal of Neuroscience Research*, vol. 70, no. 4, pp. 570–579, 2002.

[48] Z. Cai, Z.-L. Pan, Y. Pang, O. B. Evans, and P. G. Rhodes, "Cytokine induction in fetal rat brains and brain injury in neonatal rats after maternal lipopolysaccharide administration," *Pediatric Research*, vol. 47, no. 1, pp. 64–72, 2000.

[49] J. C. Fiala, J. Spacek, and K. M. Harris, "Dendritic spine pathology: cause or consequence of neurological disorders?" *Brain Research Reviews*, vol. 39, no. 1, pp. 29–54, 2002.

[50] S. Kondo, S. Kohsaka, and S. Okabe, "Long-term changes of spine dynamics and microglia after transient peripheral immune response triggered by LPS in vivo," *Molecular Brain*, vol. 4, no. 1, article 27, 2011.

[51] P. M. Carvey, Q. Chang, J. W. Lipton, and Z. Ling, "Prenatal exposure to the bacteriotoxin lipopolysaccharide leads to long-term losses of dopamine neurons in offspring: a potential, new model of Parkinson's disease," *Frontiers in Bioscience*, vol. 8, pp. s826–s837, 2003.

[52] B. Clancy, B. Kersh, J. Hyde, R. B. Darlington, K. J. S. Anand, and B. L. Finlay, "Web-based method for translating neurodevelopment from laboratory species to humans," *Neuroinformatics*, vol. 5, no. 1, pp. 79–94, 2007.

[53] S. Rees, S. Breen, M. Loeliger, G. Mccrabb, and R. Harding, "Hypoxemia near mid-gestation has long-term effects on fetal brain development," *Journal of Neuropathology & Experimental Neurology*, vol. 58, no. 9, pp. 932–945, 1999.

[54] P. R. Huttenlocher, "Morphometric study of human cerebral cortex development," *Neuropsychologia*, vol. 28, no. 6, pp. 517–527, 1990.

[55] D. E. Schendel, A. Schuchat, and P. Thorsen, "Public health issues related to infection in pregnancy and cerebral palsy," *Mental Retardation and Developmental Disabilities Research Reviews*, vol. 8, no. 1, pp. 39–45, 2002.

[56] D. K. Shah, P. J. Anderson, J. B. Carlin et al., "Reduction in cerebellar volumes in preterm infants: relationship to white matter injury and neurodevelopment at two years of age," *Pediatric Research*, vol. 60, no. 1, pp. 97–102, 2006.

[57] D. K. Thompson, S. K. Warfield, J. B. Carlin et al., "Perinatal risk factors altering regional brain structure in the preterm infant," *Brain*, vol. 130, no. 3, pp. 667–677, 2007.

[58] C. Limperopoulos, H. Bassan, K. Gauvreau et al., "Does cerebellar injury in premature infants contribute to the high prevalence of long-term cognitive, learning, and behavioral disability in survivors?" *Pediatrics*, vol. 120, no. 3, pp. 584–593, 2007.

[59] K. J. Rademaker, C. S. P. M. Uiterwaal, F. J. A. Beek et al., "Neonatal cranial ultrasound versus MRI and neurodevelopmental outcome at school age in children born preterm," *Archives of Disease in Childhood: Fetal and Neonatal Edition*, vol. 90, no. 6, pp. F489–F493, 2005.

[60] V. Chau, K. J. Poskitt, D. E. McFadden et al., "Effect of chorioamnionitis on brain development and injury in premature newborns," *Annals of Neurology*, vol. 66, no. 2, pp. 155–164, 2009.

Hindawi Publishing Corporation
BioMed Research International
Volume 2015, Article ID 718591, 8 pages
http://dx.doi.org/10.1155/2015/718591

Research Article

Sustained Reduction of Cerebellar Activity in Experimental Epilepsy

Kim Rijkers,[1,2,3] Véronique M. P. Moers-Hornikx,[1,3,4] Roelof J. Hemmes,[1] Marlien W. Aalbers,[2,3] Yasin Temel,[1,2,3] Johan S. H. Vles,[3,4] and Govert Hoogland[1,2,3]

[1]*Department of Neuroscience, Maastricht University Medical Center, P.O. Box 5800, 6202 AZ Maastricht, Netherlands*
[2]*Department of Neurosurgery, Maastricht University Medical Center, P.O. Box 5800, 6202 AZ Maastricht, Netherlands*
[3]*School for Mental Health and Neuroscience, Maastricht University, P.O. Box 616, 6200 MD Maastricht, Netherlands*
[4]*Department of Neurology, Maastricht University Medical Center, P.O. Box 5800, 6202 AZ Maastricht, Netherlands*

Correspondence should be addressed to Kim Rijkers; kimrijkers@gmail.com

Received 23 May 2014; Revised 18 February 2015; Accepted 3 March 2015

Academic Editor: Eiichi Ishikawa

Clinical and experimental evidence suggests a role for the cerebellum in seizure control, while no data are available on cerebellar activity between seizures. We hypothesized that interictal regional activity of the deep cerebellar nuclei is reduced in epilepsy and tested this in an animal model by using ΔFosB and cytochrome oxidase (COX) (immuno)histochemistry. The expression of these two markers of neuronal activity was analysed in the dentate nucleus (DN), interpositus nucleus (IN), and fastigial nucleus (FN) of the cerebellum of fully amygdala kindled rats that were sacrificed 48 hours after their last seizure. The DN and FN of kindled rats exhibited 25 to 29% less ΔFosB immunopositive cells than their respective counterpart in sham controls ($P < 0.05$). COX expression in the DN and FN of kindled animals was reduced by 32 to 33% compared to respective control values ($P < 0.05$). These results indicate that an epileptogenic state is characterized by decreased activity of deep cerebellar nuclei, especially the DN and FN. Possible consequences may include a decreased activation of the thalamus, contributing to further seizure spread. Restoration of FN activity by low frequency electrical stimulation is suggested as a possible treatment option in chronic epilepsy.

1. Introduction

The cerebellum plays a crucial role in the coordination and control of motor behaviour and cognitive processing [1]. Studies in epilepsy patients and animals models of epilepsy have demonstrated that the cerebellum takes part in the epileptogenic network as well. First of all, case reports have illustrated that the cerebellum can harbour the epileptic focus [2–4]. Furthermore, SPECT and fMRI studies in epilepsy patients have revealed that cerebellar blood flow and blood oxygen level-dependent (BOLD) signal, respectively, increase during secondary generalisation of a partial seizure [5–11]. In rats, cerebellar glucose utilization increases upon administration of proconvulsant drugs [12].

At the cellular level, it has been hypothesized that this ictally increased activity reflects increased GABAergic Purkinje cell firing [13]. Purkinje cells provide the purely inhibitory output of the cerebellar cortex [14]. These inhibitory projections modify the output of the cerebellum through the deep cerebellar nuclei, the dentate nucleus (DN), interpositus nucleus (IN), and fastigial nuclei (FN), which in turn project to the thalamus. This way, the cerebellum regulates activity of neurons elsewhere in the brain.

Thus, seizures are associated with increased activity of the Purkinje cells. Since these cells inhibit the deep cerebellar nuclei, it is likely that seizures are associated with decreased activity of these nuclei. It is not clear whether interictally these cerebellar nuclei are less active as well. The aim of the current study was therefore to assess the regional distribution of interictal neuronal activity in the deep cerebellar nuclei. To this end, we immunohistochemically analyzed cerebellar neuronal activity in fully amygdala kindled rats by evaluating the expression of ΔFosB and cytochrome C oxidase (COX, a.k.a. complex IV), in the DN, IN, and FN.

2. Materials and Methods

2.1. Animals. Experimental procedures were carried out in 12-week-old male Sprague-Dawley rats (Harlan, Horst, Netherlands). Animals were housed under controlled conditions, a 12-hour light/dark cycle (lights on 7 a.m.), background noise, and food and water *ad libitum*. Adequate measures were taken to minimize pain and discomfort. All experimental procedures were approved by the animal ethics committee of Maastricht University and complied with governmental legislation.

2.2. Amygdala Kindling

2.2.1. Electrode Placement. For amygdala kindling, rats were stereotactically implanted with an electrode in the left basolateral amygdala. Perioperative pain was minimized by administering 0.1 mL buprenorphine hydrochloride (Temgesic, Schering-Plough Inc., Amstelveen, Netherlands) subcutaneously 30 minutes before surgery. Next, rats received general isoflurane anesthesia (5% for induction and 2.5% for maintenance throughout the surgical procedure) and were fixed in a stereotactic frame (Dual Manipulator Lab Standard Stereotact, Stoelting Inc., Wood Dale, USA). The implanted electrodes were designed and manufactured by the Department of Instrument Development, Engineering and Evaluation of Maastricht University in collaboration with Professor Dr. Y. Temel (Maastricht University Medical Center, Maastricht, Netherlands). An electrode set consisted of a bipolar stimulating/recording electrode that was implanted in the left basolateral amygdala (coordinates relative to bregma: 2.5 mm posteriorly, 4.8 mm laterally, and 9.6 mm ventrally [15]) and three monopolar stainless steel electrodes that were implanted in the cortex at 1 mm depth. One cortical electrode was used for EEG, one for reference, and one for ground. Connectors for the kindling/EEG electrodes were fixed on the skull using dental acrylic.

2.2.2. Afterdischarge Threshold. Ten days after surgery the prekindling afterdischarge threshold (pre-KADT) was assessed in all rats by stimulating the amygdala with a series of pulses of increasing intensity starting at 10 μA (2 seconds, 50 Hz, 0.2 ms block pulse). Stimuli were delivered through a WPI Accupulser A310 connected to a WPI Stimulus Isolation Unit A360 (World Precision Instruments, Sarasota, FL, USA). EEG registrations from the amygdala and cortical electrodes were recorded from one minute before the kindling stimulus until the end of the behavioural seizure using a Vanguard system (Vanguard Systems, Cleveland Clinics Foundation, Cleveland, USA). Recordings were made with a sample frequency of 200 Hz, a frequency band of 0.5–70 Hz, and a 50 Hz notch filter. The afterdischarge threshold was defined as the stimulus amplitude necessary to elicit a two-second discharge with high frequency and high voltage. One day after the last kindling stimulus, a postkindling afterdischarge threshold (post-KADT) was assessed. The difference between pre-KADT and post-KADT (ΔADT) was calculated by subtracting the respective values and was considered an indirect measure of excitability.

2.2.3. Amygdala Kindling. Amygdala kindling started two weeks after surgery by administering two stimulations per day with an interstimulus interval of at least six hours. Each stimulus lasted two seconds and consisted of a 50 Hz, 400 μA, 0.2 ms block pulse. Seizure severity was assessed based on Racine's scale [16] (i.e., stage 1: freezing; stage 2: head nodding and blinking; stage 3: unilateral forelimb clonus; stage 4: bilateral forelimb clonus and rearing; stage 5: falling). Fully kindled animals were defined as animals that displayed a stage five seizure upon each of five consecutive amygdala stimulations. These fully kindled animals were subsequently stimulated once per day for two more weeks. Kindling rate was defined as the number of stimuli needed to reach the fully kindled state. Sham animals underwent the same surgical procedure and afterdischarge assessments but were not subjected to daily stimulation.

2.3. Histological Processing. Two days after the last seizures, that is, 24 h after the assessment of the post-KADT, the rats received an overdose of pentobarbital (75 mg Nembutal/kg bodyweight), followed by perfusion with Tyrode buffer (in mM: 136.9 NaCl, 2.7 KCl, 0.2 $MgCl_2$, 11.9 $NaHCO_3$, 0.3 NaH_2PO_4, and 5.0 glucose, equilibrated with 5% CO_2/95% O_2) and then with 4% paraformaldehyde dissolved in 0.1 M phosphate buffer, pH 7.6. The brains were removed, postfixed in the same fixative (4°C, 24 hours), rapidly frozen using CO_2, and stored at −80°C until sections were cut.

Coronal 10 μm serial sections from the level of the central canal fourth ventricle junction (13.6 mm posteriorly to bregma according to Paxinos [15]) caudally to the inferior colliculus (located 9.6 mm posteriorly to bregma) were cut on a cryostat, mounted on gelatin-coated glass slides, and stored at −20°C until they were processed for (immuno)histochemistry. To minimize staining-to-staining variations, staining experiments always included an equal amount of control and kindled samples.

2.3.1. ΔFosB Immunohistochemistry. Sections were rinsed in Tris-buffered saline containing 0.3% Triton (TBS-T) and then incubated (4°C, 48 hours) with polyclonal rabbit-anti-mouse for B antibody (sc-48, Santa Cruz Biotechnology Inc., Santa Cruz, CA, USA) diluted 1 : 250 in TBS-T containing 0.5% bovine serum albumin. Next, sections were rinsed in TBS-T and incubated (room temperature, overnight) with donkey-anti-rabbit biotinylated antibody (Jackson ImmunoResearch Laboratories Inc., West Grove, PA, USA) diluted 1 : 400 in TBS-T containing 0.5% bovine serum albumin. Sections were then rinsed with TBS-T, incubated for two hours in avidin/biotin diluted 1 : 800 (Vectastain ABC-kit, Vector Laboratories Inc., Burlingame, CA, USA), and visualised by 3.3′-diaminobenzidine (DAB) containing $NiCl_2$. Finally, sections were dehydrated and coverslipped.

2.3.2. COX Histology. COX was histochemically detected as described previously [17, 18]. Briefly, sections were air-dried and subsequently incubated (37°C, four hours) in the dark in a nickel enhanced 0.1 M 4-(2-hydroxyethyl)-1-piperazineethanesulfonic acid (HEPES) solution (1% $NiCl_2$,

pH 7.4) containing 0.0224% cytochrome C oxidase, 0.115% DAB, and 4.5% sucrose. The reaction was stopped by transferring the sections to an ice cold pH neutral buffered 4% paraformaldehyde medium for ten minutes. Finally, sections were dehydrated and coverslipped.

2.3.3. Quantification of Staining. The DN, IN, and FN were photographed in all sections at 4x magnification using an Olympus AX70 bright-field microscope with an Olympus DP70 camera (analySIS Imaging System, Münster, Germany). A mean of 10 sections per animal (range 4–16) for the ΔfosB staining and 16 sections per animal (range 10–19) for the COX staining were analysed. The deep cerebellar nuclei were easily identifiable due to the contrast between nuclei and surrounding white matter, allowing delineation using the freehand drawing function in ImageJ (version 1.43). Tissue artifacts were excluded from analysis.

Cells showing ΔfosB immunoreactivity in the nucleus, cytoplasm, or both were counted by an observer that was blinded for the treatment and expressed as number of immunopositive cells per square millimeter. In total, 129 sections from nine kindled animals and 72 sections from six sham animals were analysed.

Cytochrome oxidase staining was analysed by optical density (OD) using ImageJ. For each nucleus, the OD value was corrected for background staining by subtracting the OD of the adjacent white matter, resulting in negative values as ImageJ applies an inverted grey value scale. In total, 92 stained sections from six kindled animals and 101 sections from six sham animals were analysed. Due to technical problems during the staining sections from three kindled rats could not be analysed.

2.4. Statistical Analysis. A Shapiro-Wilk test was performed as test for normal distribution of data. Part of the results were not normally distributed; therefore, the data were analysed using a Mann-Whitney U test. Data are expressed as mean ± standard error of the mean (SEM). $P < 0.05$ was considered statistically significant.

3. Results

There were no significant differences in ΔFosB immunopositive cell densities or in COX grey values between left and right cerebellar nuclei in shams or in kindled animals; therefore values from both hemispheres were pooled.

3.1. ΔFosB. ΔFosB staining was not confined to the cell nucleus, as would be expected from a nuclear staining, but was seen in the cytoplasm as well (see Figure 1). This "ΔFosB-like immunoreactivity" was almost exclusively found in the most lateral regions of the deep cerebellar nuclei and was observed in the DN in particular.

Density of ΔFosB immunoreactive (ΔFosB-ir) cells was lower in the DN and FN of kindled animals than in shams (DN 108.5 ± 12.4 versus 152.1 ± 7.7, $P < 0.05$, a reduction of 29%; FN 87.2 ± 7.8 versus 115.5 ± 2.2, $P < 0.05$, a reduction of 25%); see Figure 2. In the IN, the density of ΔFosB-ir cells was also lower in kindled than in sham animals; however, this difference was not statistically significant (IN 91.3±9.1 versus 116.2 ± 3.5; $P = 0.088$).

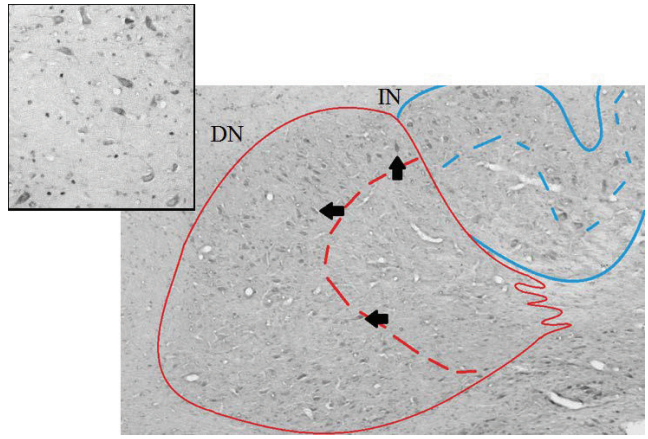

Figure 1: Photomicrograph (10x magnification) showing the distribution of ΔFosB immunoreactive cells in the lateral deep cerebellar nuclei. The cytoplasmic staining of ΔFosB is seen in relatively large cells (arrows) that are almost exclusively localized in the outer regions of the nuclei. These cells are seen in the deep cerebellar nuclei of both sham and amygdala kindled rats. The inset is a 40x magnification showing the cytoplasmic staining in more detail. DN: dentate nucleus; IN: interpositus nucleus.

3.2. COX. Kindled animals expressed significantly less COX than shams in both DN and FN (DN: −38.2 ± 6.3 versus −55.8 ± 5.2, $P < 0.05$, a reduction of 32%; FN: −22.0 ± 2.8 versus −32.9 ± 3.3, $P < 0.05$, a reduction of 33%; see Figure 3). In the IN, COX expression was also lower in kindled animals than in shams, but this difference was not statistically significant (−32.5 ± 4.7 versus −47.9 ± 4.2; $P = 0.065$).

4. Discussion

In this study, we assessed the level of neuronal activity in deep cerebellar nuclei during the interictal phase of fully kindled rats. The observed reductions in activity markers ΔFosB and COX in DN and FN suggest that a decreased seizure threshold is accompanied by reduced activity of the deep cerebellar nuclei.

4.1. Methodological Considerations. All experiments were carried out in fully kindled animals that were sacrificed 48 hours after their last kindled seizure. This means that we investigated interictal changes in a chronic epilepsy model. Sham controls did not suffer from seizures. This may have led to a difference in overall locomotor activity between kindled animals and sham controls. Data on interictal cerebellar activity in humans are scarce and are indicative of hypometabolism on PET [19] and SPECT [20]. Epileptic dogs did not show any change in cerebellar metabolism interictally [21]. These imaging studies mainly estimate cerebellar cortical

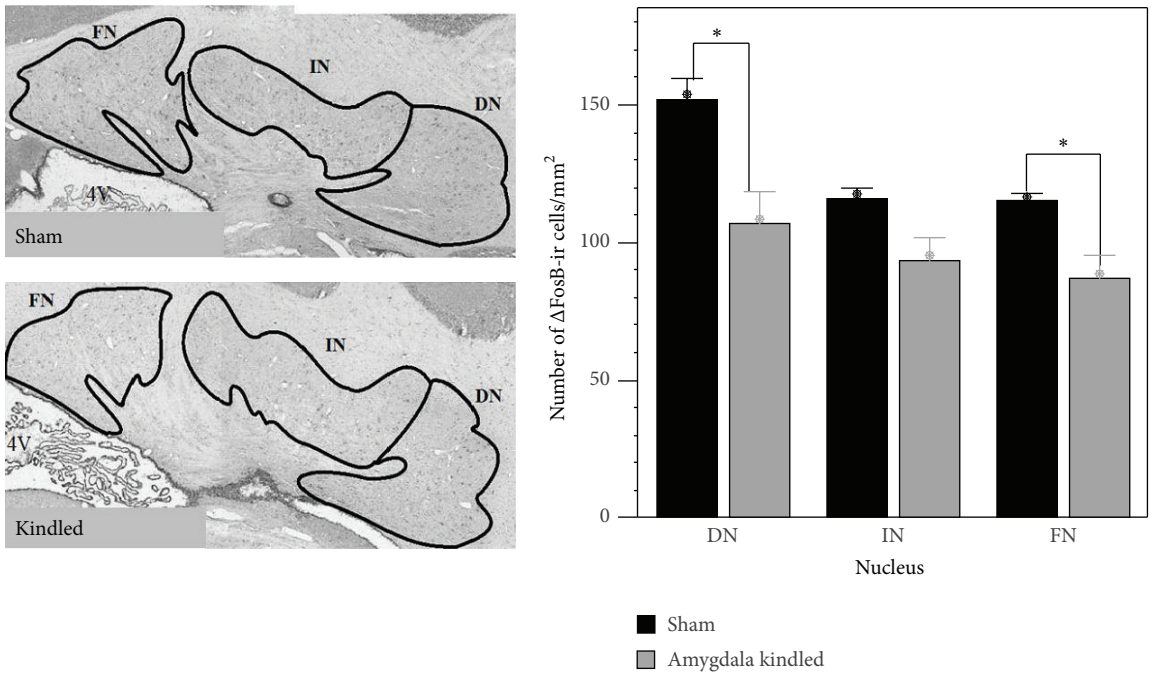

Figure 2: (a) Representative photomicrographs (4x magnification) showing ΔFosB immunoreactivity in the deep cerebellar nuclei of a sham and a fully amygdala kindled rat. Note the overall reduction in ΔFosB immunoreactivity in the kindled rat, suggesting a general decrease in neuronal activity. Coronal sections were taken at bregma level −11.30. 4V: fourth ventricle; DN: dentate nucleus; FN: fastigial nucleus; IN: interpositus nucleus. (b) Number of ΔFosB immunoreactive (ir) cells/mm^2 in the deep cerebellar nuclei. Data represent mean ± SEM of 72 sections from 6 sham animals and 129 sections from 9 kindled animals. $^*P < 0.05$.

activity, while the deep cerebellar nuclei are not evaluated this way. It is therefore not possible to compare our data with in vivo imaging data.

Some areas of the brain are more involved in generalized tonic-clonic seizures than others [9, 22–24]. The degree of involvement can be immunohistochemically determined by markers for immediately early genes, such as c-fos, FosB, and ΔFosB. C-Fos and FosB peak at two and six hours after a stimulus, respectively. ΔFosB is a highly stable FosB isoform that persists in the brain for several weeks after an initial stimulus [25]. Since the kindling protocol involves repetitive stimuli with interstimulus intervals of more than six hours, we chose to determine the ΔFosB immunopositive cell density as a marker of neuronal activation. To the best of our knowledge, no data are available in literature on basal cerebellar ΔFosB levels nor on cerebellar ΔFosB expression in epilepsy. Our results in sham rats reveal that basal expression of ΔFosB is present in all deep cerebellar nuclei and that, among the deep nuclei, the DN contains the highest density of ΔFosB immunopositive cells. The DN receives input from the more lateral parts of the cerebellar cortex while IN and FN receive input from the vermian cortex (for a review see Voogd [26]). Our data suggest that, in shams, the vermian cortex has a stronger inhibitory effect on its target nuclei than the cortex of the cerebellar hemispheres.

Furthermore, Fos immunoreactivity has been described to occur in three subcellular expression patterns, that is, solely nuclear, solely cytoplasmic, and both [27]. We found cells with nuclear ΔFosB immunoreactivity as well as cells with cytoplasmic staining. This phenomenon has been described for the hippocampus, dentate gyrus, and amygdala by others [28] and appears to be present in the deep cerebellar nuclei as well. The implication of this finding is unclear as cytoplasmic Fos staining has been described weeks to months after a stimulus and has been related to damaged or dying cells [29], while others suggest that this type of expression is related to a mechanism counteracting excitotoxicity [27, 30].

COX is a large transmembrane protein located in mitochondria. It transforms redox energy from the oxidative respiratory chain into a proton-motive force across the mitochondrial membrane. In this process, it receives an electron from four cytochrome c proteins and donates these electrons to free oxygen molecules, thereby converting them to water [31, 32]. Under physiological conditions, COX is involved in the cellular energy supply, while, in the process of seizure-induced neurodegeneration, it plays a role in the activation of proapoptotic pathways [12, 33–37]. Here, we used COX as a marker of oxidative metabolism. COX activity has been shown in the rat cerebellum previously (e.g., by using spectrophotometry and immunoblot [38]), but cerebellar COX expression has not been evaluated before using COX histology. On the other hand, COX histology has been used before to quantify the degree of cerebral oxidative metabolism after electrical stimulation in the rat [18].

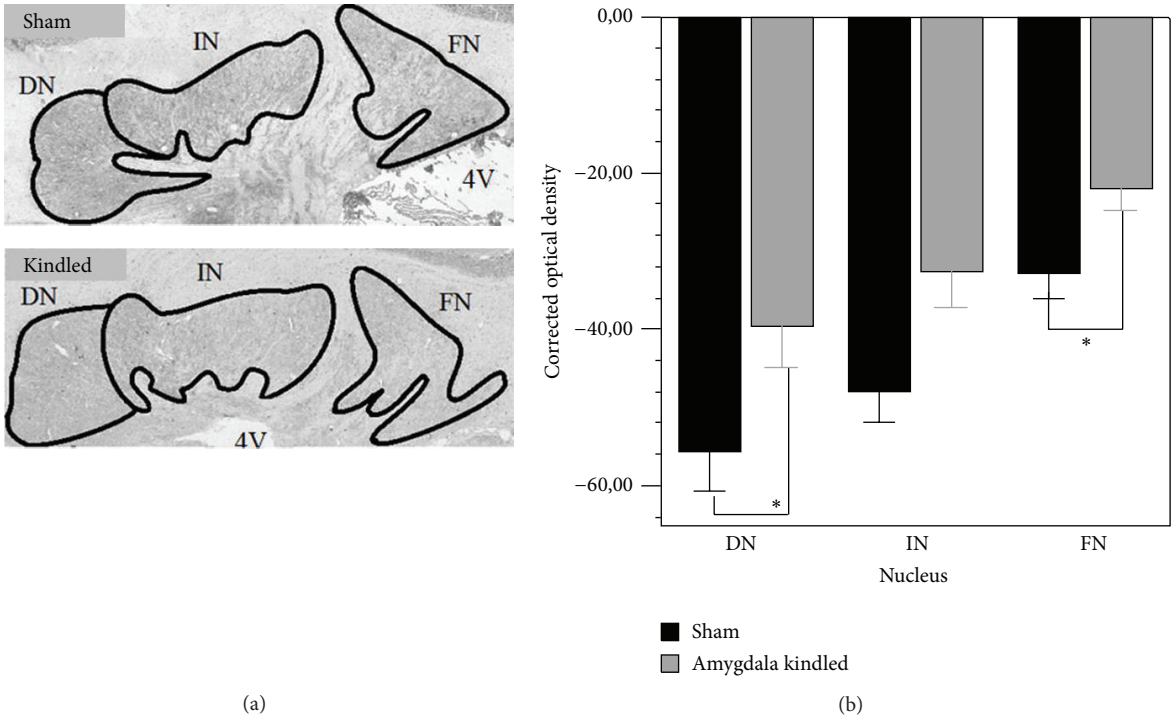

Figure 3: (a) Representative photomicrographs (4x magnification) showing COX activity in the deep cerebellar nuclei of a sham and a fully amygdala kindled rat. Note the overall reduction in COX activity in the kindled rat, suggesting a general decrease in neuronal activity. Coronal sections were taken at bregma level −11.30. 4V: fourth ventricle; DN: dentate nucleus; IN: interpositus nucleus; FN: fastigial nucleus. (b) Corrected optical density of COX activity in the deep cerebellar nuclei. The optical density was corrected for background staining by subtracting the optical density of the adjacent white matter, leading to a negative value. Data represent mean ± SEM of 101 sections from 6 sham animals and 92 sections from 6 kindled animals. $^{*}P < 0.05$.

4.2. Epilepsy Affects Activity of the Deep Cerebellar Nuclei. In kindled animals, the FN and DN showed the largest reduction in ΔFosB expression. Our COX data indicate as well that FN and DN are more affected by kindling than the IN (see Figure 3).

Apparently, amygdala kindling decreases FN and DN activity more than it reduces the activity of IN. This may be the result of direct antidromic effects of electrical stimulation of the amygdala, bearing in mind the possible anatomical connections between the FN, the DN, and the amygdala [38]. These connections have been suggested to exist based on several findings. First, changes in amygdala-related behaviour have been observed following low frequency stimulation of the FN [39] or lesioning of the deep cerebellar nuclei [40]. Second, electrophysiological studies have shown that both low [39] and higher frequency stimulation [38] of the FN can evoke bilateral responses in hippocampus and amygdala. Third, lesioning the FN leads to a bilateral degeneration of synaptic terminals in the amygdala [38]. Alternatively, the cerebellar nuclei may have been affected by the generalized seizures characterizing this model. In line with this notion, cerebellar changes have also been found in epilepsy patients suffering from generalized seizures [41, 42]. This suggestion is furthermore supported by the fact that the generalized seizure lasted up to ten minutes, while the amygdala stimulation lasted only two seconds, and by our observation that there were no left/right differences in staining patterns. Thus, decreased activity of the deep cerebellar nuclei may have been secondary to multiple generalized seizures.

Generalized seizures are associated with increased activity of the cerebellar cortex [5–11]. This cortex has purely inhibitory output [14] provided by GABAergic Purkinje cells [13] and projecting to the deep cerebellar nuclei. Decreased activity of the deep cerebellar nuclei could therefore result from ictally increased Purkinje cell firing. Experimental activation of the Purkinje fibers by electrical stimulation of the cerebellar cortex has anticonvulsive effects in animals [43, 44] and has been investigated as an anticonvulsive therapy in humans as well, with varying results [45–48]. To treat a condition that is associated with increased activity of the cerebellar cortex by activating this same cerebellar cortex may sound contradictory. The expected anticonvulsive effect can best be explained by its subsequent modulation of the deep cerebellar nuclei. Modulation of the deep cerebellar nuclei using electrical stimulation has been performed in an attempt to treat epilepsy patients [49–53], with varying results.

Output of the FN is putatively glutamatergic [53] and decreased activity of the FN may lead to a decreased activation of its most important target structure, the thalamus. This may facilitate further spread of seizures, since the thalamus has been shown to play an important role in seizure control [54–56]. Hence, the FN is of particular interest with regard to the treatment of epilepsy. It has been shown previously that both low frequency stimulation of this nucleus and

stimulation of the vermian cortex (which projects to the FN) are anticonvulsive [44, 52]. In contrast, GABA agonist injections into the FN significantly decrease seizure threshold [57]. Furthermore, complete destruction of the FN is proconvulsive, while partial destruction inhibits seizures [58]. In addition, FN lesions abolish the anticonvulsive effects of vermis stimulation [59]. On the other hand, low frequency stimulation of the DN does not affect seizure activity [60] and GABAergic injections into the DN do not affect seizures [57]. This may mean that the role of the DN in seizure control is less prominent.

5. Conclusion

The results from this study suggest that the deep cerebellar nuclei are hypoactive in amygdala kindled rats. This hypoactivity was most pronounced in the FN. Functionally located between limbic system, seizure generator, and thalamus, seizure propagator, the FN is an interesting target for epilepsy treatment.

Abbreviations

BOLD:	Blood flow and blood oxygen level-dependent
DN:	Dentate nucleus of the cerebellum
IN:	Interpositus nucleus of the cerebellum
FN:	Fastigial nucleus of the cerebellum
COX:	Cytochrome C oxidase
pre-KADT:	Prekindling afterdischarge threshold
post-KADT:	Postkindling afterdischarge threshold
OD:	Optical density.

Disclosure

Part of this work has been part of a Ph.D. thesis entitled "Deep brain stimulation and the cerebellum" by V. Moers-Hornikx, which can be found online at http://digitalarchive.maastrichtuniversity.nl/fedora/get/guid:fd1689e7-39a2-4d08-ba5d-36a8ea1450b0/ASSET1.

Conflict of Interests

The authors declare that there is no conflict of interests regarding the publication of this paper.

References

[1] J. D. Schmahmann, "Disorders of the cerebellum: ataxia, dysmetria of thought, and the cerebellar cognitive affective syndrome," *Journal of Neuropsychiatry and Clinical Neurosciences*, vol. 16, no. 3, pp. 367–378, 2004.

[2] A. H. Mesiwala, J. D. Kuratani, A. M. Avellino, T. S. Roberts, M. A. Sotero, and R. G. Ellenbogen, "Focal motor seizures with secondary generalization arising in the cerebellum: case report and review of the literature," *Journal of Neurosurgery*, vol. 97, no. 1, pp. 190–196, 2002.

[3] O. Delalande, D. Rodriguez, C. Chiron, and M. Fohlen, "Successful surgical relief of seizures associated with hamartoma of the floor of the fourth ventricle in children: report of two cases," *Neurosurgery*, vol. 49, no. 3, pp. 726–731, 2001.

[4] Y. C. Gan, M. B. C. Connolly, and P. Steinbok, "Epilepsy associated with a cerebellar arachnoid cyst: seizure control following fenestration of the cyst," *Child's Nervous System*, vol. 24, no. 1, pp. 125–134, 2008.

[5] K. Gale, "Subcortical structures and pathways involved in convulsive seizure generation," *Journal of Clinical Neurophysiology*, vol. 9, no. 2, pp. 264–277, 1992.

[6] C. Iadecola, G. Yang, T. J. Ebner, and G. Chen, "Local and propagated vascular responses evoked by focal synaptic activity in cerebellar cortex," *Journal of Neurophysiology*, vol. 78, no. 2, pp. 651–659, 1997.

[7] G. Yang and C. Iadecola, "Activation of cerebellar climbing fibers increases cerebellar blood flow: role of glutamate receptors, nitric oxide, and cGMP," *Stroke*, vol. 29, no. 2, pp. 499–508, 1998.

[8] A. D. Norden and H. Blumenfeld, "The role of subcortical structures in human epilepsy," *Epilepsy and Behavior*, vol. 3, no. 3, pp. 219–231, 2002.

[9] H. Blumenfeld, G. I. Varghese, M. J. Purcaro et al., "Cortical and subcortical networks in human secondarily generalized tonic-clonic seizures," *Brain*, vol. 132, no. 4, pp. 999–1012, 2009.

[10] T. Auer, K. Veto, T. Dóczi et al., "Identifying seizure-onset zone and visualizing seizure spread by fMRI: a case report," *Epileptic Disorders*, vol. 10, no. 2, pp. 93–100, 2008.

[11] J. H. Won, J. D. Lee, T. S. Chung, C. Y. Park, and B. I. Lee, "Increased contralateral cerebellar uptake of technetium-99m-HMPAO on ictal brain SPECT," *Journal of Nuclear Medicine*, vol. 37, no. 3, pp. 426–429, 1996.

[12] A. Ableitner and A. Herz, "Changes in local cerebral glucose utilization induced by the β-carbolines FG 7142 and DMCM reveal brain structures involved in the control of anxiety and seizure activity," *The Journal of Neuroscience*, vol. 7, no. 4, pp. 1047–1055, 1987.

[13] A. Salgado Benitez, R. Briones, and A. Fernandez Guardiola, "Purkinje cell responses to a cerebral penicillin-induced epileptogenic focus in the cat," *Epilepsia*, vol. 23, no. 6, pp. 597–606, 1982.

[14] M. Ito, M. Yoshida, K. Obata, N. Kawai, and M. Udo, "Inhibitory control of intracerebellar nuclei by the Purkinje cell axons," *Experimental Brain Research*, vol. 10, no. 1, pp. 64–80, 1970.

[15] G. Paxinos and C. Watson, *The Rat Brain in Stereotaxic Coordinates*, Academic Press, New York, NY, USA, 4th edition, 1998.

[16] R. J. Racine, "Modification of seizure activity by electrical stimulation: II. Motor seizure," *Electroencephalography and Clinical Neurophysiology*, vol. 32, no. 3, pp. 281–294, 1972.

[17] S. K. H. Tan, M. L. F. Janssen, A. Jahanshahi et al., "High frequency stimulation of the subthalamic nucleus increases c-fos immunoreactivity in the dorsal raphe nucleus and afferent brain regions," *Journal of Psychiatric Research*, vol. 45, no. 10, pp. 1307–1315, 2011.

[18] R. Vlamings, V. Visser-Vandewalle, R. Kozan, S. Kaplan, H. W. M. Steinbusch, and Y. Temel, "Bilateral high frequency stimulation of the subthalamic nucleus normalizes COX activity in the substantia nigra of Parkinsonian rats," *Brain Research*, vol. 1288, pp. 143–148, 2009.

[19] G. Schlaug, C. Antke, H. Holthausen et al., "Ictal motor signs and interictal regional cerebral hypometabolism," *Neurology*, vol. 49, no. 2, pp. 341–350, 1997.

[20] M. J. Yune, J. D. Lee, Y. H. Ryu, D. I. Kim, B. I. Lee, and S. J. Kim, "Ipsilateral thalamic hypoperfusion on interictal SPECT in temporal lobe epilepsy," *Journal of Nuclear Medicine*, vol. 39, no. 2, pp. 281–285, 1998.

[21] V. Martlé, K. Peremans, K. Audenaert et al., "Regional brain perfusion in epileptic dogs evaluated by technetium-99m-Ethyl cysteinate dimer spect," *Veterinary Radiology & Ultrasound*, vol. 50, no. 6, pp. 655–659, 2009.

[22] W. Loscher, U. Ebert, U. Wahnschaffe, and C. Rundfeldt, "Susceptibility of different cell layers of the anterior and posterior part of the piriform cortex to electrical stimulation and kindling: comparison with the basolateral amygdala and 'area tempestas'," *Neuroscience*, vol. 66, no. 2, pp. 265–276, 1995.

[23] B. J. Weder, K. Schindler, T. J. Loher et al., "Brain areas involved in medial temporal lobe seizures: a principal component analysis of ictal SPECT data," *Human Brain Mapping*, vol. 27, no. 6, pp. 520–534, 2006.

[24] K. A. Schindler, S. Bialonski, M.-T. Horstmann, C. E. Elger, and K. Lehnertz, "Evolving functional network properties and synchronizability during human epileptic seizures," *Chaos*, vol. 18, no. 3, Article ID 033119, 2008.

[25] E. J. Nestler, "Transcriptional mechanisms of addiction: role of ΔFosB," *Philosophical Transactions of the Royal Society of London Series B: Biological Sciences*, vol. 363, no. 1507, pp. 3245–3255, 2008.

[26] J. Voogd, "The human cerebellum," *Journal of Chemical Neuroanatomy*, vol. 26, no. 4, pp. 243–252, 2003.

[27] X.-Q. Duan, S.-L. Wu, T. Li et al., "Expression and significance of three types of Fos-immunoreactive cells after gamma knife irradiation of the forebrain in the rat," *Neuroscience Research*, vol. 33, no. 2, pp. 99–104, 1999.

[28] M. Dragunow, "Presence and induction of Fos B-like immunoreactivity in neural, but not non-neural, cells in adult rat brain," *Brain Research*, vol. 533, no. 2, pp. 324–328, 1990.

[29] R. J. Smeyne, M. Vendrell, M. Hayward et al., "Continuous c-fos expression precedes programmed cell death in vivo," *Nature*, vol. 363, no. 6425, pp. 166–169, 1993.

[30] G. M. Kasof, A. Mandelzys, S. D. Maika, R. E. Hammer, T. Curran, and J. I. Morgan, "Kainic acid-induced neuronal death is associated with DNA damage and a unique immediate-early gene response in c-fos-lacZ transgenic rats," *Journal of Neuroscience*, vol. 15, no. 6, pp. 4238–4249, 1995.

[31] M. Wikström, "Cytochrome c oxidase: 25 Years of the elusive proton pump," *Biochimica et Biophysica Acta—Bioenergetics*, vol. 1655, no. 1–3, pp. 241–247, 2004.

[32] P. Brzezinski and R. B. Gennis, "Cytochrome c oxidase: exciting progress and remaining mysteries," *Journal of Bioenergetics and Biomembranes*, vol. 40, no. 5, pp. 521–531, 2008.

[33] X. Saelens, N. Festjens, L. Vande Walle, M. van Gurp, G. van Loo, and P. Vandenabeele, "Toxic proteins released from mitochondria in cell death," *Oncogene*, vol. 23, no. 16, pp. 2861–2874, 2004.

[34] J. Niquet, H. Liu, and C. G. Wasterlain, "Programmed neuronal necrosis and status epilepticus," *Epilepsia*, vol. 46, no. supplement 5, pp. 43–48, 2005.

[35] T. Li, C. Lu, Z. Xia, B. Xiao, and Y. Luo, "Inhibition of caspase-8 attenuates neuronal death induced by limbic seizures in a cytochrome c-dependent and Smac/DIABLO-independent way," *Brain Research*, vol. 1098, no. 1, pp. 204–211, 2006.

[36] Y.-C. Chuang, "Mitochondrial dysfunction and oxidative stress in seizure-induced neuronal cell death," *Acta Neurologica Taiwanica*, vol. 19, no. 1, pp. 3–15, 2010.

[37] S. Zhao, E. R. Aviles Jr., and D. G. Fujikawa, "Nuclear translocation of mitochondrial cytochrome c, lysosomal cathepsins B and D, and three other death-promoting proteins within the first 60 minutes of generalized seizures," *Journal of Neuroscience Research*, vol. 88, no. 8, pp. 1727–1737, 2010.

[38] R. G. Heath and J. W. Harper, "Ascending projections of the cerebellar fastigial nucleus to the hippocampus, amygdala, and other temporal lobe sites: evoked potential and histological studies in monkeys and cats," *Experimental Neurology*, vol. 45, no. 2, pp. 268–287, 1974.

[39] R. S. Snider and A. Maiti, "Cerebellar contributions to the Papez circuit," *Journal of Neuroscience Research*, vol. 2, no. 2, pp. 133–146, 1976.

[40] G. G. Berntson and M. W. Torello, "Attenuation of septal hyperemotionality by cerebellar fastigial lesions in the rat," *Physiology and Behavior*, vol. 24, no. 3, pp. 547–551, 1980.

[41] B. P. Hermann, K. Bayless, R. Hansen, J. Parrish, and M. Seidenberg, "Cerebellar atrophy in temporal lobe epilepsy," *Epilepsy and Behavior*, vol. 7, no. 2, pp. 279–287, 2005.

[42] Y. Li, H. Du, B. Xie et al., "Cerebellum abnormalities in idiopathic generalized epilepsy with generalized tonic-clonic seizures revealed by diffusion tensor imaging," *PLoS ONE*, vol. 5, no. 12, Article ID e15219, 2010.

[43] H. Bantli, J. R. Bloedel, G. Anderson, R. McRoberts, and E. Sandberg, "Effects of stimulating the cerebellar surface on the activity in penicillin foci," *Journal of Neurosurgery*, vol. 48, no. 1, pp. 69–84, 1978.

[44] L. S. Godlevskii, K. I. Stepanenko, B. A. Lobasyuk, E. V. Sarakhan, and L. M. Bobkova, "The effects of electrical stimulation of the paleocerebellar cortex on penicillin-induced convulsive activity in rats," *Neuroscience and Behavioral Physiology*, vol. 34, no. 8, pp. 797–802, 2004.

[45] I. S. Cooper, I. Amin, M. Riklan, J. M. Waltz, and T. P. Poon, "Chronic cerebellar stimulation in epilepsy. Clinical and anatomical studies," *Archives of Neurology*, vol. 33, no. 8, pp. 559–570, 1976.

[46] J. M. van Buren, J. H. Wood, J. Oakley, and F. Hambrecht, "Preliminary evaluation of cerebellar stimulation by double-blind stimulation and biological criteria in the treatment of epilepsy," *Journal of Neurosurgery*, vol. 48, no. 3, pp. 407–416, 1978.

[47] G. D. S. Wright, D. L. McLellan, and J. G. Brice, "A double-blind trial of chronic cerebellar stimulation in twelve patients with severe epilepsy," *Journal of Neurology Neurosurgery and Psychiatry*, vol. 47, no. 8, pp. 769–774, 1984.

[48] R. Davis and S. E. Emmonds, "Cerebellar stimulation for seizure control: 17-year study," *Stereotactic and Functional Neurosurgery*, vol. 58, no. 1–4, pp. 200–208, 1992.

[49] M. Sramka and S. A. Chkhenkeli, "Clinical experience in intraoperational determination of brain inhibitory structures and application of implanted neurostimulators in epilepsy," *Stereotactic and Functional Neurosurgery*, vol. 54-55, pp. 56–59, 1990.

[50] M. Sramka, G. Fritz, M. Galanda, and P. Nádvornik, "Some observations in treatment stimulation of epilepsy," *Acta Neurochirurgica*, vol. 23, pp. 257–262, 1976.

[51] J. J. Hablitz and G. Rea, "Cerebellar nuclear stimulation in generalized penicillin epilepsy," *Brain Research Bulletin*, vol. 1, no. 6, pp. 599–601, 1976.

[52] S. Wang, D. C. Wu, M. P. Ding et al., "Low-frequency stimulation of cerebellar fastigial nucleus inhibits amygdaloid kindling acquisition in Sprague-Dawley rats," *Neurobiology of Disease*, vol. 29, no. 1, pp. 52–58, 2008.

[53] C. Batini, C. Compoint, C. Buisseret-Delmas, H. Daniel, and M. Guegan, "Cerebellar nuclei and the nucleocortical projections in the rat: retrograde tracing coupled to GABA and glutamate immunohistochemistry," *Journal of Comparative Neurology*, vol. 315, no. 1, pp. 74–84, 1992.

[54] R. Fisher, V. Salanova, T. Witt et al., "Electrical stimulation of the anterior nucleus of thalamus for treatment of refractory epilepsy," *Epilepsia*, vol. 51, no. 5, pp. 899–908, 2010.

[55] Q. Zhang, Z.-C. Wu, J.-T. Yu et al., "Anticonvulsant effect of unilateral anterior thalamic high frequency electrical stimulation on amygdala-kindled seizures in rat," *Brain Research Bulletin*, vol. 87, no. 2-3, pp. 221–226, 2012.

[56] S. Takebayashi, K. Hashizume, T. Tanaka, and A. Hodozuka, "Anti-convulsant effect of electrical stimulation and lesioning of the anterior thalamic nucleus on kainic acid-induced focal limbic seizure in rats," *Epilepsy Research*, vol. 74, no. 2-3, pp. 163–170, 2007.

[57] J. W. Miller, B. C. Gray, G. M. Turner, P. Genton, and A. Portera-Sanchez, "Role of the fastigial nucleus in generalized seizures as demonstrated by GABA agonist microinjections," *Epilepsia*, vol. 34, no. 6, pp. 973–978, 1993.

[58] J. K. Min, P. A. Valentine, and G. C. Teskey, "Effect of complete and partial bilateral lesions of the deep cerebellar nuclei on amygdaloid kindling in rats," *Epilepsia*, vol. 39, no. 7, pp. 692–699, 1998.

[59] A. Maiti and R. S. Snider, "Cerebellar control of basal forebrain seizures: amygdala and hippocampus," *Epilepsia*, vol. 16, no. 3, pp. 521–533, 1975.

[60] S. A. Chkhenkeli, M. Šramka, G. S. Lortkipanidze et al., "Electrophysiological effects and clinical results of direct brain stimulation for intractable epilepsy," *Clinical Neurology and Neurosurgery*, vol. 106, no. 4, pp. 318–329, 2004.

Hindawi Publishing Corporation
BioMed Research International
Volume 2015, Article ID 267989, 8 pages
http://dx.doi.org/10.1155/2015/267989

Research Article

Epitope Fingerprinting for Recognition of the Polyclonal Serum Autoantibodies of Alzheimer's Disease

Luiz Carlos de Oliveira-Júnior,[1,2] Fabiana de Almeida Araújo Santos,[3] Luiz Ricardo Goulart,[3] and Carlos Ueira-Vieira[1]

[1]*Laboratório de Genética, Instituto de Genética e Bioquímica, Universidade Federal de Uberlândia, Rua Acre s/n, Bloco 2E sala 230, Campus Umuarama, 38400-902 Uberlândia, MG, Brazil*
[2]*Faculdade de Medicina, Universidade Federal de Uberlândia, Avenida Para 1720, Bloco 2U sala 23, Campus Umuarama, 38400-902 Uberlândia, MG, Brazil*
[3]*Laboratório de Nanobiotecnologia, Instituto de Genética e Bioquímica, Universidade Federal de Uberlândia, Rua Acre s/n, Bloco 2E sala 230, Campus Umuarama, 38400-902 Uberlândia, MG, Brazil*

Correspondence should be addressed to Carlos Ueira-Vieira; ueira@ingeb.ufu.br

Received 28 June 2014; Accepted 18 February 2015

Academic Editor: Giovanni Scapagnini

Autoantibodies (aAb) associated with Alzheimer's disease (AD) have not been sufficiently characterized and their exact involvement is undefined. The use of information technology and computerized analysis with phage display technology was used, in the present research, to map the epitope of putative self-antigens in AD patients. A 12-mer random peptide library, displayed on M13 phages, was screened using IgG from AD patients with two repetitions. Seventy-one peptides were isolated; however, only 10 were positive using the Elisa assay technique (Elisa Index > 1). The results showed that the epitope regions of the immunoreactive peptides, identified by phage display analysis, were on the exposed surfaces of the proteins. The putative antigens MAST1, Enah, MAO-A, X11/MINT1, HGF, SNX14, ARHGAP 11A, APC, and CENTG3, which have been associated with AD or have functions in neural tissue, may indicate possible therapeutic targets.

1. Introduction

Alzheimer's disease (AD) is the most important cause of dementia. Its prevalence increases with age and, together with increasing life expectancy, has created the expectation of an increase in the number of cases, especially in developed countries [1–4]. Due to its devastating effect on cognition and high social and economic cost [5, 6], AD has become an important subject of research and, due to its characteristics, is also a challenge. This is especially true since the neurodegenerative process may progress for many years before clear behavioral and cognitive symptoms permit diagnosis [7, 8].

Following the original description of AD in 1906, the presence of β-amyloid (Aβ) deposits, senile plaques (SP), and neurofibrillary tangles (NFT) has been established as key markers of the disease [9, 10]. The search for improved understanding of its development has focused on these components, which have also been linked to numerous other neurobiological processes as well as genetic and environmental factors [11]. Despite extensive research, our understanding of AD is still limited because accurate diagnosis of the onset of the disease is often not possible [12].

Soon after it was observed that SP and NFT are accompanied by an inflammatory process in the immune system, this system began to be investigated regarding its role in AD pathogenesis [13, 14]. As in other central nervous system diseases, Parkinson's disease, Lewy corpuscles dementia, and obsessive compulsive disorder, there appears to be a relationship between inflammatory processes and humoral response to AD [15, 16].

Several studies have discovered an abundant presence of antibodies directed at targets in brain neural tissue, cerebrospinal fluid, and the serum of patients with AD. Antibodies against neurotransmitter receptors (glutamate,

dopamine, serotonin, and acetylcholine), enzymes (ATP synthase and aldolase), cytoskeletal proteins, and microglia have been described [17–20]. Their role in the development of Alzheimer's disease is still uncertain and may simply be the result of neuronal death from exposure to autoantigens or may have some contribution to the pathological process [21–23]. The characterization of these autoantibodies (aAb), their antigens, and their role in disease may be a means for the development of improved diagnostic tools and the identification of new therapeutic targets.

Phage display (Ph.D.) technology is useful for the identification of peptides or antibodies on the surface of the filamentous M13 bacteriophage capsid. This capsule permits exposure to an extensive diversity of peptides that can bind to various targets and be identified using peptide library techniques. This methodology has been proven useful not only for the selection of peptides that mimic proteins but also for the identification and description of epitopes recognized by antibodies [24, 25]. It also allows for the production of the monoclonal antibodies used to treat several diseases, vaccines, and diagnostic tests as well as several uses in nanotechnology [26].

Phage display findings can be analyzed with different bioinformatic tools: the identification of consensus motifs among selected sequences, the identification of possible targets by linear and conformational (3D structure) comparison with protein databanks, and assessments of their putative epitopes with their degree of antigenicity. This information can be extremely useful for planning experiments, designing drugs, and other applications [27–29].

The present study identified mimetic peptides of target antigens in the circulating IgG present in the serum of patients with AD. Our use of the phage display technique, together with bioinformatic tools, may represent one of the first evidences of the presence of autoantibodies and their putative epitope mapping, in AD.

2. Materials and Methods

2.1. Recruitment of Patients, Diagnostic Criteria, and Sample Collection. Serum samples from AD patients and healthy controls, matched by sex and age, were obtained from the University Hospital of Uberlandia. For the diagnosis of dementia, the DSM-IV TR criteria were used [30] and for the diagnosis of AD we used the criteria of the National Institute of Neurological and Communicative Disorders and Stroke/Alzheimer's Disease and Related Disorders Association (NINCDS-ADRDA) [31]. Patients were stratified according to the Clinical Dementia Rating (CDR), Portuguese version [32]. The controls were evaluated using the Mini-Mental State Exam [33]. This research was approved by the Research Ethics Committee of the Federal University of Uberlandia (number 304/09).

2.2. Selection of Peptides That Mimic AD Self-Antigens (Mimotopes). The phage selection was performed using a pool of sera from AD patients and healthy (control) individuals. Immunoglobulin G (IgG) was secured using magnetic beads coupled to protein G Dynabeads (Invitrogen). For subtraction of nonspecific peptides, 10 μL of the M13 phage library (PhD12, New England Biolabs Inc.; 1×10^{11} viral particles) was added to 190 μL of TBS-Tween 0.1%. After 30 minutes of incubation, magnetic separation was performed. The phage eluate was subtracted two more times prior to the positive selection, which was performed for 30 minutes against IgG-coupled beads of AD patients, completing one selection cycle. This procedure was repeated twice. Finally, bound phages were recovered from the beads by acid elution (500 μL of glycine, pH 2) for 10 minutes and then neutralized with 75 μL of Tris (pH 9).

Selected phages were amplified, purified, and titrated according to the Ph.D. Phage Display Libraries Instruction Manual (New England Biolabs).

2.3. DNA Extraction and Sequencing. After three rounds of selection, 96 blue colonies were randomly selected and their phage single strand DNA was isolated using iodide buffer extraction procedures [34].

2.4. Bead-ELISA (Enzyme Linked Immunosorbent Assay in Bead). The selected peptide-phage clones were used in the bead-ELISA assay against IgG from controls and AD patients to evaluate their reactivity and specificity.

Fifty microliters of phage supernatant was incubated with IgG coupled in magnetic beads (Invitrogen) for one hour with stirring, at room temperature. Using a magnetic apparatus, the microspheres were precipitated, washed six times with TBS-T 0.1%, and incubated with monoclonal anti-M13 peroxidase conjugate (GE Healthcare) diluted 1 : 5000 in TBS-T 0.1% and 5% BSA for one hour with stirring, at room temperature. Microspheres were again precipitated and washed six times and the reaction was observed with buffer orthophenylenediamine (OPD) to 1 mg/mL plus 3% hydrogen peroxide (H_2O_2). The results were expressed as an arbitrary ELISA Index (EI) and calculated as follows: EI = Abs of serum sample/cut-off, where the cut-off was determined as the mean absorbance of the negative control sera plus two standard deviations. Values of EI > 1.0 were considered positive.

2.5. Bioinformatics. The vector sequences were removed and the deductions of peptide sequences were performed using the ExPASy Translate Tool (http://web.expasy.org/translate). Afterwards, the peptide sequences were submitted to *in silico* analysis (Figure 1).

For a more detailed analysis, the sequence of positive peptides selected by the ELISA assay (EI > 1) was subjected to alignment using the BLAST tool (http://blast.ncbi.nlm.nih.gov/) and compared with those available in the database of nonredundant protein sequences using the BLASTP algorithm, limiting the search to *Homo sapiens* sequences.

The proteins indicated in alignment were selected for the next step of the analysis. We excluded unnamed sequences which had only been predicted or that were from unknown proteins. Those sequences with low *E*-value were analyzed to determine whether the region of alignment with the peptide

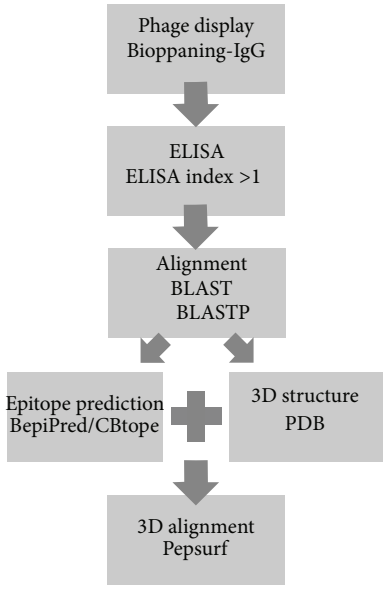

Figure 1: Bioinformatics workflow.

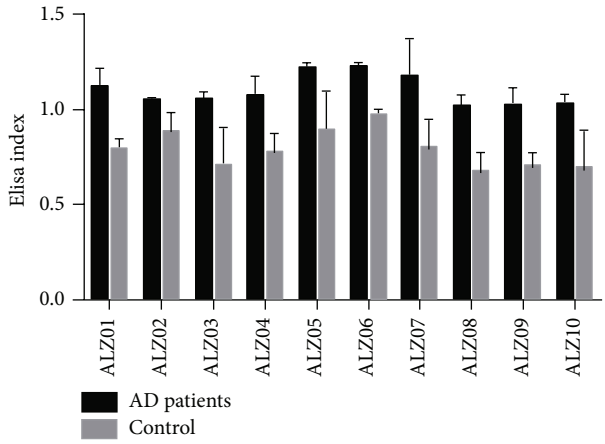

Figure 2: Detection of IgG antimimotope in serum from patients with Alzheimer's disease by Elisa using peptide-phage selected by phage display. Values of EI > 1.0 were considered positive (Student's t-test, $P < 0.05$). For clarity, peptides with Elisa Index values lower than 1 were omitted.

was a predicted epitope using BepiPred (http://www.cbs.dtu.dk/services/BepiPred/) [35] for linear B-cell epitopes and CBTOPE (http://www.imtech.res.in/raghava/cbtope/) for conformational B-cell epitopes [36]. If the region of alignment was found to be a predicted epitope and the three-dimensional structure was available in a protein databank format (http://www.rcsb.org/pdb/home/home.do), this protein was selected for the next step of analysis.

The program PEPSURF (http://pepitope.tau.ac.il/) was used to map the putative mimotope selected by phage display in the three-dimensional protein structure of the protein [29].

2.6. Statistical Analysis. Statistical analysis was performed using the GraphPad Prism version 5.00 (GraphPad Software Inc.).

3. Results

In this study 100 patients who had registered cognitive disorders were evaluated. Only 10 of these patients had complete AD diagnosis with laboratory tests, imaging, and assessment of cognitive function by neuropsychological tests. As paired healthy control (HC), we used 10 cognitively healthy individuals.

Phage display selection of a 12-mer random peptide library generated 75 peptides, of which 71 were distinct sequences. A phage ELISA assay was performed with these clones using a pool of serum from the patients and from the controls. The result showed that of the 71 peptides, only 10 were highly reactive mimotopes when compared with the controls (IE > 1). This suggested that circulating IgG from AD patients recognizes these specific peptides (Figure 2).

Those peptides with distinct sequences were subsequently chosen for in-depth characterization through bioinformatics. The data are presented in Table 1. As can be seen, only nine sequences of peptides led to the identification of targets according to established criteria for the bioinformatics analysis.

After the initial identification of targets for alignment and prediction of linear and structural epitopes, the three-dimensional alignment, using the PepSurf program, was performed. This result demonstrated that peptide sequences from phage display were mapped in exposed regions (external surfaces) of target proteins and could be accessible to antibodies (Figure 3).

4. Discussion

Phage display technology can be considered a subtractive proteomic strategy for the selection of specific molecules without known targets. This is due to its combinatorial nature, favoring the random binding to several molecules. It is, for this reason, an important tool for the identification of biomolecules because it exposes a large variety of ligands to many targets at the same time and requires only minimal knowledge of the starting proteome/immunome target [37]. However, this technology has a great disadvantage: only linear or simple cyclic peptides can be incorporated into phage pIII protein [38].

Since there was the possibility of the phage binding on components of the screening system such as plastic, magnetic bead, protein G [39], or irrelevant IgG, we performed a subtractive selection twice using IgG from a binding assay of healthy controls before selection with IgG from Alzheimer's patients. This precaution was taken to avoid the selection of peptides binding in the background.

Our selection and analysis strategy resulted in the identification of ten potential mimotopes recognized by the IgG present in the serum of patients with AD. It was possible to select peptides by phage display and prevalidate them as

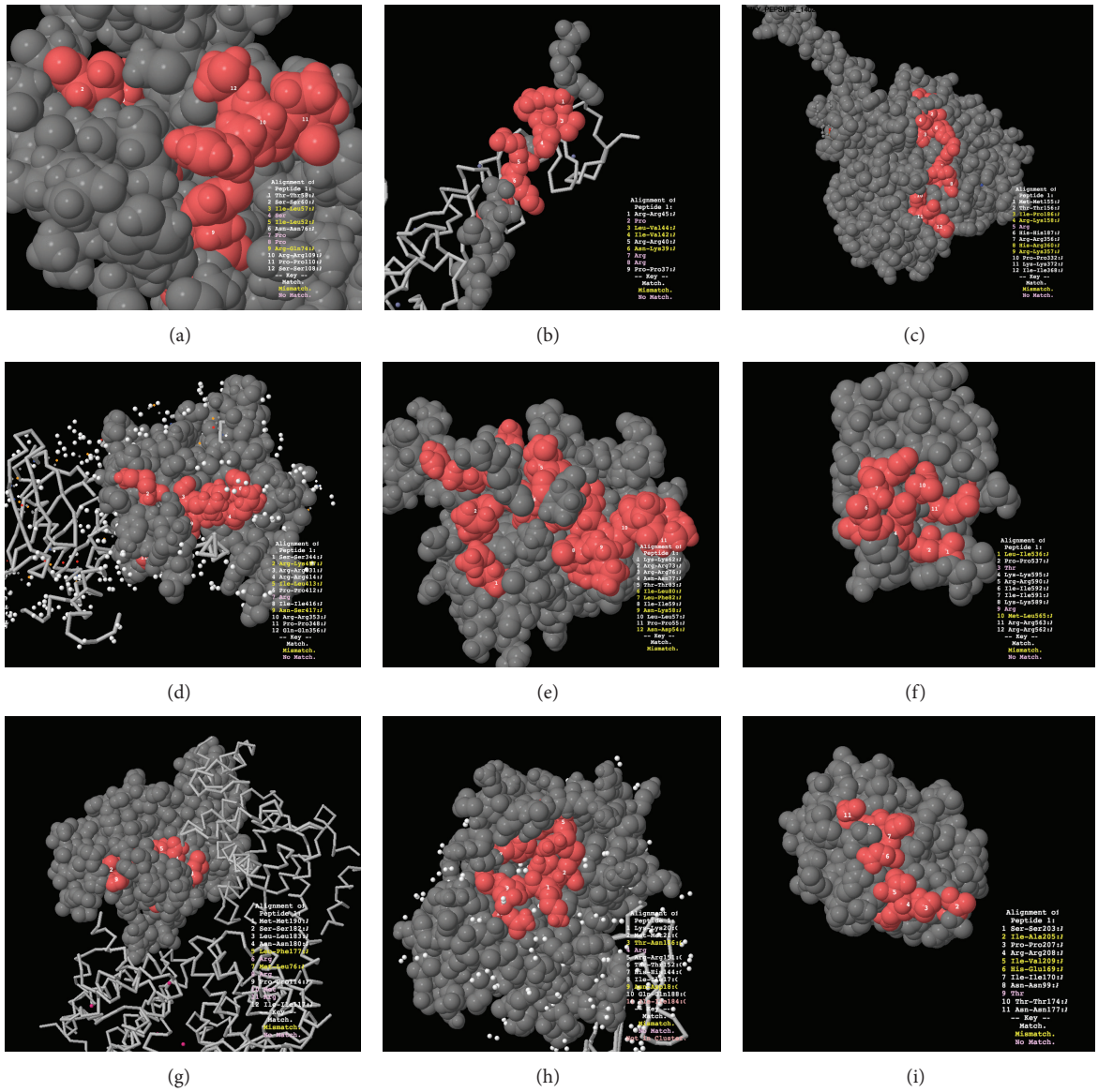

(a) (b) (c)

(d) (e) (f)

(g) (h) (i)

Figure 3: Three dimensional epitope prediction using the PepSurf program. The peptide alignment regions are shown in red. All of the peptides align with external regions. (a) MAST1; (b) Enah; (c) MAO-A; (d) X11/MINT1; (e) HGF; (f) SNX14; (g) ARHGAP 11A; (h) APC; (i) CENTG3. Source: Martz E. FirstGlance in Jmol (http://firstglance.jmol.org).

Table 1: Peptide sequence and position of alignment in putative Alzheimer's disease self-antigens.

Clone	Peptide sequence	Alignment region	Putative protein matched	PDB	Accession number NCBI
ALZ01	TSISINPPRRPS	672–683	MAST1	2M9X	AAH27985.2
ALZ02	SRPRPLIRNRRP	341–350	Enah	2XQN	AAH65238.1
ALZ03	MTIRRHRHRPKI	128–131	MAO-A	2Z5Y	P21397.1
ALZ04	SRRRIPRINRPQ	431–438	X11/MINT1	1X11	Q02410.3
ALZ05	KRRNTILINLPN	4–9	HGF	2HGF	P14210.2
ALZ06	TPIKKMIRRLPH	—	—	—	—
ALZ07	LPTKRIIKRMRR	502–508	SNX14	4BGJ	Q9Y5W7.3
ALZ08	MSLNLRMRPMRI	449–453	ARHGAP 11A	3EAP	Q6P4F7.2
ALZ09	KMTRRTHINQIS	111–115	APC	1AUT	1AUT_C
ALZ10	RSIPRIHINTTN	235–246	CENTG3	3IHW	3IHW_A

Table 2: Identity of the self-antigens mapped by mimotopes.

Database ID	Description	Protein
AAH27985.2	Microtubule associated serine/threonine kinase 1	MAST1
AAH65238.1	Enabled homolog (Drosophila)	ENAH
P21397.1	Monoamine oxidase A	MAOA
Q02410.3	Amyloid beta (A4) precursor protein-binding, family A, member 1	APBA1
P14210.2	Hepatocyte growth factor (hepapoietin A; scatter factor)	HGF
Q9Y5W7.3	Sorting nexin 14	SNX14
Q6P4F7.2	Rho GTPase activating protein 11A	ARHGAP11A
NM_000312	Protein C (inactivator of coagulation factors Va and VIIIa)	PROC
AF413079.1	Homo sapiens centaurin gamma 3 mRNA	CENTG3

potential new products for specific diagnosis of thyroid cancer [34], neurocysticercosis [40, 41], leishmaniasis, dengue, and leprosy [42]. The peptides selected in this work are also new potential tools for developing specific serum diagnostics for AD. Evaluation with large samples will be necessary for validation in serum platforms such as the ELISA assay.

Autoantibodies are important for AD progression. Patients with AD have a low titer of serum levels of the anti-beta-amyloid antibodies (Aβ1–42, Aβ1–15 and Aβ16–30) compared with age matched non-AD controls [43]. Antibodies against Aβ have potential use in AD treatment [44, 45]. However, the action of the autoantibodies on other neuroproteins is still unclear.

The putative epitopes of the self-antigens, using the mimotopes, were mapped and are presented in Table 2. The target proteins have an important function in the central nervous system or are involved in AD (Table 2).

The ALZ01 peptide is aligned with the MAST1 sequence. MAST1 is a member of the microtubule associated serine/threonine kinase family [35]. It is an important component of the postsynaptic region [46] and one of the differentially expressed genes in the brain of patients with AD [47].

The Enah or Mena proteins, with which peptide ALZ02 is aligned, are a component of the neural growth cone [48], important for neural development [49] and axonal structure [50].

Alz03 is a putative mimotope of MAO-A, an important enzyme of the catecholamine pathway. Some studies have shown changes of the catecholamine in AD. NE levels are decreased in the hippocampus of patients with AD [51]. In addition, specific variants of PS1, an important enzyme in the formation of Ab, could influence the catalytic activity of MAO-A [52].

The ALZ04 peptide sequence is aligned with the X11 protein family. These proteins, also known as Mints or APBA (APP binding family A), are multidomain adaptor proteins [53]. They are involved in many cellular processes important for neuronal function including the regulation of ion channel function, cellular traffic, synaptic vesicle docking, and exocytosis. The X11s proteins are also involved in APP processing [54, 55]. The Mint1 PTB domain interacts with APP, regulating its traffic. Several studies have shown that gene deletion or suppression interferes with the Ab levels [56].

Another interesting mimotope of a putative self-antigen identified in the present research was the HGF. This polypeptide is a growth factor that acts like a semaphorin in the neural development [57]. Some studies have shown that levels of HGF are increased in the cerebrospinal fluid of patients with AD [58]. Also, in the brain of patients with AD, there is an increase in HGF expression which may indicate a response to injury [59].

The SNX14 protein, also mapped by the peptides from phage display, is an important element for endocytosis and endosomal signaling [60]. It has been shown, in mice, that it regulates the intrinsic excitability of pyramidal neurons [61]. The SNX12, another family member of nexins sorting, is involved in the development of the cerebral cortex [62] and regulates the endocytosis of BACE-1 [63]. Its levels are diminished in the brains of AD patients [64].

The APC protein, in mice, was found to reduce the production of Ab. The mechanism involved appears to be a stimulation of the alpha secretase activity [65]. The intracerebral infusion of APC also reduced the excitotoxicity mediated by NMDA receptors [66].

The CENTG3 antibody, also known as AGAP3 and mapped by our mimotopes, is important for AMPA receptor traffic to the neural membrane during long term potentiation, which strengthens the synapse [67]. An alternative splicing variant of AGAP3, CRAG, acts like a semaphorin [68].

The involvement of aAb in neurodegenerative diseases can be varied and uncertain. Antibodies can act as receptor agonists or antagonists, coagonists, activate the complement proteins, or lead to internalization of receptors [15]. These aAb can act directly in the disease process or may be formed only as a consequence of the exposure to new antigens by neuronal death. But, interestingly, they may also become potential biomarkers to improve understanding of AD biology and progression.

The role of aAb in AD has not been determined despite frequent descriptions of its presence in the serum and

cerebrospinal fluid of AD patients. Some aAb, such as that generated against Aβ, appear to prevent the deposition and formation of fibrils and plaques by reducing neurotoxicity. Their presence in healthy individuals suggests a homeostatic role [22, 23].

Nagele et al. [69] identified several self-antigens through protein microarrays by demonstrating the presence of various aAb in the serum of patients with AD. The antigens with higher aAb reactivity were suggested as potential biomarkers. Many of the putative self-antigens identified in this study have a clear involvement with AD but the effective participation of these aAb in AD is still to be determined.

The use of mimic peptide as a diagnostic, rather than full protein, may yield increases in the specificity of the *in vitro* reaction. Since only the reactive region of the biomarker target will be in contact with the antibody, the background reactions tend to be low. Further studies with large sample sizes are necessary to define the potential of the mimotope peptide here isolated as a new biomarker.

5. Conclusion

The combination of *in silico* approaches and phage display technology was found to be an important tool in the identification of putative novel targets in Alzheimer's disease. The success of our epitope fingerprinting was based on a strategy that involved performing a subtractive selection against the IgG of AD patients. We identified mimotopes that mimic self-antigens and these mimotopes were recognized by the autoantibodies of AD patients, which may indicate potential usefulness in the diagnosis of this disease.

Conflict of Interests

The authors declare that there is no conflict of interests regarding the publication of this paper.

Acknowledgments

This research was supported by Grants from the following Brazilian research agencies: Fundação de Amparo a Pesquisa de Minas Gerais (FAPEMIG-APQ CBB-APQ-01952-13), Conselho Nacional de Desenvolvimento Científico e Tecnológico (CNPq, 445679/2014-0), and Coordenação de Aperfeiçoamento de Pessoal de Ensino Superior (CAPES).

References

[1] H. Brunnström, L. Gustafson, U. Passant, and E. Englund, "Prevalence of dementia subtypes: a 30-year retrospective survey of neuropathological reports," *Archives of Gerontology and Geriatrics*, vol. 49, no. 1, pp. 146–149, 2009.

[2] C. P. Ferri, M. Prince, C. Brayne et al., "Global prevalence of dementia: a Delphi consensus study," *The Lancet*, vol. 366, no. 9503, pp. 2112–2117, 2005.

[3] L. E. Hebert, P. A. Scherr, J. L. Bienias, D. A. Bennett, and D. A. Evans, "Alzheimer disease in the US population: prevalence estimates using the 2000 census," *Archives of Neurology*, vol. 60, no. 8, pp. 1119–1122, 2003.

[4] W. A. Rocca, A. Hofman, C. Brayne et al., "Frequency and distribution of Alzheimer's disease in Europe: a collaborative study of 1980–1990 prevalence findings," *Annals of Neurology*, vol. 30, no. 3, pp. 381–390, 1991.

[5] J. Olesen, A. Gustavsson, M. Svensson et al., "The economic cost of brain disorders in Europe," *European Journal of Neurology*, vol. 19, no. 1, pp. 155–162, 2012.

[6] L. Jönsson, M. E. Jönhagen, L. Kilander et al., "Determinants of costs of care for patients with Alzheimer's disease," *International Journal of Geriatric Psychiatry*, vol. 21, no. 5, pp. 449–459, 2006.

[7] N. C. Fox and J. M. Schott, "Imaging cerebral atrophy: normal ageing to Alzheimer's disease," *The Lancet*, vol. 363, no. 9406, pp. 392–394, 2004.

[8] R. S. Wilson, S. E. Leurgans, P. A. Boyle, and D. A. Bennett, "Cognitive decline in prodromal Alzheimer disease and mild cognitive impairment," *Archives of Neurology*, vol. 68, no. 3, pp. 351–356, 2011.

[9] E. Braak, K. Griffing, K. Arai, J. Bohl, H. Bratzke, and H. Braak, "Neuropathology of Alzheimer's disease: what is new since A. Alzheimer?" *European Archives of Psychiatry and Clinical Neuroscience*, vol. 249, no. 3, pp. S14–S22, 1999.

[10] C. R. Jack Jr., R. C. Petersen, Y. Xu et al., "Rate of medial temporal lobe atrophy in typical aging and Alzheimer's disease," *Neurology*, vol. 51, no. 4, pp. 993–999, 1998.

[11] D. J. Selkoe, "Alzheimer's disease: genes, proteins, and therapy," *Physiological Reviews*, vol. 81, no. 2, pp. 741–766, 2001.

[12] K. Gustaw-Rothenberg, A. Lerner, D. J. Bonda et al., "Biomarkers in Alzheimers disease: past, present and future," *Biomarkers in Medicine*, vol. 4, no. 1, pp. 15–26, 2010.

[13] C. Bouras, B. M. Riederer, E. Kövari, P. R. Hof, and P. Giannakopoulos, "Humoral immunity in brain aging and Alzheimer's disease," *Brain Research Reviews*, vol. 48, no. 3, pp. 477–487, 2005.

[14] P. J. Khandelwal, A. M. Herman, and C. E.-H. Moussa, "Inflammation in the early stages of neurodegenerative pathology," *Journal of Neuroimmunology*, vol. 238, no. 1-2, pp. 1–11, 2011.

[15] B. Diamond, P. T. Huerta, P. Mina-Osorio, C. Kowal, and B. T. Volpe, "Losing your nerves? Maybe it's the antibodies," *Nature Reviews Immunology*, vol. 9, no. 6, pp. 449–456, 2009.

[16] W. Maetzler, D. Berg, M. Synofzik et al., "Autoantibodies against amyloid and glial-derived antigens are increased in serum and cerebrospinal fluid of lewy body-associated dementias," *Journal of Alzheimer's Disease*, vol. 26, no. 1, pp. 171–179, 2011.

[17] M. Daniilidou, M. Tsolaki, T. Giannakouros, and E. Nikolakaki, "Detection of elevated antibodies against SR protein kinase 1 in the serum of Alzheimer's disease patients," *Journal of Neuroimmunology*, vol. 238, no. 1-2, pp. 67–72, 2011.

[18] T. V. Davydova, N. I. Voskresenskaya, V. Y. Gorbatov, V. G. Fomina, O. A. Doronina, and I. V. Maksunova, "Production of autoantibodies to glutamate during Alzheimer's dementia," *Bulletin of Experimental Biology and Medicine*, vol. 147, no. 4, pp. 405–407, 2009.

[19] E. C. Levin, N. K. Acharya, M. Han et al., "Brain-reactive autoantibodies are nearly ubiquitous in human sera and may be linked to pathology in the context of blood-brain barrier breakdown," *Brain Research*, vol. 1345, pp. 221–232, 2010.

[20] D. Vacirca, C. Barbati, B. Scazzocchio et al., "Anti-ATP synthase autoantibodies from patients with Alzheimer's disease reduce extracellular HDL level," *Journal of Alzheimer's Disease*, vol. 26, no. 3, pp. 441–445, 2011.

[21] T. Colasanti, C. Barbati, G. Rosano, W. Malorni, and E. Ortona, "Autoantibodies in patients with Alzheimer's disease: pathogenetic role and potential use as biomarkers of disease progression," *Autoimmunity Reviews*, vol. 9, no. 12, pp. 807–811, 2010.

[22] F. Neff, X. Wei, C. Nölker, M. Bacher, Y. Du, and R. Dodel, "Immunotherapy and naturally occurring autoantibodies in neurodegenerative disorders," *Autoimmunity Reviews*, vol. 7, no. 6, pp. 501–507, 2008.

[23] S. Paul, S. Planque, and Y. Nishiyama, "Immunological origin and functional properties of catalytic autoantibodies to amyloid β peptide," *The Journal of Clinical Immunology*, vol. 30, supplement 1, pp. S43–S49, 2010.

[24] H. R. Hoogenboom, A. P. de Brune, S. E. Hufton, R. M. Hoet, J.-W. Arends, and R. C. Roovers, "Antibody phage display technology and its applications," *Immunotechnology*, vol. 4, no. 1, pp. 1–20, 1998.

[25] C. Rader and C. F. Barbas, "Phage display of combinatorial antibody libraries," *Current Opinion in Biotechnology*, vol. 8, no. 4, pp. 503–508, 1997.

[26] U. Kriplani and B. K. Kay, "Selecting peptides for use in nanoscale materials using phage-displayed combinatorial peptide libraries," *Current Opinion in Biotechnology*, vol. 16, no. 4, pp. 470–475, 2005.

[27] S. F. Altschul, T. L. Madden, A. A. Schäffer et al., "Gapped BLAST and PSI-BLAST: a new generation of protein database search programs," *Nucleic Acids Research*, vol. 25, no. 17, pp. 3389–3402, 1997.

[28] J. Huang, B. Ru, and P. Dai, "Bioinformatics resources and tools for phage display," *Molecules*, vol. 16, no. 1, pp. 694–709, 2011.

[29] I. Mayrose, T. Shlomi, N. D. Rubinstein et al., "Epitope mapping using combinatorial phage-display libraries: a graph-based algorithm," *Nucleic Acids Research*, vol. 35, no. 1, pp. 69–78, 2007.

[30] American Psychiatric Association, *Diagnostic and Statistical Manual of Mental Disorders: DSM-IV-TR*, text revision, American Psychiatric Association, Washington, DC, USA, 4th edition, 2000.

[31] G. McKhann, D. Drachman, M. Folstein, R. Katzman, D. Price, and E. M. Stadlan, "Clinical diagnosis of Alzheimer's disease: report of the NINCDS-ADRDA work group under the auspices of Department of Health and Human Services Task Force on Alzheimer's disease," *Neurology*, vol. 34, no. 7, pp. 939–944, 1984.

[32] M. Montaño and L. R. Ramos, "Validade da versão em português da clinical dementia rating," *Revista de Saúde Pública*, vol. 39, no. 6, pp. 912–917, 2005.

[33] M. F. Folstein, S. E. Folstein, and P. R. McHugh, "'Mini-mental state'. A practical method for grading the cognitive state of patients for the clinician," *Journal of Psychiatric Research*, vol. 12, no. 3, pp. 189–198, 1975.

[34] C. F. Reis, A. P. Carneiro, C. U. Vieira et al., "An antibody-like peptide that recognizes malignancy among thyroid nodules," *Cancer Letters*, vol. 335, no. 2, pp. 306–313, 2013.

[35] J. E. Larsen, O. Lund, and M. Nielsen, "Improved method for predicting linear B-cell epitopes," *Immunome Research*, vol. 2, article 2, 2006.

[36] H. R. Ansari and G. P. Raghava, "Identification of conformational B-cell Epitopes in an antigen from its primary sequence," *Immunome Research*, vol. 6, no. 1, article 6, 2010.

[37] M. A. Arap, "Phage display technology—applications and innovations," *Genetics and Molecular Biology*, vol. 28, no. 1, pp. 1–9, 2005.

[38] O. H. Aina, R. Liu, J. L. Sutcliffe, J. Marik, C.-X. Pan, and K. S. Lam, "From combinatorial chemistry to cancer-targeting peptides," *Molecular Pharmaceutics*, vol. 4, no. 5, pp. 631–651, 2007.

[39] M. Vodnik, U. Zager, B. Strukelj, and M. Lunder, "Phage display: selecting straws instead of a needle from a haystack," *Molecules*, vol. 16, no. 1, pp. 790–817, 2011.

[40] M. N. Manhani, V. S. Ribeiro, R. Cardoso, C. Ueira-Vieira, L. R. Goulart, and J. M. Costa-Cruz, "Specific phage-displayed peptides discriminate different forms of neurocysticercosis by antibody detection in the serum samples," *Parasite Immunology*, vol. 33, no. 6, pp. 322–329, 2011.

[41] V. da Silva Ribeiro, M. N. Manhani, R. Cardoso, C. U. Vieira, L. R. Goulart, and J. M. Costa-Cruz, "Selection of high affinity peptide ligands for detection of circulating antibodies in neurocysticercosis," *Immunology Letters*, vol. 129, no. 2, pp. 94–99, 2010.

[42] L. R. Goulart, C. U. Vieira, A. P. P. Freschi et al., "Biomarkers for serum diagnosis of infectious diseases and their potential application in novel sensor platforms," *Critical Reviews in Immunology*, vol. 30, no. 2, pp. 201–222, 2010.

[43] B.-X. Qu, Y. Gong, C. Moore et al., "Beta-amyloid autoantibodies are reduced in Alzheimer's disease," *Journal of Neuroimmunology*, vol. 274, no. 1-2, pp. 168–173, 2014.

[44] Y. Du, X. Wei, R. Dodel et al., "Human anti-β-amyloid antibodies block β-amyloid fibril formation and prevent β-amyloid-induced neurotoxicity," *Brain*, vol. 126, no. 9, pp. 1935–1939, 2003.

[45] X.-P. Wang, J.-H. Zhang, Y.-J. Wang et al., "Conformation-dependent single-chain variable fragment antibodies specifically recognize beta-amyloid oligomers," *FEBS Letters*, vol. 583, no. 3, pp. 579–584, 2009.

[46] J. L. Richens, K. Morgan, and P. O'Shea, "Reverse engineering of Alzheimer's disease based on biomarker pathways analysis," *Neurobiology of Aging*, vol. 35, no. 9, pp. 2029–2038, 2014.

[47] M. Ray and W. Zhang, "Analysis of Alzheimer's disease severity across brain regions by topological analysis of gene co-expression networks," *BMC Systems Biology*, vol. 4, no. 1, article 136, 2010.

[48] F. Drees and F. B. Gertler, "Ena/VASP: proteins at the tip of the nervous system," *Current Opinion in Neurobiology*, vol. 18, no. 1, pp. 53–59, 2008.

[49] L. Urbanelli, C. Massini, C. Emiliani, A. Orlacchio, and G. Bernardi, "Characterization of human Enah gene," *Biochimica et Biophysica Acta—Gene Structure and Expression*, vol. 1759, no. 1-2, pp. 99–107, 2006.

[50] D. L. Franco, C. Rezával, A. Cáceres, A. F. Schinder, and M. F. Ceriani, "ENA/VASP downregulation triggers cell death by impairing axonal maintenance in hippocampal neurons," *Molecular and Cellular Neuroscience*, vol. 44, no. 2, pp. 154–164, 2010.

[51] L. Trillo, D. Das, W. Hsieh et al., "Ascending monoaminergic systems alterations in Alzheimer's disease. Translating basic science into clinical care," *Neuroscience and Biobehavioral Reviews*, vol. 37, no. 8, pp. 1363–1379, 2013.

[52] P. R. Pennington, Z. Wei, L. Rui et al., "Alzheimer disease-related presenilin-1 variants exert distinct effects on monoamine oxidase-A activity in vitro," *Journal of Neural Transmission*, vol. 118, no. 7, pp. 987–995, 2011.

[53] B. Rogelj, J. C. Mitchell, C. C. J. Miller, and D. M. McLoughlin, "The X11/Mint family of adaptor proteins," *Brain Research Reviews*, vol. 52, no. 2, pp. 305–315, 2006.

[54] J. Chaufty, S. E. Sullivan, and A. Ho, "Intracellular amyloid precursor protein sorting and amyloid-β secretion are regulated by Src-mediated phosphorylation of Mint2," *Journal of Neuroscience*, vol. 32, no. 28, pp. 9613–9625, 2012.

[55] M. F. Matos, Y. Xu, I. Dulubova et al., "Autoinhibition of Mint1 adaptor protein regulates amyloid precursor protein binding and processing," *Proceedings of the National Academy of Sciences of the United States of America*, vol. 109, no. 10, pp. 3802–3807, 2012.

[56] J.-H. Lee, K.-F. Lau, M. S. Perkinton et al., "The Neuronal Adaptor Protein X11α Reduces Aβ Levels in the Brains of Alzheimer's APPswe Tg2576 Transgenic Mice," *The Journal of Biological Chemistry*, vol. 278, no. 47, pp. 47025–47029, 2003.

[57] F. Maina and R. Klein, "Hepatocyte growth factor, a versatile signal for developing neurons," *Nature Neuroscience*, vol. 2, no. 3, pp. 213–217, 1999.

[58] Y. Tsuboi, K. Kakimoto, M. Nakajima et al., "Increased hepatocyte growth factor level in cerebrospinal fluid in Alzheimer's disease," *Acta Neurologica Scandinavica*, vol. 107, no. 2, pp. 81–86, 2003.

[59] H. Fenton, P. W. Finch, J. S. Rubin et al., "Hepatocyte growth factor (HGF/SF) in Alzheimer's disease," *Brain Research*, vol. 779, no. 1-2, pp. 262–270, 1998.

[60] P. J. Cullen, "Endosomal sorting and signalling: an emerging role for sorting nexins," *Nature Reviews Molecular Cell Biology*, vol. 9, no. 7, pp. 574–582, 2008.

[61] H.-S. Huang, B.-J. Yoon, S. Brooks et al., "*Snx14* regulates neuronal excitability, promotes synaptic transmission, and is imprinted in the brain of mice," *PLoS ONE*, vol. 9, no. 5, Article ID e98383, 2014.

[62] R. Mizutani, K. Nakamura, N. Kato et al., "Expression of sorting nexin 12 is regulated in developing cerebral cortical neurons," *Journal of Neuroscience Research*, vol. 90, no. 4, pp. 721–731, 2012.

[63] Y. Zhao, Y. Wang, J. Yang, X. Wang, X. Zhang, and Y.-W. Zhang, "Sorting nexin 12 interacts with BACE1 and regulates BACE1-mediated APP processing," *Molecular Neurodegeneration*, vol. 7, no. 1, article 30, 2012.

[64] X. Wang, Y. Zhao, X. Zhang et al., "Loss of sorting nexin 27 contributes to excitatory synaptic dysfunction by modulating glutamate receptor recycling in Down's syndrome," *Nature Medicine*, vol. 19, no. 4, pp. 473–480, 2013.

[65] B. Li, D. Yu, and Z. Xu, "Activated protein C inhibits amyloid β production via promoting expression of ADAM-10," *Brain Research*, vol. 1545, pp. 35–44, 2014.

[66] H. Guo, D. Liu, H. Gelbard et al., "Activated protein C prevents neuronal apoptosis via protease activated receptors 1 and 3," *Neuron*, vol. 41, no. 4, pp. 563–572, 2004.

[67] Y. Oku and R. L. Huganir, "AGAP3 and Arf6 regulate trafficking of AMPA receptors and synaptic plasticity," *Journal of Neuroscience*, vol. 33, no. 31, pp. 12586–12598, 2013.

[68] S. Nagashima, T. Fukuda, Y. Kubota et al., "CRMP5-associated GTPase (CRAG) protein protects neuronal cells against cytotoxicity of expanded polyglutamine protein partially via c-fos-dependent activator protein-1 activation," *The Journal of Biological Chemistry*, vol. 286, no. 39, pp. 33879–33889, 2011.

[69] E. Nagele, M. Han, C. DeMarshall, B. Belinka, and R. Nagele, "Diagnosis of Alzheimer's disease based on disease-specific autoantibody profiles in human sera," *PLoS ONE*, vol. 6, no. 8, Article ID e23112, 2011.

Hindawi Publishing Corporation
BioMed Research International
Volume 2014, Article ID 282490, 9 pages
http://dx.doi.org/10.1155/2014/282490

Research Article

Decreased Fast Ripples in the Hippocampus of Rats with Spontaneous Recurrent Seizures Treated with Carbenoxolone and Quinine

Consuelo Ventura-Mejía and Laura Medina-Ceja

Laboratory of Neurophysiology and Neurochemistry, Department of Cellular and Molecular Biology, Centro Universitario de Ciencias Biológicas y Agropecuarias (CUCBA), University of Guadalajara, Camino Ing. R. Padilla Sánchez 2100, Las Agujas, Nextipac, Zapopan, JAL, CP 45110, Mexico

Correspondence should be addressed to Laura Medina-Ceja; lauramedcej@gmail.com

Received 11 June 2014; Accepted 14 August 2014; Published 3 September 2014

Academic Editor: Antonio W. D. Gavilanes

Background. In models of temporal lobe epilepsy and in patients with this pathology, high frequency oscillations called fast ripples (FRs, 250–600 Hz) can be observed. FRs are considered potential biomarkers for epilepsy and, in the light of many *in vitro* and *in silico* studies, we thought that electrical synapses mediated by gap junctions might possibly modulate FRs *in vivo*. *Methods*. Animals with spontaneous recurrent seizures induced by pilocarpine administration were implanted with movable microelectrodes in the right anterior and posterior hippocampus to evaluate the effects of gap junction blockers administered in the entorhinal cortex. The effects of carbenoxolone (50 nmoles) and quinine (35 pmoles) on the mean number of spontaneous FR events (occurrence of FRs), as well as on the mean number of oscillation cycles per FR event and their frequency, were assessed using a specific algorithm to analyze FRs in intracranial EEG recordings. *Results*. We found that these gap junction blockers decreased the mean number of FRs and the mean number of oscillation cycles per FR event in the hippocampus, both during and at different times after carbenoxolone and quinine administration. *Conclusion*. These data suggest that FRs may be modulated by gap junctions, although additional experiments *in vivo* will be necessary to determine the precise role of gap junctions in this pathological activity associated with epileptogenesis.

1. Introduction

Epilepsy is a neuronal disorder that is characterized by the abnormal, continued discharge and hypersynchronous activity of neurons [1]. The existing models of epilepsy provide good tools to study the basic mechanisms by which seizures are generated, and the model of temporal lobe epilepsy (TLE) induced by pilocarpine or kainic acid (KA) simulates most of the characteristics of this pathology [2–4]. In this TLE model, high frequency oscillations known as fast ripples (FRs, 250–600 Hz) have been observed, as in tetrodotoxin and tetanus toxin models of epilepsy [5–7], in computational models *in silico* [8, 9] and in patients with TLE [2, 10, 11].

FRs can be evoked by electrical stimulation of the same brain areas where they occur spontaneously and they reflect bursts of population spikes from synchronously firing principal cells in relatively small areas of the hippocampus (HIP, 1 mm^3) [12–14]. According to electrophysiological studies in animals with spontaneous recurrent seizures, these are areas that contain groups of pathologically interconnected neurons [2, 15, 16]. However, FRs have only been recorded in the HIP and entorhinal cortex (EC) ipsilateral to the lesion during slow wave sleep and immobility, albeit for periods ranging from days to months [2, 17]. In addition, various studies have confirmed that the onset of focal seizures coincides with fast ripple (FR) activity [10, 18, 19]. Accordingly, FRs are considered to be potential biomarkers for epilepsy as they can be

recorded both before seizure onset and during seizure activity [3, 16].

Electrical synapses enable electrical activity to be synchronized between neurons and they permit the spread of depolarization (excitation) or hyperpolarization (inhibition) across a particular neural network [20]. Several studies have highlighted the involvement of electric coupling in epileptiform activity, both in *in vitro* and *in vivo* models [19, 20]. Moreover, the loss of electrical coupling provoked by gap junction blockers (e.g., carbenoxolone [CBX], a nonspecific blocker of connexins, or quinine, a dose-dependent blocker of connexin 36) [21, 22] or through a deficiency in connexins, the structural proteins that form gap junctions, produces antiepileptic effects [23–30]. Indeed, recent *in silico* studies [31] supported the participation of gap junctions localized in axons in the generation and persistence of gamma and FR activity.

Based on this information, we have considered the possible involvement of electrical synapses mediated by gap junctions in the modulation of FRs in animals experiencing spontaneous recurrent seizures. For this propose, we evaluated the effects of CBX and quinine on the mean number of spontaneous FR events (FR occurrence), as well as the mean number of oscillation cycles per FR event and frequency.

2. Methods

2.1. Model of Temporal Lobe Epilepsy Induced by Intracerebroventricular Pilocarpine Administration. Male Wistar rats (190–200 g) were housed individually in cages in a temperature-controlled room (22 ± 2°C), on a 12 h light/dark cycle (lights on from 7:00 a.m. to 7:00 p.m.) and with *ad libitum* access to food and water. All experimental procedures were designed to minimize animal suffering and the total number of animals used. The protocols used were in accordance with the Rules for Research in Health Matters (Mexican Official Norms NOM-062-ZOO-1999, NOM-033-ZOO-1995) and they were approved by the local Animal Care Committee.

To induce acute status epilepticus (SE) [32], rats were anesthetized with isofluorane (Sofloran, PISA, Laboratories, Mexico) in 100% oxygen and secured in a Stoelting stereotaxic frame with the incisor bar positioned at −3.3 mm. A hole was drilled in the skull above the right lateral ventricle at the following stereotaxic coordinates relative to bregma: AP −4.1 mm, L −5.2 mm, and V 7 mm. A single dose of pilocarpine hydrochloride (1.2 mg/μL, total volume 2 μL; Sigma-Aldrich, USA) was injected through a needle connected to an injection pump (flow rate: 1 μL/min; Stoelting Co., IL, USA). After recovery, the animals returned to their cages for observation, convulsive behavior was scored according to the Racine scale [33], and animals with a score of 4/5 were considered to exhibit SE. After 90–120 minutes, SE was abolished by administering diazepam (5–10 mg/kg, i.p.) to increase their survival and, when necessary, two doses of diazepam were administered. The convulsive behavior of all the animals after pilocarpine injection was monitored visually and 15 days after SE induction the rats were video monitored for 24 hours every day, scoring their spontaneous recurrent seizures. Animals exhibiting spontaneous recurrent seizures were selected for microelectrode implantation.

2.2. Surgery. Control rats were anaesthetized as indicated above and they were positioned in a stereotaxic frame such that lambda and the bregma were in the same horizontal plane. In the control group, fixed recording microelectrodes, consisting of pairs of tungsten wires (60 μm in diameter) with a 1.5 mm vertical tip separation, were implanted in the right anterior (RAH: AP −3.5 mm; ML 2.00 mm; DV 4.0 mm) and posterior hippocampus (RPH: AP −5.0 mm relative to bregma; ML 5.0 mm; DV 5.5 mm). In addition, two stainless steel screws were driven into the bone, one above the bregma and one above the cerebellum, which served as indifferent and ground electrodes, respectively. Finally, a stainless steel guide cannula (0.5 mm internal diameter) was implanted through a hole drilled in the skull and positioned in the region of the right EC (AP −8.00 mm, ML 4.0 mm, DV 5.0 mm) in order to insert a needle for the injection of various chemical agents (CBX, quinine, and saline solution). This arrangement of microelectrodes was placed on a pin connector and, along with the guide cannula, fastened to the skull with dental cement. For experimental groups, an arrangement of eight microelectrodes with the same characteristics as those described above was mounted in a mobile device and implanted into the right region of the hippocampus (RAH, AP −3.5 mm, ML 3.0 mm, DV 2.5 mm; RPH, AP −5.0 mm, ML 3.0 mm, DV 2.5 mm) in order to move this device to different depths of the hippocampus and easily detect FRs in experiments carried out in freely moving rats.

2.3. Drug Administration. To determine the involvement of electrical synapses, we used three control ($n = 3$ rats each one) and three experimental groups of animals ($n = 6$ each one) with recurrent spontaneous seizures, the latter receiving CBX (50 mM, final dose 50 nmoles), quinine (35 mM, final dose 35 pmoles), or the vehicle alone (NaCl 0.9%; Sigma Chemical Co. St. Louis, MO, USA). These drugs were administered through an injection needle placed into the guide cannula (0.2 μL/min flow for 5 minutes) and using a microsyringe mounted to a microinjection pump (WPI, Fl. USA).

2.4. Intracranial EEG Recordings and Analysis. Intracranial EEG activity was recorded in freely moving rats. Five 4-channel MOSFET small amplifiers were attached to the cable connector to eliminate movement artifacts. Hippocampal electrical activity was recorded on a polygraph with eight amplifiers (Model 7D, Grass Technologies, RI, USA) at a bandwidth of 0.1 to 3 kHz and with a sensitivity of 75 μV/cm per channel. The sampling rate was set at 5 kHz/channel with 12-bit precision using an iMac A1048 (Apple, USA) and MP150 software system (BIOPAC Systems, CA, USA). The basal electrical activity of each control group was analyzed, and the amplitude and frequency averaged over a 15 min recording period. In contrast, once recorded, EEG traces from all recordings of experimental animals were converted

to MATLAB readable files to process and identify the FRs using an algorithm designed specifically for this purpose [34–36]. Accordingly, each of the signals selected was passed through a 100–650 Hz band-pass filter using the Hamming method with 60 coefficients. To identify FRs, the filtered signal was processed using the root mean square (RMS) in a sliding window of 3 ms and through its successive values. Values that were over 5 times the standard deviation of the mean value of the filtered signal and that lasted at least 6 ms were considered possible FR events. A second criterion was also used for FR classification, whereby the changes in the approximate entropy of the signal were analyzed [36, 37] and those that were over twice the mean value were considered putative FRs. Signals that fulfilled these two criteria were processed with the fast Fourier transform (FFT) to calculate their frequency in Hz. In addition, the results from the automated FRs detection algorithm were manually inspected. The FRs parameters evaluated were the mean number of spontaneous FR events (occurrence of FRs per 15 min) and the mean number of oscillation cycles per FR event, as well as the frequency before, during, and after CBX or quinine administration.

2.5. Histological Evaluation. After each experiment the animals were anesthetized with sodium pentobarbital and perfused transcardially with 100 mL of normal saline (0.9%) in 0.12 M buffer/$CaCl_2$, followed by 300 mL of 4% paraformaldehyde in 0.12 M buffer/$CaCl_2$ (pH 7.3). The animal's brain was then removed, and coronal sections (50 μm thick) were obtained and stained with cresyl violet to confirm the correct positioning of the guide cannula and microelectrodes. Only animals that showed a correct implantation of cannula and microelectrodes were included in the present work.

2.6. Statistical Analysis. In the control groups the data are expressed as the mean ± SEM of the amplitude and frequency of electrical activity recorded in the RAH, LAH, RPH, and LPH (right/left anterior/posterior hippocampus). Significant differences between control groups were obtained by an analysis of variance (ANOVA, one-way) followed by Tukey's test. The data from the experimental groups are expressed as the mean ± SEM of each parameter evaluated before, during, and after CBX or quinine administration. Significant differences were analyzed by ANOVA followed by Dunnett's post hoc test, with P values < 0.05 considered significant.

3. Results

3.1. Behavior and Analysis of Intracranial EEG Recordings in Control Animals. Animals from the three control groups showed normal behavior before, during, and after drug administration into the EC (CBX 50 nmoles, quinine 35 pmoles, and NaCl 0.9%). In these animals normal grooming, chewing movements, exploratory behavior, and sleep periods were observed. The analysis of the intracranial EEG recordings from these control rats revealed a low amplitude and frequency of electrical activity (Figure 1) in all the regions analyzed, both before and after drug administration. The only significant difference observed was in the frequency parameter in the 150–165 min period analyzed between animals from the control groups treated with NaCl and quinine (1.16 ± 0.09 Hz versus 1.55 ± 0.12 Hz, resp., Figure 1).

3.2. Effect of Carbenoxolone on the Fast Ripples Observed in Animals with Spontaneous Seizures. In terms of their behavior, the rats that received CBX showed vibrissae movements, and while they remained in a state of sleep for most of the analysis, spontaneous seizures were observed in some animals at level 5 of the Racine scale during the experiments.

When the intracranial EEG recordings from experimental animals ($n = 6$) with spontaneous and recurrent seizures were analyzed, spontaneous FRs were evident in all the regions registered (Figure 2(a)). The administration of CBX (50 nmoles) produced a significant decrease in the mean number of FRs in the RAH and RPH compared to those that received NaCl (Figures 3 and 4), both during and at different times after CBX administration (RAH: during 4.8 ± 1.4 versus 0.8 ± 0.2; after 30–45 min, 4.2 ± 1.4 versus 0.6 ± 0.1; after 150–165 min 4.6 ± 1.7 versus 0.6 ± 0.2. RPH: during, 5.0 ± 1.5 versus 0.4 ± 0.1; after 30–45 min, 6.0 ± 1.6 versus 0.5 ± 0.1; after 150–165 min, 5.8 ± 1.7 versus 0.7 ± 0.2). By contrast, the mean number of oscillation cycles per FR event decreased in the RPH during and at different times after CBX administration (during 6.3 ± 1.4 versus 1.4 ± 0.5; after 30–45 min 6.8 ± 0.3 versus 2.9 ± 0.8; after 150–165 min 6.48 ± 0.2 versus 2.9 ± 0.8), yet only during CBX administration in the RAH (5.69 ± 0.9 versus 2.5 ± 0.7). The mean frequency of FRs also decreased in the RPH compared with the rats that received NaCl alone, both during and at different times after CBX administration (during 342.1±77.3 versus 93±39; after 30–45 min 414.6±14.5 versus 175±51; after 150–165 min 386.6±10.5 versus 169±49), yet only during CBX administration in the RAH (317.2 ± 51 versus 115 ± 41 Hz).

3.3. Effect of Quinine on the Fast Ripples Observed in Animals with Spontaneous Seizures. The animals that received quinine exhibited vibrissae movements and they remained in a state of sleep for most of the analysis, although level 5 spontaneous seizures of the Racine scale were observed in some of these animals.

Like the animals that received CBX, spontaneous FRs were evident in all the regions analyzed when rats received quinine (Figure 2(b)), although there were fewer FRs during quinine administration in the RAH and 150–165 min after quinine administration (Figures 3 and 4: during 4.8 ± 1.4 versus 1.0 ± 0.3; after 150–165 min 4.6 ± 1.7 versus 1.7 ± 0.4). By contrast, there were fewer FRs in the RPH at all the EEG recording periods analyzed (during 5.0 ± 1.5 versus 1.0 ± 0.5; after 30–45 min 6.0 ± 1.6 versus 3.0 ± 0.7; after 150–165 min 5.8 ± 1.7 versus 2.0 ± 0.5). While in the RPH a significant decrease in the mean number of oscillation cycles per FR was observed only during quinine administration (6.3 ± 1.4 versus 3.0 ± 0.7) there was no difference in the mean frequency of FRs in the R AH and R PH.

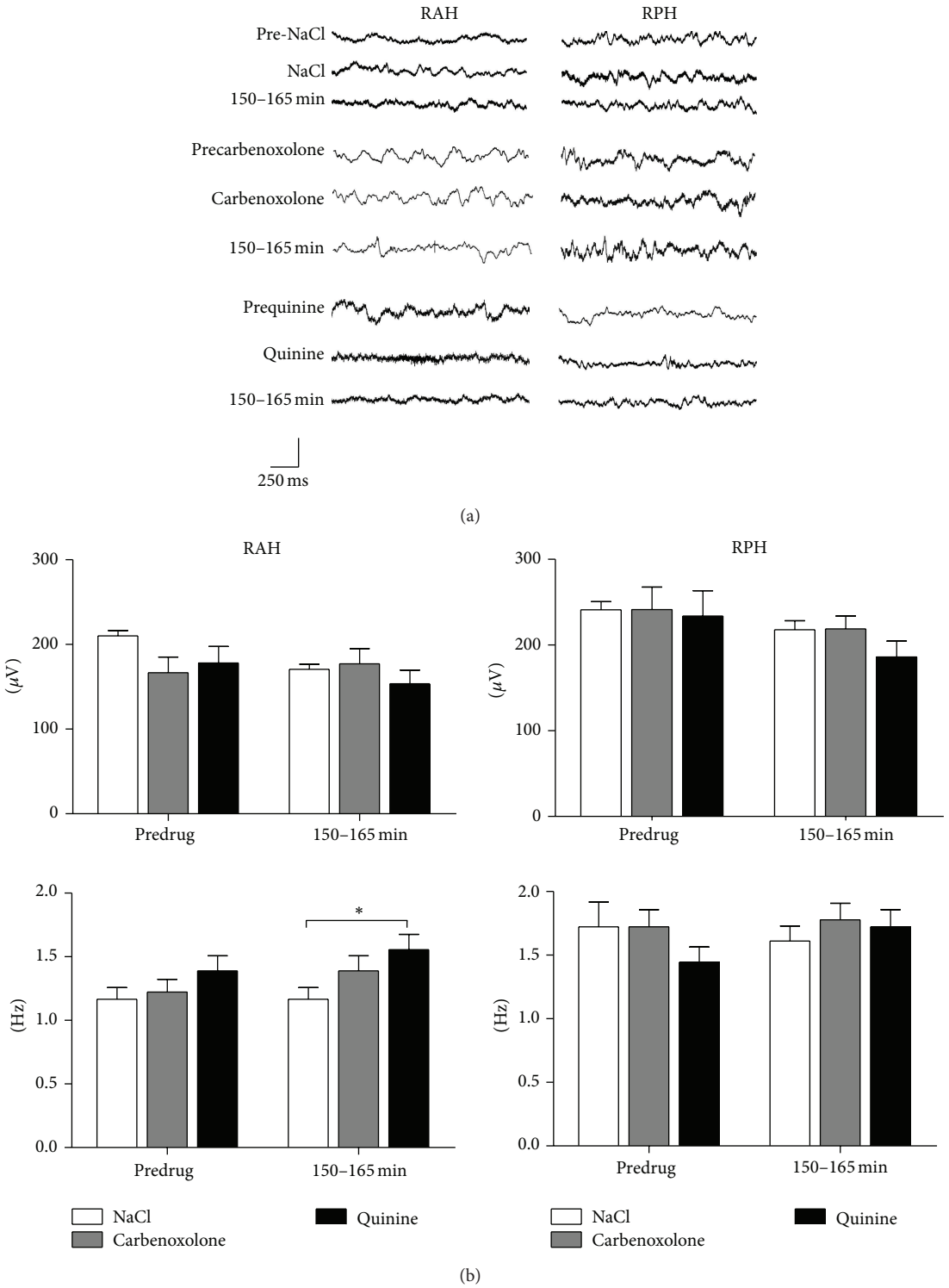

Figure 1: Representative intracranial EEG recordings from the different brain regions studied in three different rats from the NaCl, CBX, and quinine control groups ($n = 3$ each one). The lower graphs show the mean amplitude (μV ± SEM) and frequency (Hz ± SEM) of the electrical activity observed before (PRE-DRUG) and 150–165 min after drug administration. The y-axis calibration bar corresponds to the amplitude: 0.4 mV for NaCl, 1 mV for CBX, and 0.5 mV for quinine groups ($^*P < 0.05$).

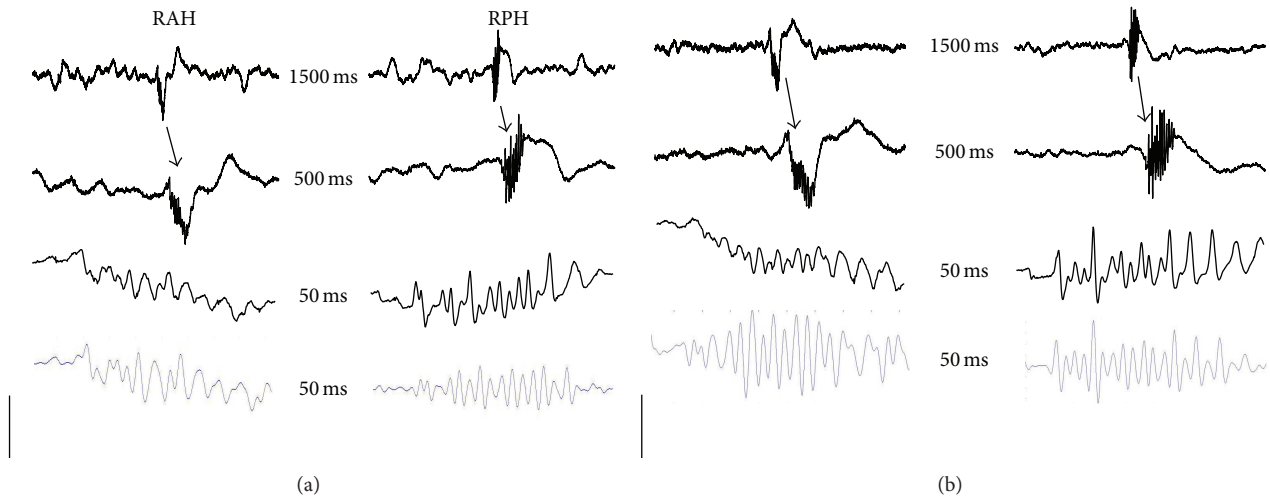

Figure 2: Representative intracranial EEG recordings taken before drug administration from the different brain regions studied in two rats from the experimental groups ($n = 6$ each one) with CBX (a) and quinine (b), in which spontaneous fast ripples (FRs) were observed simultaneously: right anterior hippocampus (RAH) and right posterior hippocampus (RPH). An EEG trace of 1.5 s with a spontaneous FR (arrow in the first trace) followed by extended EEG traces of the same activity. The last EEG trace is with an 80 Hz filter. The numbers in the centre correspond to the time of each EEG trace and the y-axis calibration bar corresponds to the amplitude: 1 mV for the first and 0.4 mV for the rest of the EEG traces.

4. Discussion

In the present study, no differences were found in the behavior observed in animals from control groups and electrical activity was characterized by the presence of slow physiological waves of low amplitude and frequency, although a slight increase in the frequency was observed between the saline solution control animals and those that received quinine. However, this difference could be due to different behavioral states of control animals considering that these animals were observed quiet and asleep, 150–165 min after drug administration. Moreover this difference did not appear to be physiologically relevant for our study given that the frequency of both groups did not exceed 2 Hz.

In this study spontaneous FRs were detected in all the hippocampal brain regions analyzed from animals with spontaneous and recurrent seizures induced by the i.c.v. administration of pilocarpine, animals chosen after analyzing their intracranial EEG recordings with an algorithm exclusively designed to detect FRs. The movable recording microelectrodes that we used in the experimental animals were situated at different depths of hippocampal regions in order to detect FRs, which are generated in relatively small areas ($1\,mm^3$) [15, 16]. The mean number and frequency of spontaneous FRs observed here were similar to those described previously in animals administered unilateral hippocampal injections of KA [2, 15]. Moreover, unlike other studies, spontaneous FRs were observed during immobile, waking, and sleeping states of the animals, although periods of slow-wave sleep were not specifically analyzed, when FRs are more frequent [15, 38]. There have been many studies into FRs and their probable mechanism of generation [5, 12–16, 39], considering that FRs may be potential biomarkers for epilepsy and useful to detect candidate areas for resection [40]. Nevertheless, there are no *in vivo* studies about factors that could modulate FRs by electrical synapses.

We found that the nonspecific blocker of gap junctions, CBX, decreased the mean number of FRs in the RAH and RPH, as well as the mean number of oscillation cycles per FR event, and the frequency in the RPH during and at different times after CBX administration. These data indicate a probable role of gap junctions in modulating FRs, although there is no data to date from studies *in vivo* with which the results of present study can be compared. Nevertheless, similar results were reported in some *in vitro* studies. In a study carried out on slices from epileptic patients, CBX (0.2 mM) provoked a 50% decrease in FRs [31] as in other study [9], while ripple activity (150–250 Hz) was also blocked by the gap junction blocker halothane [41, 42]. Likewise, quinine decreased the mean number of FRs in the RAH and RPH during and at different times after its administration, while the mean number of oscillation cycles per FR event only decreased in the RPH, suggesting only a partial modulatory effect of quinine on FRs. This effect could be due to quinine blocking gap junctions formed only by Cx36, which are found in neurons, and we speculate that gap junctions formed by different connexins are required for FR activity, as observed here through the effects of the nonspecific blocker, CBX.

There are currently no *in vivo* studies to compare our results regarding the effects of quinine, although there is significant data supporting the important role of gap junctions in epileptiform activity in different *in vitro* and *in vivo* models. Indeed, the disruption of electrical coupling induced

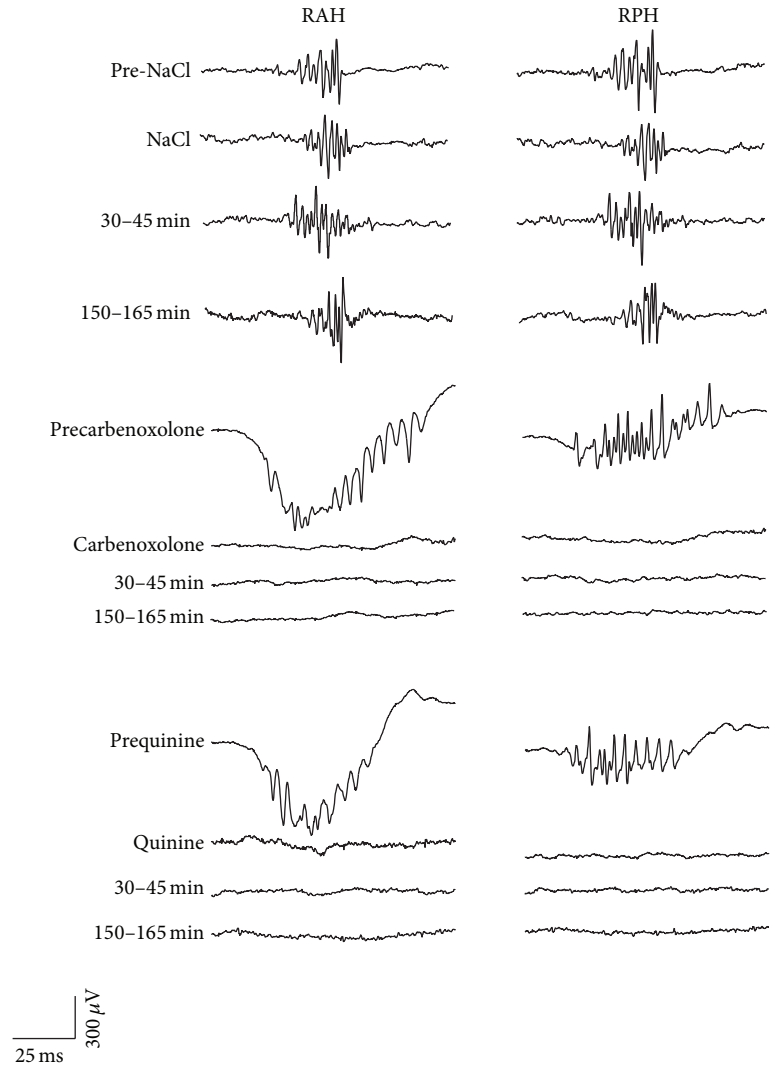

Figure 3: Representative intracranial EEG recordings from the different brain regions studied and obtained from three different rats in the NaCl, CBX, and quinine experimental groups ($n = 6$ each one) in which spontaneous fast ripples (FRs) were observed: right anterior hippocampus (RAH) and right posterior hippocampus (RPH) before, during, and at different times after drug administration. Note the effects of CBX and quinine on the FRs.

by gap junction blockers or through a deficiency in certain Cx proteins that make up gap junctions has antiepileptic effects [20, 24, 27–30]. Similarly, a role for Cx36 was shown in the generation of high frequency oscillations (100–200 Hz) and epileptiform field bursts recorded in slices from the hippocampus of deficient mice [26]. other *in silico* study has demonstrated the importance of axoaxonal gap junctions in FR generation [31]. These data support our data regarding the modulation of FRs by gap junctions, although we cannot rule out the influence of other factors that could modulate FRs, such as the chemical neurotransmission. In relation to this, serotonin was found to reduce electric coupling through protein kinase C, via IP_3/Ca^{2+} [43], and probable through 5-HT2 receptor activation [44]. In addition, the frequency of FRs was higher during slow wave sleep, a period in which serotonin levels are low in the model of chronic seizures induced by KA [2, 11, 15]. Indeed, a modulatory effect of serotonin was observed on electric synapses in weakly electrical coupled neural networks of the *Helisoma* ganglia [45]. In conjunction with our data regarding serotonin and FR modulation [46], these facts also suggest a possible influence of serotonin neurotransmission on gap junction activity and, hence, in the modulation of FRs.

The CBX and quinine have been clinically used against malaria and ulcers but they have not been completely tested for their anticonvulsant effects in patients; therefore it is necessary to carry out more *in vivo* experiments to find the role of gap junctions in the FRs modulation in order to consider this strategy as a possible clinical implication.

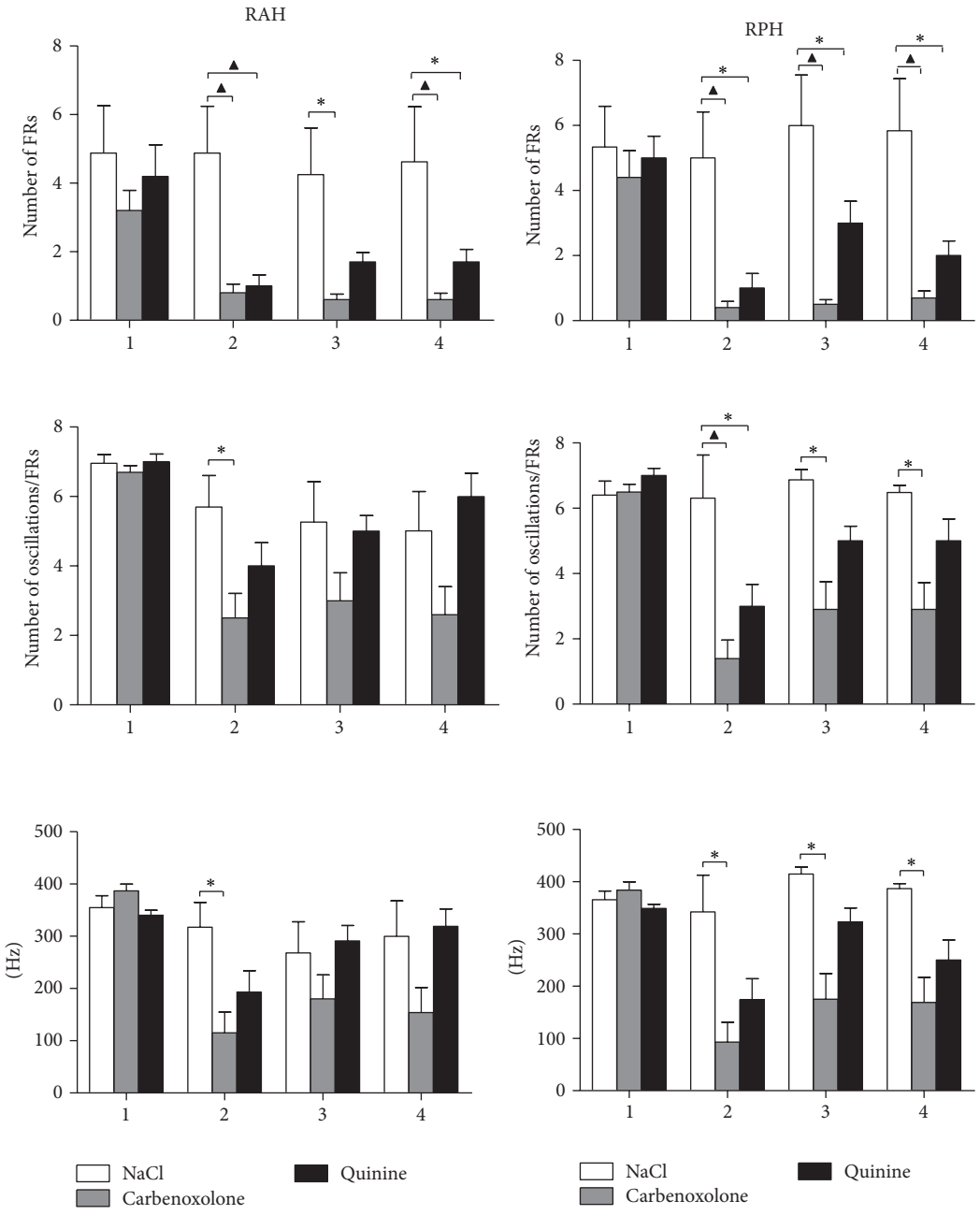

Figure 4: Graphs show the mean number of spontaneous FR events (spontaneous FRs ± SEM) and the oscillation cycles per spontaneous FR, as well as the mean frequency (Hz), before (1), during (2), and at different times after NaCl (NaCl, 0.9%), CBX (50 nmoles), and quinine (35 pmoles) administration (3, 30–45 min; 4, 150–165 min) in the regions studied: right anterior hippocampus (RAH) and right posterior hippocampus (RPH). A significant decrease in FR number was provoked by CBX and quinine administration in the RAH and RPH ($^{*}P < 0.05$; $^{\blacktriangle}P < 0.001$).

5. Conclusions

Through the present data, we conclude that gap junctions could exert a modulatory effect on FRs in the hippocampus of rats with spontaneous seizures induced by pilocarpine. While these effects probably occur through gap junctions formed by different connexins, we cannot rule out the possible participation of chemical synapses in FR modulation, such as that of serotonin neurotransmission. Finally, it is necessary to perform additional *in vivo* experiments to determine the precise role of gap junctions in the modulation of FRs associated with epilepsy in the hippocampus.

Conflict of Interests

The authors declare that there is no conflict of interests regarding the publication of this paper.

Authors' Contribution

Laura Medina-Ceja participated in supervising experiments, analysis and discussion of results, paper preparation, and final revision; Consuelo Ventura-Mejía contributed in experiments and analysis of results. Consuelo Ventura-Mejía and Laura Medina-Ceja contributed equally to this work.

Acknowledgments

This study was supported by Grant sponsor CONACYT-SEP-CB, Grant no. 106179 to Laura Medina-Ceja.

References

[1] A. Bragin, J. Engel Jr., and R. J. Staba, "High-frequency oscillations in epileptic brain," *Current Opinion in Neurology*, vol. 23, no. 2, pp. 151–156, 2010.

[2] A. Bragin, J. Engel Jr., C. L. Wilson, E. Vizentin, and G. W. Mathern, "Electrophysiologic analysis of a chronic seizure model after unilateral hippocampal KA injection," *Epilepsia*, vol. 40, no. 9, pp. 1210–1221, 1999.

[3] A. Bragin, C. L. Wilson, J. Almajano, I. Mody, and J. Engel Jr., "High-frequency oscillations after status epilepticus: epileptogenesis and seizure genesis," *Epilepsia*, vol. 45, no. 9, pp. 1017–1023, 2004.

[4] D. F. He, D. L. Ma, Y. C. Tang, J. Engel Jr., A. Bragin, and F. R. Tang, "Morpho-physiologic characteristics of dorsal subicular network in mice after pilocarpine-induced status epilepticus," *Brain Pathology*, vol. 20, no. 1, pp. 80–95, 2010.

[5] P. Jiruska, A. D. Powell, W.-C. Chang, and J. G. R. Jefferys, "Electrographic high-frequency activity and epilepsy," *Epilepsy Research*, vol. 89, no. 1, pp. 60–65, 2010.

[6] J. D. Frost Jr., C. L. Lee, R. A. Hrachovy, and J. W. Swann, "High frequency EEG activity associated with ictal events in an animal model of infantile spasms," *Epilepsia*, vol. 52, no. 1, pp. 53–62, 2011.

[7] J. D. Frost, C. L. Lee, J. T. Le, R. A. Hrachovy, and J. W. Swann, "Interictal high frequency oscillations in an animal model of infantile spasms," *Neurobiology of Disease*, vol. 46, no. 2, pp. 377–388, 2012.

[8] R. D. Traub and A. Bibbig, "A model of high-frequency ripples in the hippocampus based on synaptic coupling plus axon-axon gap junctions between pyramidal neurons," *Journal of Neuroscience*, vol. 20, no. 6, pp. 2086–2093, 2000.

[9] A. K. Roopun, J. D. Simonotto, M. L. Pierce et al., "A nonsynaptic mechanism underlying interictal discharges in human epileptic neocortex," *Proceedings of the National Academy of Sciences of the United States of America*, vol. 107, no. 1, pp. 338–343, 2010.

[10] A. Bragin, J. Engel Jr., C. L. Wilson, I. Fried, and G. Buzsáki, "High-frequency oscillations in human brain," *Hippocampus*, vol. 9, no. 2, pp. 137–142, 1999.

[11] A. Bragin, C. L. Wilson, R. J. Staba, M. Reddick, I. Fried, and J. Engel Jr., "Interictal high-frequency oscillations (80-500Hz) in the human epileptic brain: entorhinal cortex," *Annals of Neurology*, vol. 52, no. 4, pp. 407–415, 2002.

[12] A. Bragin, P. Claeys, K. Vonck et al., "Analysis of initial slow waves (ISWs) at the seizure onset in patients with drug resistant temporal lobe epilepsy," *Epilepsia*, vol. 48, no. 10, pp. 1883–1894, 2007.

[13] A. Bragin, C. L. Wilson, and J. Engel Jr., "Voltage depth profiles of high-frequency oscillations after kainic acid-induced status epilepticus," *Epilepsia*, vol. 48, supplement 5, pp. 35–40, 2007.

[14] D. E. Bragin, R. C. Bush, W. S. Müller, and E. M. Nemoto, "High intracranial pressure effects on cerebral cortical microvascular flow in rats," *Journal of Neurotrauma*, vol. 28, no. 5, pp. 775–785, 2011.

[15] A. Bragin, C. L. Wilson, and J. Engel Jr., "Chronic epileptogenesis requires development of a network of pathologically interconnected neuron clusters: a hypothesis," *Epilepsia*, vol. 41, no. 6, pp. S144–S152, 2000.

[16] A. Bragin, I. Mody, C. L. Wilson, and J. Engel Jr., "Local generation of fast ripples in epileptic brain," *Journal of Neuroscience*, vol. 22, no. 5, pp. 2012–2021, 2002.

[17] A. Bragin, C. L. Wilson, and J. Engel Jr., "Spatial stability over time of brain areas generating fast ripples in the epileptic rat," *Epilepsia*, vol. 44, no. 9, pp. 1233–1237, 2003.

[18] R. S. Fisher, W. R. S. Webber, R. P. Lesser, S. Arroyo, and S. Uematsu, "High-frequency EEG activity at the start of seizures," *Journal of Clinical Neurophysiology*, vol. 9, no. 3, pp. 441–448, 1992.

[19] R. D. Traub, A. Bibbig, A. Piechotta, A. Draguhn, and D. Schmitz, "Synaptic and nonsynaptic contributions to giant IPSPs and ectopic spikes induced by 4-aminopyridine in the hippocampus in vitro," *Journal of Neurophysiology*, vol. 85, no. 3, pp. 1246–1256, 2001.

[20] J. L. Perez Velazquez and P. L. Carlen, "Gap junctions, synchrony and seizures," *Trends in Neurosciences*, vol. 23, no. 2, pp. 68–74, 2000.

[21] G. R. Juszczak and A. H. Swiergiel, "Properties of gap junction blockers and their behavioural, cognitive and electrophysiological effects: animal and human studies," *Progress in Neuro-Psychopharmacology and Biological Psychiatry*, vol. 33, no. 2, pp. 181–198, 2009.

[22] M. Srinivas, M. G. Hopperstad, and D. C. Spray, "Quinine blocks specific gap junction channel subtypes," *Proceedings of the National Academy of Sciences of the United States of America*, vol. 98, no. 19, pp. 10942–10947, 2001.

[23] F. M. Ross, P. Gwyn, D. Spanswick, and S. N. Davies, "Carbenoxolone depresses spontaneous epileptiform activity in the CA1 region of rat hippocampal slices," *Neuroscience*, vol. 100, no. 4, pp. 789–796, 2000.

[24] R. Köhling, S. J. Gladwell, E. Bracci, M. Vreugdenhil, and J. G. R. Jefferys, "Prolonged epileptiform bursting induced by 0-Mg2+ in rat hippocampal slices depends on gap junctional coupling," *Neuroscience*, vol. 105, no. 3, pp. 579–587, 2001.

[25] D. G. Margineanu and H. Klitgaard, "Can gap-junction blockade preferentially inhibit neuronal hypersynchrony vs. excitability?" *Neuropharmacology*, vol. 41, no. 3, pp. 377–383, 2001.

[26] N. Maier, M. Güldenagel, G. Söhl, H. Siegmund, K. Willecke, and A. Draguhn, "Reduction of high-frequency network oscillations (ripples) and pathological network discharges in hippocampal slices from connexin 36-deficient mice," *Journal of Physiology*, vol. 541, part 2, pp. 521–528, 2002.

[27] I. Pais, G. H. Sheriar, H. Monyer et al., "Sharp wave-like activity in the hippocampus in vitro in mice lacking the gap junction protein connexin 36," *Journal of Neurophysiology*, vol. 89, no. 4, pp. 2046–2054, 2003.

[28] Z. Gajda, E. Gyengési, E. Hermesz, K. Said Ali, and M. Szente, "Involvement of gap junctions in the manifestations and control

of the duration of seizures in rats in vivo," *Epilepsia*, vol. 44, no. 12, pp. 1596–1600, 2003.

[29] L. Medina-Ceja, A. Cordero-Romero, and A. Morales-Villagrán, "Antiepileptic effect of carbenoxolone on seizures induced by 4-aminopyridine: a study in the rat hippocampus and entorhinal cortex," *Brain Research*, vol. 1187, no. 1, pp. 74–81, 2008.

[30] L. Medina-Ceja and C. Ventura-Mejía, "Differential effects of trimethylamine and quinine on seizures induced by 4-aminopyridine administration in the entorhinal cortex of vigilant rats," *Seizure*, vol. 19, no. 8, pp. 507–513, 2010.

[31] A. Simon, R. D. Traub, N. Vladimirov et al., "Gap junction networks can generate both ripple-like and fast ripple-like oscillations," *European Journal of Neuroscience*, vol. 39, no. 1, pp. 46–60, 2014.

[32] L. Medina-Ceja, K. Pardo-Peña, and C. Ventura-Mejía, "Evaluation of behavioral parameters and mortality in a model of temporal lobe epilepsy induced by intracerebroventricular pilocarpine administration," *NeuroReport*, 2014.

[33] R. J. Racine, "Modification of seizure activity by electrical stimulation: II. Motor seizure," *Electroencephalography and Clinical Neurophysiology*, vol. 32, no. 3, pp. 281–294, 1972.

[34] J. Csicsvari, H. Hirase, A. Czurkó, A. Mamiya, and G. Buzsáki, "Oscillatory coupling of hippocampal pyramidal cells and interneurons in the behaving rat," *The Journal of Neuroscience*, vol. 19, no. 1, pp. 274–287, 1999.

[35] R. J. Staba, C. L. Wilson, A. Bragin, I. Fried, and J. Engel Jr., "Quantitative analysis of high-frequency oscillations (80–500 Hz) recorded in human epileptic hippocampus and entorhinal cortex," *Journal of Neurophysiology*, vol. 88, no. 4, pp. 1743–1752, 2002.

[36] A. López-Cuevas, B. Castillo-Toledo, L. Medina-Ceja, C. Ventura-Mejía, and K. Pardo-Peña, "An algorithm for on-line detection of high frequency oscillations related to epilepsy," *Computer Methods and Programs in Biomedicine*, vol. 110, no. 3, pp. 354–360, 2013.

[37] S. M. Pincus, "Approximate entropy as a measure of system complexity," *Proceedings of the National Academy of Sciences of the United States of America*, vol. 88, no. 6, pp. 2297–2301, 1991.

[38] M. Lévesque, A. Bortel, J. Gotman, and M. Avoli, "High-frequency (80-500Hz) oscillations and epileptogenesis in temporal lobe epilepsy," *Neurobiology of Disease*, vol. 42, no. 3, pp. 231–241, 2011.

[39] G. Foffani, Y. G. Uzcategui, B. Gal, and L. Menendez de la Prida, "Reduced spike-timing reliability correlates with the emergence of fast ripples in the rat epileptic hippocampus," *Neuron*, vol. 55, no. 6, pp. 930–941, 2007.

[40] T. Akiyama, B. McCoy, C. Y. Go et al., "Focal resection of fast ripples on extraoperative intracranial EEG improves seizure outcome in pediatric epilepsy," *Epilepsia*, vol. 52, no. 10, pp. 1802–1811, 2011.

[41] A. Draguhn, R. D. Traub, D. Schmitz, and J. G. R. Jefferys, "Electrical coupling underlies high-frequency oscillations in the hippocampus in vitro," *Nature*, vol. 394, no. 6689, pp. 189–192, 1998.

[42] A. Ylinen, A. Bragin, Z. Nádasdy et al., "Sharp wave-associated high-frequency oscillation (200 Hz) in the intact hippocampus: network and intracellular mechanisms," *The Journal of Neuroscience*, vol. 15, part 1, pp. 30–46, 1995.

[43] B. Rörig and B. Sutor, "Serotonin regulates gap junction coupling in the developing rat somatosensory cortex," *European Journal of Neuroscience*, vol. 8, no. 8, pp. 1685–1695, 1996.

[44] B. Rörig and B. Sutor, "Nitric oxide-stimulated increase in intracellular cGMP modulates gap junction coupling in rat neocortex," *NeuroReport*, vol. 7, no. 2, pp. 569–572, 1996.

[45] T. M. Szabo, J. S. Caplan, and M. J. Zoran, "Serotonin regulates electrical coupling via modulation of extrajunctional conductance: H-current," *Brain Research*, vol. 1349, pp. 21–31, 2010.

[46] K. Pardo-Peña, L. Medina-Ceja, and A. Morales-Villagrán, "Serotonin modulates fast ripple activity in rats with spontaneous recurrent seizures," *Brain Research*, 2014.

Hindawi Publishing Corporation
BioMed Research International
Volume 2014, Article ID 981219, 8 pages
http://dx.doi.org/10.1155/2014/981219

Review Article

Clinical Metabolomics and Nutrition: The New Frontier in Neonatology and Pediatrics

Angelica Dessì,[1] Flaminia Cesare Marincola,[2] Alice Masili,[1] Diego Gazzolo,[3] and Vassilios Fanos[1]

[1] *Neonatal Intensive Care Unit, Puericulture Institute and Neonatal Section, Azienda Ospedaliera Universitaria, University of Cagliari, SS 554, Monserrato, 09042 Cagliari, Italy*
[2] *Department of Chemical and Geological Sciences, University of Cagliari, Cittadella Universitaria, SS 554, km 4.5, Monserrato, 09042 Cagliari, Italy*
[3] *Department of Maternal, Fetal and Neonatal Health, C. Arrigo Children's Hospital, Spalto Marengo 46, 15100 Alessandria, Italy*

Correspondence should be addressed to Vassilios Fanos; vafanos@tiscali.it

Received 11 April 2014; Accepted 14 August 2014; Published 27 August 2014

Academic Editor: Giovanni Li Volti

In the pediatric clinic, nutritional research is focusing more and more on preventing the development of long-term diseases as well as supporting the repair processes important in the therapy of already fully developed diseases. Most children who are hospitalized or affected by chronic diseases could benefit from specific and careful attention to nutrition. Indeed, the state of nutrition modulates all body functions, including the different metabolic processes which, all together, have a profound effect on the development of the health and future of all individuals. Inappropriate food, even in the first periods of life, can accelerate the development of chronic metabolic diseases, especially in the pediatric age. To gain further insights into metabolic cycles and how they are connected with diet and health, nutrition and metabolomics interact to develop and apply modern technologies for metabolic assessment. In particular, nutritionists are evaluating the metabolomic approach to establish the single nutritional phenotypes, that is, the way in which diet interacts with individuals' metabolisms. This strategy offers the possibility of providing a complete definition of the individual's nutritional and health status, predict the risk of disease, and create metabolomic databases supporting the development of "personalized nutrition," in which diet is attuned to the nutritional needs of individual patients.

1. Introduction

Metabolomics, one of the most recent "omics" sciences, can be defined as an approach based on the systematic study of the complete set of metabolites (metabolome) present in a given biological system, whether fluids, cells, or organisms [1]. The metabolome represents the complete set of low molecular weight (typically < 1500 Da) metabolites produced by an organism, which are the end products of gene expression. Thus, it can be viewed as a mirror that reflects the physiological, evolutionary, and pathological state of a biological system. By measuring the metabolome, metabolomics allows us to photograph the genome in its interaction with the environment and thus investigate the metabolic status of an organism in determined physiological conditions as a consequence of drug treatment, environmental influences, nutrition, lifestyle, genetic effects, and so on. Metabolomic analyses can generally be classified as targeted or untargeted. Targeted analyses focus on the characterization of a specific class of metabolites and are used to measure the concentration of a limited number of known metabolites precisely. This approach is important for assessing the behavior of a specific group of compounds in the sample under given conditions. Untargeted metabolomics focuses on the analysis of the metabolome profile to obtain fingerprints without attempting to identify or precisely quantify all the metabolites in the sample. This approach is most useful in biomarker discovery, diagnostics, and revealing specific metabolic patterns of disease. The study of the complex metabolic fingerprint and the comparative analyses of metabolomes are performed by a combined approach of spectrometric and spectroscopic techniques and computer programs. The techniques commonly employed

are nuclear magnetic resonance (NMR) spectroscopy, gas or liquid chromatography-mass spectrometry (GC-MS and LC-MS), Fourier transform infrared spectrometry, and capillary electrophoresis-MS (CE-MS). One of the difficulties with all these techniques is that they provide complex datasets, due to the large numbers of metabolites generated by multiple subjects. Thus, the analysis and interpretation of data relies on pattern recognition and discriminant analysis techniques [2]. One of the areas of greatest interest and in which metabolomics has revealed its great potential is that of nutrition. This is at the origin of nutrimetabolomics or nutritional metabolomics, that is, the study of the human or animal metabolome as a function of nutritional status or as a function of a nutritional challenge. Nutrimetabolomics, together with nutrigenomics, is the foundation on which personalized diets are shaped and planned: through the study of the metabolome it is possible to assess changes induced by diet in gene expression and thus, by modifying the nutriments and biomolecules assumed in the diet, we can intervene in the interaction between nutrients and the human metabolism to reach and maintain the best state of health [3, 4]. Thanks to metabolomics, it appears to be possible to assess an individual's state of nutrition to understand how single nutrients influence metabolic regulation and thus to formulate personalized diets which, if followed at an early age, may prevent the onset of certain chronic diseases such as diabetes, inflammatory diseases, and obesity. Nutrimetabolomics appears to be a promising technique also in pediatric and neonatal research. Studies in this field are evolving continuously towards an improvement in pediatric and neonatological practices in hospitals and clinics. It has been found more and more that exogenous factors such as nutrition, especially in the early stages of life, are of fundamental importance owing to their impact on the proper growth of children and their possible implication for diseases in adulthood, in the case of an inappropriate diet [5]. Comprehension of changes in metabolic profiles during one's lifespan, starting from the earliest stages, may represent an important point of reference in arriving at an understanding of their fundamental mechanisms and their consequent metabolic alterations. This review focuses on the applications of metabolomic technology in the context of neonatology and pediatrics with emphasis on the potential preclinical and clinical applications of this technology in the area of nutrition.

2. Metabolomics and Nutrition in Neonatology

In the last ten years, many steps forward have been taken by experts in the field of nutrition in identifying nutrients essential for the growth and good health of the newborn. Milk is a key component in the diet of infants all over the world and especially breast milk is the primary source of nutrition for neonates. Human breast milk (HBM) is a complex biological fluid capable of satisfying the nutritional requirements of a rapidly growing child. Besides the normal nutritional substances such as proteins, carbohydrates, fats, vitamins, and minerals, HBM also contains many other biologically active components such as growth factors, antimicrobic compounds, and immunostimulating components that educate neonates' immune system and protect them against pathogens [6, 7]. Many studies have demonstrated the advantages of breastfeeding, especially in the case of preterm neonates who, because of their low weight at birth, are more exposed to the onset of diseases, both in the first months of life and in adulthood [8, 9]. For these patients, it is thus important to have the best possible nutritional support to ensure proper growth and long-term effects on health and wellbeing. Recently, NMR-based metabolomic studies have been performed to better understand the nutritional properties of HBM. The first investigation was carried out by Marincola et al. [10] who compared the metabolic profiles of the hydrosoluble extract from breast milk of mothers who gave premature birth (between 26 and 36 weeks of gestation) with those of formula milk. A detailed NMR spectral analysis of the human milk oligosaccharides (HMOs) was performed by Praticò et al. [11]. Finally, Smilowitz et al. [12] investigated the interindividual variation in the milk metabolome in terms of maternal secretor status, phenotype, and diet. All of these studies pointed out the contribution of several factors to milk composition variation, among which time of collection, mother's diet and length of pregnancy.

At present, nutritionists and dietologists are turning their attention to the discovery of new ways to treat or prevent diseases connected with nutrition such as obesity, diabetes, cardiovascular diseases, and the metabolic syndrome. Several studies have demonstrated that certain chronic pathologies are caused not only by postnatal conditions but also by exposure to epigenetic factors that may influence and permanently alter fetal "programming" [13–15]. It would in fact appear that fetal malnutrition, both excessive and insufficient, may permanently alter the metabolic processes of the fetus and increase the risk of chronic diseases in adulthood [5]. An altered glucid metabolism during fetal development in neonates with intrauterine growth retardation (IUGR) has recently been suggested to be reflected by the increase in extracellular myoinositol that may be considered a valid predictive marker of the development of obesity and type 2 diabetes (T2D) in adulthood [16, 17]. Inositol is in fact known as a secondary messenger of the insulin transducer signal; it is also known that insulin plays a role in favoring lipid and provide synthesis as well as cell growth [18]. In the case of fetal malnutrition (both too much and not enough), it is thus possible to hypothesize that at birth there is a situation of reduced sensitivity to insulin which may be revealed by an increase in extracellular inositol. Recently, the metabolomics approach has been adopted to analyze the urine NMR profiles in large-for-gestational-age (LGA) and IUGR neonates and to define the metabolic patterns associated with such pathologies [19]. The metabolomic analysis made it possible to identify molecules responsible for the different metabolic profiles of IUGR and LGA newborns with respect to a control group. Among these metabolites, myoinositol stood out, whose urine content was higher in both IUGR and LGA neonates. This finding appears to confirm the fact that exposure to a hyperglycemic or

hypoglycemic environment in the uterus leads to a common condition of reduced glucid tolerance at birth which tends to persist during growth and into adulthood and consequently to a higher risk of developing pathologies such as obesity and T2D (Figure 1). Thus, comprehension of changes in metabolic profiles during one's lifespan, starting from the earliest stages, may represent an important point of reference in arriving at an understanding of their fundamental mechanisms and their consequent metabolic alterations. Indeed, if it is true that genetics regulates an individual's response to food (nutrigenetics), it is being more and more affirmed that nutrients can control the gene expression (nutrigenomics) and products of the metabolism (nutrimetabolomics).

3. Metabolomics and Nutrition in Pediatrics

A number of studies applying metabolomics to nutritional research in pediatrics have been performed (Table 1). Bertram et al. [20] were the first to demonstrate the potential of NMR-based metabolomics in identifying the overall biochemical effects of consumption of different animal proteins in children. In their work the authors investigated the biochemical effects and metabolic differences linked with assumption of large amounts of milk or meat proteins for a limited period of time in children eight years of age. They discovered that the diet based on milk protein generated an increase in urinary excretion of hippurate (mainly derived via gut microfloral breakdown of plant phenolics and aromatic amino acids), thus demonstrating alterations in gut microflora. Differently, the meat diet caused increased urinary excretion of creatine and histidine, whose presence is consistent with the fact that meat is the primary creatine and histidine source, and urea. The NMR analysis of serum revealed a slight influence of the milk diet on the lipid profile, while the meat diet appeared not to have any effect on the serum metabolic profile. These findings confirmed that the metabolomic phenotype is the result not only of genetic factors and diet, but also of the individual's intestinal microbiome. How nutritional habits interfere with the intestinal microbiota is far from understood. The human body contains thousands of millions of microorganisms. They are greater in number than the cells and represent about 3% of body mass. For example, the bacteria that live in the intestinal tract make it possible to digest food and absorb nutritional substances by decomposing most of the proteins, lipids and carbohydrates in our diet, which otherwise would not be assimilated. The microbiome is able to contribute to human survival, with a larger number of genes compared to those of humans themselves. Several experts have hypothesized that a person's intestinal flora has a specific metabolic efficiency and that certain characteristics of microbiome composition may predispose towards a group of obesity-related metabolic abnormalities that increase an individual's risk of developing type 2 diabetes and cardiovascular disease [21]. Even though the microbiome of each individual begins at birth, it is possible to modify its composition through variations in the diet. It has been demonstrated that the kind of diet is capable of modifying certain risk factors for the development of the metabolic syndrome in obese individuals by causing variations in the composition of the bacterial population. In the light of a relationship among obesity, microbiome, and major susceptibility to the metabolic syndrome, it is thus clear that diet assumes a central role in modulating the risk of the disorder.

Infantile obesity is one of the most frequent problems in the pediatric age. The risk of an obese child becoming an obese adult increases with age and is directly related to the amount of excess weight. Moreover, an association between a rapid weight increase in early infancy and an increased risk of obesity in adulthood has been found [22]. Since obesity predicts both short- and long-term adverse health outcomes, including T2D, cardiovascular diseases, hypertension, certain forms of cancer and other obesity-associated problems, research into early-life determinants of obesity could lead to innovative strategies for prevention. Different metabolomic investigations both on animals and humans have been performed on the metabolic state of obese children. As will be shown shortly, since growth might have an impact on metabolism, data in the literature on metabolomic changes related to obesity show some inconsistencies, especially when a comparison between adults and children is made. Mihalik et al. [23] performed a target metabolomic study to determine whether or not obese youth with or without T2D would show the fasting plasma metabolic signatures of elevated amino acid (AA) and medium- to short-chain acylcarnitine (AcylCN) species reported in adults. To this end, tandem mass spectrometry (MS/MS) was used to assess the concentration of AcylCN species and AA in plasma of obese (OB), normal weight (NW), and T2D obese adolescents. The findings demonstrated that long-chain AcylCNs were similar in the three groups. Differently, short- and medium-chain AcylCN and AA concentrations were lower in the plasma of both the OB and the diabetic youths. Furthermore, OB adolescents with T2D demonstrated lower concentrations of the later β-oxidation intermediates along with higher rates of fat oxidation. Contrary to what has been reported for adults, the absence of defective fatty acid or amino acid metabolism in OB and T2D adolescents compared with NW support the hypothesis that adolescents and young adults with obesity and T2D have not yet developed the mitochondrial defects that are documented in older adults, and they may even have enhanced mitochondrial activity as an adaptation.

Plasma samples from normal weight, overweight and obese children were profiled by Zeng et al. [24] using GC-MS. Several metabolites (isoleucine, glyceric acid, serine, 2,3,4-trihydroxybutyric acid, and phenylalanine) were screened as potential biomarkers of childhood obesity. Moreover, the waist-hip ratio together with total triglycerides, total cholesterol, high density lipoprotein and low density lipoprotein were suggested to be the most important parameters that correlated with the metabolic disturbances of childhood obesity. Wahl et al. [25] analysed serum samples of OB and NW children between 6 and 15 years of age by using a MS-based metabolomics approach. Metabolite concentrations and metabolite ratios were compared between the two groups of children as well as between children of different pubertal

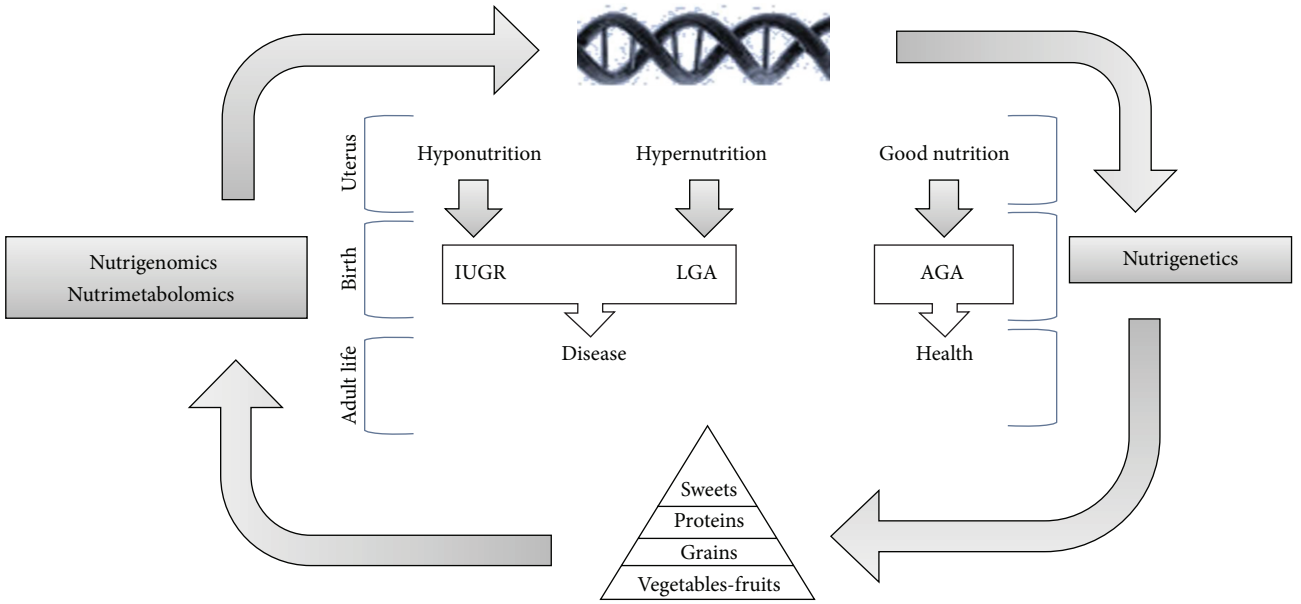

Figure 1: Nutrimetabolomics, nutrigenomics, and nutrigenetics in the life cycle: between genetics and environment and between hypo- and hypernutrition.

stages. Fourteen metabolites and 69 metabolite ratios were found to be significantly different in OB compared to NW children. In particular, the observed higher concentrations of the acylcarnitines in OB compared to NW were consistent with findings in adults. Differently, a significant reduction of glutamine, methionine, proline, and acyl-alkyl phosphatidylcholine (PC) concentrations was found in OB compared to NW children. Furthermore, OB children exhibited significantly decreased concentrations of the unsaturated lysophosphatidylcholines (LPCs) and increased ratios between saturated LPCs and phatidylcholines. The identified biomarkers were indicative of oxidative stress and changes in sphingomyelin metabolism, in β-oxidation, and in pathways associated with energy expenditure.

In the search for weight loss predictors, Wahl et al. [26] analyzed the MS serum metabolite profile of obese children during the Obeldicks lifestyle intervention program, a one-year weight loss program tailored to obese children aged 6–15 years and based on physical activity, nutritional education and behavior therapy that includes individual psychological care of the child and his/her family. Eighty obese children completed the Obeldicks program and were analyzed: 40 achieved a substantial reduction of their body mass index standard deviation score (BMI-SDS) during this program and 40 did not improve their overweight status. The combination of MS data with anthropometric and clinical parameters highlighted long-chain unsaturated phosphatidylcholines and smaller waist circumference as significant predictors of BMI-SDS reduction during the study, thus suggesting a role of phosphatidylcholine metabolism and abdominal obesity in body weight regulation. To enhance the understanding of relationships between obesity and gut microbiota, lifestyle and genetic background in humans, some animal species have been evaluated as experimental models for obesity research. Because of similarities in nutrition and metabolism between pigs and humans [12, 13], genetically obese and lean pigs are useful in childhood obesity research in understanding the mechanisms responsible for development of adiposity. He et al. [27] used NMR-based metabonomics to investigate differences in the serum of genetically obese and lean growing pigs to explore the feasibility of using the obese Ningxiang pig as an animal model for childhood obesity research. The results of this study clearly demonstrated marked differences in serum metabolites, hormones and body composition between obese and lean pigs under the same nutritional and environmental conditions. The altered serum metabonome of obese pigs was mainly ascribed to increased lipogenesis, adipose accumulation, reduced conversion of amino acid nitrogen into urea, and reduced protein synthesis. In addition, changes in gut microbiota-related metabolites, including trimethylamine-N-oxide and choline, were observed in sera of obese pigs compared to lean pigs. Most of these changes are similar to those reported for other animal models as well as children and teenagers. These findings justify the use of the Ningxiang pig as an animal model for childhood obesity research.

Increasing rates of obesity in children have focused attention also on the development of type 1 diabetes (T1D). Indeed, the risk of T1D might rise with increased weight gain as a result of increased insulin resistance and additional stress to beta cells [28]. Zuppi et al. [29] were the first to test the potential of NMR-based metabolomics in highlighting differences between urines from children and adolescents with T1D, but without renal complications, and from healthy individuals matched for sex and age. The levels of alanine, lactate, acetate and citrate were significantly higher in the diabetic patients than in controls. No correlation was found

Table 1: A summary of metabolomic studies assessing variations in nutritional health and/or disease status in paediatrics.

Disease	Population studied	Samples	Platform	Biological processes associated with the metabolic disorder	Reference
Obesity	Adolescents: (i) Normal weight ($n = 39$) (ii) Obese ($n = 64$) (iii) T2D ($n = 17$)	Plasma	MS/MS	No defects in fatty acid and amino acid metabolism	Mihalik et al. [23]
	Children: (i) Normal weight ($n = 16$) (ii) Obese ($n = 32$) (iii) Overweight ($n = 13$)	Plasma	GC-MS	Changes in lipid metabolism	Zeng et al. [24]
	Children: (i) Normal weight ($n = 40$) (ii) Obese ($n = 80$)	Serum	MS	Oxidative stress, changes in sphingomyelin metabolism, in β-oxidation, and in pathways associated with energy expenditure.	Wahl et al. [25]
	Obese children: (i) With substantial overweight reduction ($n = 40$) (ii) Without substantial overweight reduction ($n = 40$)	Serum	MS	Phosphatidylcholine metabolism	Wahl et al. [26]
	Pigs (4 months of age): (i) Obese type ($n = 10$) (ii) Lean type ($n = 8$)	Serum	NMR	Lipogenesis, lipid oxidation, energy utilization and partition, protein and amino acid metabolism, and fermentation of gastrointestinal microbes	He et al. [27]
Diabetes 1	Children: (i) T1D ($n = 25$) (ii) Control ($n = 25$)	Urine	^{1}H-NMR	Increased glomerular filtration rateand/or a modification of the transport mechanisms at thetubular level.	Zuppi et al. [29]
	Children: (i) Who progressed to T1D ($n = 50$) (ii) Who remained healthy and autoantibody negative ($n = 67$)	Serum	UPLC-MS	Dysregulation of lipid and amino acid metabolism preceding islet autoimmunity	Orešič et al. [30]
	Children: (i) T1D ($n = 34$) (ii) Control ($n = 16$)	Urine	CE-UV	—	Balderas et al. [31]
	Children: (i) T1D ($n = 34$) (ii) Control ($n = 15$)	Plasma Urine	LC-MS CE-MS	Dysregulation of lipid metabolism and activity of the gut microflora Protein and amino acid metabolism, glycation	Balderas et al. [32]
	Children: (i) T1D ($n = 19$) (ii) Control ($n = 90$)	Urine	^{1}H-NMR	Carbohydrate metabolism and gut microbial metabolism	Culeddu et al. [33]
	(i) Diabetic children and teenagers with T1D ($n = 30$) (ii) Control ($n = 12$)	Urine	^{1}H-NMR	Endogenous glucose production pathway from proteins	Deja et al. [34]
Inflammatory bowel disease	Mice (4–24 weeks of age)	Hydrophilic and lipophilic extracts from intestinal compartments	NMR LC-MS	Modifications of the general cell membrane composition, alteration of energy homeostasis, and the generation of inflammatory lipid mediators	Baur et al. [35]
Celiac disease	Infants genetically susceptible for CD ($n = 47$)	Stool	NMR	GI tract microbiota metabolism	Sellitto et al. [36]

between the duration of T1D and the urinary excretion of the different metabolites. This result was hypothesized to reflect the increased glomerular filtration rate and/or modification of the transport mechanism at the tubular lumen in T1D. Changes in the serum metabolome were assessed prospectively in children who later progressed to T1D by Oresic et al. [30]. For this study, ultraperformance liquid chromatography coupled to mass spectrometry (UPLC-MS) was used. The authors compared the serum metabolome from children who, during followup, progressed to type 1 diabetes-associated autoimmunity and, further, to clinical diabetes or who remained permanently healthy and autoantibody negative. The individuals who developed diabetes had low serum levels of succinic acid and PC at birth, reduced levels of triglycerides and antioxidant ether phospholipids throughout the follow up, and increased levels of proinflammatory lysoPCs several months before seroconversion to autoantibody positivity. The appearance of insulin and glutamic acid decarboxylase autoantibodies was preceded by diminished ketoleucine and elevated glutamic acid. These findings strongly suggested that the metabolic dysregulation precedes overt autoimmunity in T1D.

Balderas et al. [31] used capillary electrophoresis with UV detection to reveal differences in urines of diabetic children as compared to controls and to study the effects of a special additive containing rosemary extract, vitamin E and polyunsaturated fatty acids added to their standard diet through the meat. Analysis of urines obtained after a 12-month treatment evidenced clear differences between treated and nontreated diabetic children. Some of the metabolites associated with T1D were identified, among which guanidinoacetate, creatinine, urea, phenyllactate and p-OH-phenyllactate, phenaceturate, and benzoate. To analyze more in depth the metabolic changes characterizing T1D children, Balderas et al. [32] later also investigated the alterations in plasma and urine of T1D diabetic children who were under insulin treatment with good glycemic control. Plasma samples were analyzed with LC-MS, while urines with CE-MS. Compared to the control group, the main changes in plasma of T1D patients were associated with the lipid metabolism and some markers of the differential activity of the gut microflora. Changes in urine composition were associated with the protein and amino acid metabolism. Furthermore, one early glycation end product (fructosamine) was excreted in higher proportion in the diabetic group. A detailed analysis of the NMR-based metabolomics profiles of diabetic and healthy children's urine was presented by Culeddu et al. [33]. By excluding from the statistical analysis the NMR signals of sugars and citrate (related to the carbohydrate metabolism) and of hippurate (a metabolite of bacterial origins) whose presence overwhelmed all the other compound effects on classification models, the authors evidenced other metabolites (p-cresol sulphate and phenylacetylglycine) as relevant biomarkers. These metabolites were suggested to reflect changes in gut microbiota composition of T1D children with respect to the control group. Additional urine biomarkers associated with T1D were found by Deja et al. [34]. They investigated the relation between the level of glycated hemoglobin (HbA1c) and concentration of metabolites in urines of T1D children and teenagers by using 1H NMR target analysis. Differences among patients with HbA1c levels below (L-T1D) and above (H-T1D) 6.5% showed the importance not only of glucose, ketone bodies and HbA1c, but also of other urine metabolites such as alanine, valine, acetate, pyruvate and citrate, probably related to the endogenous glucose production pathway from proteins.

Recently, the biochemical conditions at the root of inflammatory intestinal disease and their impact on the systemic and gastrointestinal metabolism was studied by Baur et al. [35]. The authors monitored the metabolic events associated with the progressive development of Crohn's disease in a mouse model (from the age of 4 up to 24 weeks). The metabolic profiles of different intestinal compartments were generated by combining NMR spectroscopy and LC-MS. Data revealed shifts in the intestinal lipid metabolism concomitant with the histological onset of inflammation. Moreover, the condition of advanced disease was characterized by a significantly altered metabolism of cholesterol, triglycerides, phospholipids and sphingomyelin in the inflamed tissue (ileum) and the adjacent parts of the intestine (proximal colon). Finally, the effects of nutrition on the metabolic and kinetic equilibrium in children affected by the celiac disease (CD) were assessed in a metabolomic work by Sellitto et al. [36]. The authors combined high-resolution culture-independent methods based on pyrosequencing of barcoded 16SrRNA gene amplicons, quantitative PCR and NMR-based metabolomics to determine the composition and temporal changes of the gut microbiota and to identify potential biomarkers associated with onset of CD in infants with genetic predisposition for CD over the first two years of life. The results showed that infants genetically susceptible to CD who were exposed to gluten at an early age mounted an immune response against gluten and developed CD autoimmunity more frequently than at-risk infants in which gluten exposure was delayed until 12 months of age. Furthermore, the metabolomic analysis of fecal samples revealed potential biomarkers for the prediction of the disease.

4. Conclusions

On the basis of published studies, it can be stated that metabolomics is showing itself to be a powerful investigative tool in pediatric and neonatological nutrition research and, in particular, in searching for new biomarkers associated with nutritional health and/or disease status. The final goal is to arrive at an understanding of the biological behavior of a cell system in response to outside stimuli and clear the way to a comprehension of the complex network of interactions between nutrients and molecules (nutrimetabolomics). It is the study of cell metabolites of low molecular weight in response to dietetic treatments that will make it possible to design a kind of nutrition tailored to the genes of each individual, especially in the fields of neonatology and pediatrics.

Conflict of Interests

The authors declare that there is no conflict of interests regarding the publication of this paper.

References

[1] J. K. Nicholson and J. C. Lindon, "Systems biology: metabonomics," *Nature*, vol. 455, no. 7216, pp. 1054–1056, 2008.

[2] J. C. Lindon and J. K. Nicholson, "Spectroscopic and statistical techniques for information recovery in metabonomics and metabolomics," *Annual Review of Analytical Chemistry*, vol. 1, no. 1, pp. 45–69, 2008.

[3] V. Fanos, R. Antonucci, and L. Atzori, "Metabolomics in the developing infant," *Current Opinion in Pediatrics*, vol. 25, no. 5, pp. 604–611, 2013.

[4] V. G. Makarov, M. N. Makarova, A. V. Rydlovskaya, and S. V. Tesakova, "Nutrimetabolomics from the points of systemic estimation of function of metabolomic complexes," *Voprosy Pitaniia*, vol. 76, no. 3, pp. 4–10, 2007.

[5] A. Dessì, M. Puddu, G. Ottonello, and V. Fanos, "Metabolomics and fetal -neonatal nutrition: between "not enough" and "too much"," *Molecules*, vol. 18, pp. 11724–11732, 2013.

[6] A. L. Morrow and J. M. Rangel, "Human milk protection against infectious diarrhea: implications for prevention and clinical care," *Seminars in Pediatric Infectious Diseases*, vol. 15, no. 4, pp. 221–228, 2004.

[7] L. Fernández, S. Langa, V. Martín et al., "The human milk microbiota: origin and potential roles in health and disease," *Pharmacological Research*, vol. 69, no. 1, pp. 1–10, 2013.

[8] A. I. Eidelman, R. J. Schanler, M. Johnston et al., "Breastfeeding and the use of human milk," *Pediatrics*, vol. 129, pp. 827–841, 2012.

[9] A. Reali, F. Greco, S. Fanaro et al., "Fortification of maternal milk for very low birth weight (VLBW) pre-term neonates," *Early Human Development*, vol. 86, no. 1, pp. S33–S36, 2010.

[10] F. C. Marincola, A. Noto, P. Caboni et al., "A metabolomic study of preterm human and formula milk by high resolution NMR and GC/MS analysis: preliminary results," *Journal of Maternal-Fetal and Neonatal Medicine*, vol. 25, no. 5, pp. 62–67, 2012.

[11] G. Praticò, G. Capuani, A. Tomassini, M. E. Baldassarre, M. Delfini, and A. Miccheli, "Exploring human breast milk composition by NMR-based metabolomics," *Natural Product Research*, vol. 28, no. 2, pp. 95–101, 2014.

[12] J. T. Smilowitz, A. O'Sullivan, D. Barile, J. B. German, B. Lönnerdal, and C. M. Slupsky, "The human milk metabolome reveals diverse oligosaccharide profiles," *Journal of Nutrition*, vol. 143, pp. 1709–1718, 2013.

[13] D. J. P. Barker, "Fetal origins of coronary heart disease," *British Medical Journal*, vol. 311, no. 6998, pp. 171–174, 1995.

[14] A. Dessì, G. Ottonello, and V. Fanos, "Physiopathology of intrauterine growth retardation: from classic data to metabolomics," *Journal of Maternal-Fetal and Neonatal Medicine*, vol. 25, no. 5, pp. 13–18, 2012.

[15] C. Berti, I. Cetin, C. Agostoni et al., "Pregnancy and infants' outcome: nutritional and metabolic implications," *Critical Reviews in Food Science and Nutrition*, 2014.

[16] H. C. Bertram, P. M. Nissen, C. Nebel, and N. Oksbjerg, "Metabolomics reveals relationship between plasma inositols and birth weight: possible markers for fetal programming of type 2 diabetes," *Journal of Biomedicine and Biotechnology*, vol. 2011, Article ID 378268, 8 pages, 2011.

[17] A. Dess, L. Atzori, A. Noto et al., "Metabolomics in newborns with intrauterine growth retardation (IUGR): urine reveals markers of metabolic syndrome," *Journal of Maternal-Fetal and Neonatal Medicine*, vol. 24, no. 2, pp. 35–39, 2011.

[18] A. Dessì and V. Fanos, "Myoinositol: a new marker of intrauterine growth restriction?" *Journal of Obstetrics & Gynaecology*, vol. 33, pp. 776–780, 2013.

[19] L. Barberini, A. Noto, C. Fattuoni et al., "Urinary metabolomics reveals that low and high birth weights infants share elevated inositol concentrations at birth," *Journal of Maternal-Fetal and Neonatal Medicine*. In press.

[20] H. C. Bertram, C. Hoppe, B. O. Petersen, J. Ø. Duus, C. Mølgaard, and K. F. Michaelsen, "An NMR-based metabonomic investigation on effects of milk and meat protein diets given to 8-year-old boys," *British Journal of Nutrition*, vol. 97, no. 4, pp. 758–763, 2007.

[21] J. K. DiBaise, H. Zhang, M. D. Crowell, R. Krajmalnik-Brown, G. A. Decker, and B. E. Rittmann, "Gut microbiota and its possible relationship with obesity," *Mayo Clinic Proceedings*, vol. 83, no. 4, pp. 460–469, 2008.

[22] B. Koletzko, B. Brands, L. Poston, K. Godfrey, and H. Demmelmair, "Early nutrition programming of long-term health," *Proceedings of the Nutrition Society*, vol. 71, no. 3, pp. 371–378, 2012.

[23] S. J. Mihalik, S. F. Michaliszyn, J. de las Heras et al., "Metabolomic profiling of fatty acid and amino acid metabolism in youth with obesity and type 2 diabetes: evidence for enhanced mitochondrial oxidation," *Diabetes Care*, vol. 35, no. 3, pp. 605–611, 2012.

[24] M. Zeng, Y. Liang, H. Li et al., "Plasma metabolic fingerprinting of childhood obesity by GC/MS in conjunction with multivariate statistical analysis," *Journal of Pharmaceutical and Biomedical Analysis*, vol. 52, no. 2, pp. 265–272, 2010.

[25] S. Wahl, Z. Yu, M. Kleber et al., "Childhood obesity is associated with changes in the serum metabolite profile," *Obesity Facts*, vol. 5, no. 5, pp. 660–670, 2012.

[26] S. Wahl, C. Holzapfel, Z. Yu et al., "Metabolomics reveals determinants of weight loss during lifestyle intervention in obese children," *Metabolomics*, vol. 9, no. 6, pp. 1157–1167, 2013.

[27] Q. He, P. Ren, X. Kong et al., "Comparison of serum metabolite compositions between obese and lean growing pigs using an NMR-based metabonomic approach," *Journal of Nutritional Biochemistry*, vol. 23, no. 2, pp. 133–139, 2012.

[28] D. Daneman, "Type 1 diabetes," *The Lancet*, vol. 367, no. 9513, pp. 847–858, 2006.

[29] C. Zuppi, I. Messana, P. Tapanainen et al., "Proton nuclear magnetic resonance spectral profiles of urine from children and adolescents with type 1 diabetes," *Clinical Chemistry*, vol. 48, no. 4, pp. 660–662, 2002.

[30] M. Oresic, S. Simell, M. Sysi-Aho et al., "Dysregulation of lipid and amino acid metabolism precedes islet autoimmunity in children who later progress to type 1 diabetes," *Journal of Experimental Medicine*, vol. 205, no. 13, pp. 2975–2984, 2008.

[31] C. Balderas, A. Villaseñor, A. García et al., "Metabolomic approach to the nutraceutical effect of rosemary extract plus Ω-3 PUFAs in diabetic children with capillary electrophoresis," *Journal of Pharmaceutical and Biomedical Analysis*, vol. 53, pp. 1298–1304, 2010.

[32] C. Balderas, F. J. Rupérez, E. Ibañez et al., "Plasma and urine metabolic fingerprinting of type 1 diabetic children," *Electrophoresis*, vol. 34, no. 19, pp. 2882–2890, 2013.

[33] N. Culeddu, M. Chessa, M. C. Porcu et al., "NMR-based metabolomic study of type 1 diabetes," *Metabolomics*, vol. 8, no. 6, pp. 1162–1169, 2012.

[34] S. Deja, E. Barg, P. Młynarz, A. Basiak, and E. Willak-Janc, "1H NMR-based metabolomics studies of urine reveal differences between type 1 diabetic patients with high and low HbAc1 values," *Journal of Pharmaceutical and Biomedical Analysis*, vol. 83, pp. 43–48, 2013.

[35] P. Baur, F. Martin, L. Gruber et al., "Metabolic phenotyping of the Crohn's disease-like IBD etiopathology in the TNFΔARE/WT mouse model," *Journal of Proteome Research*, vol. 10, no. 12, pp. 5523–5535, 2011.

[36] M. Sellitto, G. Bai, G. Serena et al., "Proof of concept of microbiome-metabolome analysis and delayed gluten exposure on celiac disease autoimmunity in genetically at-risk infants," *PLoS ONE*, vol. 7, no. 3, Article ID e33387, 2012.